PB-236 647

DESIGN OF AN OPTIMUM DISTILLATE OIL BURNER FOR CONTROL OF POLLUTANT EMISSIONS

R. A. Dickerson, et al

Rockctdyne

Prepared for:

National Environmental Research Center

June 1974

DISTRIBUTED BY:

NTIS
National Technical Information Service
U. S. DEPARTMENT OF COMMERCE
5285 Port Royal Road, Springfield Va. 22151

PB-236 647

302052

EPA-650/2-74-047

June 1974

Environmental Protection Technology Series

DESIGN OF AN OPTIMUM DISTILLATE OIL BURNER FOR CONTROL OF POLLUTANT EMISSIONS

Reproduced by
NATIONAL TECHNICAL
INFORMATION SERVICE
U S Department of Commerce
Springfield VA 22151

Office of Research and Development
U.S. Environmental Protection Agency
Washington, DC 20460

PB 236 647

TECHNICAL REPORT DATA

(Please read Instructions on the reverse before completing)

1. REPORT NO. EPA-650/2-74-047	2.	3. RECIPIENT'S ACCESSION NO.
4. TITLE AND SUBTITLE Design of an Optimum Distillate Oil Burner for Control of Pollutant Emissions		5. REPORT DATE June 1974
		6. PERFORMING ORGANIZATION CODE
7. AUTHOR(S) R. A. Dickerson and A. S. Okuda		8. PERFORMING ORGANIZATION REPORT NO.
9. PERFORMING ORGANIZATION NAME AND ADDRESS Rocketdyne Division, Rockwell International 6633 Canoga Avenue, Canoga Park, CA 91304		10. PROGRAM ELEMENT NO. 1AB014; ROAP 21ADG-44
		11. CONTRACT/GRANT NO. 68-02-0017
12. SPONSORING AGENCY NAME AND ADDRESS EPA, Office of Research and Development NERC-RTP, Control Systems Laboratory Research Triangle Park, NC 27711		13. TYPE OF REPORT AND PERIOD COVERED Final
		14. SPONSORING AGENCY CODE
15. SUPPLEMENTARY NOTES		

16. ABSTRACT
The report describes results of a research study of the pollution characteristics of high-pressure atomizing, No. 2 distillate fuel oil burners. The main emphasis was on optimizing burner design to minimize pollutant emissions when firing into refractory-lined combustion chambers. The atomizing characteristics, and flow and composition profiles in the combustion zones of several commercial burners were determined experimentally. Mass median droplet diameters were 60-90 microns for 0.50-1.50 gph oil spray nozzles. Nitric oxide (NO) formation was most prevalent in the near-stoichiometric combustion zones where local flow conditions led to vigorous gas mixing. These data were used to design variable geometry burners, used to optimize burner geometry for minimizing pollutant emissions. The optimum geometry burners were fabricated in fixed-geometry versions and tested extensively to verify their low air pollutant emissions. Substantial reductions (about 50 percent) in NO emissions were achieved by optimizing conventional designs, with negligible emissions of other pollutants. Also, several nonconventional burner designs were built and tested: two of these led to very low NO emissions. Program results have been used to develop recommendations for burner design to minimize pollutant emissions.

17. KEY WORDS AND DOCUMENT ANALYSIS

a. DESCRIPTORS		b. IDENTIFIERS/OPEN ENDED TERMS	c. COSATI Field/Group
Air Pollution	Distillates	Air Pollution Control	13B
Combustion	Heating Equipment	Stationary Sources	21B
Oil Burners		Burner Design	13A
Design		Oil Spray Characterization	07B
Nitrogen Oxides		Flow Field Measurement	11H, 21D
Fuel Oil			

18. DISTRIBUTION STATEMENT Unlimited	19. SECURITY CLASS *(This Report)* Unclassified	21. NO. OF PAGES 270
	20. SECURITY CLASS *(This page)* Unclassified	22. PRICE $16.00

EPA Form 2220-1 (9-73)

I

Reproduced by
NATIONAL TECHNICAL
INFORMATION SERVICE
U S Department of Commerce
Springfield VA 22151

DESIGN OF AN OPTIMUM DISTILLATE OIL BURNER FOR CONTROL OF POLLUTANT EMISSIONS

by

R. A. Dickerson and A. S. Okuda

Rocketdyne Division
Rockwell International
6633 Canoga Avenue
Canoga Park, California 91304

Contract No. 68-02-0017
ROAP No. 21ADG-44
Program Element No. 1AB014

EPA Project Officer: G. B. Martin

Control Systems Laboratory
National Environmental Research Center
Research Triangle Park, North Carolina 27711

Prepared for

OFFICE OF RESEARCH AND DEVELOPMENT
U. S. ENVIRONMENTAL PROTECTION AGENCY
WASHINGTON, D.C. 20460

June 1974

This report has been reviewed by the Environmental Protection Agency and approved for publication. Approval does not signify that the contents necessarily reflect the views and policies of the Agency, nor does mention of trade names or commercial products constitute endorsement or recommendation for use.

ABSTRACT

This report describes results from a research study of the pollution characteristics of high-pressure atomizing, No. 2 distillate fuel oil burners. The main emphasis was on optimizing burner design to minimize pollutant emissions when these burners are fired into refractory-lined combustion chambers. The atomization characteristics, flow profiles, and composition profiles in the combustion zones of several commercial burners were determined experimentally. Mass median droplet diameters ranged from 60 to 90 microns for 0.50- to 1.50-gph oil spray nozzles. Nitric oxide formation was most prevalent in the near-stoichiometric combustion zones where local flow conditions led to vigorous mixing of gases. These data were used to guide the design of variable geometry burners that were used to optimize the burner geometry for minimization of pollutant emissions. The optimum geometry burners were fabricated in fixed geometry versions and tested extensively to verify their low air pollutant emissions. Substantial reductions in NO (~50 percent) emissions were achieved by optimizing conventional designs, with negligible emissions of other pollutants. Additionally, several nonconventional burner designs were built and tested, two of which led to very low nitric oxide emissions. Results from the program have been used to develop recommendations for burner design to minimize pollutant emissions.

This report was submitted in fulfillment of Contract No. 68-02-0017 by Rocketdyne Division, Rockwell International, Canoga Park, California, under the sponsorship of the Environmental Protection Agency. Work was completed as of 1 February 1974.

CONTENTS

Page

Abstract iii

List of Figures vi

List of Tables xvi

Summary 1

  Atomization Measurements 2

  Tests of Commercial Burners 2

  Versatile Burner Experiments 4

  Optimized Fixed Geometry Burners 5

  Nonconventional Burner Concepts 7

  Conclusions 9

  Summary of Recommended Design Practices 10

Introduction 15

Apparatus and Data Reduction 23

  Atomization Test Facility 23

  Air Flow Patterns 26

  Oil Spray Patterns 34

  Combustion Gas Flow Patterns 39

  Combustion Chambers 43

  Furnaces 49

  Combustion Gas Composition Patterns 51

  Exhaust Gas Analyses 63

  Thermal Radiation 64

  Nonconventional Burners 66

  Oil Nozzles 75

Experimental Results 79

  Atomization Measurements 80

  Commercial Burner Studies 82

  Interpretation of Commercial Burner Results 173

  Burner Geometry Optimization Studies 188

  Simulated Field Testing of Optimum Geometry Burners 207

  Nonconventional Burners 218

CONTENTS (Continued)

Page
Conclusions 238
Optimum Burner Geometry 238
Burner Design Philosophy 238
Combustion Chamber Wall Temperature 240
Combustion Chamber Geometry 240
Appendix A
Commercial Design Practices 241
Appendix B
Factors for the Conversion of Units to the Metric System 251

FIGURES

No.		Page
1	Photographs of a 1-gph, Low Pollutant Emission Optimized Oil Burner Head	12
2	Choke Diameter Versus Oil Flowrate for Minimum Nitric Oxide Emissions, Low Smoke and Carbon Monoxide Emissions	13
3	Typical High-Pressure, Oil-Fired Gun Burner	17
4	Simplex Oil Spray Nozzle	19
5	Three Typical Air Diffuser Designs Used in the Ends of Oil Burner Blast Tubes	19
6	Wax Flow Facility	24
7	Velocity Direction Indicator Probes	28
8	Schematic of Directional Probe Gimbaling Apparatus Used to Alter Probe Angle While Keeping the Probe Tip Stationary	29
9	Probe Gimbaling Apparatus	31
10	Interpretation of β Angle Curves	33
11	Location of Horizontal and Vertical Planes for Determination of Gas Velocity Vectors	35
12	Liquid Spray Mass Flux Sampling Apparatus	37
13	Effects of Sampling Velocity on Oil Collection Rate	38
14	Oil Burner Cold-Flow Facility Schematic	40
15	Water-Cooled Probes	41
16	Schematic of Oil Burner Flame Gas Velocity Probe System	42
17	Schematic of the 8.0-Inch-Diameter Insulated Cylindrical Combustor With Semicircular Mixing Baffles	44
18	Schematic of 30-Inch-Diameter, Hot/Cold Wall, Coaxial Cylindrical Research Combustor for 6- to 12-gph Oil Burners	47
19	Schematic of Oil Burner Combustion Gas Sampling System	50
20	United Sensor Model GB 24-125 Gas Sampling Probe	53
21	Analytical System for Fuel Oil Burner Emission Analysis	54
22	Land 2π Radiometer Used for Radiation Measurements	65
23	Schematic of Modified Versatile Burner With Variable Rate, Mechanically Driven, Multiple Vane Swirler	67

FIGURES (Continued)

No. Page

24 Cross-Section View of the Fixed Geometry, 1.65-Inch-Diameter, 30-Degree Convergent Choke 69

25 Photographs of the Mechanically Rotated, Six-Vane Intense Swirl Burner in Various Stages of Assembly 70

26 Schematic of Displaced Oil Injection Burner Prototypes Constructed and Hot Fired 71

27 Schematic of the Forced Recirculated Combustion Gas Experimental Burner 73

28 Photograph of the Forced Recirculating Combustion Gas Burner (fully instrumented) With an 8-Vane, 60-Degree Swirler Ring, and 4 of 12 Combustion Gas Inlet Ports Plugged 74

29 Schematic of the Preheated Air Burner Test Apparatus Using a 2-Inch-Diameter Blast Tube with an 8-Vane, 75-Degree Swirl Ring, and a 0.75-80°-C Oil Nozzle 76

30 Cross-Sectional Schematic Showing the Internal Construction of a Typical High-Pressure Oil Atomizing Nozzle and the Various Spray Cone Patterns 77

31 Spray Dropsize Data Obtained Using the Method of Frozen Wax on Various Oil Burner Spray Nozzles 81

32 Extrapolation of Delavan Data to the Mass Median Particle Diameter Obtained for the Delavan 0.75-gph/80°-C Nozzle 83

33 Spray Dropsize Distribution for a Delavan 0.75-80°-B Nozzle at 100-psi Pressure 84

34 Spray Dropsize Distribution for a Delavan 0.75-80°-C Nozzle Operating at 100 psi 85

35 Spray Dropsize Distribution for a Delavan 1.00-80°-C Nozzle at 100-psi Pressure 86

36 Spray Dropsize Distribution for a Monarch 1.50-80°-R Nozzle at 100-psi Pressure 87

37 Spray Dropsize Distribution for a Delavan 0.50-80°-C Nozzle at 100-psi Pressure 88

38 Spray Dropsize Distribution for a Delavan 0.75-80°-C Nozzle at 75-psi Pressure 89

FIGURES (Continued)

No.		Page
40	Air Flow Parameters at 1.5 Inches Downstream in the Horizontal Plane of a 55-J Burner	92
41	Air Flow Parameters at 1.5 Inches Downstream in the Vertical Plane of a 55-J Burner	93
42	Air Flow Parameters at 3 Inches Downstream in the Horizontal Plane of a 55-J Burner	95
43	Air Flow Parameters at 3 Inches Downstream in the Vertical Plane of a 55-J Burner	96
44	Air Flow Parameters at 6 Inches Downstream in the Horizontal Plane of a 55-J Burner	97
45	Air Flow Parameters at 6 Inches Downstream in the Vertical Plane of a 55-J Burner	98
46	Measured Cold-Flow Air Velocity Vectors in the Horizontal Plane of a 55-J Burner	99
47	Measured Cold-Flow Air Velocity Vectors in the Vertical Plane of a 55-J Burner	100
48	Air Velocity Vectors for the Horizontal Plane of a 55-J Burner	101
49	Air Velocity Vectors for the Vertical Plane of a 55-J Burner	102
50	Air Velocity Vectors and Fuel Spray Mass Flux Data for a 55-J Burner Incorporating a 0.75-80°-C Nozzle (Horizontal Plane)	104
51	Air Velocity Vectors and Fuel Spray Mass Flux Data for a 55-J Burner Incorporating 0.75-80°-C Nozzle (Vertical Plane)	105
52	Air Velocity Vectors and Fuel Spray Mass Flux Data for a 55-J Burner Incorporating a 1.50-80°-C Nozzle (Vertical Plane)	106
53	Combustion Gas Velocity Vectors in the Horizontal Plane for the ABC 55-J Burner Mounted in an 8-Inch-Diameter, Cylindrical, Coaxial Chamber	107

FIGURES (Continued)

No.		Page
54	Combustion Gas Velocity Vectors in the Vertical Plane for the ABC 55-J Burner Mounted in an 8-Inch-Diameter, Cylindrical, Coaxial Chamber	108
55	Local Combustion Gas Analysis Profiles for the ABC 55-J Burner at a Nominal Stoichiometric Ratio of 1.25 With a 0.75-70°A Nozzle (Horizontal Plane)	109
56	Local Combustion Gas Analysis Profiles for the BAC 55-J Burner at a Nominal Stoichiometric Ratio of 1.50 With a 0.75-70°A Nozzle (Horizontal Plane)	110
57	Carbon Monoxide Emissions Measured by Mixed Combustion Gas Sampling in the Coaxial, 8-Inch-Diameter Cylindrical Combustion Chamber	112
58	Nitric Oxide Emissions Measured by Mixed Combustion Gas Sampling in the Coaxial, 8-Inch-Diameter Combustion Chamber	113
59	Smoke Emissions Measured by Mixed Combustion Gas Sampling, Coaxial 8-Inch-Diameter Combustion Chamber	114
60	Carbon Monoxide Emissions Measured by Lennox Furnace Flue Gas Sampling	115
61	Nitric Oxide Concentrations Measured in the Lennox Furnace Flue Gas Samples	116
62	Total Hydrocarbon Emissions Measured by Lennox Furnace Flue Gas Sampling	117
63	Smoke Emissions Measured by Lennox Furnace Flue Gas Sampling	118
64	Air Flow Parameters at 1.5 Inches Downstream of the Mite Burner in an 8-Inch-Diameter, Cylindrical, Coaxial Chamber	120
65	Air Flow Parameters at 3 Inches Downstream of the Mite Burner Installed in an 8-Inch-Diameter Cylindrical, Coaxial Chamber	121
66	Air Flow Parameters at 6 Inches Downstream of the Mite Burner in an 8-Inch-Diameter Cylindrical, Coaxial Chamber	122

FIGURES (Continued)

No.		Page
67	Air Flow and Oil Spray Flux Patterns in the Horizontal Plane of the Mite Burner Mounted in an 8-Inch-Diameter Cylindrical, Coaxial Chamber	123
68	Air Flow and Oil Spray Flux Patterns in the Vertical Plane of the Mite Burner, Mounted in an 8-Inch-Diameter, Cylindrical, Coaxial Chamber	124
69	Combustion Gas Velocity Vectors in the Horizontal Plane for the ABC Mite Burner Mounted in an 8-Inch-Diameter, Cylindrical, Coaxial Chamber	126
70	Combustion Gas Velocity Vectors in the Vertical Plane for the ABC Mite Burner Mounted in an 8-Inch-Diameter, Cylindrical, Coaxial Chamber	127
71	Combustion Gas Analysis Profiles for the ABC Mite Burner at a Nominal Stoichiometric Ratio of 1.25 With a 0.75-70°-A Nozzle	128
72	Combustion Gas Analysis Profiles for the ABC Mite Burner at a Nominal Stoiochiometric Ratio of 1.50 With a 0.75-70°-A Nozzle	129
73	Combustion Gas Analysis Profiles for the ABC Mite Burner at a Nominal Stoichiometric Ratio of 1.80 With a 0.75-70°-A Nozzle	130
74	Air Flow and Oil Spray Flux Patterns in the Horizontal Plane of the Model AFC Burner Mounted in an 8-Inch-Diameter Cylindrical, Coaxial Combustion Chamber	133
75	Air Flow and Oil Spray Flux Patterns in the Vertical Plane of the Model AFC Burner Mounted in an 8-Inch-Diameter, Cylindrical, Coaxial Chamber	134
76	Combustion Gas Analysis Profiles for the Model AFC Burner at a Nominal Stoichiometric Ratio of 1.25 With a 0.75-70°-A Nozzle	136
77	Combustion Gas Analysis Profiles for the Model AFC Burner at a Nominal Stoichiometric Ratio of 1.50 With a 0.75-70°-A Nozzle	137

FIGURES (Continued)

No. Page

78 Air Flow and Oil Spray Flux Patterns in the Horizontal Plane of the Nu-Way Burner Mounted in an 11-Inch-Diameter, Cylindrical, Coaxial Chamber 139

79 Air Flow and Oil Spray Flux Patterns in the Vertical Plane of the Nu-Way Burner Mounted in an 11-Inch-Diameter, Cylindrical, Coaxial Chamber 140

80 Combustion Gas Velocity Vectors in the Horizontal Plane for the Nu-Way Burner Mounted in an 11-Inch-Diameter, Cylindrical, Coaxial Chamber 142

81 Combustion Gas Velocity Vectors in the Vertical Plane for the Nu-Way Burner Mounted in an 11-Inch-Diameter, Cylindrical, Coaxial Chamber 143

82 Effect of Combustion Chamber Size on Nitric Oxide Emissions 144

83 Smoke Content of the Exhaust Gases for the 6-gph Nu-Way Burner Operating in the 30-Inch-Diameter, Coaxial Combustion Chamber Under Cold- and Hot-Wall Conditions 145

84 Hot-Wall, Local Combustion Gas Analysis Profiles for the 6-gph Nu-Way Burner at Nominal Stoichiometric Ratio of 1.16, With Twin 3-60°-B Oil Nozzles 147

85 Hot-Wall, Local Combustion Gas Analysis Profiles for the 6-gph Nu-Way Burner at a Nominal Stoichiometric Ratio of 1.16, With Twin 3-60°-B Nozzles 148

86 Comparison Plots of Local Combustion Zone Sampled Stoichiometric Ratio 149

87 Comparison of Combustion Gas Composition Profiles of the 6-gph Nu-Way Model CO Burner in Hot- and Cold-Wall Enclosures of Different Diameters 152

88 Radiant Energy Profiles for the 6-gph Nu-Way Burner at a Nominal Stoichiometric Ratio of 1.25 153

89 Radiant Energy Profiles for the 6-gph Nu-Way Burner at a Nominal Stoichiometric Ratio of 1.50 154

FIGURES (Continued)

No. Page

90 Diagram of the Carlin Company FFD Flame Funnel Series Burner Showing the Semi-Staged Combustion 158

91 Nitric Oxide Emissions Obtained From the Carlin 250 FFD Flame Funnel, the Nu-Way Model CO, and the Sun-Ray Model PHC Burners 160

92 Air Flow Parameters in the Horizontal Plane at 1.5 Inches Downstream of the Sun-Ray Burner With No Chamber and No Oil Flow 162

93 Air Flow Parameters in the Horizontal Plane 3 Inches Downstream of the Sun-Ray Burner With No Chamber and No Oil Flow 163

94 Air Flow Parameters in the Horizontal Plane at 6 Inches Downstream of the Sun-Ray Burner With No Chamber and No Oil Flow 164

95 Air Velocity Vectors in the Horizontal Plane for the Sun-Ray PHC-34 Burner With No Chamber and No Oil Flow 165

96 Air Velocity Vectors in the Vertical Plane for the Sun-Ray PHC-34 Burner With No Chamber and No Oil Flow 166

97 Comparison of Nitric Oxide Emissions in the Flue Gas for the Sun-Ray Model PHC Burner Operating at 11.5 gph 167

98 Smoke Content of the Flue Gases for the Sun-Ray Model PHC Burner Fired at 11.5 gph in the 30-Inch-Diameter Coaxial Combustion Chamber Under Cold- and Hot-Wall Conditions 168

99 Hot-Wall, Local Combustion Gas Analysis Profile for the Sun-Ray Burner at 11.5 gph and a Nominal Stoichiometric Ratio of 1.03 169

100 Hot-Wall, Local Combustion Gas Analysis Profiles for the Sun-Ray Burner at 11.5 gph and a Nominal Stoichiometric Ratio of 1.03 170

101 Hot-Wall, Local Combustion Gas Analysis Profiles for the Sun-Ray Burner at 11.5 gph and a Nominal Stoichiometric Ratio of 1.03 171

FIGURES (Continued)

No.		Page
102	Comparison Plots of Local Combustion Zone Sampled Stoichiometric Ratio	172
103	Nitric Oxide Content of Locally Sampled Combustion Gases, as a Function of Combusted Fuel Content, for the ABC 55-J Burner	184
104	Nitric Oxide Content of Flue Gases Produced by the Well-Stirred Burner	187
105	Overall Photograph of the 3- to 12-gph Versatile Research Burner	190
106	Photographs of the Variable Geometry Burner Heads of Both the 1- to 3-gph and the 6- to 12-gph Versatile Burners	192
107	Versatile Burner Flue Gas Emissions Obtained With 10-percent Excess Air in the 30-Inch-Diameter Hot-Wall Chamber	194
108	Versatile Burner Flue Gas Emission Obtained With 10-Percent Excess Air in the 30-Inch-Diameter Hot-Wall Chamber	195
109	Versatile Burner Flue Gas Emissions Obtained With 10-Percent Excess Air in the 30-Inch-Diameter Hot-Wall Chamber	196
110	Versatile Burner Flue Gas Emissions Obtained With 10-Percent Excess Air in the 30-Inch-Diameter Hot-Wall Chamber	197
111	Versatile Burner Flue Gas Emissions Obtained With 10-Percent Excess Air in the 30-Inch-Diameter Hot-Wall Chamber	199
112	Comparison of Nitric Oxide Emission Results From the 1- to 3-gph Versatile Burner Experiments as a Function of Air Swirl Vane Angle	201
113	Nitric Oxide Emissions as a Function of Choke Diameter for the Versatile Research Oil Burner at a Nominal Oil Flowrate of 0.75 gph with 25-Percent Excess Air	202
114	Choke Diameter Versus Oil Flowrate for Minimum Nitric Oxide Emissions, Low Smoke, and Carbon Monoxide Emissions	203
115	Nitric Oxide Emission Results From 1-gph Versatile Burner Experiments in a Perpendicular Port Combustor	206
116	Closeup Photograph of the 1-gph Optimum Oil Burner Head	208

FIGURES (Continued)

No.		Page
117	Nitric Oxide Emissions From the Fixed Geometry, 1-gph Optimum Burner Fired in the 8-Inch-Diameter, Hot-Wall, Coaxial Combustor	209
118	Comparison of Nitric Oxide Emission Profiles for Several 1-gph Oil Burners Fired in the 8-Inch-Diameter, Hot-Wall, Perpendicular Combustor	210
119	Exhaust Gas Composition Profiles as a Function of Time for the 1-gph Optimum Oil Burner in a Refractory-Lined Chamber, Hydronic Furnace	212
120	Comparison of Nitric Oxide Emission Profiles for Various Oil Burners in the 6- to 12-gph Firing Rate Range	214
121	Oscilloscope Frequency Trace of Noise Generated by the 9-gph Fixed Geometry Optimum Burner, Measured at the Exhaust of the 30-Inch-Diameter, 10-Foot-Long Coaxial Combustor	216
122	Exhaust Gas Composition Profiles as a Function of Time for the 9-gph Cptimum Oil Burner in a Cold-Wall, 30-Inch-Diameter, Coaxial Combustor	217
123	Nitric Oxide Emissions, Comparison of the Effect of Swirl on the 30-Degree Convergence, 1.65-Inch-Diameter, Mechanically Rotated, Six-Vane Swirler, With No Spark Igniter	220
124	Effects of Varying Recirculated Combustion Gas With the Forced Combustion-Gas Recirculation Burner	223
125	Effects of Combustion Chamber Wall Temperature With Forced Combustion-Gas Recirculation Burner	225
126	Forced Combustion Gas Recirculation Burner Emissions at an Oil Flowrate of 0.75 gph	227
127	Schematic of the Two-Stage, Intense-Swirl, Concentric-Tube Oil Burner Head Extension	229
128	Nitric Oxide Emission Results of Fuel-Rich Combustion Experiments With a Fixed-Vane Intense-Swirl Burner Head	231

FIGURES (Concluded)

No.		Page
129	Cross-Section View of the Fixed Geometry, 1.65-Inch-Diameter No-Swirl Optimum Burner Head	232
130	Nitric Oxide Emissions of the Fixed Geometry, Convergent and Expansion Sections Head, Optimum Geometry, No-Swirl Burner	233
131	Variation of the Nitric Oxide Profiles for the 1.65-Inch-Diameter, Fixed Geometry Versatile Burner With a 0.75-90°-A Nozzle Tested on Different Days	235
132	Comparison of Nitric Oxide Emissions of Commercially Available Burners With Spark Igniter Modifications	236
133	Comparison of Nitric Oxide Emissions From the 1.65-Inch-Diameter, No-Swirl, Fixed Geometry, Versatile Burner With Spark Igniter Modifications	237

TABLES

No.		Page
1	Contributors to Air Pollution in the United States	16
2	Exhaust Analysis Instruments	55
3	Pure Air Composition	56
4	Validity of Stoichiometric Ratio Calculations of Eq. 7	59
5	Equilibrium Flame Properties for No. 2 Distillate Fuel Oil	60
6	Calculated Equilibrium Gas Composition, Mole Percent	61
7	Commercial Burners Evaluated Experimentally	90

SUMMARY

This report describes the results of a program to study pollutant formation and emissions from No. 2 distillate fuel oil burners.

Emphasis was placed on high-pressure atomizing, luminous flame, No. 2 distillate fuel oil burners fired into refractory combustion chambers. The studies included burners ranging in oil flowrate from 0.5 to 12 gallons per hour (gph).

The objective of this study was to develop information that would allow minimization of the pollutant emissions from a burner by optimizing the burner geometry design within practical constraints. The pollutants to be minimized were nitric oxide, carbon monoxide, smoke, and unburned gaseous hydrocarbons.

The approach taken to achieving this objective was to: (1) relate emitted pollutant concentrations to mixing and flow characteristics of the burner, (2) relate the mixing and flow characteristics to burner design parameters, and (3) select the optimum design which minimized pollutant emissions while maintaining high combustion efficiency. This approach was implemented by: (1) studying the characteristics of several commercially available oil burners, namely, atomization, oil spray, and air flow patterns in the combustion zone, combustion gas composition patterns in the combustion zone, and overall pollutant emissions; (2) interpreting the results from the commercial burners to determine which design parameters are most important to the formation of pollutants; (3) building and testing "versatile" burners capable of continuous variation of the design parameters found to

be most important to pollutant formation; and (4) building and testing fixed design burners corresponding to the design found from the versatile burner tests to be optimum for pollutant minimization.

ATOMIZATION MEASUREMENTS

Atomization measurements were made with a number of high-pressure oil burner nozzles rated for oil flowrates of 0.75 to 1.50 gph. These tests were conducted with pressure drops from 75 to 125 psig. The frozen wax method was used for these measurements. Mass median droplet diameters obtained from these tests ranged from 65 to 90 microns. These results show that the commercially used atomization nozzles which are available at very low cost (less than about $1.00 per nozzle, nominally) do an excellent job of atomization.

TESTS OF COMMERCIAL BURNERS

The air flow patterns produced by several commercially available burners under noncombustion conditions were determined through the use of a directional impact probe that could be located at various positions in the oil burner flowfield. Additionally, oil spray flux patterns were measured with an aspirated sampling probe. The commercial burners tested in this manner were the ABC Model 55-J-1 (0.75 gph), the ABC Mite (1.0 gph), the Union Model AFC (0.75 gph), the Nu-Way Model CO (6 gph), and the Sun-Ray Model PHC (12 gph). Maximum air velocities were found to be, typically, about 30 ft/sec from the 0.75- and 1-gph burners, and about 60 ft/sec from the 6- and 12-gph burners. The measurements of flow patterns were repeated under combustion conditions with a cooled, directional impact probe being used. The flow patterns from these tests were found to differ very little, except for velocity magnitude, from those obtained from cold-flow measurements.

The same commercial burners were test fired in specially constructed, refractory-lined, cylindrical combustion chambers with the burner blast tubes mounted coaxially. During these test firings, combustion gas samples from various locations (including those where velocity measurements were made) in the combustion zones just downstream of the burner blast tubes were withdrawn through water-cooled sample probes. The samples were analyzed for nitric oxide, carbon monoxide, carbon dioxide, unburned hydrocarbon, and oxygen content of the sampled gases. The most important observation from these gas sampling studies was that the amount of nitric oxide formed, per unit mass of fuel burned, tended to be highest in the regions where both: (1) the combustion gas composition was near stoichiometric, and (2) the velocity patterns tended to promote gas mixing. In these regions, the nitric oxide concentration tended to be exceptionally high. The velocity patterns referred to in (2) above included regions where local combustion gas recirculation was taking place, but away from the cooling effects of walls and, also, regions where the velocity gradients were relatively steep, thus promoting turbulent mixing. A careful examination of the experimental data revealed that thorough mixing of the gas phase, so that the combustion process resembled a well-stirred reactor (at least locally), led to high concentrations of nitric oxide only when the local burned gas composition corresponded to 0 to 80 percent excess air. At local excess air levels greater than 80 percent, the opposite was true (i.e., thorough mixing led to low nitric oxide emissions). Because practical oil burners must operate at near stoichiometric conditions (nominally, between zero and about 25 percent excess air) to achieve satisfactory system efficiency, it was concluded that local recirculation, agitation of the gas flow, and steep gradients must be avoided if nitric oxide emissions are to be minimized. The flame-retention devices, used in the end of the blast tube of some burners, were found to promote the unwanted local recirculation, agitation, and steep velocity gradients. Therefore, the flame-retention device was found to be undesirable from a pollution standpoint.

VERSATILE BURNER EXPERIMENTS

Based on the results from the commercial burner studies, versatile geometry burners were constructed that simulated the construction of nonflame-retention burners. The variable geometry features of these burners included a continuously variable choke diameter, variable nozzle recess, and six peripheral, variable-angle air swirler vanes. Two such versatile geometry burners were constructed, one for use with flowrates of 1- to 3-gph (4-inch-diameter, 9-inch-long blast tube), and one for use with flowrates of 3- to 12-gph (5-inch-diameter, 12-inch-long blast tube). Combustion experiments were conducted with these versatile burners in refractory-lined, coaxial, cylindrical combustion chambers, over the 1- to 12-gph range of oil flowrates and over practical ranges of choke diameters, air swirler vane angles, and oil spray nozzle types. During all of these experiments, the pollutant emissions were measured. The results showed that usually the smoke, unburned hydrocarbons, and carbon monoxide emissions decreased, often monotonically, with increasing air swirler vane angle, whereas nitric oxide emissions increased, often monotonically, also with increasing air swirler vane angle. An air swirler vane angle of 25 degrees (measured relative to the blast tube axis) was found to be a good compromise over the entire oil flowrate range from 1- to 12-gph. The primary effect of the blast tube choke diameter was on the nitric oxide emissions, the choke diameter for minimization of nitric oxide emissions being given by choke diameter (inches) = $(2.7 \times \text{gph})^{0.4}$. The oil spray atomizer characteristics and oil nozzle recess were found to have little effect on the emissions, with the exception that nozzles producing smaller dropsizes (i.e., small orifice nozzles operated at high pressure drop) tended to produce less smoke than the larger dropsize nozzles (i.e., large orifice nozzles operated at low pressure drop). Oil nozzle position and spray angle had little effect on emissions in the versatile geometry burner studies, although later studies with fixed geometry burners required a trial and error selection of oil nozzle spray angle necessary for elimination of smoke emissions, with the best spray angle apparently being dependent on chamber geometry (implying that a nozzle must be selected which eliminates impingement of raw oil on the chamber walls). The optimum burner geometry criteria, therefore, reduced to utilizing six peripheral air swirler vanes at an angle of 25 degrees relative to the blast tube axis, and a choke diameter given by $(2.7 \times gph)^{0.4}$.

OPTIMIZED FIXED GEOMETRY BURNERS

Fixed geometry burners, sized to burn nominally 1-gph and 9-gph of No. 2 fuel oil, were designed according to the optimum criteria obtained from the versatile geometry burner results. Combustion tests were conducted with the burners to verify the low pollutant operation.

1-gph Optimum Burner

The 1-gph optimum, fixed geometry burner was test fired in a refractory lined, coaxial combustion chamber. As expected from the versatile burner geometry optimization experiments, the optimum burner produced negligible smoke, unburned hydrocarbon and carbon monoxide emissions, and the nitric oxide emissions were only ∿1 gm NO/kg fuel burned, which may be compared with nominal levels of 1.5 to 2 gm NO/kg fuel from typical commerical burners fired into the same combustion chamber. Additionally, the optimum geometry burner was capable of operating at only 5 to 10 percent excess air without smoke, whereas typical commercial burners require up to 25 percent excess air to achieve smoke free operation.

Moreover, when the 1-gph optimum, fixed geometry burner was fired into an air-cooled combustion chamber, the nitric oxide emissions were reduced by 20 percent relative to similar emissions obtained in a hot-wall chamber.

When the 1-gph optimum, fixed geometry burner was fired into a refractory wall, perpendicular port combustion chamber, with the combustion chamber axis perpendicular to the axis of the burner blast tube, the nitric oxide emissions increased to a nominal 2 gm NO/kg fuel, compared with nitric oxide emissions of 2 to 3 gm/kg for typical commerical burners fired into the same chamber. The higher emissions in the perpendicular port combustion chamber apparently resulted from a high level of gas-phase mixing caused by the right-angle turn from the burner blast tube axis to the combustion chamber axis. As noted above, strong mixing in the combustion zone tends to induce high nitric oxide emissions.

The 1-gph optimum fixed geometry burner was subjected to simulated field tests, accumulating a total time of 128 hours while being cycled on and off to simulate field usew The tests were conducted in a Unitron A100 hydronic/warm air furnace having a coaxial, refractory-lined combustion chamber. During this testing, no adjustments were made on the burner. The 1-gph optimum burner performed over the entire test period with little variation and no noticeable degradation. The nominal stoichiometric ratio drifted upward slightly (about 2 percent, from 1.08 to 1.10 to 1.10 to 1.12), probably due to changes in ambient conditions associated with the outdoor test facility. None of the exhaust pollutant emission concentrations increased during the testing, with nitric oxide at about 0.95 gm NO/kg fuel burned, no measurable unburned gaseous hydrocarbons, and no smoke (Bacharach smoke scale = 0). Carbon monoxide decreased slightly (0.60 → 0.35 gm CO/kg fuel), probably due to the shift in stoichiometric ratio. Removal and inspection of the 1-gph optimum burner after completion of testing revealed no soot or sludge accumulation nor any evidence of deterioration of either the burner or the furnace.

9-gph Optimum Burner

The 9-gph, optimum, fixed geometry burner was test fired only in a coaxial, water-cooled combustion chamber. The inside diameter of the combustion chamber was 30 inches, nominally sized for 12 gph. The nitric oxide emissions from the 9-gph burner were very low, at a level of about 0.6 gm NO/kg fuel, compared to 1.2 gm NO/kg fuel for both the 6- and 12-gph commercial burners when fired into the same combustion chamber. The 9-gph optimum burner was found to be capable of operating smoke free at as low as 2-percent excess air, whereas the commercial burners required from 5- to 25-percent excess air to eliminate smoke.

Simulated field testing of the 9-gph optimum burner also was conducted, with a total of 112 hours being accumulated with this burner in the 30-inch-diameter, water-cooled, coaxial combustor. The performance of this larger optimum burner also showed little variation and no noticeable degradation. The stoichiometric ratio increased slightly from 1.02 to 1.03 to 1.03 to 1.04. A slight improvement was noted in the NO emission level, which decreased from about 0.5 to 0.6 gm NO/kg fuel to 0.45 to 0.50 gm NO/kg fuel burned. The CO emission level varied slightly, probably with changes in ambient conditions, but emissions as low as 0.6 to 0.7 gm CO/kg fuel burned were still being obtained at the end of the test series. The emission level of unburned hydrocarbons was zero and the Bacharach smoke number was zero. Inspection of the 9-gph optimum burner at the end of the test series revealed only a slight oily accumulation around the perimeter of the 5-inch-diameter burner head, and no evidence of deterioration of the burner head assembly.

The overall results from the optimum fixed geometry burner tests are considered very good. They show that the design criteria generated from the versatile geometry burner experiments do lead to low pollution burner designs. The optimum geometry burners are capable of operation at very low excess air levels while still producing emissions significantly lower than presently obtained with commercial burners. Low excess air levels lead to high furnace efficiency because of the resultant high flame temperatures that benefit heat transfer rates.

NONCONVENTIONAL BURNER CONCEPTS

In addition to the above-described studies of conventional, high-pressure atomizing, luminuous-flame burners designed for operation in refractory-lined combustion chambers, a portion of the program effort also was directed toward nonconventional burners. Several types of nonconventional burners were investigated, with the most notable results being obtained with an intense swirl burner and a forced combustion gas recirculation burner.

The intense swirl burner contained a mechanically rotated paddle wheel located at the end of the burner blast tube for swirling the inlet combustion air. The paddle was rotated by an electrical motor at rates as high as 3450 rpm. Combustion gas analyses from samples obtained in the combustion zones of commerically available burners had led to the conclusion that such an intense swirl burner would produce very high nitric oxide emissions at excess air levels near stoichiometric, but very low nitric oxide emissions at extremely high excess air levels (in excess of 80-percent excess air). The intense swirl burner behaved essentially as predicted from the commercial burner data. The nitric oxide emissions were very high at low excess air levels (about 3 gm NO/kg fuel burned at 25-percent excess air) and very low at high excess air (about 0.35 gm/kg fuel at 120-percent excess air). The smoke, unburned hydrocarbon, and carbon monoxide emissions were all minimal for these tests. The tests were conducted in a perpendicular port, refractory-lined combustion chamber, and the low nitric oxide emissions observed at high excess air levels were lower than those observed in commercial burners (operated in similar combustion chambers) by a factor of from 3:1 to 5:1. Operation at such high excess air levels requires a very large heat exchanger to maintain the furnace efficiency at a high level, because the low flame temperatures coincident with the high excess air levels reduce heat transfer efficiency. Operation at these high excess air levels is, therefore, unacceptable, and the intense swirl burner was regarded as a tool to investigate combustion phenomena rather than as a commercially viable burner.

The forced combustion-gas recirculation burner was designed for operation in either air-cooled or water-cooled combustion chambers. In this burner, a fan is used to draw combustion gases out of the combustion chamber from the zones near the wall where the gases are likely to have been cooled by convective heat transfer to the wall. These combustion gases are mixed with the burner primary air and reinjected into the chamber. Thus, this burner was designed to achieve the same benefits as those obtained with flue gas recirculation without requiring a duct from the flue to the burner.

Simulated field testing of the 9-gph optimum burner also was conducted, with a total of 112 hours being accumulated with this burner in the 30-inch-diameter, water-cooled, coaxial combustor. The performance of this larger optimum burner also showed little variation and no noticeable degradation. The stoichiometric ratio increased slightly from 1.02 to 1.03 to 1.03 to 1.04. A slight improvement was noted in the NO emission level, which decreased from about 0.5 to 0.6 gm NO/kg fuel to 0.45 to 0.50 gm NO/kg fuel burned. The CO emission level varied slightly, probably with changes in ambient conditions, but emissions as low as 0.6 to 0.7 gm CO/kg fuel burned were still being obtained at the end of the test series. The emission level of unburned hydrocarbons was zero and the Bacharach smoke number was zero. Inspection of the 9-gph optimum burner at the end of the test series revealed only a slight oily accumulation around the perimeter of the 5-inch-diameter burner head, and no evidence of deterioration of the burner head assembly.

The overall results from the optimum fixed geometry burner tests are considered very good. They show that the design criteria generated from the versatile geometry burner experiments do lead to low pollution burner designs. The optimum geometry burners are capable of operation at very low excess air levels while still producing emissions significantly lower than presently obtained with commercial burners. Low excess air levels lead to high furnace efficiency because of the resultant high flame temperatures that benefit heat transfer rates.

NONCONVENTIONAL BURNER CONCEPTS

In addition to the above-described studies of conventional, high-pressure atomizing, luminuous-flame burners designed for operation in refractory-lined combustion chambers, a portion of the program effort also was directed toward nonconventional burners. Several types of nonconventional burners were investigated, with the most notable results being obtained with an intense swirl burner and a forced combustion gas recirculation burner.

When this burner was tested, the nitric oxide emissions were found to be very low, about 0.3 to 0.4 gm NO/kg fuel, at nearly stoichiometric conditions, with no measurable smoke, and very low emissions of carbon monoxide and unburned hydrocarbon. In some cases, this burner was found to operate under fuel-rich conditions with no significant smoke. When this burner was tested in refractory wall combustion chambers, significantly increased nitric oxide emissions were obtained, as expected, becuase of the higher temperature of the recirculated combustion gases. Increasing the oil flowrate of this burner from 0.5 to 0.75 gph, in a cooled chamber, also resulted in increased nitric oxide emissions, apparently due to a limitation in the available amount of cooled combustion gases near the walls of the combustion chamber. The forced combustion gas recirculation burner, or some modification thereof, appears to be a good choice for the burner design when a nonrefractory-lined, cooled-wall combustion chamber is available.

CONCLUSIONS

The major conclusions from this study may be summarized as follows:

1. In refractory-lined combustion chambers, minimum nitric oxide emissions are obtained from nonflame-retention burners having peripheral swirlers at 25-degree angles (relative to the burner blast tube axis) and choke diameters corresponding to:

   $$\text{Dia. (inches)} = (2.7 \times \text{gph})^{0.4}.$$

2. Variations of oil nozzle position (0- to 1-inch recess), oil pressure drop (75 to 125 psi), and spray cone angle (45 to 90 degrees) affected smoke emissions but had no significant effects on other pollutants. Proper matching of the atomizer spray angle to the combustion chamber geometry is necessary to avoid smoke emissions.

3. Coaxial combustion chambers result in lower pollutant emissions than perpendicular port combustion chambers. This has been demonstrated for refractory lined combustion chambers.

4. Cool-wall combustion chambers result in lower nitric oxide emissions than refractory wall combustion chambers.
5. In cool-wall chambers some form of combustion gas recirculation is beneficial to the minimization of nitric oxide emissions, but in refractory wall combustion chambers, this recirculation is not as beneficial.

SUMMARY OF RECOMMENDED DESIGN PRACTICES

Design recommendations for minimizing exhaust emissions have been developed especially for high-pressure atomizing, gun-type oil burners firing into adiabatic (uncooled) wall combustion chambers, with emphasis being placed on remaining within the current conventional oil burner manufacturing practices. These optimized burner criteria are also applicable to cooled-wall combustion chambers, but under cooled-wall conditions, other methods (i.e., "blue flame" burners and combustion/flue gas recirculation burners) are available to reduce pollutant emissions further.

Combustion Chambers

The coaxial combustion chamber configuration was found to be more favorable for obtaining low pollutant emissions than the perpendicular burner port enclosures. Design of combustion chambers with the burner insertion port aligned along the axis of the chamber is recommended. A cooled chamber wall also is favorable in achieving lower nitric oxide emissions levels.

Air Swirl Devices

Omission of flame-retention devices (i.e., flame cones and flame-retention swirler rings) is recommended. However, some air swirl (rotational energy) is needed to promote mixing of the air and the oil spray. Simple peripheral swirl vanes (six vanes) that extend from the blast tube perimeter to within 0.3 inch of the oil nozzle assembly, and having a length/width ratio of about 1.5, are recommended. Vanes that project radially, that are spaced equally around the burner head, and are set at an angle of 25 degrees relative to the blast tube axis (Fig. 1) are recommended. Minor modifications to the existing spark electrode designs will probably be required to avoid interference with the large vanes. The configuration shown in Fig. 1 was typical of those tested during this study. Other slightly different configurations, designed for greater ease of fabrication or servicing, may be equally acceptable.

Choke Diameter

The choke diameter (exit area) has a significant effect on nitric oxide emissions. Minimum nitric oxide is obtained with a diameter given by the following relationship:

$$\text{Dia} = (2.7 \times \text{gph})^{0.4}$$

where

Dia = optimum choke diameter, inches

gph = oil flowrate, gal/hr

This correlation is shown graphically in Fig. 2, where the shaded area represents the suggested allowable deviation from the specified diameter.

Oil Nozzles

The high-pressure (100 to 300 psig), swirl-atomizing, simplex nozzles are entirely adequate oil atomizing devices. In larger oil burners, the use of higher oil supply pressure (300 psig) or multiple nozzle assemblies (which are frequently used in current commercial practice) tends to reduce smoke emissions because smaller oil dropsizes are formed. The additional pump power requirements of the higher oil supply pressure system suggest the multiple nozzle system is the more favorable of these two design recommendations.

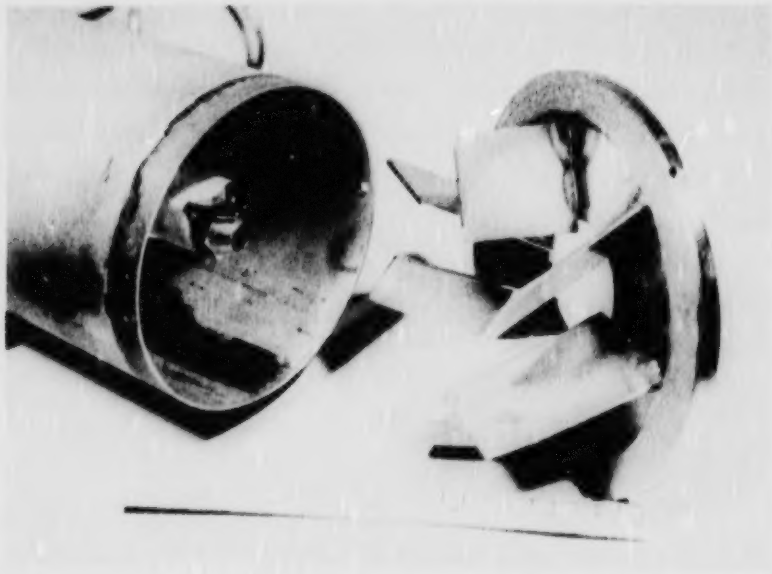

(a) Closeup of a 1-gph optimized oil burner head

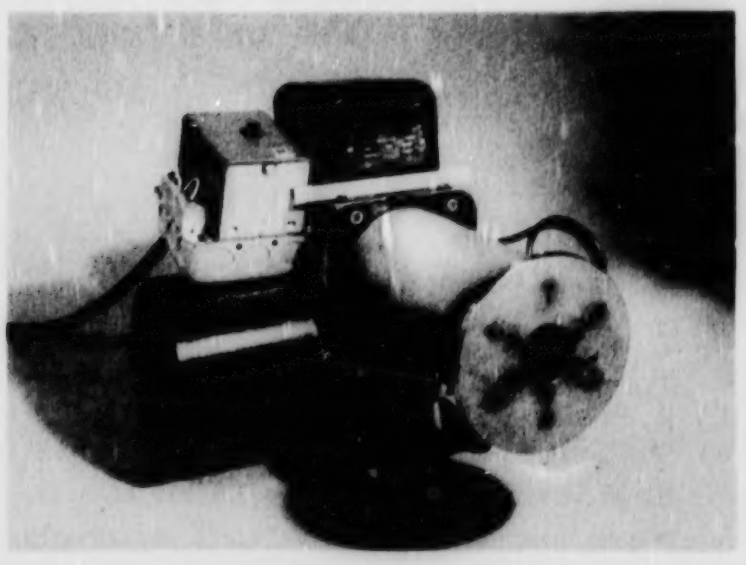

(b) Optimized burner head mounted on a typical oil burner body

Figure 1. Photographs of a 1-gph, low pollutant emission optimized oil burner head

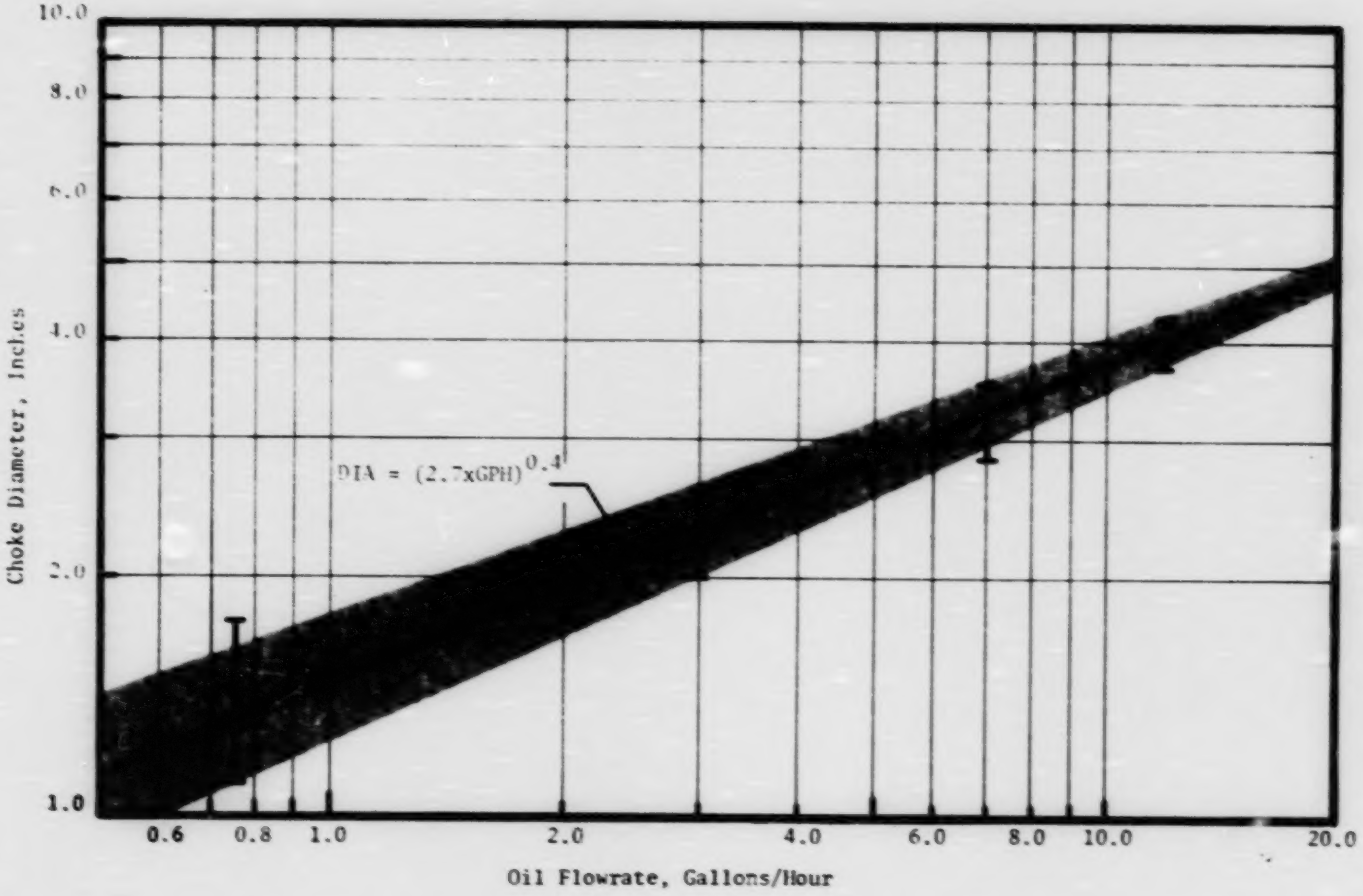

Figure 2. Choke diameter versus oil flowrate for minimum nitric oxide emissions, low smoke and carbon monoxide emissions (Applicable to burners incorporating a six-vane, 25-degree air swirler)

Electrical Spark Igniter

The operation of the 10,000- to 12,000-volt electrical spark igniter has shown some significant effects on nitric oxide emission levels from non-flame-retention-type burners. Avoidance of continuous operation of the spark igniter throughout the burner firing time is recommended, although continuous spark may be necessary to ensure nonoscillatory combustion. Burner designs that incorporate spark operation only during burner start-up are recommended. Considering the power consumption of a typical spark igniter of 250 watts (∿1000 Btu/hr), this recommendation should reduce the power requirement significantly.

INTRODUCTION

The combustion of fossil fuels currently generates approximately three-fourths of all air pollution. As shown in Table 1, the major contributors to overall air pollution are: 50 percent from transportation (cars, trucks, and airplanes), 20 percent from stationary fuel combustion (electrical power generation and space heating), and 13 percent from industrial processes. Stationary fuel combustion contributes 28 percent of the particulates and 39 percent of the nitric oxide emissions.

Of particular interest to this program is the air pollution caused by distillate oil burners for commercial or residential space heating. During the peak heating season, such oil burners contribute heavily to the particulate and nitric oxide pollution in urban areas. They also contribute unburned hydrocarbons and carbon monoxide to a less significant extent.

In large measure the control and/or elimination of such emissions is directly related to the care and maintenance of oil burning equipment. Hydrocarbons and particulate matter, for example, can be virtually eliminated by proper adjustment of fuel oil burners and careful maintenance to avoid degradation. Burner combustion efficiency and emissions of oxides of nitrogen are interrelated parameters which can be varied by burner design and operating characteristics. Emissions of oxides of sulfur are largely determined by the fuel and can be restricted through the use of low sulfur fuel.

Table 1. CONTRIBUTORS TO AIR POLLUTION IN THE UNITED STATES

Type of Pollutant	Transportation	Stationary Fuel Combustion	Industrial Processes	Solid Waste Disposal	Miscellaneous*
	Quantity, millions of tons per year				
Carbon Monoxide	71.2	1.9	7.8	4.5	8.6
Sulfur Oxides	0.4	22.1	7.2	0.1	0.6
Hydrocarbons	13.8	0.7	3.5	1.4	6.5
Particulates	1.2	6.0	5.9	1.2	7.2
Nitrogen Oxides	8.0	6.7	0.2	0.7	1.4
Total	94.6	37.4	24.6	7.9	24.3
Percent of Total	50	20	13	4	13

Source: National Air Pollution Control Administration
*Forest fires, etc.

The primary pollutants emitted into the atmosphere by oil burners are: oxides of nitrogen, smoke, carbon monoxide, and gaseous hydrocarbons. All except nitrogen oxides can be minimized by operating at sufficiently high air-to-fuel ratios. Unfortunately, operation at high air-to-fuel ratios generally leads to lowered performance, and frequently to higher nitric oxide emissions.

The broad purposes of the program described in this report were to determine the effects of burner design parameters on pollutant emissions for stationary energy conversion devices that use No. 2 fuel oil, and to define designs which allow pollutants to be minimized while maintaining high efficiency. The effort has been directed primarily toward reduction of pollutant emissions from high-pressure atomizing, 1- to 12-gph No. 2 distillate oil burners fired in refractory combustion chambers.

The typical oil burner of this type, Fig. 3, has spark ignition, achieves oil atomization by pumping the oil at high pressure (100 to

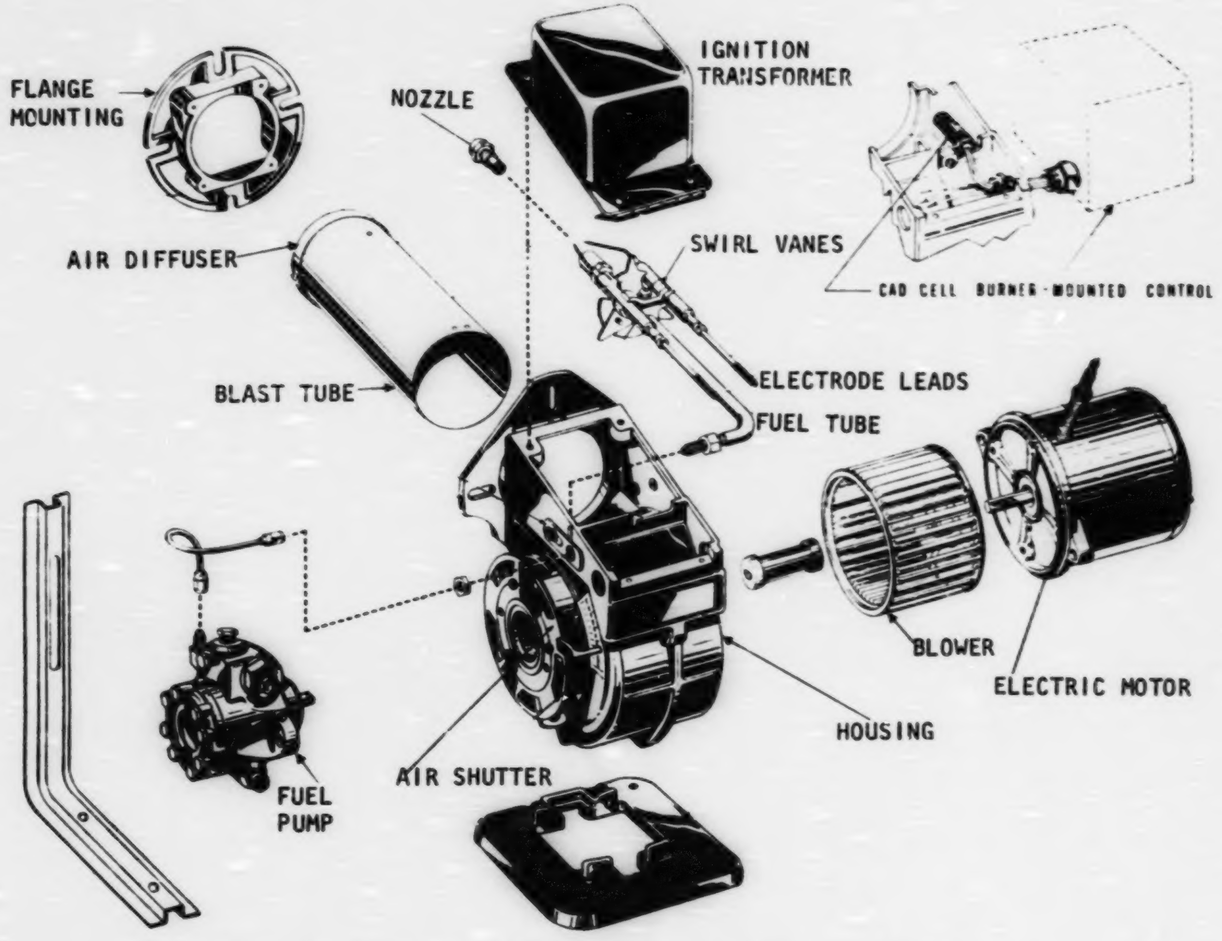
FLANGE MOUNTING
NOZZLE
IGNITION TRANSFORMER
CAD CELL
BURNER-MOUNTED CONTROL
SWIRL VANES
AIR DIFFUSER
BLAST TUBE
ELECTRODE LEADS
FUEL TUBE
BLOWER
ELECTRIC MOTOR
HOUSING
AIR SHUTTER
FUEL PUMP

Figure 3. Typical high-pressure, oil-fired gun burner

300 psig) through a conical spray simplex nozzle, Fig. 4, and supplies air for the combustion process through an electrically driven blower. The oil nozzle and spark ignition electrodes are located in the end of a cylindrical tube (blast tube) through which the combustion air flows into the combustion chamber. The design of the air diffuser located at the blast tube end (Fig. 5) strongly affects the air flow pattern and, hence, the combustion process. Many different blast tube end designs are available, ranging from a sinple choke ring (an orifice plate affixed to the end of the blast tube to restrict the air flow) to elaborate swirl vane and flame-retention assemblies intended to enhance mixing and to provide regions of low-velocity air/fuel-spray mixture to allow flame attachment. The levels of pollutant emissions from such commercially available burners vary significantly, depending on the design selected. Several oil burner manufacturers were contacted to determine present state-of-the-art burner design practices. The information obtained from these contacts is summarized in Appendix A.

This study has been directed toward defining burner modifications that would minimize emissions and maximize efficiency of the high-pressure gun burner, and be economically feasible to manufacture, install, and operate. The economics are important because there are almost 12 million oil burners in operation in the United States today, of which well over 90 percent are the high-pressure gun burner type. An example of a desirable device for pollution control would be one that could be simply and economically installed at the time of fuel nozzle replacement. This would result in rapid improvement of the existing oil burner installations because high-pressure fuel nozzles are normally replaced every 2 to 3 years. In contrast, a device requiring major burner modification or replacement of significant portions of the burner assembly and its auxiliary components would be less desirable.

Burner design and operation are significantly affected by the type of combustion chamber in which the burner is operated. The largest number of oil

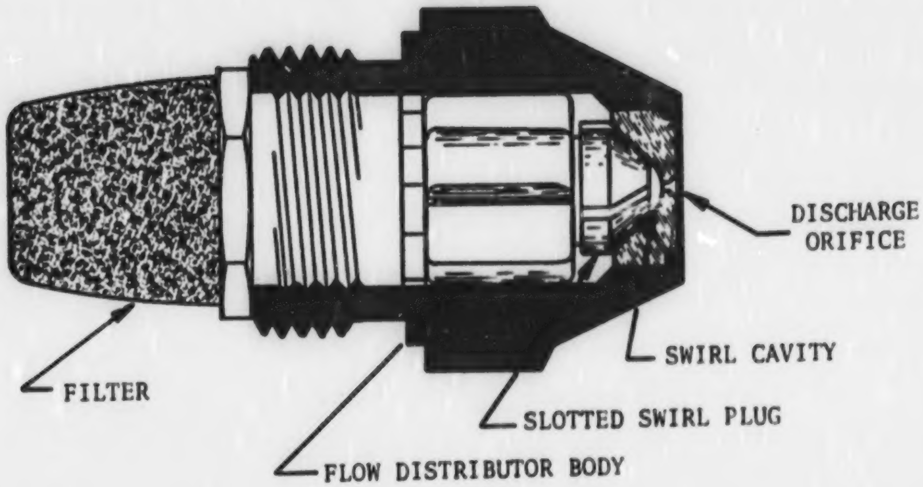
DISCHARGE ORIFICE
SWIRL CAVITY
FILTER
SLOTTED SWIRL PLUG
FLOW DISTRIBUTOR BODY

Figure 4. Simplex oil spray nozzle

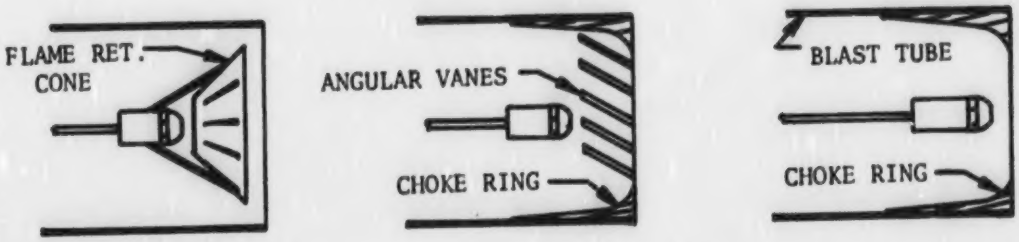
FLAME RET. CONE
ANGULAR VANES
CHOKE RING
BLAST TUBE
CHOKE RING

Figure 5. Three typical air diffuser designs used in the ends of oil burner blast tubes

burners are used in furnace installations. Most modern oil furnaces are warm air delivery systems; however, a large percentage of the heating installations in the northeast are hydronic (warm water) systems. The combustion chambers in the furnaces vary widely in configuration and characteristics; for example, many of the older warm air furnaces have a heavy refractory lining and the chambers are large. The most recent warm air combustion chambers contain a lightweight, cast refractory lining and are smaller. Many hydronic systems have one or more cold walls exposed to the combustion system. The predominant number of residential furnace combustion chambers are refractory or refractory lined and, therefore, this study has been centered primarily on improvement of burners operated in refractory combustion chambers.

A wide variation in fuel flowrates is used in existing installations. Almost all of the residential heating installations are operated in a range from 0.5 to 1.2 gal/hr, with 80 percent in the 0.6 to 0.9 gal/hr range. Commercial installations, however, are operated predominantly in the 1 to 3 gal/hr range, with some higher flowrates also used. Some oil-fired, hot-water heaters operate with flowrates as low as 0.5 gal/hr. Consequently, an air pollution-improving device should be effective over this wide flowrate range. The major portion of effort in this study has concerned the nominal flowrate of 1 gph, with a significant but lesser effort concerned with oil flowrates up to 12 gph.

All oil burners must meet stringent safety standards to be acceptable for installation in the United States. Safety standards are set by the Underwriters Laboratory (UL) and conformance is evaluated by tests. The basic UL specification applying to the high-pressure oil burner design is UL Specification 296, "Standard for Domestic Oil Burners." Some of the UL requirements related to the burner head are as follows: (1) ability to remove the ignition electrodes and fuel nozzle assembly without removal of the entire burner, (2) high-tension wiring must be installed with a minimum separation from other components, (3) materials having sufficient temperature capability must be used within the combustor head, and

(4) specific provision must be made for oil dripping from the fuel nozzle and for handling oil that may accumulate on the electrodes. Any burner design modifications must be compatible with these requirements.

The role of the serviceman is paramount in the oil equipment business. Installation, maintenance, and service training requirements for new equipment must be minimal to provide an acceptable product. Excessive complexity of any device could prevent its use.

Because all oil burners deteriorate with time, a desirable characteristic of a pollution control device would be insensitivity to degradation. A survey conducted by Rocketdyne prior to start of the present study indicated that the typical oil furnace installation set for less than No. 1 Bacharach smoke at the initiation of a heating season usually operates at greater than No. 4 smoke by the end of the heating season. This indicates the need for more frequent service, at least once per year compared to the typical once every 2 or 3 years.

In view of the safety, cost, serviceability, furnace compatibility, and degradation factors, and the basic program objective of producing low pollutant emissions in conjunction with high efficiency, the following approach was selected for this program: (1) study the mixing, atomization, and flow characteristics of several commercially available burners; (2) determine the pollutant formation and emission characteristics of these burners; (3) relate the mixing, atomization, and flow characteristics to the pollutant formation and emission; and (4) determine optimum burner design criteria that would lead to the atomization, mixing, and flow characteristics yielding the best compromise between low pollutant emissions and high efficiency.

APPARATUS AND DATA REDUCTION

This section describes the apparatus used to characterize burner processes experimentally, and, where appropriate, includes the methods used to reduce the experimental data to reported form. The apparatus described includes those items other than the commercially available burners. These burners are described later, together with data obtained from each.

ATOMIZATION TEST FACILITY

A wax flow technique was used to determine the dropsize distribution produced by the oil spray nozzles. The facility used for those tests is shown in Fig. 6. The system consists of two molten-wax tanks, one hot-water tank, pneumatic control valves, and a thermostatically controlled oil bath vessel in which the wax and water tanks are immersed. Associated flow and collection equipment includes Taber injection pressure transducers, turbine flowmeters, a particle collector surface, and a particle catch basin into which the particles are washed from the particle collector. This facility is used extensively at Rocketdyne for characterization of rocket engine injectors. The hot-water flow system is used to simulate bipropellant rocket flows, but was not required for the oil burner atomizer flows.

The hot-oil bath is heated by a 30-kilowatt, thermostatically controlled heater. An electrically operated pump circulates the oil from the oil bath container through the heater and back again to ensure uniform temperature. In addition, hot oil is forced through jacketed run lines and

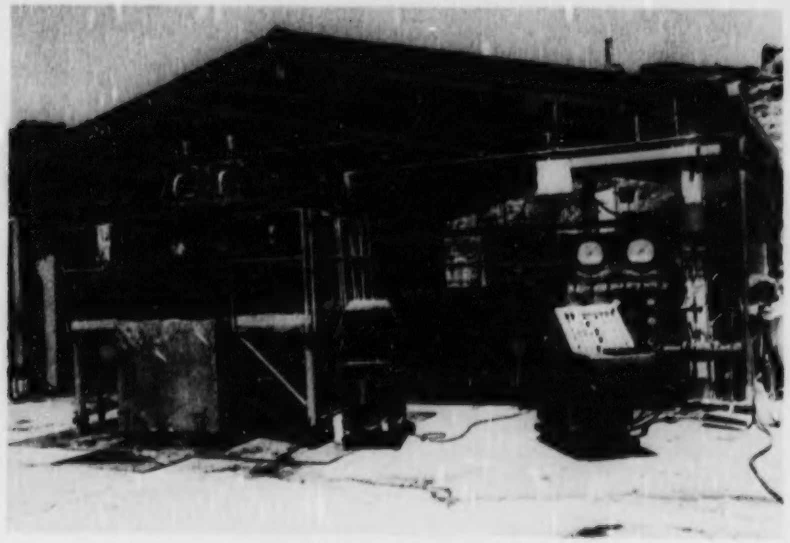

5AD21-6/13/69-S1B

(a) Wax flow system

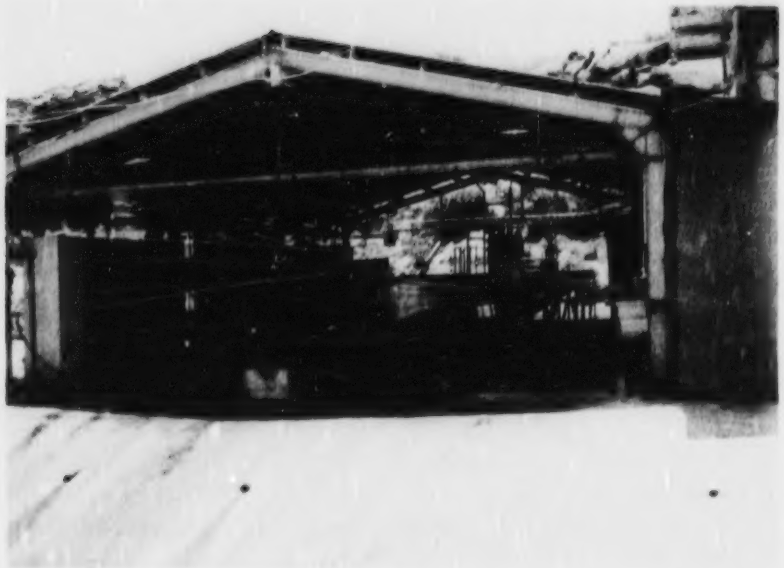

5AD21-6/13/69-S1C

(b) Particle collector platform

Figure 6. Wax flow facility

valves to ensure that the wax does not freeze or cool prior to spraying. The wax flow system has three parallel line sections each containing a flowmeter, a thermocouple, and a hand shutoff (flow control) valve. A wide range of flowrates can be obtained by opening one of the three hand shutoff valves leading to the appropriate flowmeter spanning the desired flowrate range.

Between the atomizer and the frozen droplet collector surface, a deflector tube is used that ducts the wax spray away from the collector until steady-state wax flow conditions are established. Through use of a high-speed pneumatic actuator, the tube is removed for the duration of the run and is replaced prior to flow cutoff, thus eliminating wax-particle collection during flow start and cutoff transients. The particle collector is an 18- by 50-foot, epoxy-coated, wooden platform that slopes gradually toward the center of the platform and away from the atomizer. The entire platform is located under a semi-enclosed structure that shields the collection area from wind currents that might cause the smaller particles to be blown away. The slope of the platform causes the wax droplets to be directed into a relatively small-particle catch basin when the impact surface is washed down with water. The catch basin has several baffles to ensure that none of the wax particles are washed overboard.

For the present study, wax flow tests were made with the oil burner atomizer nozzles mounted in the end of a hot-oil-jacketed wax flow line, with no attempt being made to simulate the air flow patterns produced by typical oil burners. This was believed valid because the nature of the conical spray nozzles being used causes most of the atomization to take place very close to the nozzle exit where the liquid films are shielded from air flow by the body of the atomizer.

The wax utilized for the spray dropsize experiments was Shell Type 270 wax (Petrochemicals Division, Shell Chemical Company). This wax has a melting point of 140 F, and was sprayed at a temperature of approximately 200 F. The Type 270 wax was chosen because of its high block point temperature of 120 F, which implies that the wax particles are not sticky at temperatures below 120 F. The nonsticky quality of the wax particles is very important for particle size determination. The high block point wax allows the collected wax particles to be sieved much like dry sand, whereas lower block point waxes yield particles which tend to congeal into sticky masses which are very difficult to sieve. At the 200 F spraying temperature, the Type 270 wax has a viscosity of 0.0027 lbm/ft-sec, a density of 48 lbm/ft^3, and a surface tension of 17 dynes/cm. The viscosity and density of Type 270 wax are reasonably comparable with the viscosity and density (0.0026 lbm/ft-sec and 56 lb/ft^3) of No. 2 fuel oil.

For the nozzles tested, the mass median droplet diameters, $\overline{D}$, of the collected frozen wax particles were in the 60- to 100-micron (25.4 microns = 0.001 inch) range. The mass median droplet diameter is defined as the diameter for which one-half of the spray mass has larger diameters and the remaining half has smaller diameters. For the 60- to 100-micron range, the size distribution of the collected particles was most conveniently determined by the Sharples Micromerograph, a commercially available sedimentation-in-air device. Particles from one test run were also sized by sifting through a series of standard testing sieves. For the test on which both sizing techniques were utilized, size distribution data obtained by means of the Micromerograph were found to yield a mass median droplet diameter approximately 10 percent larger than was obtained from the parallel analysis using the sieving technique. This discrepancy is probably due to the loss of small particles to the wall of the Micromerograph, but its magnitude is small.

AIR FLOW PATTERNS

Air flow patterns were determined by measuring both the direction and magnitude of air velocity at many points throughout the flowfield created by the oil burners.

Air flow patterns were determined near the blast tube exits of several burners, with the flow constrained within short, cylindrical sheet metal chambers mounted coaxially with the burner blast tubes. For the nominal 1-gph burners, an 8-inch-diameter coaxial cylindrical chamber was used while, for the 6- and 12-gph burners, an 11-inch-diameter coaxial cylindrical chamber was used. The coaxial chamber extended approximately 9 inches beyond the end of the burner blast tube, and air velocity vector profiles were determined at several planes perpendicular to the blast tube axes, at distances up to 9 inches downstream from the blast tube exit.

Two different gas velocity-vector direction-indicator probes were built for initial checkout. These two probes are shown schematically in Fig. 7. They were designed to make use of the fact that the pressure indicated by an impact tube varies most rapidly with angular orientation when the tube inlet is inclined at 45 degrees to the flow. Flow direction in one plane was determined by changing the probe angle until the indicated pressures from opposed impact tubes with inlets inclined at 90 degrees to one another were equal. Flow direction in the other plane was obtained by similarly balancing the second pair of impact tubes of the quadruple tube probes. For this purpose, the probe was mounted on a gimbaling apparatus, as shown in Fig. 8 which allowed changes in probe angle without changing the location of the probe tip. The probe was mounted so that one of the adjustable angles corresponded to movement in the plane of one pair of probe tubes, and the remaining adjustable angle corresponded to the plane of the other pair of tubes. The two gas velocity-vector direction-indicator probes shown in Fig. 7 differ primarily in the manner by which the tube inlets are inclined to the axis of the probes. In the compact probe (Fig. 7a), the inclined inlets result from cutting each of the tubes in the four-tube bundle at 45 degrees to the bundle axis while, with the standard probe, the inlet inclination was obtained by bending the tubes as shown in Fig. 7b. It was expected that the standard probe (Fig. 7b) would give more precise information concerning the flow angle than the compact probe; however, the experimental results indicated no significant differences between the two probe types. Therefore, the compact probe

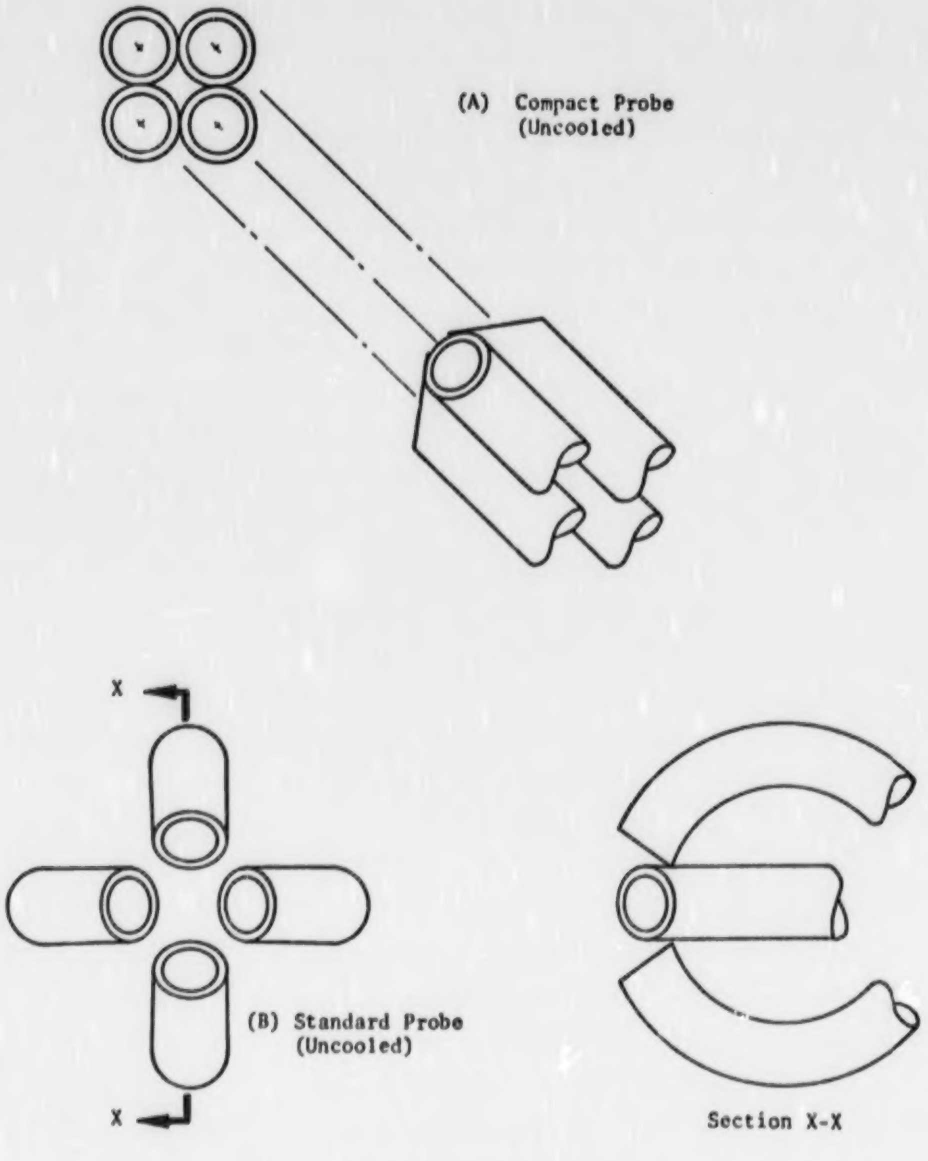
(A) Compact Probe
(Uncooled)
X
(B) Standard Probe
(Uncooled)
X
Section X-X

Figure 7. Velocity direction indicator probes

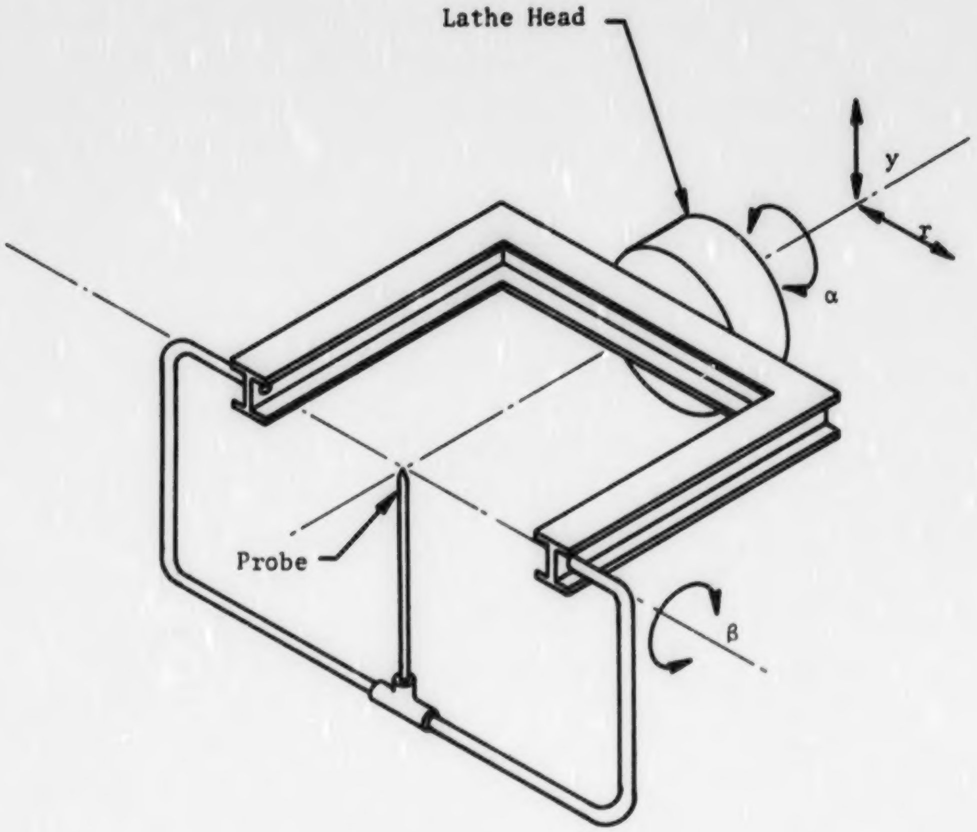
Lathe Head
y
r
α
Probe
β

Figure 8. Schematic of directional probe gimbaling apparatus used to alter probe angle while keeping the probe tip stationary

probe design, which offers less interference with the flow and the combustion chamber walls, was used for determination of gas velocity vector directions. The probe was calibrated in gas flows of known direction. Once calibrated, the probes gave direction indications which were reproducible to within ±2 degrees, with oil burner air flows of about 10 ft/sec. The primary factor limiting reproducibility appeared to be nonsteadiness of the flows produced by the oil burner.

The probes shown in Fig. 7 indicate only the vector direction of the gas flow. Another probe was used to determine the magnitude of the air velocity, a commercially available 1/16-inch-OD pitot probe. After determining the flow vector directions, the multiple-port impact probe was replaced on the gimbaling apparatus by the pitot probe. The pitot probe was aligned with the previously determined air velocity vector directions before making a measurement of the velocity head. For both the multiport vector direction probe and the pitot probe, the required pressures were measured with an MKS Baratron electronic pressure meter. A 30-millimeter pressure sensor was used in conjunction with the Baratron which allowed measurement of impact pressures as low as 0.001 mm Hg.

The apparatus used for these experiments is shown in Fig. 9. The gimbaling device was fabricated from a rotatable lathe, used for one of the gimbal directions, and a tube and aluminum I-beam structure for the other gimbal direction. In addition to the effective gimbaling action available from rotation of the lathe table, the lathe table allowed translational movement in two directions. Also shown in Fig. 9 is the 55-J burner and the Baratron electronic pressure meter.

With the gimbaling apparatus shown in Fig. 8, it was possible to define the flow vector at any point of interest in terms of two angles and an impact velocity head. The angle of rotation provided by the rotatable

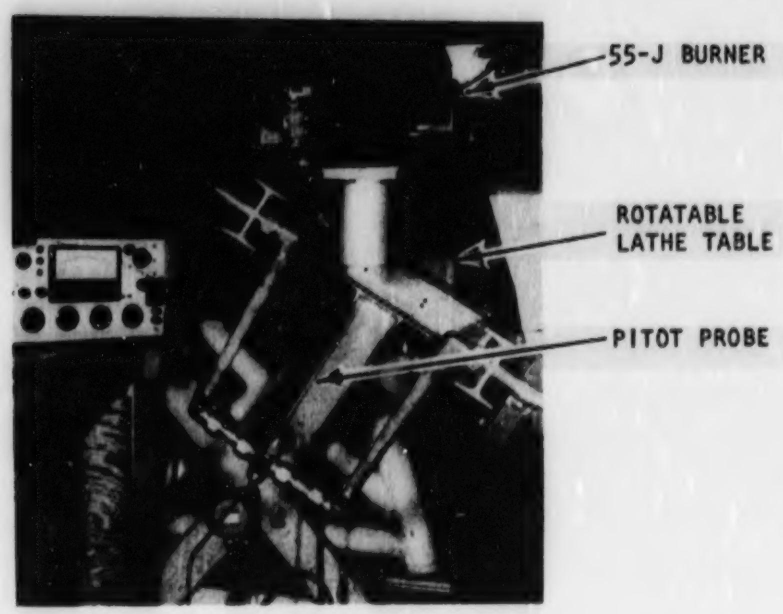
55-J BURNER
ROTATABLE LATHE TABLE
PITOT PROBE

(a) Set for a compound angle

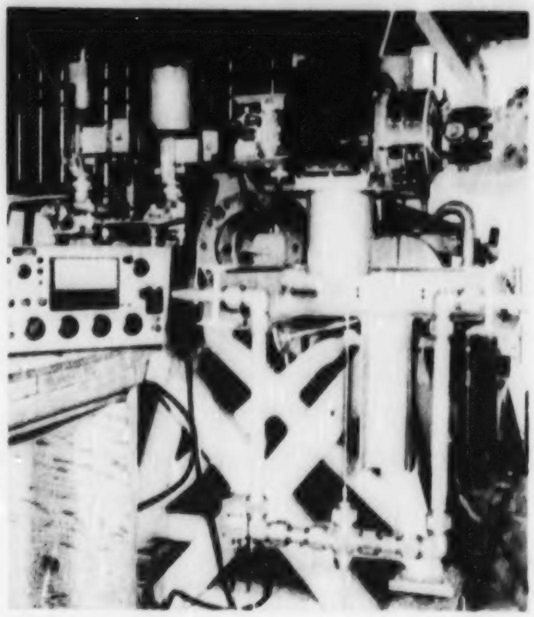

(b) Set for straight axial flow

Figure 9. Probe gimbaling apparatus

lathe head was termed α, and the angle of rotation provided by the tube and I-beam structure was termed β. With these parameter definitions, the components of velocity are obtained from the following equations:

$$\begin{aligned} V_T &= V \sin\beta \\ V_R &= V \cos\beta \sin\alpha, \quad V = \left(\frac{2\, g_c\, \Delta P}{\rho}\right)^{1/2} \\ V_A &= V \cos\beta \cos\alpha \end{aligned} \qquad (1)$$

where

V = velocity scalar magnitude, ft/sec

V_T = tangential velocity component, ft/sec

V_R = radial velocity component, ft/sec

V_A = axial velocity component, ft/sec

α = velocity angle, measured in degrees of rotation about an axis perpendicular to both the burner tube axis and the radial ray being traversed

β = velocity angle, measured in degrees of rotation about an axis inclined at an angle α to the radial ray being traversed, and located in the plane established by the burner tube axis and the radial ray being traversed

g_c = gravitational constant, ft-lbm/lbf-sec^2

ΔP = impact head, lbf/ft^2

ρ = gas (air) density, lbm/ft^3

To interpret the data giving the β angle as a function of location, it is helpful to realize that a curve of β versus radius consisting of a straight line passing through the burner axis ($r = 0$), such as shown in Fig. 10, corresponds to a flowfield rotating at a uniform rpm about the axis, while the dashed curve corresponds to a flowfield rotating at a higher rpm on the outer radii, and the dotted curve corresponds to a flowfield rotating at a

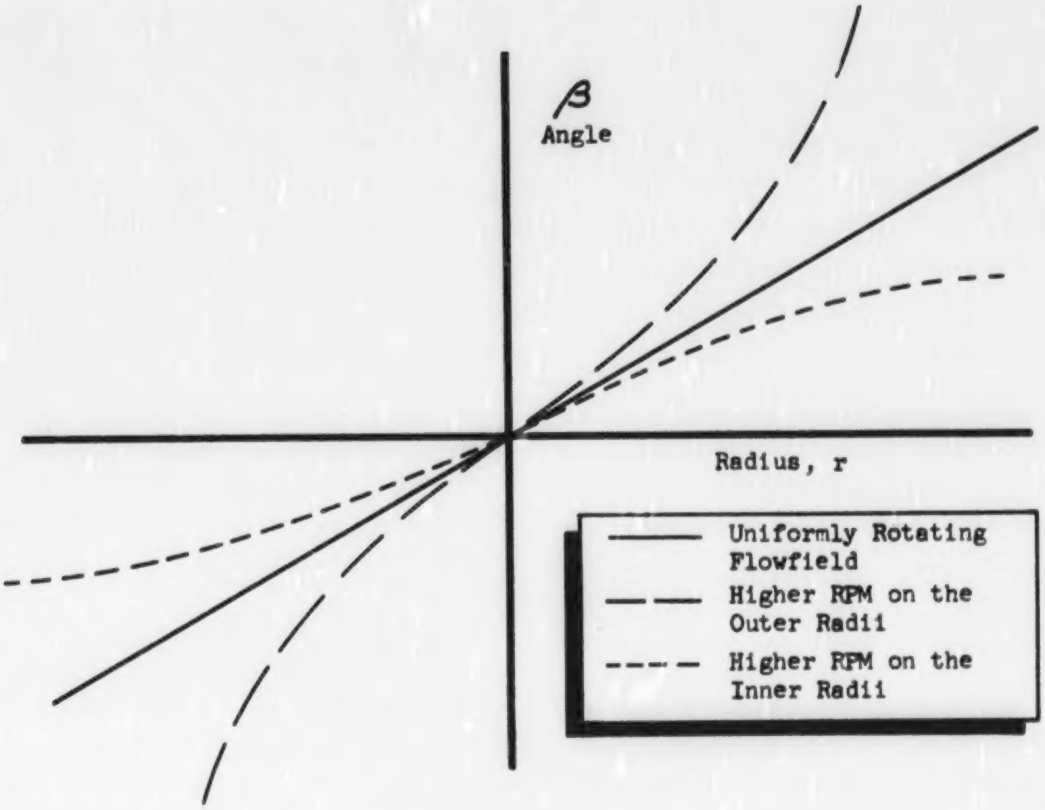
β
Angle
Radius, r
Uniformly Rotating Flowfield
Higher RPM on the Outer Radii
Higher RPM on the Inner Radii

Figure 10. Interpretation of β angle curves

higher rpm at the inner radii. Strictly speaking, these generalizations require flowfield symmetry which is not obtained with most burners tested, but the trends are applicable.

Prior to the start of testing for any particular burner, the velocity vector direction probe was calibrated by flowing gaseous nitrogen through a 3/8-inch-diameter tube and impinging on the probe. Generally, the 3/8-inch-diameter calibration tube was aligned parallel with the axis of the burner blast tube. When the gimbal was used to orient the direction of the multiport impact tube to obtain null pressure readings for both planes, the α and β angle scales were then adjusted to each read zero degrees, indicating precisely axial flow. The traversing capabilities of the lathe table were used to accurately move the probe tip from point to point in the flowfield. The lathe table allowed translation of the probe tip in a plane corresponding to a major diameter of the blast tube axis, and in the axial direction corresponding to various distances downstream of the blast tube exit. For these movements, the axis of rotation of the α angle was maintained in the same plane. To make measurements in two perpendicular planes required mounting the burner twice. In general, measurements were made in two planes which were termed the horizontal and the vertical planes, as shown schematically in Fig. 11.

OIL SPRAY PATTERNS

Under cold-flow conditions, oil spray mass fluxes were determined as a function of location in the gas flowfield. To obtain meaningful oil spray mass flux data, it is necessary to use an oil spray collector that is aligned with the local air flow velocity vector. It is also necessary to sample isokinetically, so that air velocity entering the sample tube is equal to the local air velocity. If air is entering the sample tube at less than local air velocity, a high-pressure (partial stagnation) zone is created near the tip of the sample tube, deflecting droplets away from the sample tube inlet. On the other hand, if air is pulled into the tube at a higher than local velocity, a low-pressure zone is created near the sample tube inlet, and more than the desired oil sample rate is obtained.

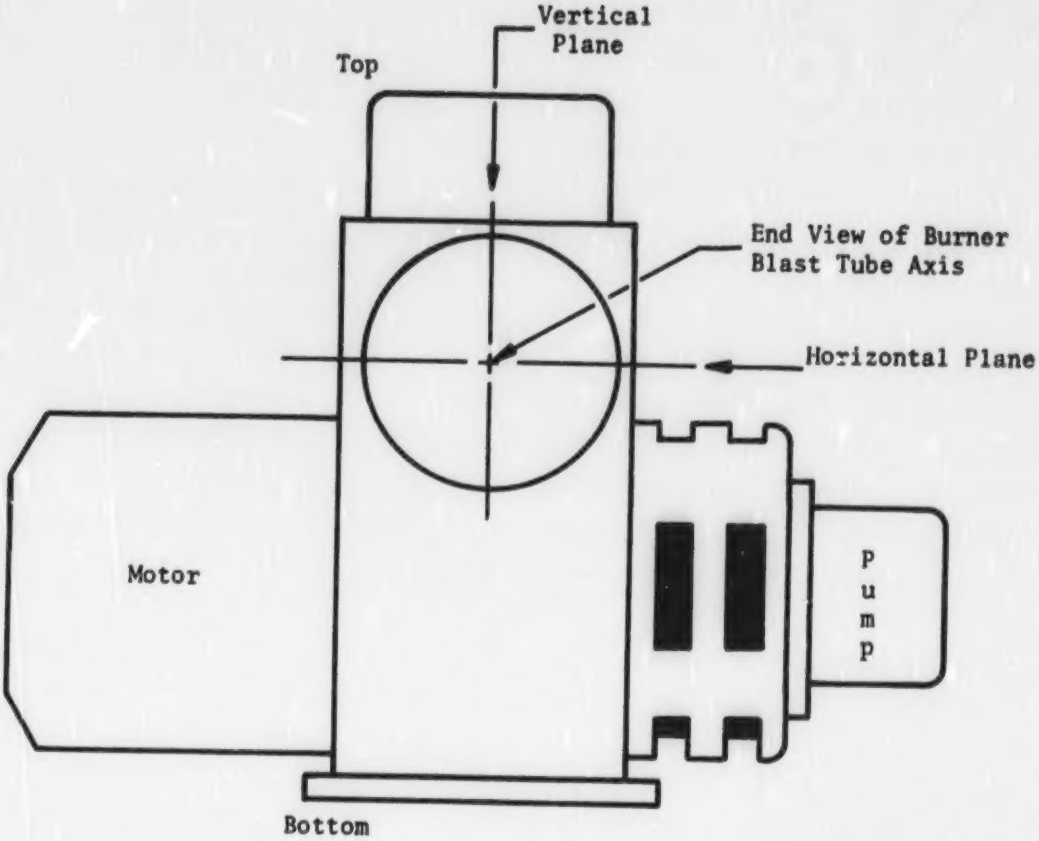
Vertical Plane
Top
End View of Burner Blast Tube Axis
Horizontal Plane
Motor
Pump
Bottom

Figure 11. Location of horizontal and vertical planes for determination of gas velocity vectors

Apparatus used for determination of oil spray mass flux under isokinetic sampling conditions is shown in Fig. 12. A sampler tube is mounted on the gimbaling apparatus, and is aligned with the previously measured local vector direction of the air flow. Gas is sucked into the tube at a rate giving a gas entry velocity corresponding to the previously measured local gas velocity. The air is sucked by means of an aspirator. The rate of air movement into the probe is indicated by an in-line rotameter, and controlled by a small valve. Oil that enters the sampler tube along with the air constitutes the desired sample, and it is separated out by a miniature cyclone separator located in the sample line upstream of the air rotameter. The small cyclone separator was very efficient at removing oil spray from the airstream, as indicated by cleanliness of the gas exiting from the cyclone. The oil collected by the cyclone separator flowed into a 2-cc pipette, plugged at one end so that the oil collected therein. The oil-sampling rate was determined by timing the rate of oil accumulation in the pipette after a quasi-steady-state condition was established.

The effects of nonisokinetic sampling on liquid collection rate were investigated. The results for one particular location in the flowfield of a 55-J burner are shown in Fig. 13. At the location in question, the local free stream air velocity was 14 ft/sec, and oil sampling was performed at velocities from 6 to 30 ft/sec. The data shown in Fig. 13 indicate that sampling at a velocity which is too low (i.e., lower than local air velocity) results in larger magnitude liquid collection rate errors than sampling at velocities which are too high. For example, sampling at a velocity of 6 ft/sec too high results in a liquid collection rate 4 percent too high, while sampling at a velocity 6 ft/sec too low results in a liquid collection rate 21 percent too low. The experiments relating to Fig. 13 utilized an 0.75-gph oil burner nozzle which produces droplets having a mass median droplet diameter of about 75 microns. Most oil burners produce approximately this same size or larger droplets. Since nonisokinetic sampling errors tend to be most significant for small droplets, the errors represented by Fig. 13 can be interpreted as about the most severe that normally would be encountered because of nonisokinetic effects.

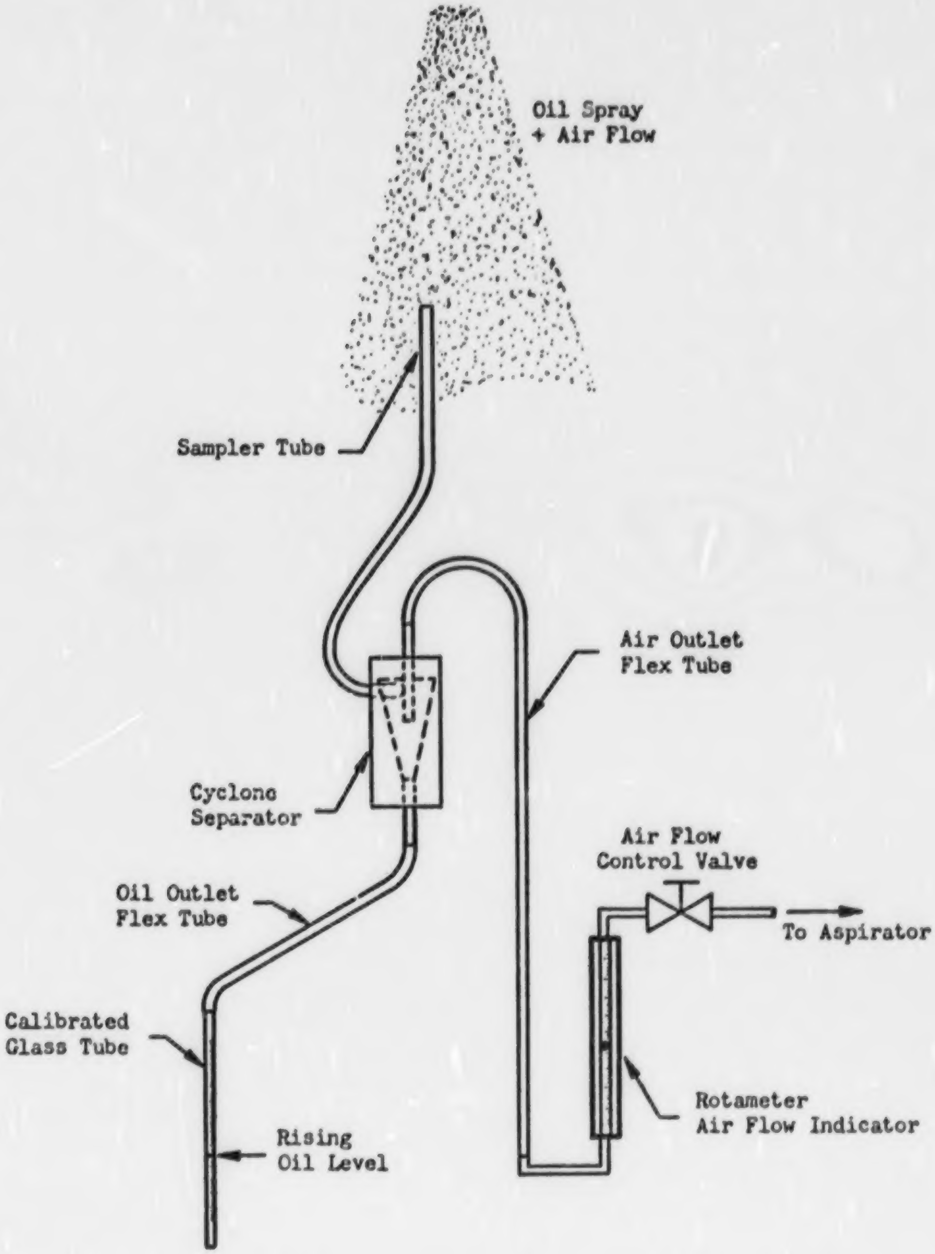
Oil Spray
+ Air Flow
Sampler Tube
Air Outlet
Flex Tube
Cyclone
Separator
Air Flow
Control Valve
To Aspirator
Oil Outlet
Flex Tube
Calibrated
Glass Tube
Rotameter
Air Flow Indicator
Rising
Oil Level

Figure 12. Liquid spray mass flux sampling apparatus

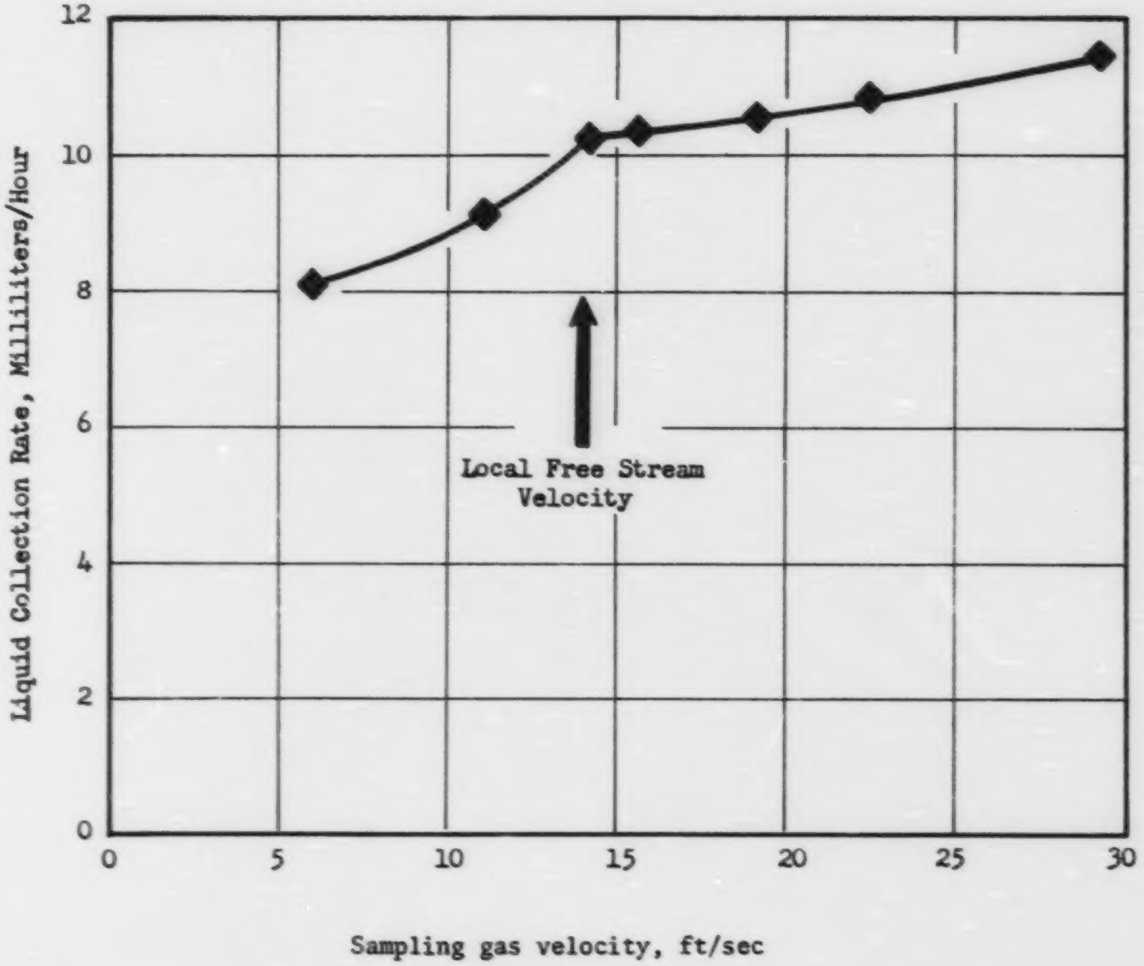

Figure 13. Effects of sampling velocity on oil collection rate

Oil mist and vapors that arise from cold-flowing burners (without ignition, for oil spray collection) were found to be irritating to personnel. To minimize exposure of personnel, a plastic curtain was hung around the oil burner under test, and air flow from behind the curtain was ducted through a blower and directed 30 feet up the adjacent hillside. The apparatus is shown schematically in Fig. 14. Air exhausting from the end of the duct appeared to be free of fuel mist, and irritation of operating personnel was eliminated. The oil sampler and the cyclone separator were mounted on the gimbal apparatus inside the curtain.

COMBUSTION GAS FLOW PATTERNS

Burner geometry effects were characterized by air flow pattern determination in the absence of oil spray and combustion. To characterize the effects of combustion on the flow patterns, the same experiments were repeated, except that they were conducted with combustion. The apparatus used for these experiments was fundamentally the same as used for the experiments involving air flow only, except that several modifications were required to make the system compatible with oil spray and combustion.

One important modification required for measurements under hot-fire conditions was the use of cooled probes. Shown schematically in Fig. 15 are the water-cooled versions of the multiport impact probe for velocity direction determinations, and a separate water-cooled pitot probe for velocity magnitude determination.

The burners were fired using the same coaxial, cylindrical sheet-metal combustion chambers previously described. However, for the hot-fire experiments, the burners were fired vertically upward rather than downward. The upward orientation, as shown in Fig. 16, had two advantages: (1) hot combustion gases were allowed to rise without contacting the burner hardware and (2) oil drainage out of the probes was promoted. The latter is desirable since it is important to keep oil from entering the Baratron

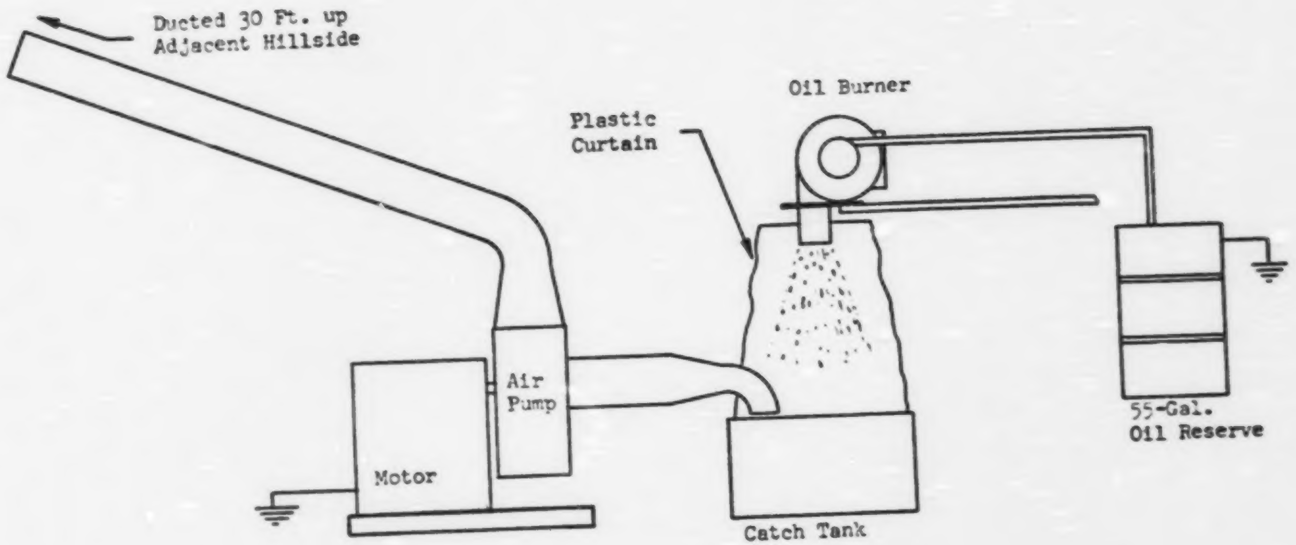
Ducted 30 Ft. up
Adjacent Hillside
Oil Burner
Plastic
Curtain
Air
Pump
Motor
Catch Tank
55-Gal.
Oil Reserve

Figure 14. Oil burner cold-flow facility schematic

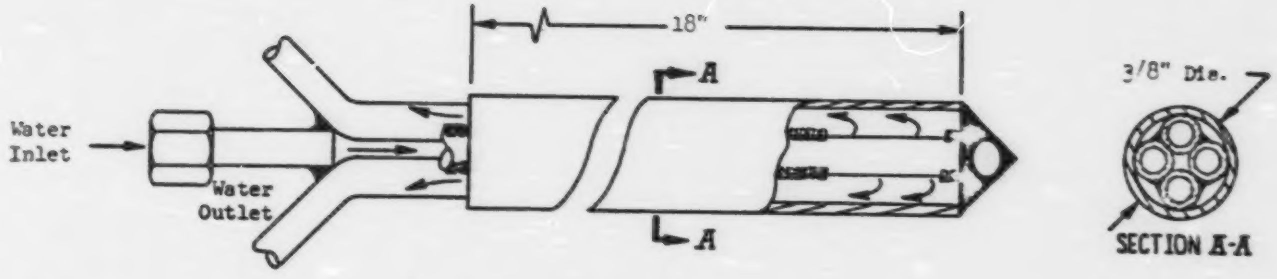
18"
A
A
Water
Inlet
Water
Outlet
3/8" Dia.
SECTION A-A

Water-cooled four-tube directional probe

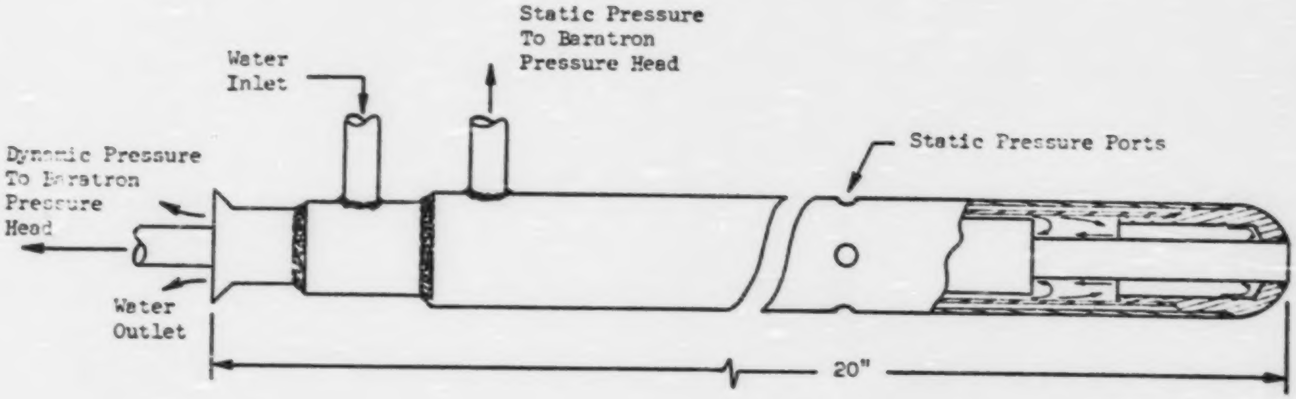
Water
Inlet
Static Pressure
To Baratron
Pressure Head
Dynamic Pressure
To Baratron
Pressure
Head
Water
Outlet
Static Pressure Ports
20"

Water-cooled pitot probe

Figure 15. Water-cooled probes

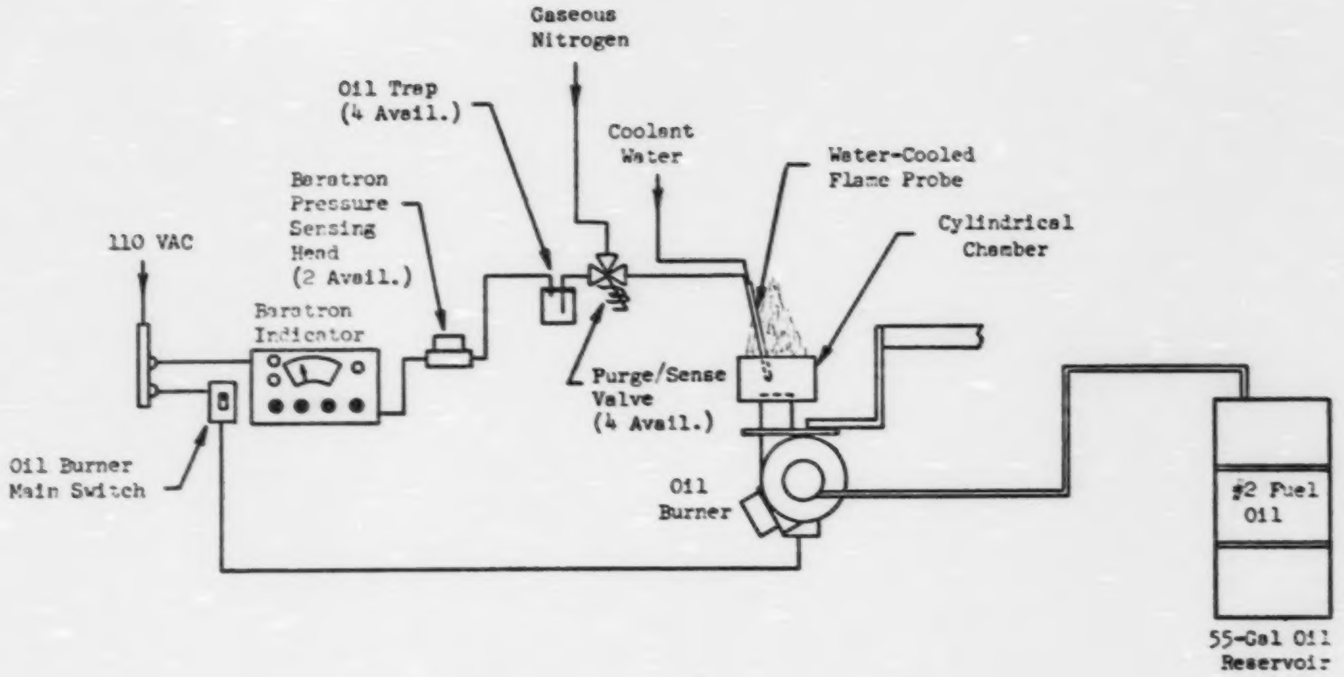
Gaseous Nitrogen
Oil Trap (4 Avail.)
Coolant Water
Water-Cooled Flame Probe
Baratron Pressure Sensing Head (2 Avail.)
Cylindrical Chamber
110 VAC
Baratron Indicator
Purge/Sense Valve (4 Avail.)
Oil Burner Main Switch
Oil Burner
#2 Fuel Oil
55-Gal Oil Reservoir

Figure 16. Schematic of oil burner flame gas velocity probe system

pressure-sensing head which, for electronic stability, is thermostatically maintained at an elevated temperature. The composite test system is shown in Fig. 16. Included are electrical purge/sense valves which allow periodic purging of the probes and lines to clear any oil or soot deposits from the probe lines. Also included are oil traps to inhibit any possible oil migration to the Baratron pressure-sensing heads.

At the time the combustion gas flow pattern measurements were being made, there was no provision for analysis of the gases as a function of the location at which the impact pressures were measured. Calculation of velocity requires knowledge of the gas density (see Eq. 1). Therefore, in the absence of local combustion gas analyses, the combustion gas was assumed to have a density corresponding to a molecular weight of 29 and a temperature of 2300 F. These assumptions were used in the calculation of all combustion gas velocities reported herein. Localized combustion gas compositions were determined at a later stage in the program, but not at a sufficient number of locations to include all of the velocity measurements previously taken and, hence, the composition measurements were not incorporated into calculation of any of the combustion gas velocities reported herein.

COMBUSTION CHAMBERS

There were four research cylindrical combustion chambers used in the combustion gas and exhaust gas analysis studies. The four chambers were of 8-, 11-, 18-, and 30-inch diameters for a hot-firing oil flowrate range of 0.50 to 12.0 gph.

The 8-inch-ID chamber was fabricated to accommodate oil burners of 0.50- to 1.50-gph flowrate, with oil spray-chamber wall impingement being the primary limiting factor. Figure 17 is a drawing of the 8-inch-diameter, cylindrical combustor showing the various locations of the sampling probes, the semicircular mixing baffles, and a perpendicular burner port extension. In the coaxial chamber configuration, the distance from the burner port to

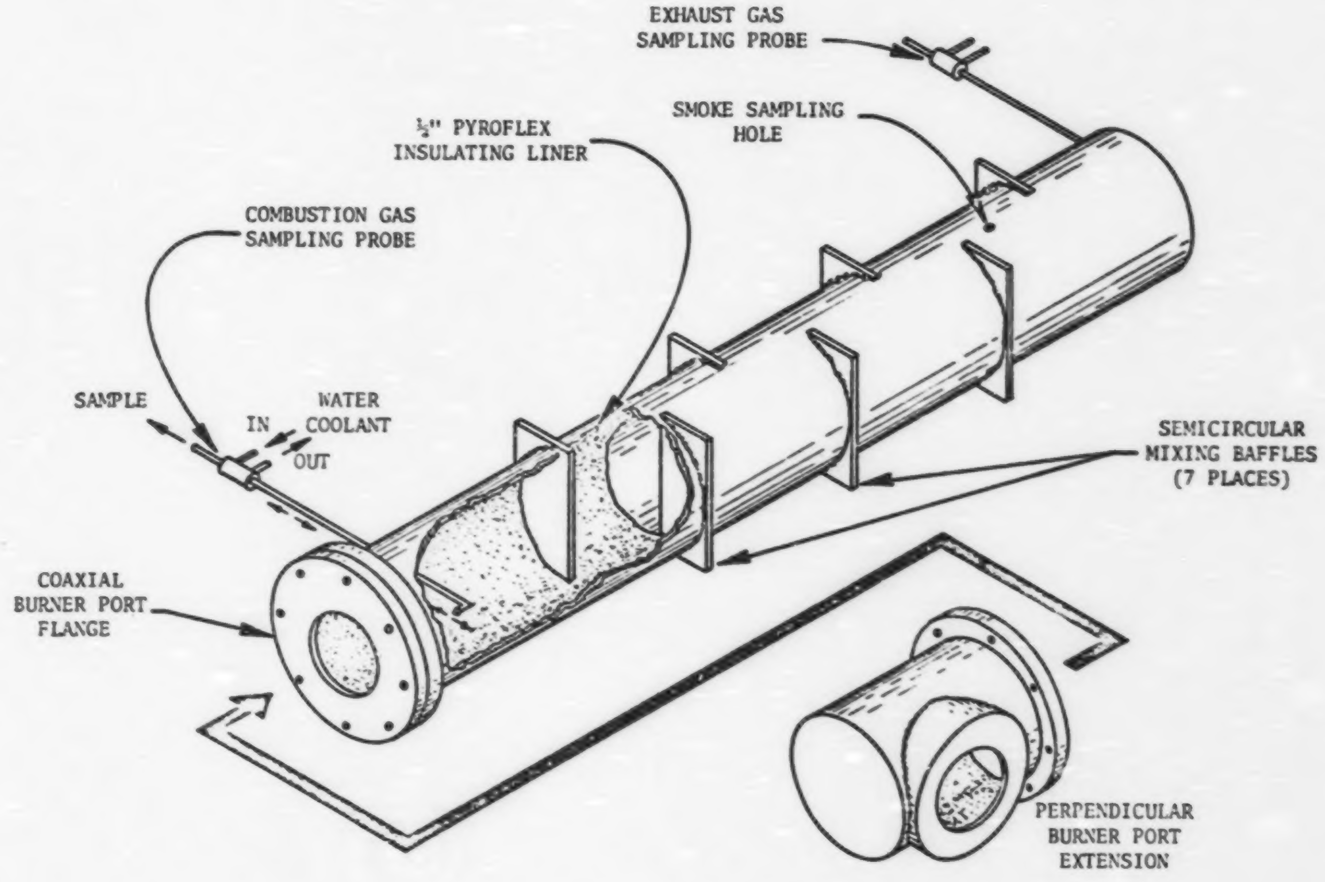
EXHAUST GAS
SAMPLING PROBE
SMOKE SAMPLING
HOLE
½" PYROFLEX
INSULATING LINER
COMBUSTION GAS
SAMPLING PROBE
SAMPLE
IN
WATER
COOLANT
OUT
SEMICIRCULAR
MIXING BAFFLES
(7 PLACES)
COAXIAL
BURNER PORT
FLANGE
PERPENDICULAR
BURNER PORT
EXTENSION

Figure 17. Schematic of the 8.0-inch-diameter insulated cylindrical combustor with semicircular mixing baffles

the first baffle (combustion chamber length) is 16 inches, with a total of 7 semicircular mixing baffles spaced 6 inches apart down the remaining length of the chamber. These baffles are installed 0.50 inch short of either side of the chamber centerline, leaving a 1-inch gap down the center through which the flame can be observed from the end of the combustion chamber. The combustion chamber section is completely insulated with 1/2-inch-thick Pyroflex liner, which is a vacuum-cast alumina silicate fiber matting that is flexible when purchased, but sets up firmly after being fired for approximately 15 minutes. The insulating characteristics of the Pyroflex lining maintains the inside wall temperature of the combustion chamber section at about 3000 to 3200 F. This extremely high wall temperature minimizes soot formation on the wall since the carbon oxidizes off at this temperature. Three combustion zone sampling ports are located on the combustion chamber section to allow local combustion gas sampling traverses at 1.5, 3 and 6 inches downstream from the burner head. An additional end probe is mounted near the exit of the combustor to sample the completely combusted, mixed exhaust gases to obtain overall conditions. The end probe is inserted approximately 12 inches in from the exit, past the exit baffle to avoid ambient air ingestion into the probe that would dilute the sample. The probes used for both the combustion gas and exhaust gas sampling were water-cooled United Sensor Corporation Model GB 24-125. A water jacket, 19 inches in length, could also be attached to the combustion chamber section and, with the removal of the Pyroflex insulation, the inside wall temperature could be lowered to about 350 to 450 F to simulate a water-base (cold-wall) type furnace. The water-jacket enclosure was sealed on the burner port end flange and open at the other end, permitting cold-wall operation only when the chamber assembly is mounted vertically.

An 8-inch-diameter, perpendicular burner port combustion extension, also shown in Fig. 17, was fabricated to mate to the 8-inch-diameter cylindrical combustor. The perpendicular burner port configuration is quite common in commercially available furnaces, and the dimensions of this enclosure closely duplicated the Lennox furnace combustion chamber (described later in this section) that was also used in experiments. The perpendicular port extension added 11 inches to the length of the combustion section but, being perpendicular, the closest obstruction to the flame was the opposing wall 8 inches away. Pyroflex insulation (1/2-inch thick) was used to line the inside of the extension, and no wall temperature variation experiments were attempted with this combustor configuration.

An 11-inch-diameter, hot-wall, cylindrical, coaxial combustor was fabricated for combustion zone gas sampling experiments for the larger (6 and 12 gph) burners. The size of this combustor was marginally acceptable for experiments at the 12-gph flowrate, as some fuel spray impingement on the chamber wall was noted. This 11-inch combustor was similar to the basic configuration of the smaller 8-inch-diameter combustor described previously, with 2 probe-mounting locations (combustion section and exhaust), coaxial port, and straight cylindrical geometry. The mixing baffles differed in that, instead of semicircular plates, it used turbulence generators in the form of a convergent section (choke) and a 1 in. sq mesh grid of 0.25-inch water-cooled tubing. The overall length of this combustion chamber was 7 feet, and the first 22 inches were insulated with Pyroflex liner making it a hot-wall combustion chamber with an inside wall temperature of approximately 3000 F. The combustion chamber section had 2 additional probe ports (5 total) allowing combustion gas-sampling traverses at 1.5, 3, 6, 9, and 12 inches from the oil burner head.

A 30-inch ID, hot/cold wall, coaxial combustor was fabricated for the 6- to 12-gph oil burner experiments. Figure 18 is a schematic of the 3-section combustor, showing the hot- or cold-wall combustion chamber section and the 2-piece mixing/exhaust section. The combustion chamber section consisted of a 30-inch-diameter chamber with a 31.5-inch-diameter water-jacket shroud surrounding it, leaving a 0.75-inch, water coolant passage with 3 inlet and 3 outlet fittings. The water jacket was sectioned by an

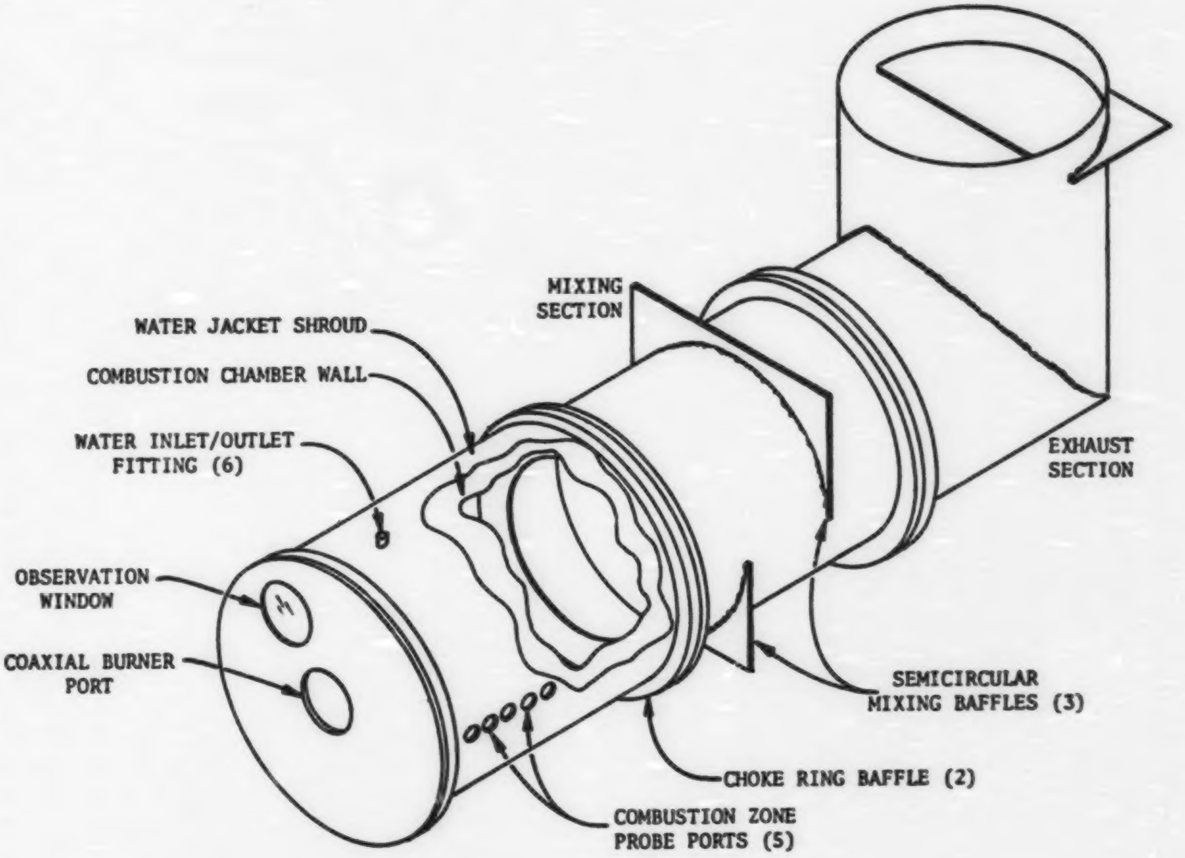
WATER JACKET SHROUD
COMBUSTION CHAMBER WALL
WATER INLET/OUTLET FITTING (6)
OBSERVATION WINDOW
COAXIAL BURNER PORT
MIXING SECTION
EXHAUST SECTION
SEMICIRCULAR MIXING BAFFLES (3)
CHOKE RING BAFFLE (2)
COMBUSTION ZONE PROBE PORTS (5)

Figure 18. Schematic of 30-inch-diameter, hot/cold wall, coaxial cylindrical research combustor for 6-to 12-gph oil burners

expansion joint to compensate for differential expansion between the jacket wall and the hotter combustion chamber wall where the wall temperature differential may be as great as 1000 F in the "hot-wall" mode. There are 5 combustion gas sampling ports that permit sampling traverses at 3, 6, 9, 12 and 15 inches from the burner head. The ports were bellowed tubes welded at the inner and outer cylinder walls to prevent water leakage and allow differential expansion of the walls. The combustion chamber can be run in the "cold-wall" mode by flowing water coolant (5 to 6 gpm at 12 gph firing rate) through the water jacket, which results in an inside chamber wall temperature of about 350 to 400 F. The "hot-wall" configuration required the installation of 1/2-inch Pyroflex lining held in place by a water-cooled support grid of 1/4-inch stainless-steel tubing. A trickle flow of water must be maintained through the waterjacket to prevent the inner cylinder wall from overheating ($T \approx$ 1500 F). The combustion section was 36 inches in length, terminating with a choke ring-type mixing baffle of 22 inches ID. Downstream of the choke ring were the mixing/exhaust sections consisting of 2 semicircular mixing baffles and another choke ring baffle, spaced at 12-inch intervals. The exhaust was turned 90 degrees vertically and terminated near the exit with another semicircular baffle to avoid ambient air ingestion that would dilute the gas samples. The sample probe extends 18 inches into the exhaust section to further prevent sample dilution. A 5-inch-diameter Pyrex glass window in the burner port flange allowed observation of the flame in the combustion chamber.

An 18-inch-diameter, hot-wall, coaxial combustor extension to the 30-inch-diameter mixing/exhaust section was fabricated to allow 3-gph burner experiments with a minimal of test stand modifications. The combustion chamber was 18 inches in length, lined with 1/2-inch-thick Pyroflex insulation, and terminated with a 12.5-inch-ID choke ring baffle/mating flange combination. The chamber was designed for hot-wall experiments only, with no provisions for water cooling the wall. There were 4 combustion zone probe ports that allowed sampling traverses to be made at 1.5, 3, 6, and 9 inches from the burner head. The chamber mated directly to the 30-inch-diameter mixing section and required only a partial covering of the exhaust outlet to avoid air ingestion at the lower firing rate.

Figure 19 shows a schematic of the general test stand setup of both the 8-inch- and 30-inch-diameter combustors. This is a schematic showing general locations rather than detail of flow systems, and does not show the combustion zone probe locations.

FURNACES

Two commercially available, home-sized (0.5 to 1.50 gph), heating furnaces were used in oil burner flue gas sampling experiments. A Lennox Model OF7-105M, 0.75-gph warm-air furnace and a Unitron Model A100, 1.10-gph combination warm-air/hydronic (warm water) furnace were used to test the 0.5- to 1.50-gph oil burners.

The Lennox warm-air furnace had an 8-inch-ID by 14-inch-tall upright circular combustion chamber with the burner port mounted perpendicular to the chamber axis. The chamber was refractory-lined (hot wall) with the heat exchanger section mounted directly above the combustion chamber. The combustion chamber configuration was very similar to the 8-inch-diameter, perpendicular port, research combustor extension designed from basic dimensions taken from the Lennox furnace. The flue samples were removed from the 6-inch-diameter stack through an uncooled, 1/4-inch-OD, stainless-steel tube having its entrance bent perpendicular into the direction of the gas flow.

The Unitron Model A100 warm-air/hydronic furnace is rather unique in its combination heat transfer system, using both forced air and hot water for heat distribution. This furnace had a coaxial combustion chamber very similar to the 8-inch-diameter research combustor described earlier in this section. The furnace combustion chamber is cylindrical, 10.5-inch ID, 24 inches in length, and lined with 1/2-inch Pyroflex insulation. The

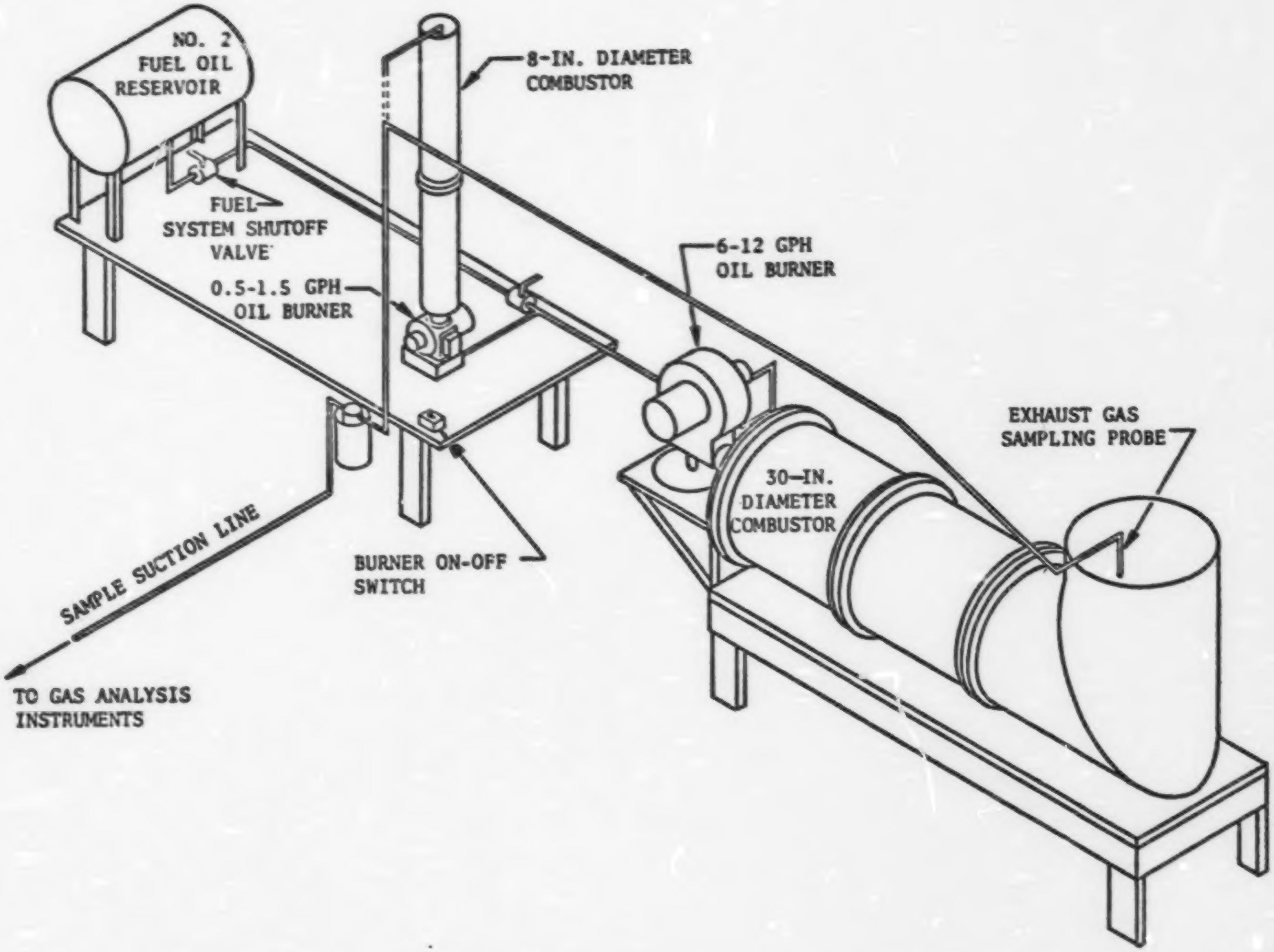
NO. 2
FUEL OIL
RESERVOIR
8-IN. DIAMETER
COMBUSTOR
FUEL-
SYSTEM SHUTOFF
VALVE
0.5-1.5 GPH
OIL BURNER
6-12 GPH
OIL BURNER
EXHAUST GAS
SAMPLING PROBE
30—IN.
DIAMETER
COMBUSTOR
SAMPLE SUCTION LINE
BURNER ON-OFF
SWITCH
TO GAS ANALYSIS
INSTRUMENTS

Figure 19. Schematic of oil burner combustion gas sampling system

hot combustion gases are then turned 90 degrees upward into a manifold and 90 degrees again through a multitube hot gas-to-water heat exchanger to heat the water, which is the primary heat transfer medium. Part of the hot water flows through an internal, finned radiator which, with the blower, constitutes the warm-air heat distribution system.

COMBUSTION GAS COMPOSITION PATTERNS

As a tool for diagnosis to determine the local combustion effects leading to formation of the various pollutants, it is desirable to know not only the local flow patterns, but also the local composition patterns of the combustion gases. To accomplish this required localized sampling and analysis of combustion gases. The localized sampling was conducted using the combustion chambers having probe ports, as described in the previous section.

Accurate measurement of nitric oxide concentration by gas sampling from a gas stream sufficiently hot to allow non-negligible nitric oxide chemical kinetics requires that the sample probe instantaneously quench the temperature of the gas sample as it enters the probe. If the temperature is not instantly quenched to a temperature sufficiently low so that nitric oxide kinetics are negligible, there is a definite probability that the nitric oxide content of the gas sample will change within the probe as a result of chemical processes on surfaces and in the bulk gas flowing through the probe. For the present program of study, the likelihood of quantitative changes in nitric oxide concentration due to sample quenching technique was recognized; however, the nature of this study (pollutant minimization) was such that exact concentrations of nitric oxide are of considerably less importance than relative concentrations at various locations and for various burners. It was chosen, therefore, to utilize a simple water-cooled convective quench sample probe rather than a more costly, difficult-to-operate probe designed specifically to achieve rapid thermal quench.

The gas sample probe utilized to obtain gas samples from within the burner combustion zone was a low-cost, commercially available model (GB 24-125) manufactured by United Sensor Corporation. A photograph of this probe is shown in Fig. 20. It is a simple tubular probe with a short right-angle turn at the sampling end. The right-angle end allows the probe to be inserted from a position at right angles to the flow, with the probe inlet still being pointed upstream. No attempt was made to align the gas sample probe inlet with the local vector direction of the gas flow. The gas velocity within the 1/8-inch-diameter inlet to the probe was maintained relatively constant for all experiments at approximately 250 ft/sec.

In one instance, the velocity was reduced by a factor of 4:1, changing the thermal quench conditions, and the nitric oxide analysis was found to be insensitive to this change.

The sample flow train used for the experiments is shown in Fig. 21. Gas aspirated through the sample probe entered an air-cooled condensibles trap where particulates and heavy oils were separated out. Next, the gas passed into an ice-cooled, stainless-steel condensibles trap where most of the water and all but the most volatile hydrocarbons were removed. After the condenser, the gas passed into a pyrex wool-filled glass cylinder. The last item served as a final separator for heavy oils and particulates, and provided a visual indication of the cleanliness of the gas being admitted to the analysis instruments. Table 2 gives a summary of the gas analysis instruments used. The gas leaving the glass wool filter was split into three parallel paths. One path led directly to the total hydrocarbon analyzer. A second path led through a Drierite bed where water was removed, and then into the series-plumbed carbon monoxide, carbon dioxide, and oxygen analyzers. The third path passed through a combined Drierite and 3 Å molecular sieve bed for total water removal, and then into the nitric oxide analyzer. The gas was pumped through the system by three diaphragm pumps located downstream of the nitric oxide analyzer, total hydrocarbon, and carbon monoxide + carbon dioxide analyzers. The

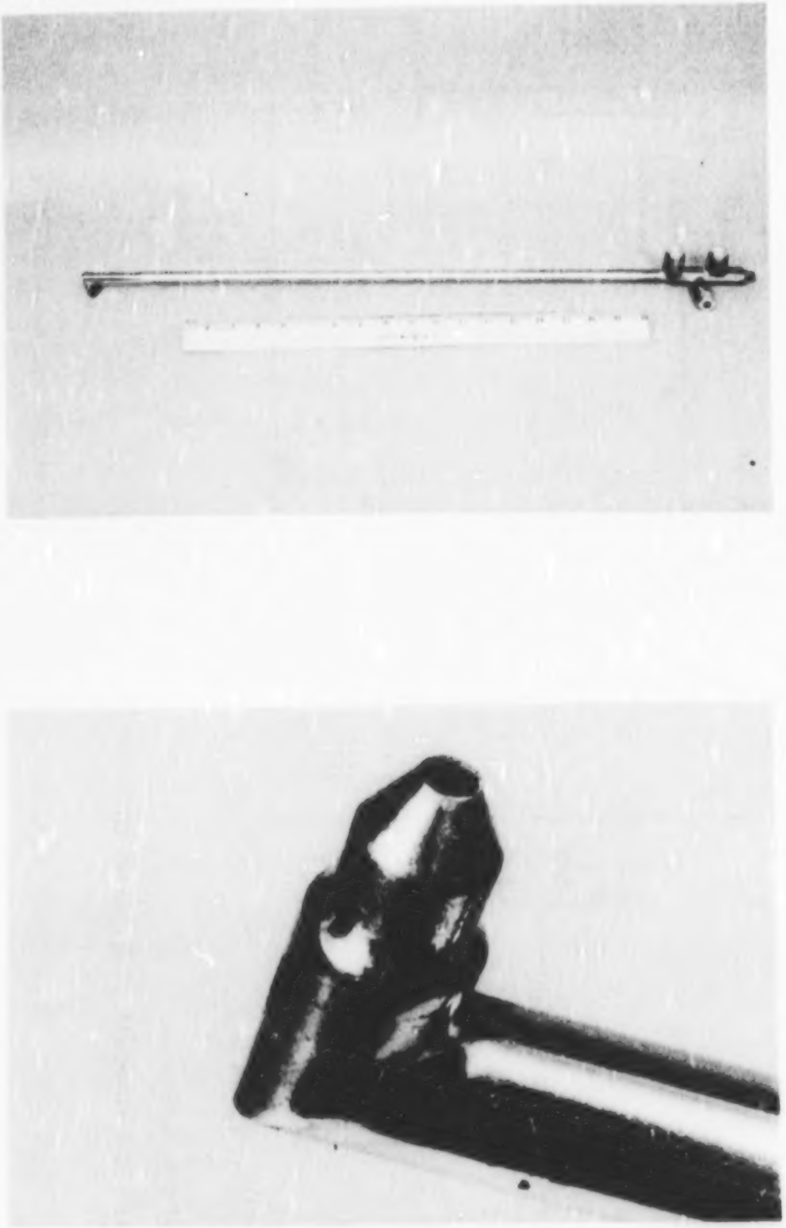

Figure 20. United Sensor model GB 24-125 gas sampling probe

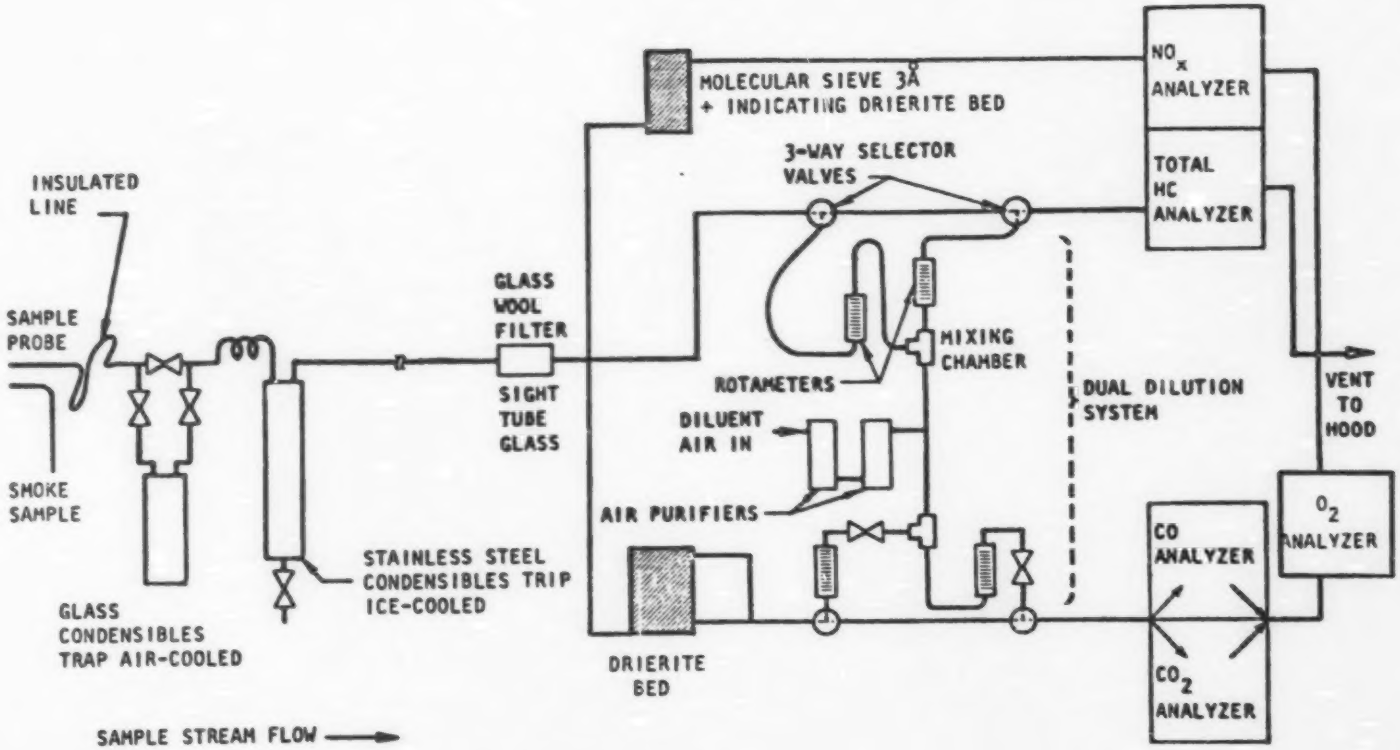
INSULATED LINE
SAMPLE PROBE
SMOKE SAMPLE
GLASS CONDENSIBLES TRAP AIR-COOLED
STAINLESS STEEL CONDENSIBLES TRIP ICE-COOLED
GLASS WOOL FILTER
SIGHT TUBE GLASS
MOLECULAR SIEVE 3Å + INDICATING DRIERITE BED
3-WAY SELECTOR VALVES
ROTAMETERS
MIXING CHAMBER
DILUENT AIR IN
AIR PURIFIERS
DRIERITE BED
DUAL DILUTION SYSTEM
NO$_x$ ANALYZER
TOTAL HC ANALYZER
VENT TO HOOD
O$_2$ ANALYZER
CO ANALYZER
CO$_2$ ANALYZER

SAMPLE STREAM FLOW ⟶

ALL LINES 1/4-INCH STAINLESS STEEL TUBING (THIN WALL)

Figure 21. Analytical system for fuel oil burner emissions analysis

Table 2. EXHAUST ANALYSIS INSTRUMENTS

	CO	CO_2	NO	Total HC	Oxygen	Smoke
Type	MSA Nondispersive IR LIRA Model 300	MSA Nondispersive IR LIRA Model 300	MSA Nondispersive IR LIRA Model 200	MSA H_2 flame ionization detector	Beckman polarographic	Bacharach (manual)
Range	0 to 1500 ppm (mole)	0 to 20 mole %	0 to 500 ppm (mole)	0.2 to 800 ppm total HC by volume as CH_4	0 to 100%	0 to 9
Sensitivity	30 ppm minimum detectable	0.25% minimum detectable	10 ppm minimum detectable	10 ppm minimum detectable	~0.1%	1
Calibration	1000 ppm CO in N_2 standard gas	14% CO_2 in N_2 standard gas	0.82% C_2H_4 in N_2 used as simulant for 410-ppm NO standard	3% CH_4 in helium used as a standard	Air - 21% N_2 = 0%	Ten spots of monotonically varying darkness

system also contained capability for dilution of gas passing through the carbon monoxide, carbon dioxide, and oxygen path. Dilution was achieved by admission of air metered through parallel rotameters, and it allowed use of the analytical instruments on gas samples more concentrated than the highest range of the instruments.

When the analytical system shown in Fig. 21 is used to analyze gases sampled from within the combustion zone, there are two major factors that must be considered when reducing the data: (1) only burned or partly pyrolyzed fuel is included in the analysis, since liquid or vaporized fuel is non-quantitatively removed by the cold trap, and (2) water formed from hydrogen and oxygen during the combustion process is also removed by the cold trap from the analyzed sample.

Values calculated from the local combustion gas sampling data include: the local stoichiometric ratio of the gases (this necessarily excludes unburned fuel vapor or liquid which is removed at the cold trap), the weight content of nitric oxide per unit weight content of burned fuel, and the weight of carbon monoxide per unit weight of burned fuel. The method of calculation to obtain these values is described below.

The calculations are based on air having the nominal composition given in Table 3.

Table 3. PURE AIR COMPOSITION

Component	Mole Percent
N_2	78.08
O_2	20.95
Ar + He + Ne	0.94
CO_2	0.03
	100.00

The composition of the fuel is assumed to be characterized by the formula CH_x where, for use herein, x = 1.814. The following symbols are used in the calculations:

AIR = moles of air to produce 100 moles of dry sample
FUEL = moles of fuel to produce 100 moles of dry sample
CO = moles of carbon monoxide in 100 miles of dry sample
CO_2 = moles carbon dioxide in 100 moles of dry sample
NO = moles of nitric oxide in 100 moles of dry sample
O_2 = moles of oxygen in 100 moles of dry sample
HC = moles of hydrocarbon, as CH_4, in 100 moles of dry sample
x = number 2 fuel oil composition, CH_x, $x \simeq 1.814$

The values of CO, CO_2, NO, O_2, and HC are obtained directly from the analysis instruments. In the following, it is assumed that all hydrogen is oxidized to water and condensed out of the system at the cold trap, prior to analysis.

An oxygen balance yields:

$$0.2095\ AIR = CO_2 - 0.0003\ AIR + 0.5\ CO + 0.25X\ (CO_2 + CO - 0.0003\ AIR) + 0.5\ NO + O_2 \qquad (2)$$

The left-hand side of the above equation represents the total free oxygen contributed by the air. The first two items on the right side represent moles of oxygen tied up in CO_2, less the amount of CO_2 originally present in the air. The third term represents moles of oxygen tied up as carbon monoxide. The fourth term represents oxygen consumed to oxidize hydrogen yielding the water condensed out in the cold trap. The fifth term is the oxygen tied up in nitric oxide. The sixth term is free oxygen remaining in the sample reaching the analysis instruments. Equation 2 can be arranged to yield:

$$AIR = \frac{(1 + \frac{x}{4})\ CO_2 + (1/2 + \frac{x}{4})\ CO + 1/2\ NO + O_2}{0.2095 + 0.0003 + 0.0003\ x/4} \qquad (3)$$

A carbon balance can be used to calculate the moles of burned fuel per 100 moles of dry sample gas:

$$\mathrm{FUEL} = \mathrm{CO_2} - 0.0003\ \mathrm{AIR} + \mathrm{CO} \tag{4}$$

The moles of air available per mole of burned fuel in the sample gas can be obtained by taking the ratio of the values from Eq. 3 and 4. AIR must be calculated first, before calculation of FUEL. If the combustion were in stoichiometric proportions, the moles of air would be, by an oxygen demand calculation:

$$\mathrm{AIR}_{\mathrm{stoich}} = \frac{(1 + x/4)\ \mathrm{FUEL}}{0.2095} \tag{5}$$

The stoichiometric ratio of the locally sampled burned gases is a parameter frequently used in this report. It is defined as the ratio of AIR to $\mathrm{AIR}_{\mathrm{stoich}}$:

$$\mathrm{SR} = \text{stoichiometric ratio} = \frac{\mathrm{AIR}}{\mathrm{AIR}_{\mathrm{stoich}}} \tag{6}$$

Combination of Eq. 3 through 6 yields a direct calculation of the burned gas stoichiometric ratio in terms of the measured parameters:

$$\mathrm{SR} = \frac{\dfrac{(1 + \frac{x}{4})\ \mathrm{CO_2} + (1/2 + \frac{x}{4})\ \mathrm{CO} + 1/2\ \mathrm{NO} + \mathrm{O_2}}{0.2095 + 0.0003 + 0.0003x/4}}{\dfrac{(1 + \frac{x}{4})}{0.2095}\left[\mathrm{CO_2} + \mathrm{CO} - 0.0003\ \dfrac{(1 + \frac{x}{4})\ \mathrm{CO_2} + (1/2 \times \frac{x}{4})\ \mathrm{CO} + 1/2\ \mathrm{NO} + \mathrm{O_2}}{0.2095 + 0.0003 + 0.0003x/4}\right]} \tag{7}$$

According to the above definition, when the sample contains just a sufficient amount of air to oxidize all of the fuel in the sample to $\mathrm{CO_2}$ plus condensed-out water, then SR = 1; and, as a second example, if there is twice the required amount of air for complete oxidation of the fuel, then SR = 2. Note that the stoichiometric ratio, as calculated from Eq.7 does not require that the product in the sample be in chemical equilibrium.

Note that the accuracy of the stoichiometric ratio calculation would be affected very little if all terms in Eq. 7 containing the factors 0.0003 and NO were ignored. These factors represent the carbon dioxide originally present in free air, and the oxygen tied up in nitric oxide, respectively.

One partially questionable assumption made in the formulation of Eq. 7 was that all hydrogen originally present in the fuel becomes oxidized to water and removed in the cold trap. This was a necessary assumption, since there was no instrument available to measure the actual hydrogen content of the sample gas. The assumption is very good under the combined conditions of air-rich stoichiometric ratios (SR > 1) and chemical equilibrium. To test this assumption, the Rocketdyne thermochemical computer code was used to calculate the species concentrations under conditions of chemical equilibrium for stoichiometric ratios from 0.8 to 2.8. These calculations included the equilibrium presence of free H_2. The actual stoichiometric ratios of these combustion gases, compared to the stoichiometric ratios calculated from Eq. 7 (which does not recognize the presence of H_2) are given in Table 4, where it can be seen that Eq. 7 is quite accurate except for SR < 1. The calculated equilibrium conditions for these results are given in Tables 5 and 6.

TABLE 4. VALIDITY OF STOICHIOMETRIC RATIO CALCULATIONS OF EQ. 7

Actual Stoichiometric Ratio	Stoichiometric Ratio Calculated from Eq. 7
0.800	0.844
1.000	1.003
1.200	1.197
1.400	1.400
1.600	1.600
2.000	2.002
2.400	2.404
2.800	2.804

Table 5. EQUILIBRIUM FLAME PROPERTIES FOR NO. 2 DISTILLATE FUEL OIL

($CH_{1.814}$, 18,443 Btu/lb Heat of Combustion With Air at 14.67 psia)

Stoich. Ratio*	Oil + Air Inlet Temp., F	Flame Temperature, F	C_p Frozen, Btu/lb-R	γ Frozen	Viscosity, centipoise	Thermal Conductivity, Btu/hr-ft-F	Prandtl Number	Molecular Weight
0.8	0	3429	0.346	1.261	0.0666	0.0702	0.7946	27.73
1.0 ↑		3614	0.341	1.254	0.0687	0.0711	0.7984	28.80
1.2		3290	0.333	1.260	0.0653	0.0661	0.7954	29.00
1.4		2940	0.324	1.267	0.0615	0.0610	0.7915	29.03
1.6 Air		2649	0.318	1.275	0.0581	0.0567	0.7880	29.03
2.0 Rich		2209	0.307	1.288	0.0527	0.0500	0.7820	29.02
2.4		1897	0.298	1.298	0.0487	0.0452	0.7771	29.01
2.8 ↓		1663	0.291	1.308	0.0456	0.0415	0.7730	29.00
0.8	70	3778	0.347	1.261	0.0671	0.0709	0.7948	27.72
1.0		3649	0.341	1.254	0.0691	0.0715	0.7984	28.77
1.2		3336	0.333	1.259	0.0658	0.0667	0.7956	29.00
1.4		2991	0.325	1.267	0.0621	0.0617	0.7918	29.03
1.6		2703	0.318	1.274	0.0589	0.0574	0.7884	29.03
2.0		2765	0.308	1.286	0.0535	0.0509	0.7825	29.02
2.4		1955	0.299	1.297	0.0495	0.0461	0.7778	29.01
2.8		1722	0.193	1.306	0.0464	0.0425	0.7738	29.00
0.8	200	3567	0.347	1.260	0.0681	0.0720	0.7951	27.71
1.0		3709	0.342	1.257	0.0698	0.0723	0.7983	28.73
1.2		3418	0.334	1.259	0.0668	0.0678	0.7958	28.98
1.4		3085	0.326	1.266	0.0632	0.0629	0.7923	29.02
1.6		2802	0.320	1.273	0.0600	0.0588	0.7890	29.02
2.0		2369	0.309	1.284	0.0548	0.0524	0.7834	29.02
2.4		2061	0.301	1.294	0.0509	0.0477	0.7790	29.01
2.8		1831	0.295	1.303	0.0479	0.0441	0.7751	29.00

*Stoichiometric ratio is unity at 14.49 pounds of air per pound of fuel, and proportionately greater than unity for increasing amounts of air; S.R. = (AIR/FUEL)/14.49

Table 6. CALCULATED EQUILIBRIUM GAS COMPOSITION, MOLE PERCENT

Stoich. Ratio	Oil + Air Inlet Temp., F	H	O	Ar	OH	H_2	H_2O	CO	CO_2	NO	N_2	O_2
0.8	0	0.0630	0.0000	0.821	0.0499	2.016	12.263	7.243	8.687	0.000	68.837	0.000
1.0		0.0397	0.0313	0.866	0.2816	0.250	11.690	1.393	12.052	0.253	72.522	0.619
1.2		0.000	0.0217	0.882	0.1862	0.030	10.141	0.161	11.247	0.390	73.784	3.160
1.4		0.000	0.0000	0.890	0.0757	0.000	8.832	0.0203	9.841	0.2955	74.465	5.566
1.6		0.000	0.0000	0.895	0.0790	0.000	7.799	0.000	8.679	0.2080	74.947	7.444
2.0		0.000	0.0000	0.902	0.000	0.000	6.297	0.000	7.000	0.0829	75.603	10.107
2.4		0.000	0.0000	0.907	0.000	0.000	5.276	0.000	5.864	0.0339	76.028	11.888
2.8		0.000	0.0000	0.910	0.000	0.000	4.541	0.000	5.046	0.000	76.326	13.161
0.8	70	0.0737	0.0000	0.821	0.0613	1.996	12.271	7.268	8.659	0.017	68.901	0.000
1.0		0.0455	0.0362	0.866	0.3072	0.269	11.647	1.501	11.934	0.272	72.456	0.666
1.2		0.0000	0.0261	0.882	0.2082	0.036	10.121	0.195	11.210	0.404	73.751	3.159
1.4		0.0000	0.0000	0.890	0.0885	0.000	8.824	0.026	9.835	0.322	74.447	5.553
1.6		0.0000	0.0000	0.895	0.0351	0.000	7.795	0.000	8.678	0.223	74.933	7.432
2.0		0.0000	0.0000	0.902	0.000	0.000	6.297	0.000	7.000	0.096	75.596	10.100
2.4		0.0006	0.0000	0.907	0.000	0.000	5.276	0.000	5.863	0.041	76.023	11.884
2.8		0.0000	0.0000	0.910	0.000	0.000	4.541	0.000	5.046	0.018	76.323	13.159
0.8	200	0.0964	0.0000	0.821	0.0878	1.964	12.273	7.318	8.604	0.027	68.796	0.000
1.0		0.0577	0.0468	0.864	0.3579	0.304	11.562	1.710	11.705	0.310	73.328	0.754
1.2		0.0000	0.0356	0.882	0.2533	0.048	10.078	0.270	11.127	0.451	73.683	3.162
1.4		0.0000	0.0000	0.890	0.1157	0.000	8.806	0.042	9.816	0.373	74.405	5.526
1.6		0.0000	0.0000	0.895	0.0493	0.000	7.787	0.000	8.672	0.268	74.905	7.406
2.0		0.0000	0.0000	0.902	0.0000	0.000	6.295	0.000	7.000	0.125	75.582	10.085
2.4		0.0000	0.0000	0.907	0.0000	0.000	5.276	0.000	5.863	0.059	76.015	11.876
2.8		0.0000	0.0000	0.910	0.0000	0.000	4.541	0.000	5.046	0.028	76.319	13.154

The primary cause of the inaccuracy at SR < 1 is the presence of H_2. In nonequilibrium gases, there is likely to be H_2 present even where none would be indicated from equilibrium calculations and, at fuel-rich conditions, there could be more or less than indicated from the equilibrium calculations. Because of this likelihood of nonequilibrium, no attempt was made to correct the calculations of Eq. 7 by means of equilibrium calculations.

The other parameters of interest for the sampled combustion gases are the mass ratio of nitric oxide to burned fuel, the mass ratio of carbon monoxide to burned fuel, and the mass ratio of unburned hydrocarbons (as CH_4) to burned fuel. These ratios are generally expressed herein as grams of nitric oxide per kilogram of burned fuel (gm NO/kg fuel) grams of methane per kilogram of fuel (gm CH_4/kg fuel), and grams of carbon monoxide per kilogram of burned fuel (gm CO/kg fuel). These parameters are calculated by aid of Eq. 3 and 4 from the following relations:

$$\frac{\text{gm NO}}{\text{kg fuel}} = \frac{1000 \times \text{NO} \times MW_{NO}}{(CO_2 - 0.0003\ \text{AIR} + CO)\ MW_F} \tag{8}$$

$$\frac{\text{gm CO}}{\text{kg fuel}} = \frac{1000 \times \text{CO} \times MW_{CO}}{(CO_2 - 0.0003\ \text{AIR} + CO)\ MW_F} \tag{9}$$

$$\frac{\text{gm HC}}{\text{kg fuel}} = \frac{1000 \times \text{HC} \times MW_{CH_4}}{(CO_2 - 0.0003\ \text{AIR} + CO)\ MW_F} \tag{10}$$

where

MW_{NO} = molecular weight of NO = 30.01

MW_F = molecular weight of fuel
= 12.01 + 1.01 x = 13.83

MW_{CO} = molecular weight of CO = 28.01

MW_{CH_4} = molecular weight of methane = 16.04

For calculation of the above quantities, the term 0.0003 air can be assumed zero without introducing more than about 0.1-percent error in the calculations, or AIR can be computed from Eq. 3 and included in the calculation. The numbers given in this report include the effect of the term. The experimental data were reduced, according to the above equation, by means of a remote terminal timeshare computer program.

EXHAUST GAS ANALYSES

In several instances, the totally mixed exhaust gases from oil burner combustion processes were analyzed. These measurements can be used to compute the total emissions of the burner. The mixed exhaust gases were analyzed: (1) in the exhaust stack from the furnaces used, and (2) downstream of the mixing baffles of the research combustion chambers described previously.

When the exhaust gases were sampled from the exhaust stack of the furnaces, the gases were, of course, already cool (approximately 600 F) from passage through the furnace heat exchanger. Since the flue gases were precooled, the sample for analysis was withdrawn through an uncooled, 1/4-inch-OD, stainless-steel tube with its entrance perpendicular to the direction of gas flow. The gas withdrawn through this uncooled tube was then input to the sample analysis system shown in Fig. 21.

When the exhaust gases were sampled from the end of the mixing section of one of the previously described research combustors, the gases were still relatively hot due to the absence of a heat exchanger. Therefore, the sample gases were removed by means of the convective quench probe shown in Fig. 20. From the probe, the gases passed to the sample analysis system shown in Fig. 21.

The parameters calculated for the exhaust gases were stoichiometric ratio, nitric oxide-to-burned fuel mass ratio, carbon monoxide-to-burned fuel mass ratio, and unburned hydrocarbon-to-burned fuel mass ratio. These parameters were calculated from Eq. 7 through 10.

In addition to the gaseous pollutants described above, the smoke content of the mixed gases was also measured. The instrument utilized for this purpose was a Bacharach smoke meter. It is manufactured by the Bacharach Instrument Company, Pittsburgh, Pennsylvania. This is a hand-held device which, when pumped, sucks flue gases from a 1/4-inch-OD, uncooled sample probe through a piece of white filter paper; 10 strokes of the pump, over a period of about 15 seconds, causes the passage of 2250 in.^3 of flue gas per in.^2 of filter paper. The smoke particles deposit out on the filter paper. A reading is taken by comparing the darkness of the smoke deposition spot to a scale of 10 such calibrated spots provided with the instrument. The readings vary from 0 to 9. A reading of zero corresponds to no visually detectable deposition on the filter paper, while a reading of 9 corresponds to a dark black deposition. Intermediate readings are varying shades of black and gray, increasing in darkness with increasing reading numbers. A reading of 1 is generally accepted by the industry as a very acceptable degree of smoke. At the opposite extreme, a reading of 9, which is totally unacceptable, still does not correspond to sufficient smoke to be easily visible from observation of the exhaust stack outlet. In some instances, reported herein, when the reading was obviously greater than 9, the number of strokes was halved and smoke spot reading doubled, thus extending the smoke scale to a maximum of 18.

THERMAL RADIATION

Several experiments were performed with an instrument for measuring thermal radiation. This instrument is shown in Fig. 22. The detection end of the radiometer probe has a small hole, which is at one focus of an ellipsoidal polished cavity. At the other focus of the cavity is a hemispherical detector which acts as a blackbody to soak up the thermal radiation. Heat is conducted away from the blackbody detector through a small metal rod. Thermocouples at two locations on the metal rod detect thermal gradients therein, which are an indication of the heat flux through the rod and, hence, an indication of radiant heat flux impinging on the blackbody detector. The ellipsoidal cavity was purged continuously with gaseous

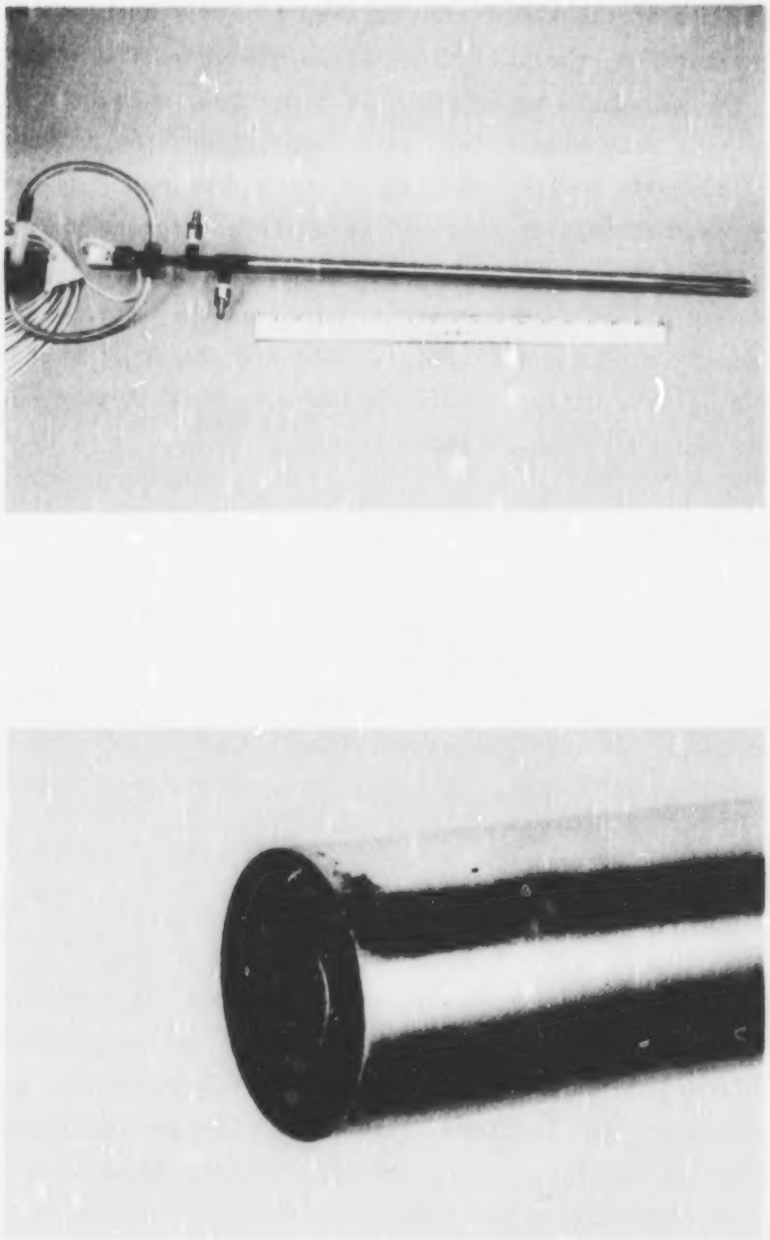

Figure 22. Land 2π radiometer used for radiation measurements

nitrogen during use of the radiometer to keep possibly harmful combustion gases from entering the polished ellipsoidal cavity. The probe was calibrated by the manufacturer in terms of radiation, using the specific nitrogen purge rate recommended for use. In practice, the nitrogen purge was apparently adequate to keep combustion gases from entering the probe cavity, but it was not able to stop oil spray from entering the cavity. After a few experiments, the oil spray which entered the cavity deteriorated the blackbody coating (apparently a paint) on the detector and nullified the calibration of the radiometer. The data reported with this instrument in a later section of this report should, therefore, be considered only as semiquantitative indications.

NONCONVENTIONAL BURNERS

There were four nonconventional burners designed and fabricated to investigate either the effects on exhaust pollutants or the feasibility of various designs utilizing known pollutant-reducing burner concepts. These designs are called: (1) mechanically rotated, intense swirl burner, (2) displaced oil injection burner, (3) forced recirculating combustion gas burner, and (4) heated air burner.

Intense Swirl Burner

An existing burner was modified to accept a variable rate, mechanically rotated, multiple-vane swirler assembly to be used to investigate low to very high air swirl rates. Figure 23 shows a schematic of the modified burner with the motorized swirler assembly. A six-vane swirler was mounted on a hollow rotating shaft, through which an inner stationary tube held the oil spray nozzle in position and also served as the oil feedline to the nozzle. The outer shaft was pulley driven by a V-belt link to a 1/7-hp ($\approx$ 1/12 hp required), 1725-rpm electric motor. The 4-cluster pulley arrangement allowed a swirl spin rate variation from 812 to 3450 rpm, varying the ratio of angular momentum to axial momentum (swirl number) of the

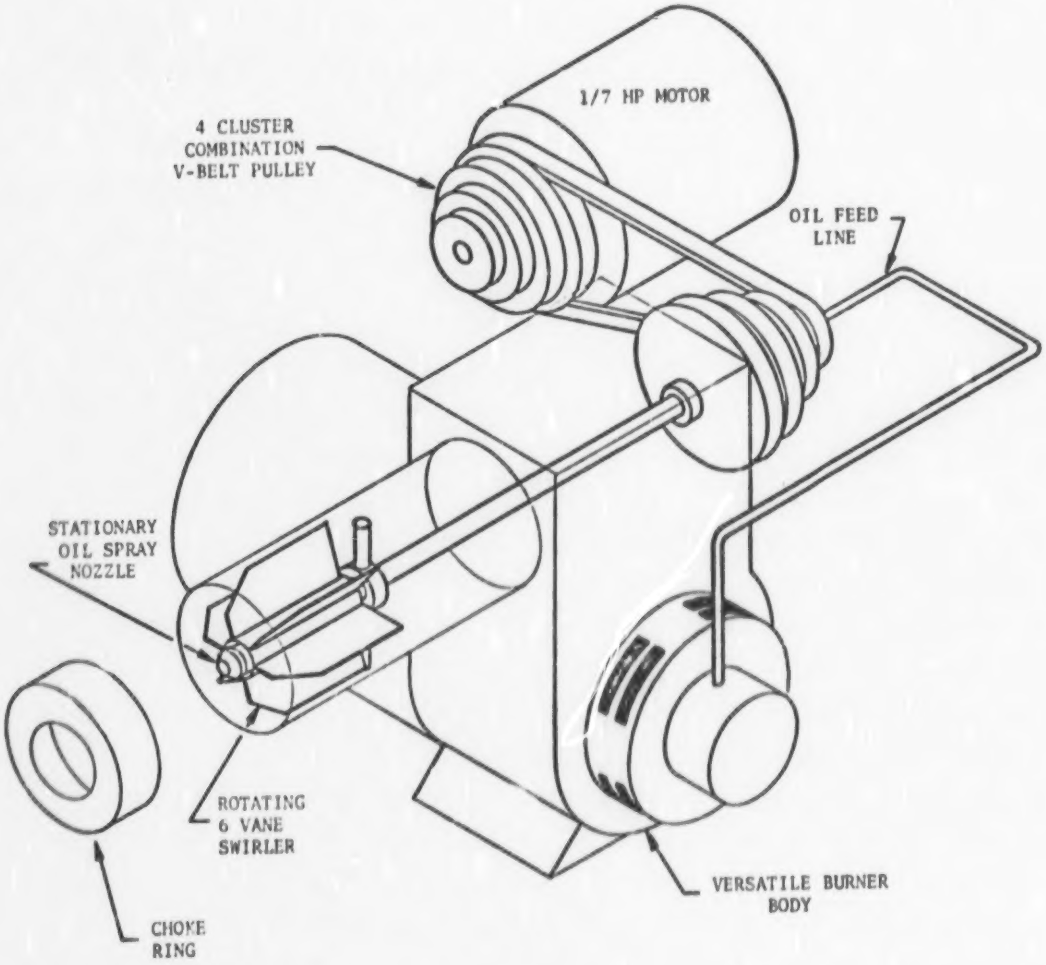
1/7 HP MOTOR
4 CLUSTER COMBINATION V-BELT PULLEY
OIL FEED LINE
STATIONARY OIL SPRAY NOZZLE
ROTATING 6 VANE SWIRLER
VERSATILE BURNER BODY
CHOKE RING

Figure 23. Schematic of modified versatile burner with variable rate, mechanically driven, multiple vane swirler

air from 2.2 to 8.8. The swirler assembly was mounted in a standard 4.0-inch-diameter blast tube and utilized a 30-degree convergence, 1.65-inch choke diameter, fixed geometry burner head (Fig. 24). Figure 25 shows photographs of this mechanically rotated, intense swirl burner in various stages of assembly.

Displaced Oil Injection Burner

A displaced injection experimental burner (Fig. 26) was constructed and tested. The intent of this injection concept was to utilize cool, recirculated combustion gases to aid fuel vaporization and, thereby, alter stoichiometric ratio at which combustion occurred. The primary air was introduced tangentially into the chamber, causing a recirculation pattern, and the oil nozzle was displaced circumferentially downstream into the combustion chamber. This extension allowed time for the primary air and the recirculated combustion gases to mix prior to encountering the oil spray. The first burner (prototype A, Fig. 26a) was designed to minimize modifications to the conventional burner. A burner was fitted with a 4-inch-diameter blast tube cut at 45 degrees at the exit with an oil nozzle canted 60 degrees to the blast tube centerline. The choke plate configuration was established by trial through visual observation of the flame. It was found that substantial air flow was needed near the chamber wall to keep the fuel spray from impinging on the chamber wall and causing smoke formation. The minimum height of the oil nozzle was dictated by the length of the nozzle and the chosen 60-degree cant angle. This combination of requirements for the nozzle height and chamber wall air flow resulted in a choke plate configuration that produced poor mixing of the primary air and fuel. Very smoky, high NO emission profiles were obtained. The lowest smoke reading obtained in the hot-firings with a No. 2 Bacharach smoke scale.

Modifications were made (prototype B, Fig. 26b) to decrease the oil nozzle height (i.e., extension into the chamber) and improve the oil spray contact

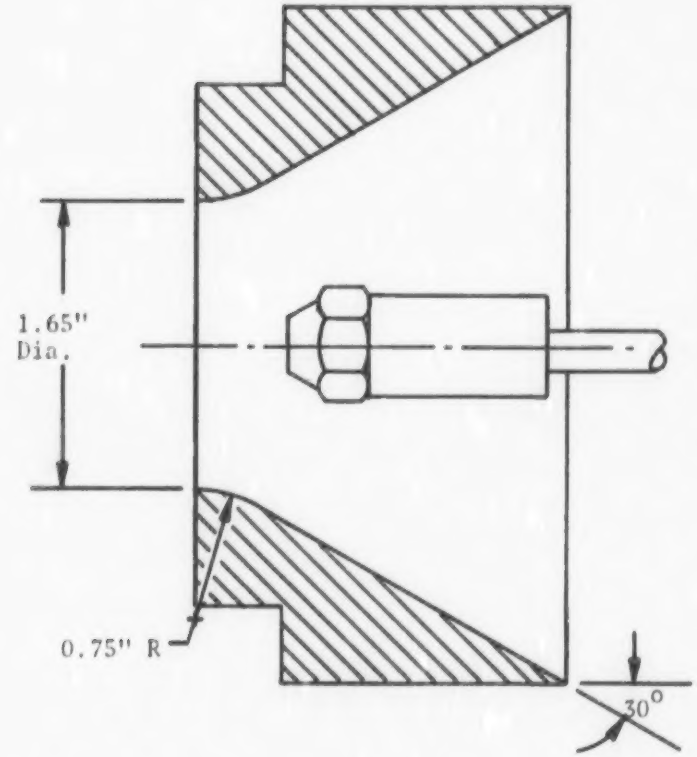
1.65"
Dia.
0.75" R
30°

Figure 24. Cross-section view of the fixed geometry, 1.65-inch-diameter, 30-degree convergent choke

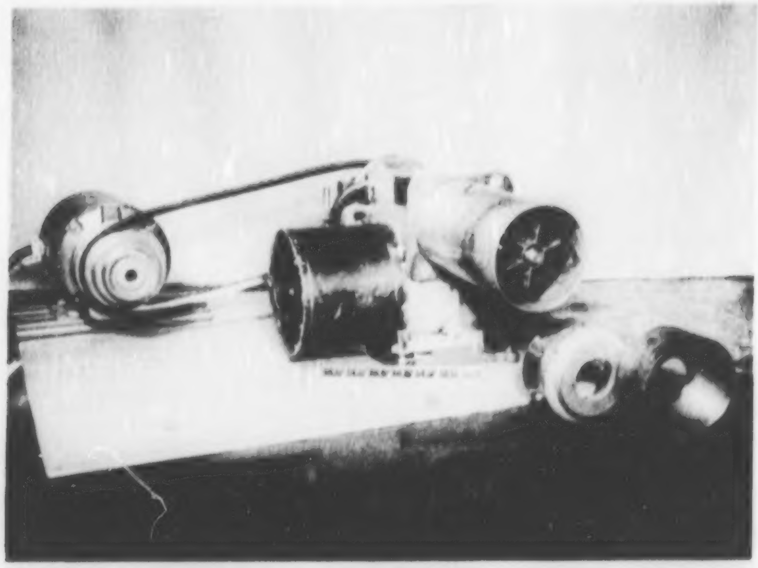

5AD26-7/17/73-S1D

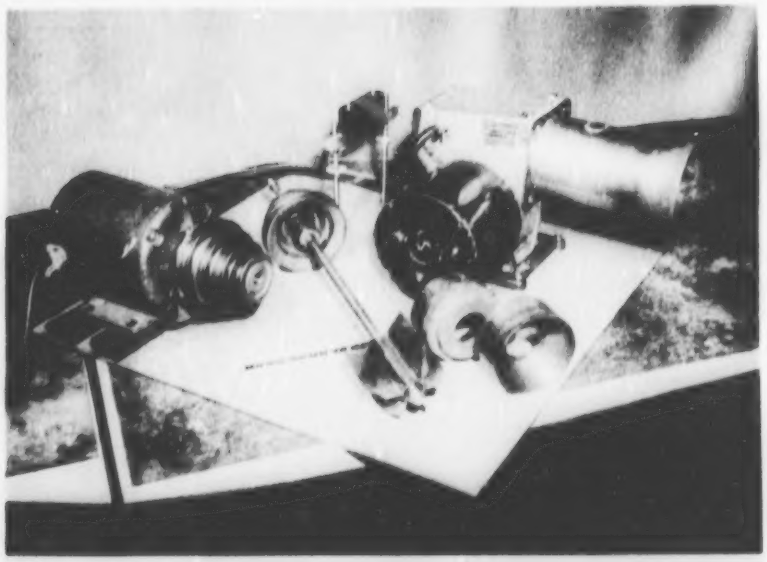

5AD26-7/17/73

Figure 25. Photographs of the mechanically rotated, six-vane intense swirl burner in various stages of assembly

(a) Prototype A

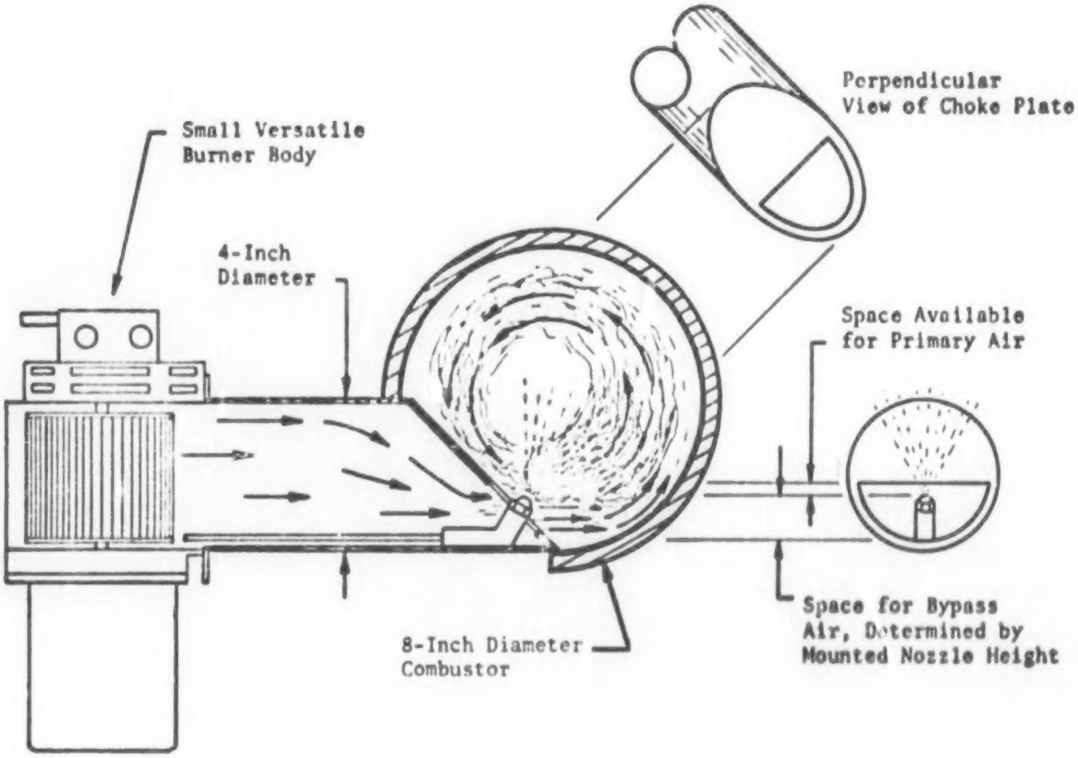
Small Versatile Burner Body
4-Inch Diameter
Perpendicular View of Choke Plate
Space Available for Primary Air
Space for Bypass Air, Determined by Mounted Nozzle Height
8-Inch Diameter Combustor

(b) Prototype B

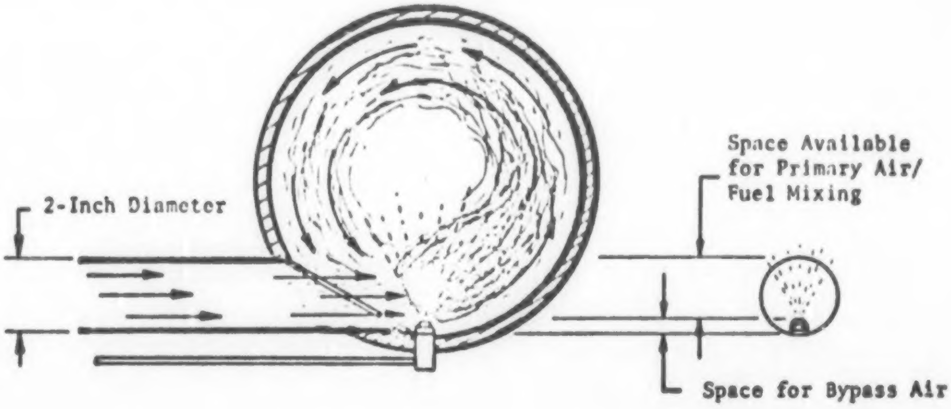
2-Inch Diameter
Space Available for Primary Air/ Fuel Mixing
Space for Bypass Air

Figure 26. Schematic of displaced oil injection burner prototypes constructed and hot fired

with the primary air flow. To accomplish this, the oil nozzle was inserted through the chamber wall and a smaller, 2.0-inch-diameter blast tube was used to concentrate the air flow near the wall and oil spray. No choke plate evaluation hot firings were made and the burner was fired with the straight 2-inch-diameter blast tube. The oil spray, now much closer to the wall, was blown onto the wall insulation and "cooked out," producing excessive white, unburned fuel smoke. No further modifications were made to improve the mixing in the displaced injection prototypes.

Recirculating Combustion Gas Burner

An experimental burner was designed and fabricated that would force mixing between inlet air and combustion gases withdrawn from the combustion chamber. This mixture was then to be used as the air supply for the burner.

The forced recirculation burner was designed so that the recirculated combustion gases were withdrawn from portions of the chamber where heat may have been lost from the gas to the chamber wall and, therefore, the burner to some extent simulated flue gas (i.e., cooled gas) recirculation without the required external ducting. The flow directions are shown schematically in Fig. 27. Air entered at the eight side ports, flowed to the front of the burner, where it made a 180-degree turn, simultaneously mixing with combustion gas drawn in through the 12 end ports. The mixed gases flowed back into the internal cavity of the squirrel cage blower wheel (later replaced by a centrifugal blower wheel), where centrifugal forces generated by the blower forced the gases radially outward into the plenum from which they then flowed through holes in the back plate of the blower wheel, into the blast tube funnel inlet and down the blast tube toward the blast tube exit (burner head). The air flow was regulated by a cover band that slid over the air inlet holes. The combustion gas flow was regulated by the size of the combustion gas inlet holes, which could be plugged or drilled out as necessary. The ignition source was external or manually operated. Figure 28 is a photograph of the assembled burner with a mixed-gas temperature probe (iron/constantan thermocouple) and a mixed-gas sampling port.

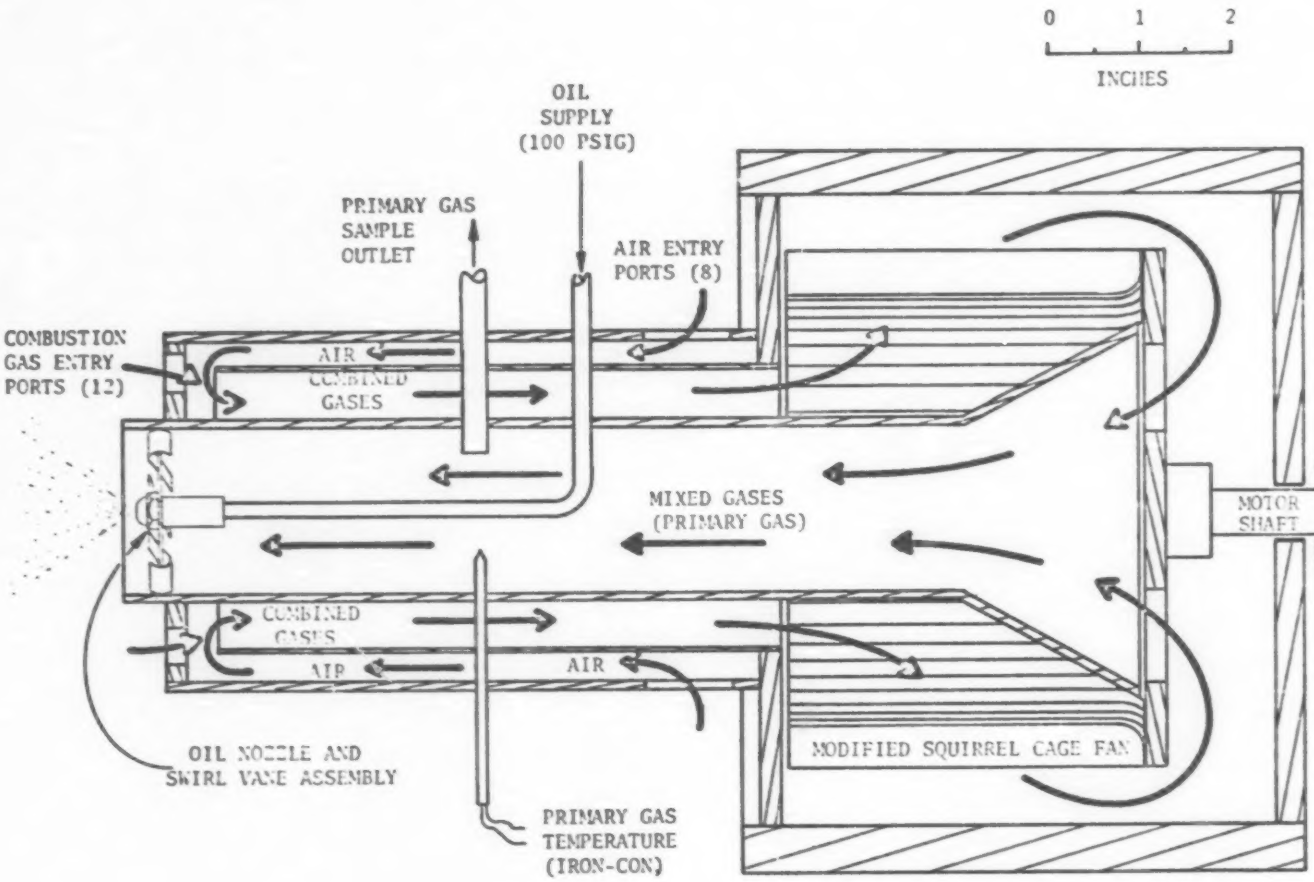
0
1
2
INCHES
OIL SUPPLY (100 PSIG)
PRIMARY GAS SAMPLE OUTLET
AIR ENTRY PORTS (8)
COMBUSTION GAS ENTRY PORTS (12)
AIR
COMBINED GASES
MIXED GASES (PRIMARY GAS)
MOTOR SHAFT
COMBINED GASES
AIR
AIR
OIL NOZZLE AND SWIRL VANE ASSEMBLY
MODIFIED SQUIRREL CAGE FAN
PRIMARY GAS TEMPERATURE (IRON-CON)

Figure 27. Schematic of the forced recirculated combustion gas experimental burner

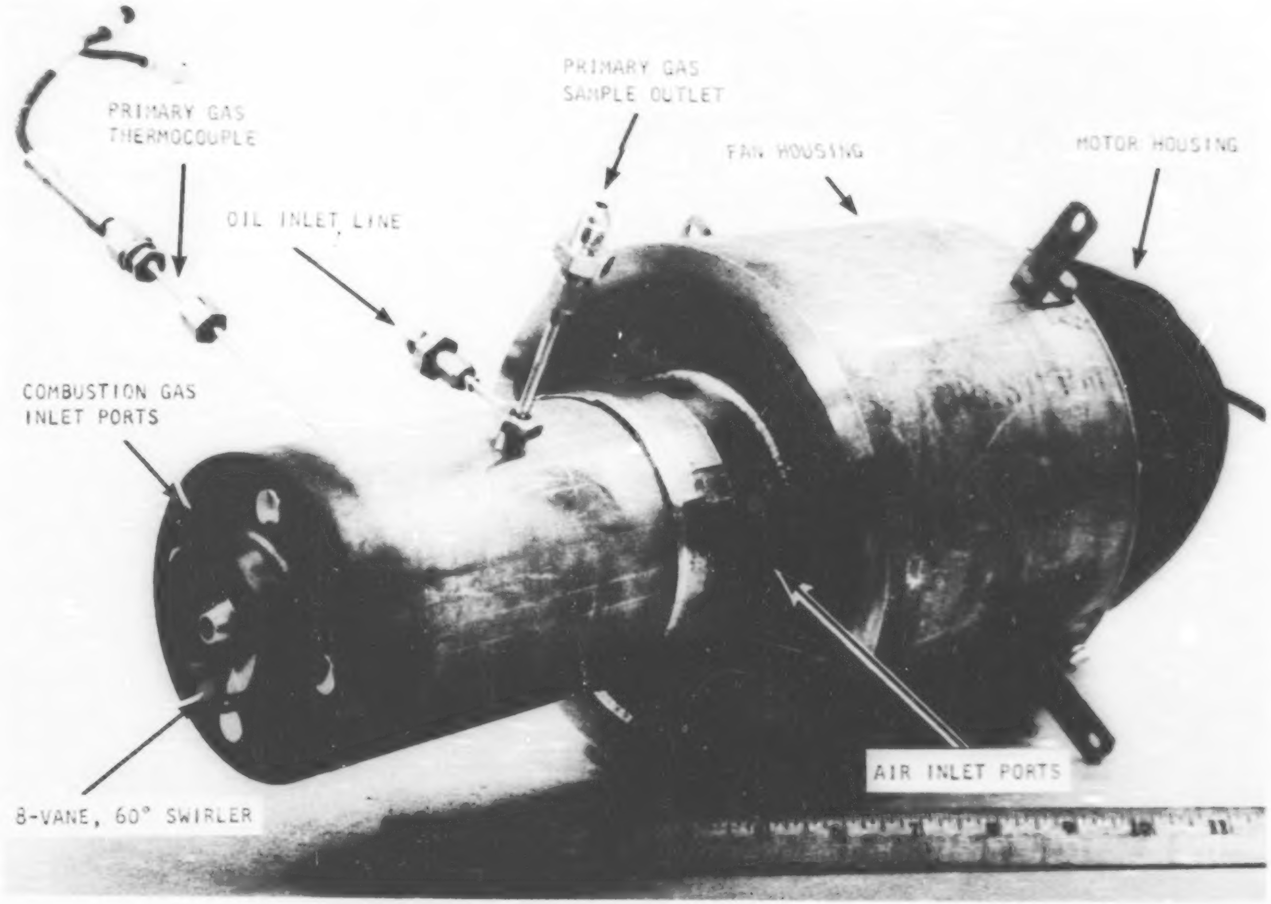
PRIMARY GAS THERMOCOUPLE
PRIMARY GAS SAMPLE OUTLET
FAN HOUSING
MOTOR HOUSING
OIL INLET LINE
COMBUSTION GAS INLET PORTS
AIR INLET PORTS
8-VANE, 60° SWIRLER

5AD24-6/27/73-S1A

Figure 28. Photograph of the forced recirculating combustion gas burner (fully instrumented) with an 8-vane, 60-degree swirler ring, and 4 of 12 combustion gas inlet ports plugged

Heated Air Burner

The heated air, oil burner concept was investigated as a part of a three-stage combustion burner concept. The preheating of inlet air was to be the initial conditioning for the first, fuel-rich combustion stage. The heated air burner was designed and fabricated to investigate the effect of the inlet air temperature on exhaust emissions, especially that of smoke emission. The added stage of preheating the inlet air was intended to accelerate the primary combustion process (fuel-rich combustion) by prevaporization and thus avoid quenching the air/hydrocarbon kinetics in the free-carbon stage, thereby inhibiting the formation of smoke. High smoke emission levels are a common problem in two-stage combustion processes, as the free carbon from the primary stage is not easily oxidized in the secondary combustion stage. Figure 29 shows a schematic of the heated air burner assembly. The system utilized the Carlin 250 FFD burner body to provide the air and oil flows, a 16-inch-diameter by 22-inch-long, sealed air shroud, and a 2-inch-diameter burner head with an eight-vane, 75-degree swirler ring. An iron-constantan thermocouple mounted near the entrance to the burner head measured the preheated air temperature which reached as high as 590 F.

OIL NOZZLES

All oil burners tested were of the high-pressure atomizing type. These burners all used high pressure (100 to 300 psig), swirl atomizing, simplex nozzles requiring only oil supplied at high pressure for spray atomization. Figure 30 shows a cross-section schematic of a typical nozzle. The high-pressure oil flows through the filter, then the flow direction is aligned axially by the flow distributor body for a controlled entrance into the swirl plug. The swirl plug contains a number of slots (oil flow channels) that direct flow tangentially into the swirl cavity, imparting rotational energy to the oil flow before it is discharged through the discharge orifice. The combination of the small orifice size and high swirl

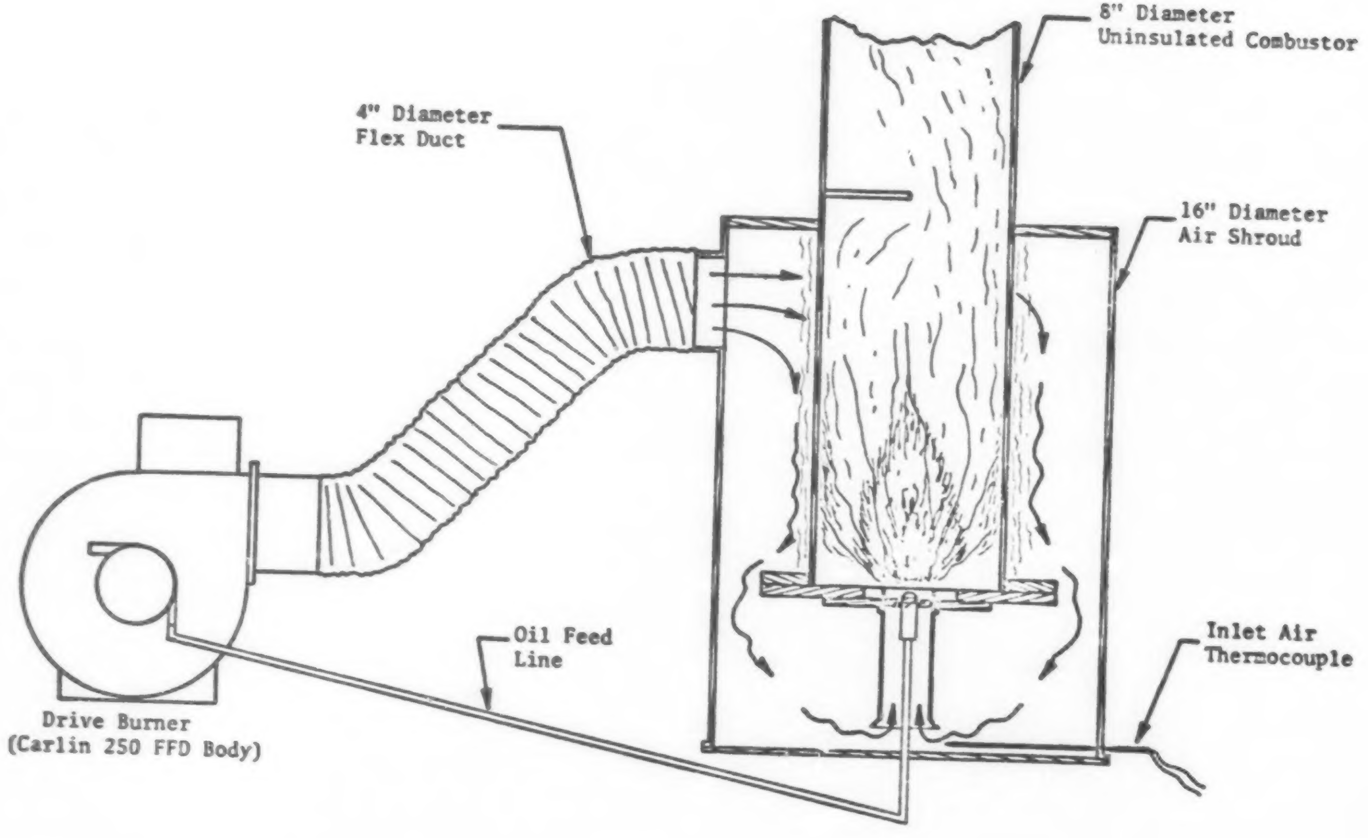
8" Diameter
Uninsulated Combustor
4" Diameter
Flex Duct
16" Diameter
Air Shroud
Oil Feed
Line
Inlet Air
Thermocouple
Drive Burner
(Carlin 250 FFD Body)

Figure 29. Schematic of the preheated air burner test apparatus using a 2-inch-diameter blast tube with an 8-vane, 75-degree swirl ring, and a 0.75-80°-C oil nozzle

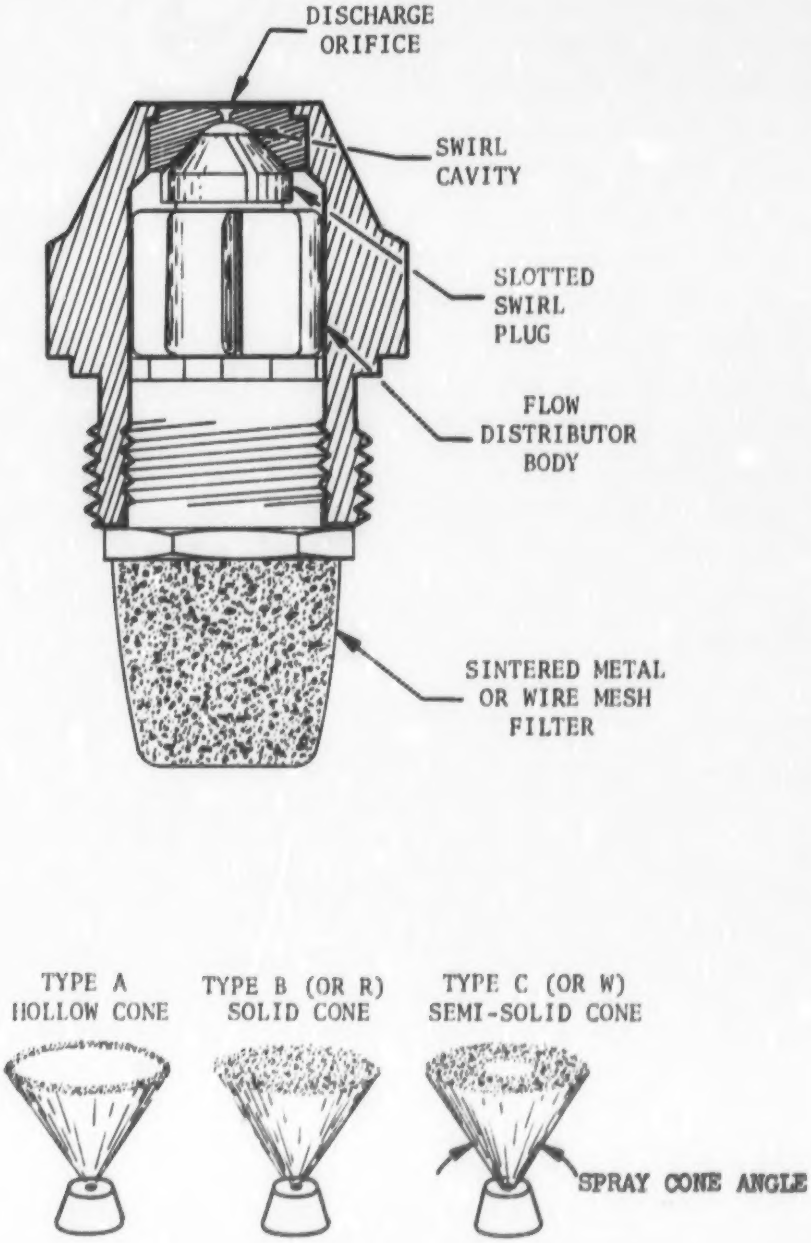
DISCHARGE ORIFICE
SWIRL CAVITY
SLOTTED SWIRL PLUG
FLOW DISTRIBUTOR BODY
SINTERED METAL OR WIRE MESH FILTER
TYPE A HOLLOW CONE
TYPE B (OR R) SOLID CONE
TYPE C (OR W) SEMI-SOLID CONE
SPRAY CONE ANGLE

Figure 30. Cross-sectional schematic showing the internal construction of a typical high-pressure oil atomizing nozzle and the various spray cone patterns

(rotational energy) causes the oil to self-atomize without requiring the addition of more energy from other sources. The resulting droplets are very small, with the mass median dropsize ($\overline{D}$), less than 100 microns (1 micron = 10^{-6} meters) up to nozzles as large as 25-gph flowrate at 100-psig oil supply pressure. Various combinations of discharge orifices and swirl plugs produce a variety of spray patterns which are generally categorized into three groups: hollow cone, solid cone, and semi-solid cone. Figure 30 shows these three spray patterns and their type of nomenclature. The hollow cone pattern is generally recommended for the 0.5- to 3.0-gph burners and the solid cone pattern for the larger burners. The spray cone angle is usually recommended by the burner manufacturer for each specific burner and it is an important parameter in mixing and also flame front stability, especially in "conventional" (nonflame-retention head) oil burners. The nozzles are labeled according to their nominal oil flowrate (gph at 100 psig), the spray cone angle (degrees) and the spray pattern type.

Except where otherwise noted, oil nozzles used in the experimental studies described herein were manufactured for oil burner applications by Delavan.

EXPERIMENTAL RESULTS

Presented in this section are discussions and results of experimental studies conducted with the oil burner apparatus. It is separated into: (1) Atomization Measurements, (2) Commercial Burner Studies, (3) Interpretation of Commercial Burner Results, (4) Burner Geometry Optimization Studies, (5) Optimum Burner Operation, and (6) Nonconventional Burner Studies.

The section on atomization results is a description of experiments conducted to determine the spray dropsize distributions produced by typical oil burner atomizers. These experiments were carried out using a molten wax technique which allowed collection and sizing of solidified droplets.

The description of commercial burner studies includes experimentally measured air velocity vectors, combustion gas velocity vectors, oil spray patterns, combustion gas composition patterns, flue gas emissions, and combustion chamber wall temperature effects.

The interpretation of commercial burner results includes a detailed discussion of the rationale behind selection of the versatile burner design with the rationale being based on the commercial burner studies and related to consideration of well-stirred versus plug flow combustion processes.

The description of versatile burner studies includes a description of the reasons for the versatile burner design and a description of versatile burner geometry variation studies which led to the optimum burner geometry design criteria.

Description of the optimum burner operation involves the fabrication and operation of two burners, the designs of which were based on the optimum criteria developed from the versatile burner studies. Included are comparisons with commercial burners, showing the beneficial effects of the optimum designs.

The unique concepts section describes experimental results obtained with a number of burners of very nonconventional design, including some which are not fired in refractory-lined combustion chambers.

ATOMIZATION MEASUREMENTS

Conical spray nozzles for use with No. 2 distillate fuel oil burners are available from various manufacturers. Such nozzles vary in flowrate, conical spray angle, and spray density patterns. Solid-cone spray nozzles have a more or less uniform spray mass flux over the circular spray area, and hollow-cone spray nozzles have high mass flux near the outer edges of the circular spray pattern. Intermediate nozzles have lower spray mass flux in some central portions of the circular area than on the outside, but the difference is not as extreme as for hollow-cone sprays. Figure 30 in the Apparatus section shows these differences schematically.

Five oil burner spray nozzles were wax flowed, each at three different pressures, nominally 75, 100, and 125 psig. The experimental data from these wax flows, in terms of mass median diameter of the collected frozen wax particles, are presented graphically in Fig. 31. The oil spray nozzle designations given in Fig. 31 have three terms, e.g., 0.75-80°C. The first term (0.75) is the rated oil flowrate at 100-psi pressure drop. The second term (80°) is the full included angle of the spray cone produced. The last term ("C") is an indication of the nature of the spray pattern, "A" being a hollow cone, "B" or "R" being a solid cone, and "C" or "W" being a semisolid cone (see Fig. 30). The nozzles tested were all in the residential-size range of 0.5- to 1.5-gph rated flow at 100-psig pressure. At the

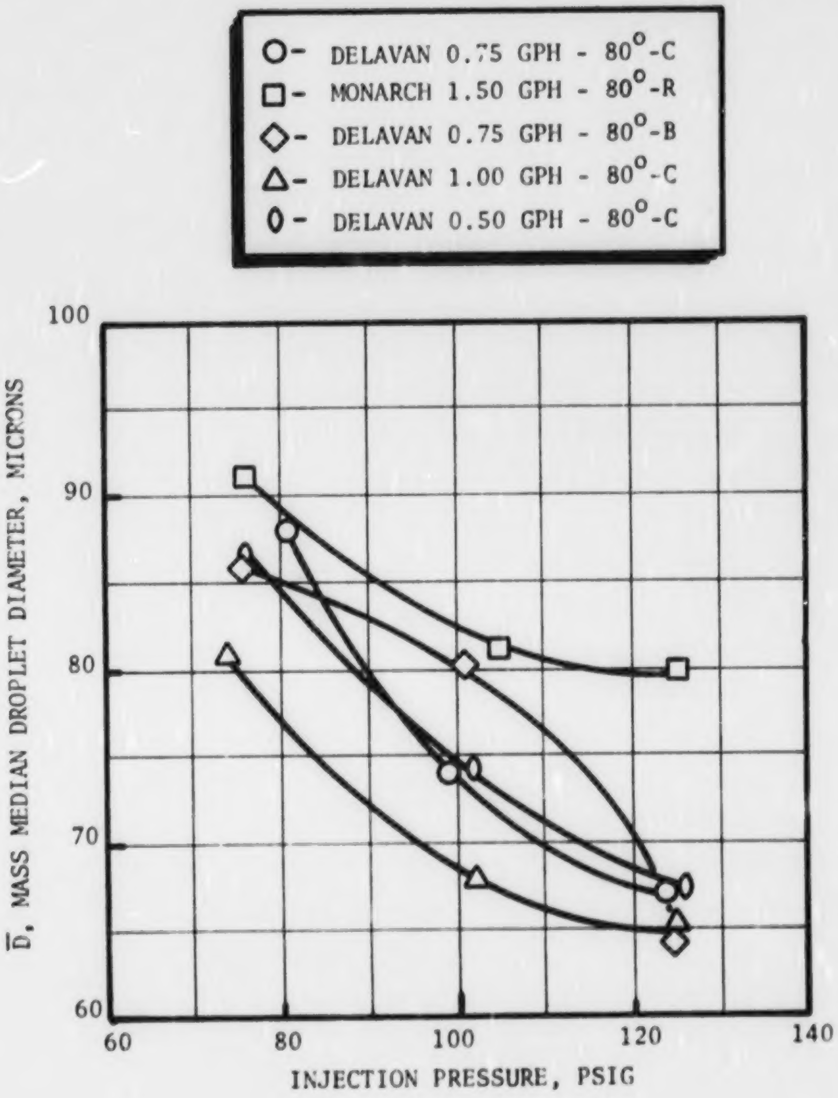

Figure 31. Spray dropsize data obtained using the method of frozen wax on various oil burner spray nozzles

rated pressure of 100 psig, these residential-size burners typically produced mass median particle diameters of approximately 75 microns.

Shown in Fig. 32 are mass median droplet size data reported in a Delavan nozzle brochure. When extrapolated down to the residential nozzle size range, the value of 75 microns is in agreement with the Delavan curve, despite the use of a different fluid and a different droplet size experimental determination technique.

Size distribution curves for the tests conducted at a nominal wax spray pressure of 100 psig are shown in Fig. 33 through 37. Except for left-to-right expansion, these curves differ very little in basic shape. The curves shown are cumulative fraction curves, the derivatives of which yield the familiar bell curve. All of the distribution curves shown in Fig. 33 through 37, were obtained by sizing of the collected particles on a Sharples micromerograph, a sedimentation-in-air analyzer. For one case, the particles size analysis was checked by means of standard sieves, and the comparison shown in Fig. 38 was obtained. It is noted that the mass median particle diameter determined by the sieving technique was approximately 10-percent smaller than that obtained by the micromerograph technique. The reason for the 10-percent discrepancy is not apparent, and its magnitude was not sufficiently large to provoke a thorough investigation.

COMMERCIAL BURNER STUDIES

To provide a baseline for later development studies, several commercial burners were characterized.

Commercial burners experimentally evaluated to determine pollutant formation and emission characteristics included three burners sized for residential applications (~ 0.75 gph) and three larger burners (6 to 12 ghp). Table 7 presents data pertinent to these burners.

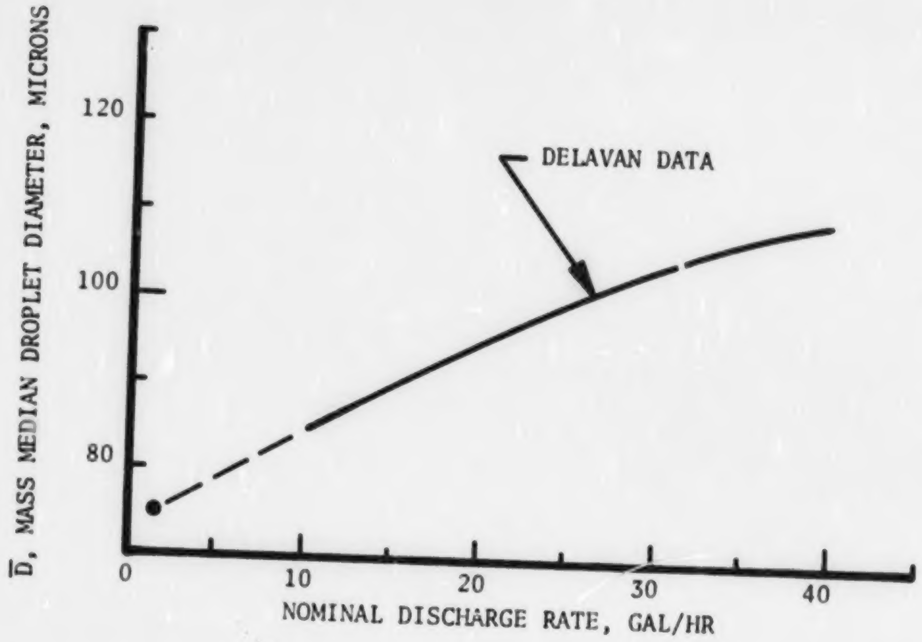

Figure 32. Extrapolation of Delavan data to the mass median particle diameter obtained for the Delavan 0.75-gph/80°-C nozzle

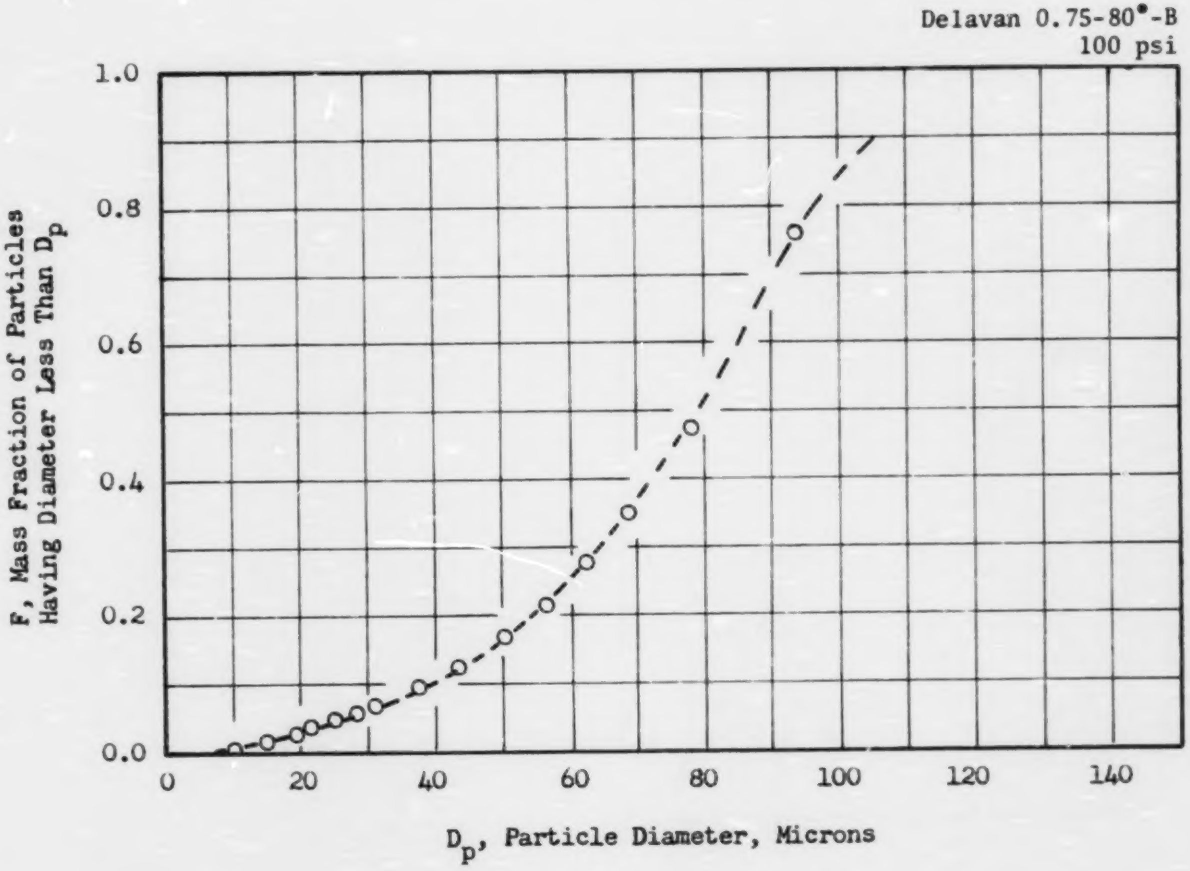

Figure 33. Spray dropsize distribution for a Delavan 0.75-80°-B nozzle at 100-psi pressure (micromerograph analysis)

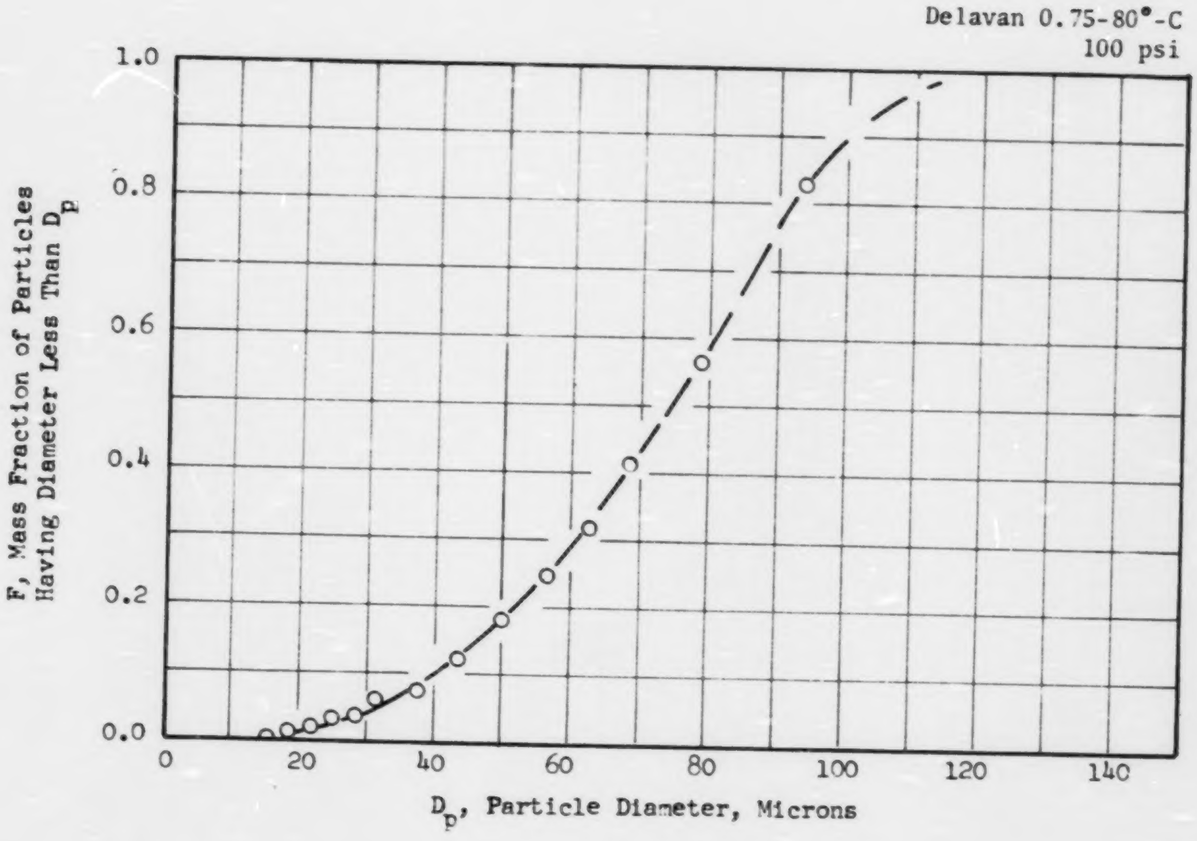

Figure 34. Spray dropsize distribution for a Delavan 0.75-80°-C nozzle operating at 100 psi (micromerograph analysis)

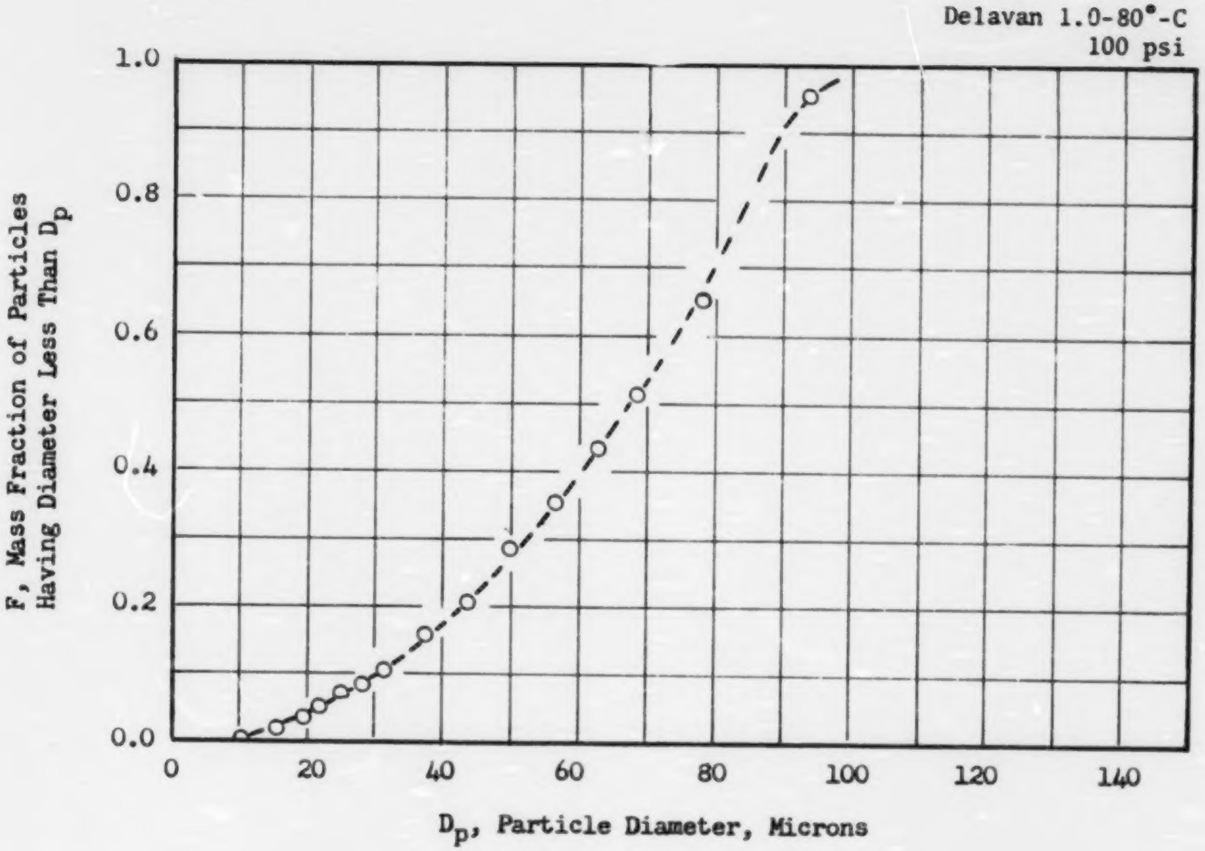

Figure 35. Spray dropsize distribution for a Delavan 1.00-80°-C nozzle at 100-psi pressure (micromerograph analysis)

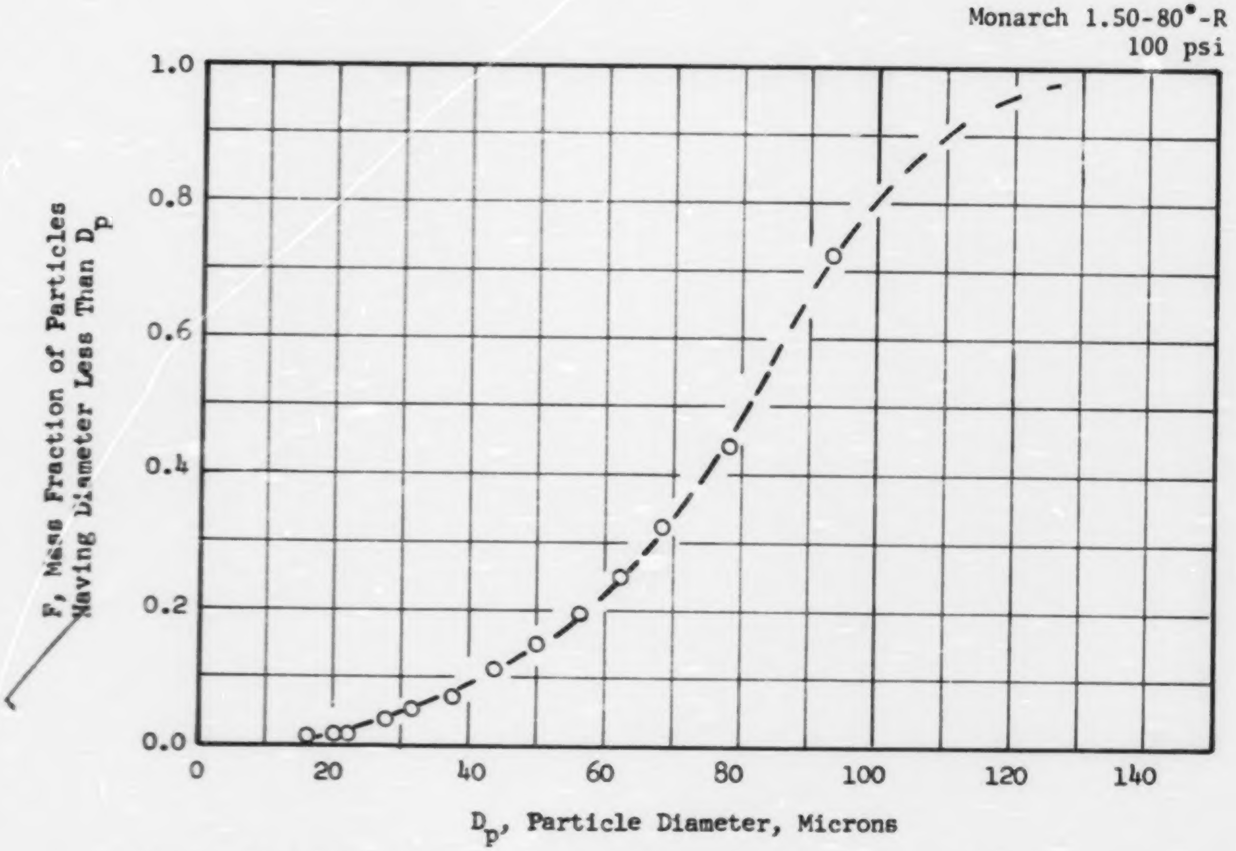

Figure 36. Spray dropsize distribution for a Monarch 1.50-80°-R nozzle at 100-psi pressure (micromerograph analysis)

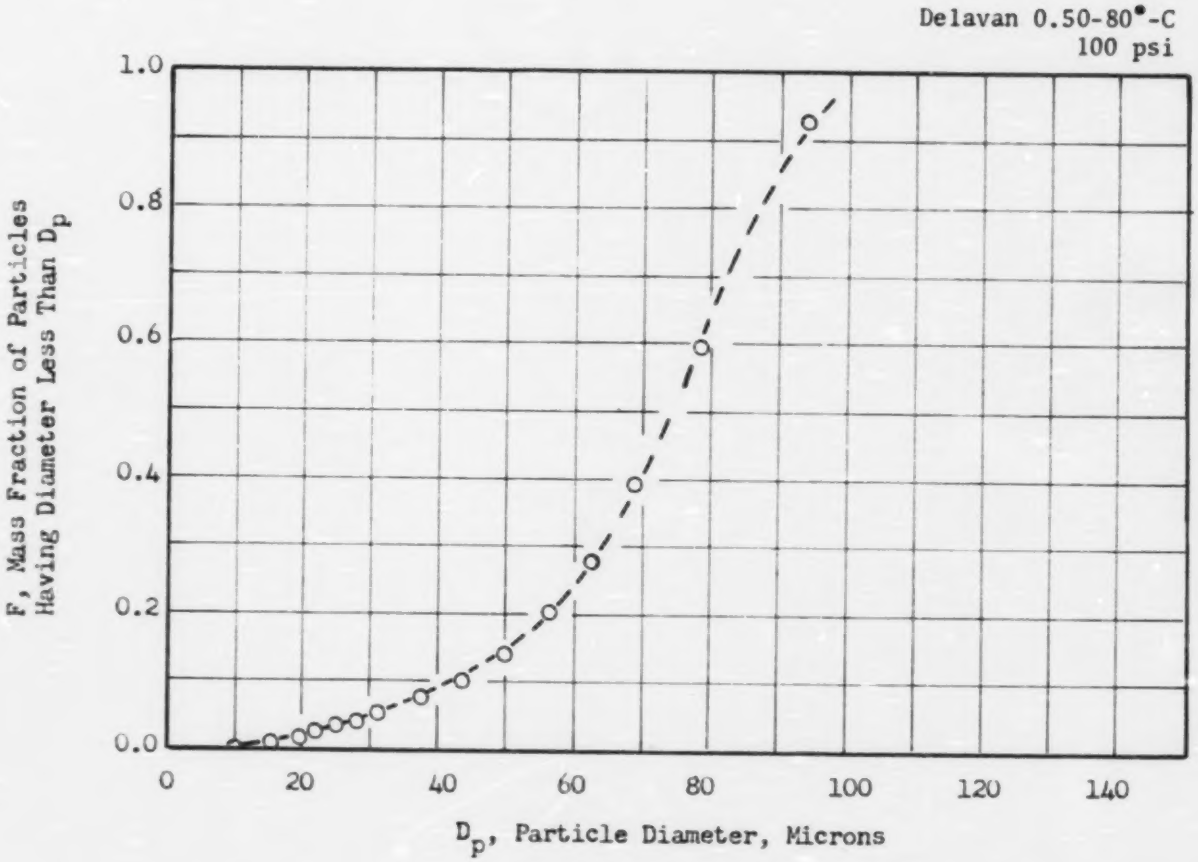

Figure 37. Spray dropsize distribution for a Delavan 0.50-80°-C nozzle at 100-psi pressure (micromerograph analysis)

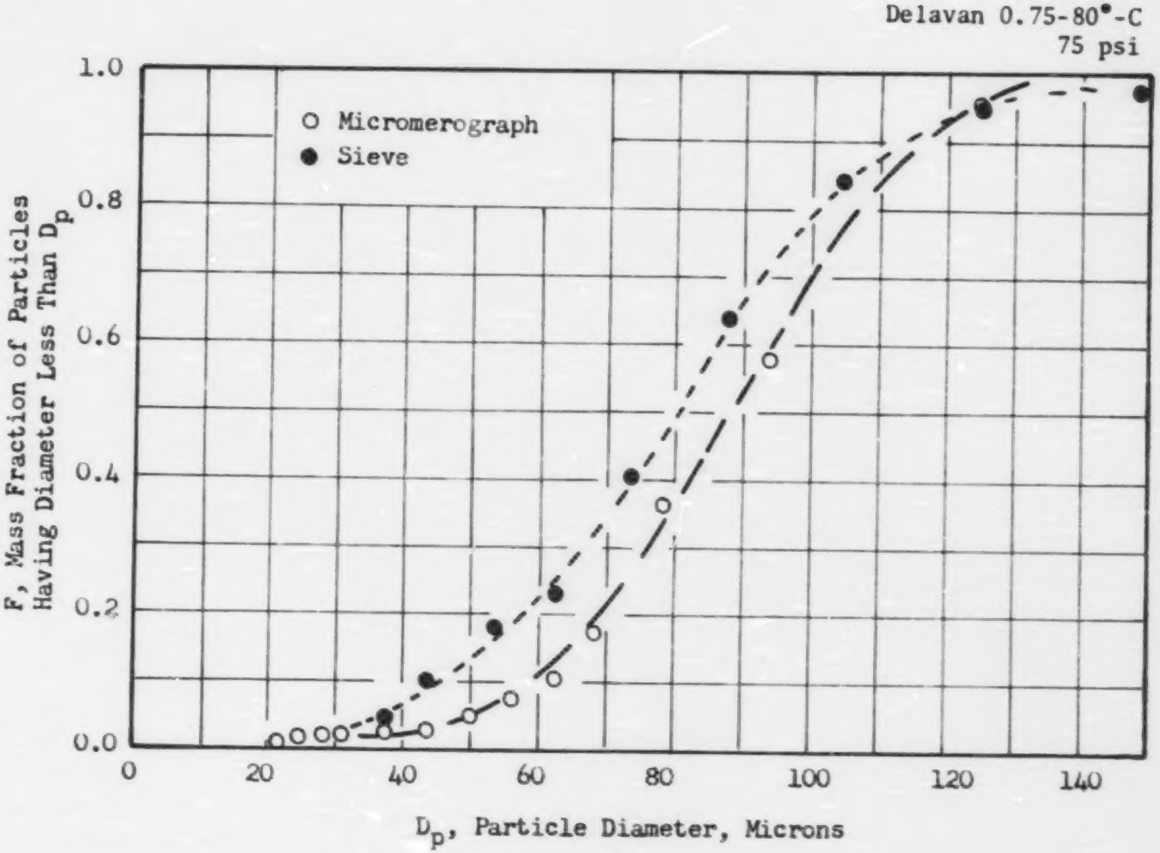

Figure 38. Spray dropsize distribution for a Delavan 0.75-80°-C nozzle at 75-psi pressure (comparison of frozen wax particle analyses by micromerograph, sedimentation in air, and sieve techniques)

Table 7. COMMERCIAL BURNERS EVALUATED EXPERIMENTALLY

Model	Manufacturer	Oil Flowrate, gph	Type
55-J-1	ABC	0.60 to 1.10	Nonflame Retention
Mite	ABC	1.00 to 1.25	Flame Retention
AFC	Union (Beckett)	0.50 to 2.50	Flame Retention
Nu-Way "CO"	White-Rodgers	6.00 to 10.00	Nonflame Retention
250 FFD	Carlin	5.00 to 12.00	Flame Funnel Retention
PHC-34	Sun Ray Burner	5.00 to 14.00	Flame Retention

The experimental studies included determination of smoke, unburned hydrocarbons, carbon monoxide, and nitric oxide emissions. Typically, at conditions under which low smoke emissions are obtained, the unburned hydrocarbon and carbon monoxide emissions tend to be acceptably low, while nitric oxide emissions may or may not be low, depending on the burner design. The crux of the problem, therefore, is achieving complete fuel combustion (i.e., no smoke, unburned hydrocarbons, or carbon monoxide in the exhaust), while simultaneously minimizing nitric oxide formation. Among the experimental results obtained with the commercial burners, those which have been most enlightening with respect to nitric oxide minimization are the velocity vector and combustion gas composition profiles in the combustion zones just downstream of the end of the burner blast tube.

The results obtained with each of the burners in Table 7 are presented separately below, after which, the results are discussed and interpretated collectively.

ABC Model 55-J Burner (0.75 gph)

The ABC 55-J is one of the most common types of residential-size No. 2 distillate fuel oil burners in use in the U.S.A. The end of its blast tube provides a restriction from 4-1/8 to 2 inches, with six peripheral swirler vanes. The oil spray nozzle is located in the center and toward the blast tube end, with electrodes just upstream for purposes of ignition.

Since the 55-J was accepted as a "standard" oil burner, it was subjected to the most extensive testing of any of the burners used in the program. Measurements performed with this burner included: (1) cold-flow air velocity vector measurements in both an 8- and an 11-inch-ID coaxial cylindrical chamber, (2) cold-flow oil mass flux determinations, (3) furnace flue gas sampling, (4) combustion gas velocity vector determinations, (5) combustion gas composition pattern measurements, and (6) mixed combustion gas composition output from an 8-inch-diameter coaxial cylindrical combustion chamber.

Cold-flow air velocity vector measurements involved determination of the dynamic head and flow angles α and β, as described previously in the Experimental Apparatus section. These measurements were made on both horizontal and vertical diameters at axial locations 1.5, 3, and 6 inches downstream of the end of the blast tube. The velocity vectors include the axial, tangential, and radial components of the measured velocities. Figures 40 and 41 show the experimental data in the horizontal and the vertical planes at the 1.5-inch axial location. It is readily apparent that there is significant nonsymmetry with respect to the centerline axis (represented by zero radius in Fig. 40 and 41) of the burner blast tube. The nonsymmetrical characteristics are apparently induced by effects due to the locations of the blower wheel, the blower inlet, the ignition system, and the static pressure plate, all of which are relatively close to the exit of the short blast tube. As previously discussed, the β angle infers rotation of the flow as it progresses down the chamber. At the 1.5-inch axial location in the horizontal plane, the β angle reaches a value of approximately ±20

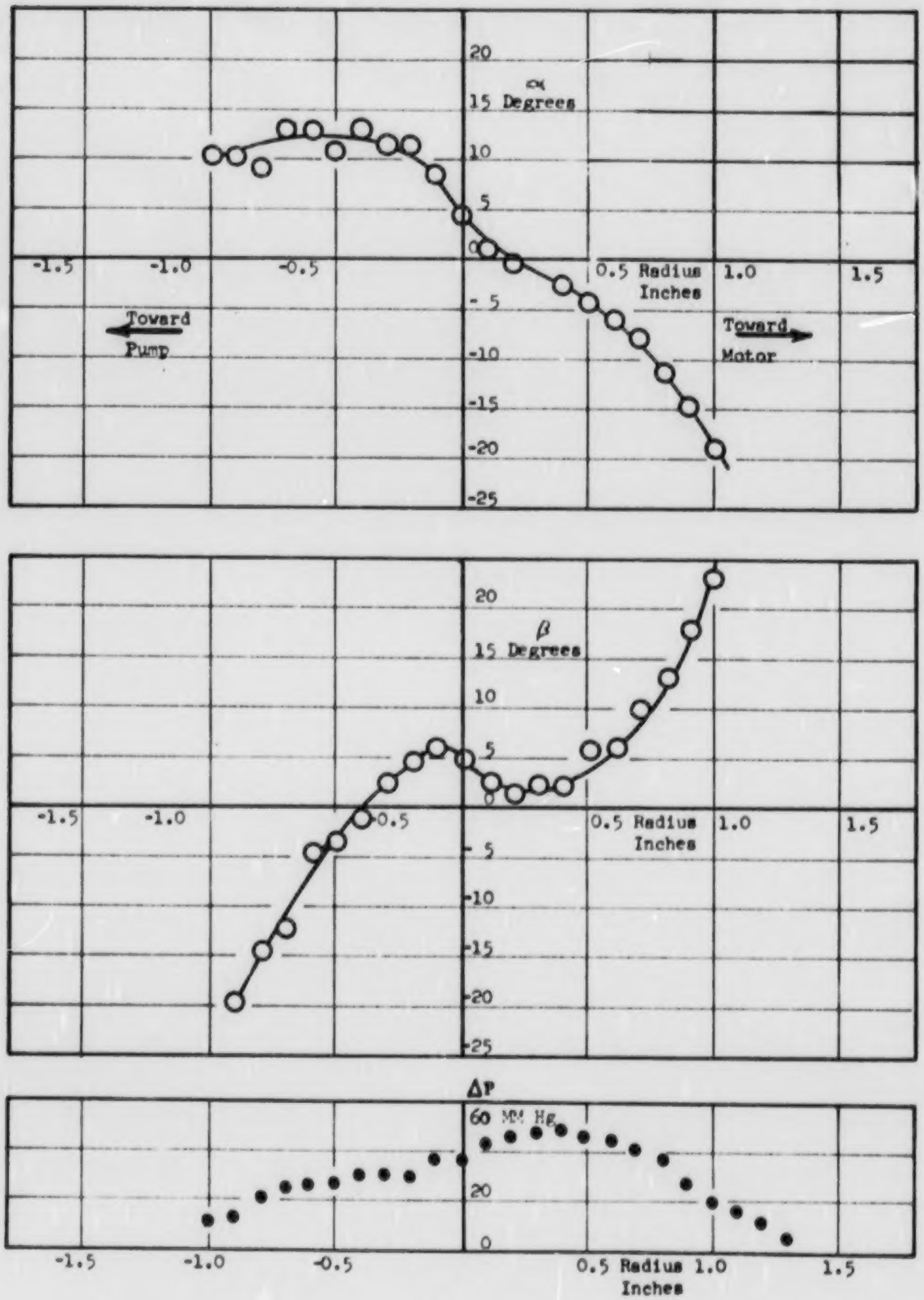

Figure 40. Air flow parameters at 1.5 inches downstream in the horizontal plane of a 55-J burner

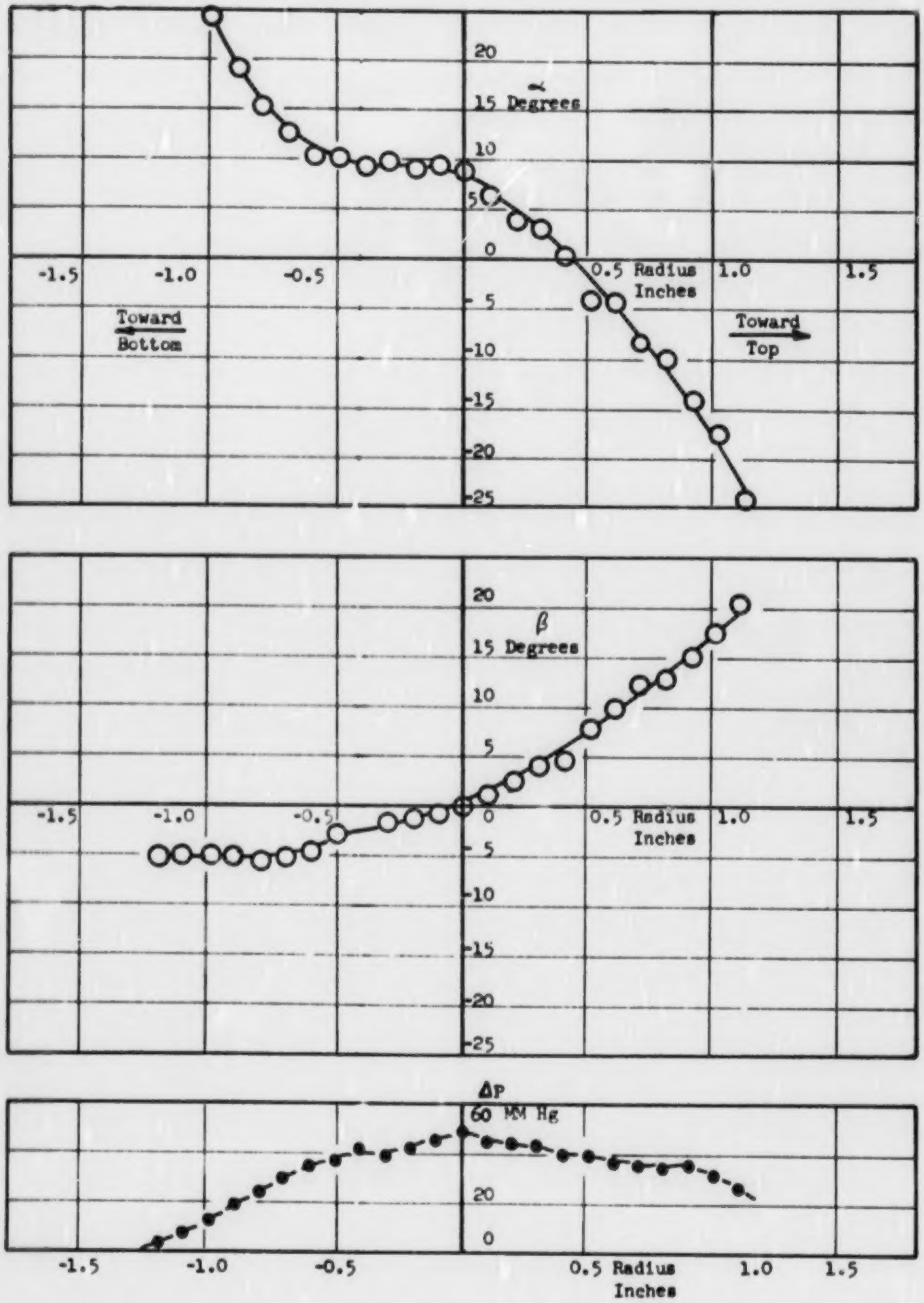

Figure 41. Air flow parameters at 1.5 inches downstream in the vertical plane of a 55-J burner

degrees at radii of ±1 inch, while α at the same point is also approximately 20 degrees. These experimental values can be shown to infer that the airflow at the point in question is rotating approximately 22 degrees about the burner axis for each inch of axial travel. It would be expected, therefore, that should these α and β angles remain constant, a 90-degree rotation would be achieved in approximately 4 inches of axial travel. In reality, as shown in Fig. 42 through 45, the β angle decreases as the flow continues downstream (primarily due to the cone-shaped expansion of the flow), and a 90-degree rotation would therefore require somewhat more than 4 inches of axial travel. A 90-degree rotation of the flow for every few inches of axial travel is realistic. As shown in Fig. 40 through 45, the nonsymmetry of the flow patterns persists even to the 6-inch downstream axial position.

The figures showing flow angles α and β , and dynamic head, ΔP, accurately describe the flow; however, it is easier to visualize the flow patterns if they are presented as linear vectors as in Fig. 46 and 47. The vectors shown in Fig. 46 and 47 represent those components of the air velocity which are in the plane represented by the paper. In general, each velocity vector shown in Fig. 42 and 43 has an additional component (the tangential velocity component) either into or out of the paper, but that component is not shown since the paper has only two dimensions.

Assessment was desired of the effects of chamber dimensions on the air velocity patterns created by the 55-J burner. The measurements carried out with the 8-inch-ID, coaxial, cylindrical combustion chamber were repeated with a larger diameter (11 inches) chamber. The results of the larger chamber dimensions are shown in Fig. 48 and 49 which compare air velocity vectors in the two different diameter chambers. The difference in chamber dimensions is seen to have a measurable, but not a significant effect on the flow patterns.

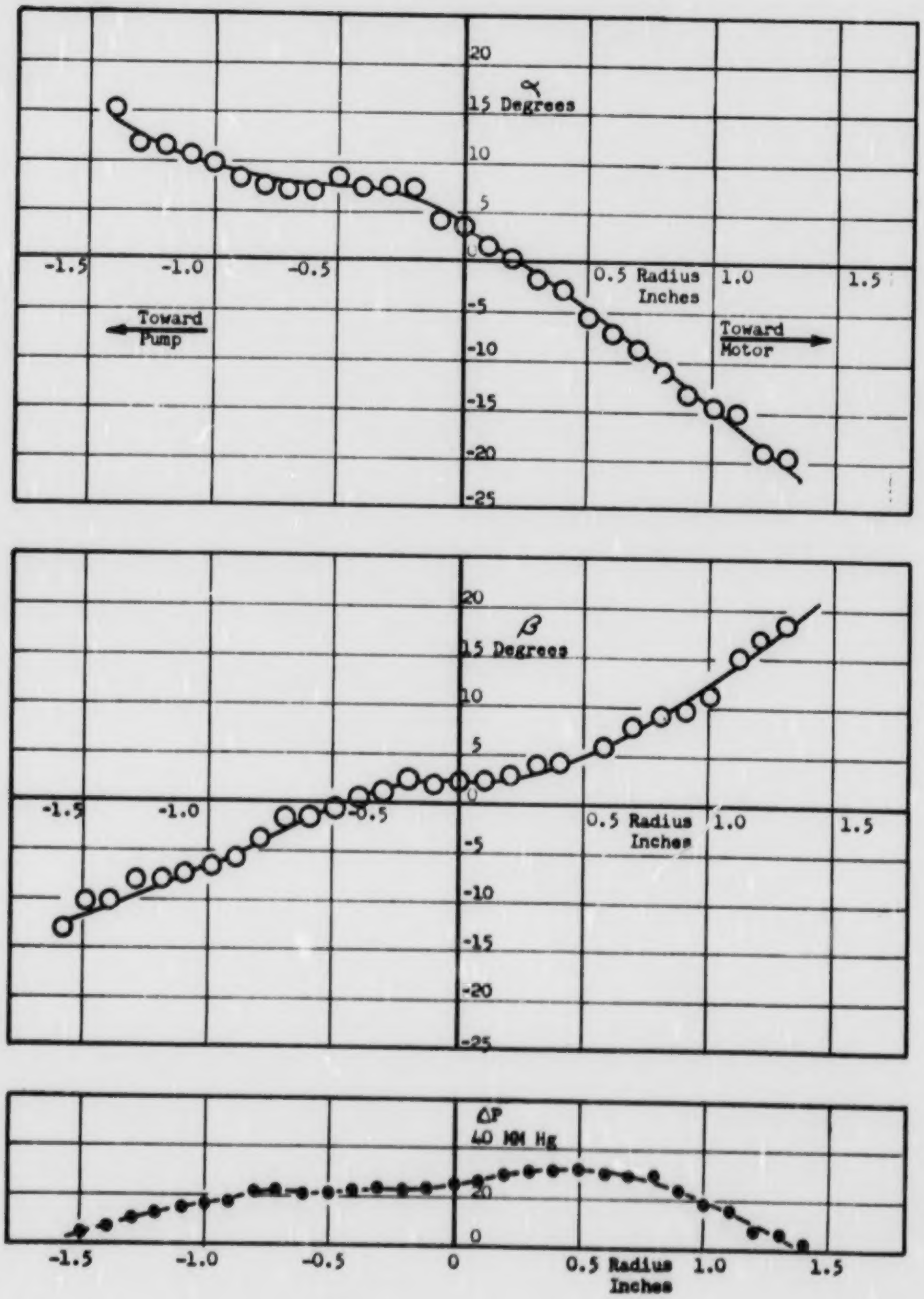

Figure 42. Air flow parameters at 3 inches downstream in the horizontal plane of a 55-J burner

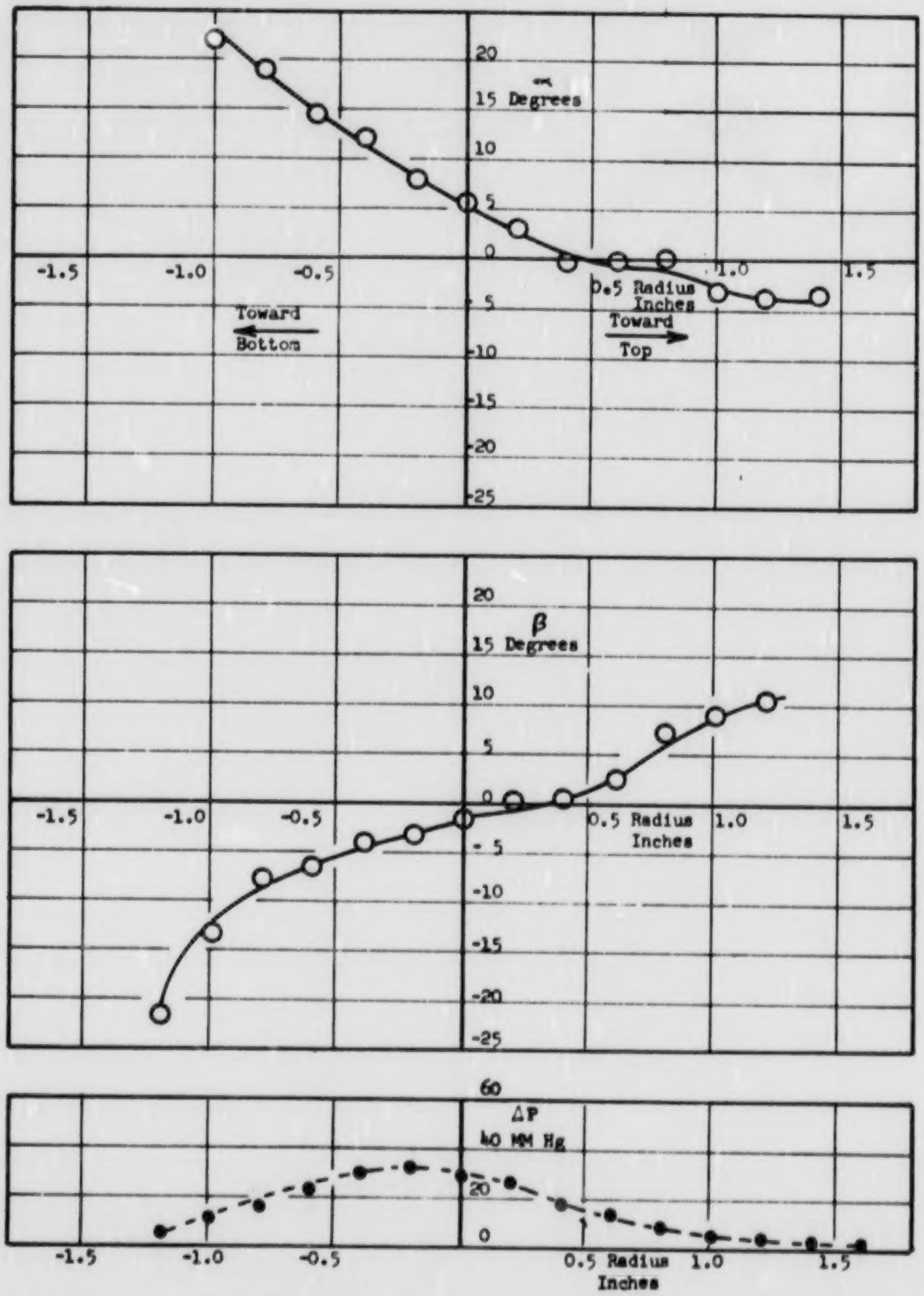

Figure 43. Air flow parameters at 3 inches downstream in the vertical plane of a 55-J burner

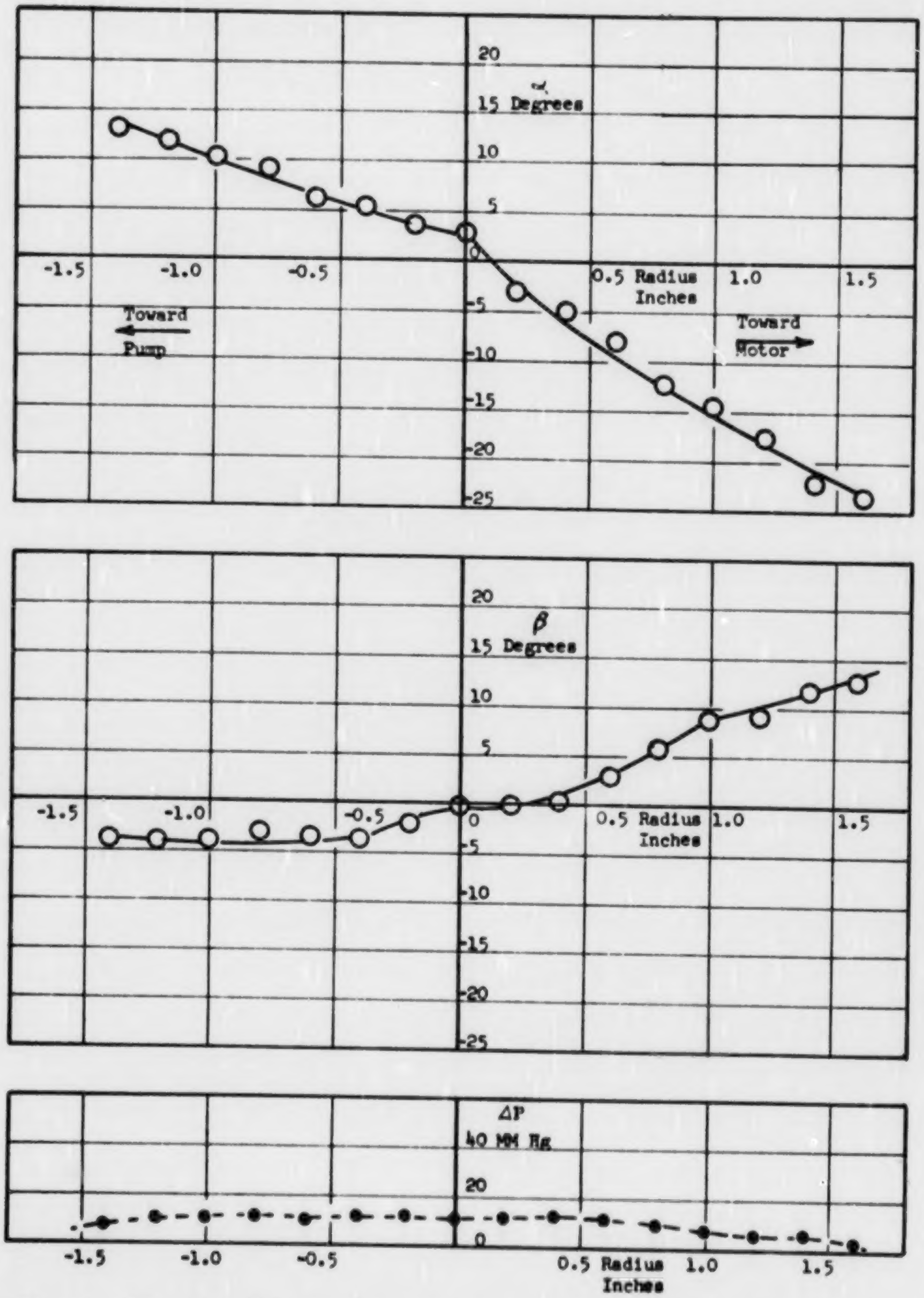

Figure 44. Air flow parameters at 6 inches downstream in the horizontal plane of a 55-J burner

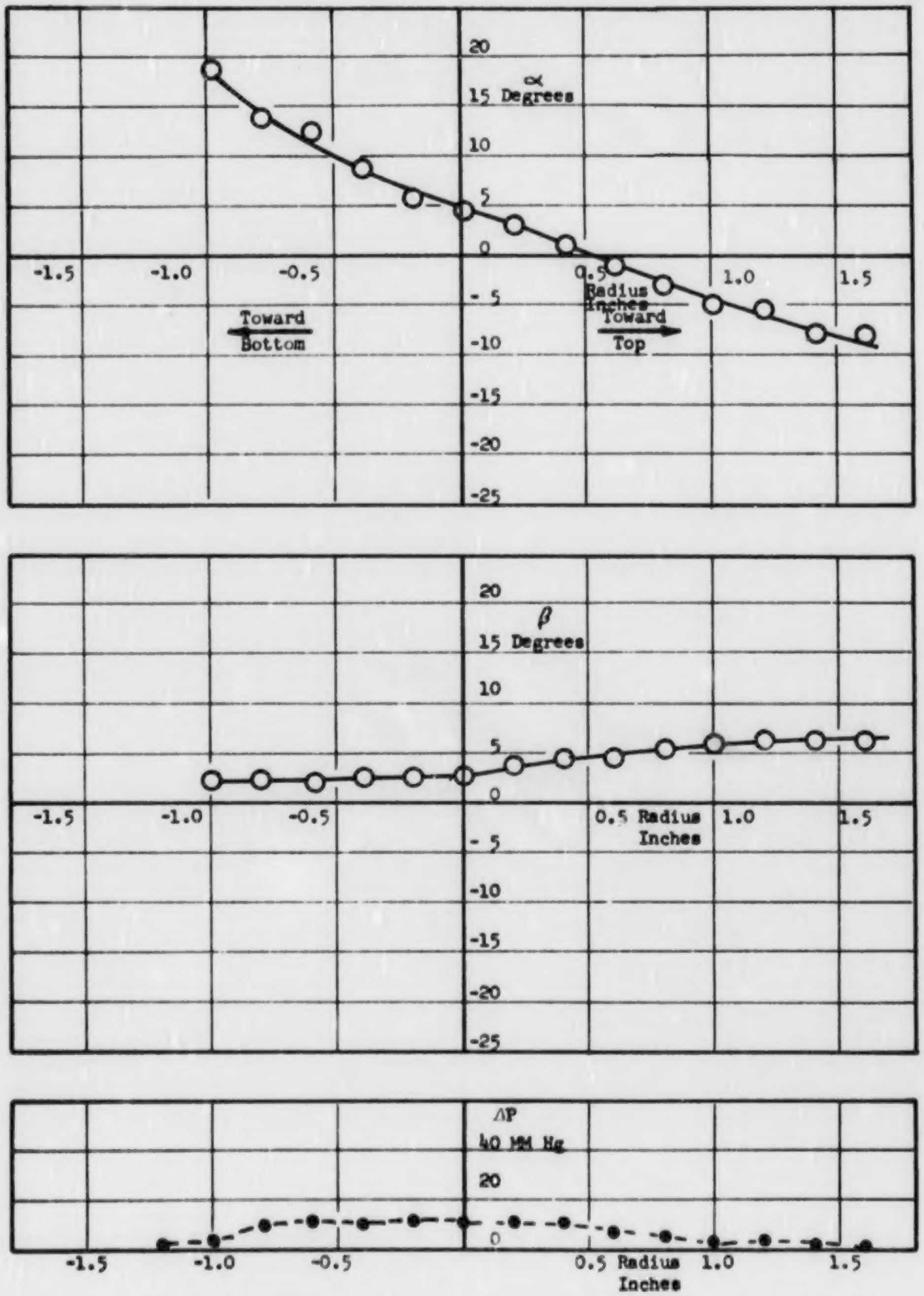

Figure 45. Air flow parameters at 6 inches downstream in the vertical plane of a 55-J burner

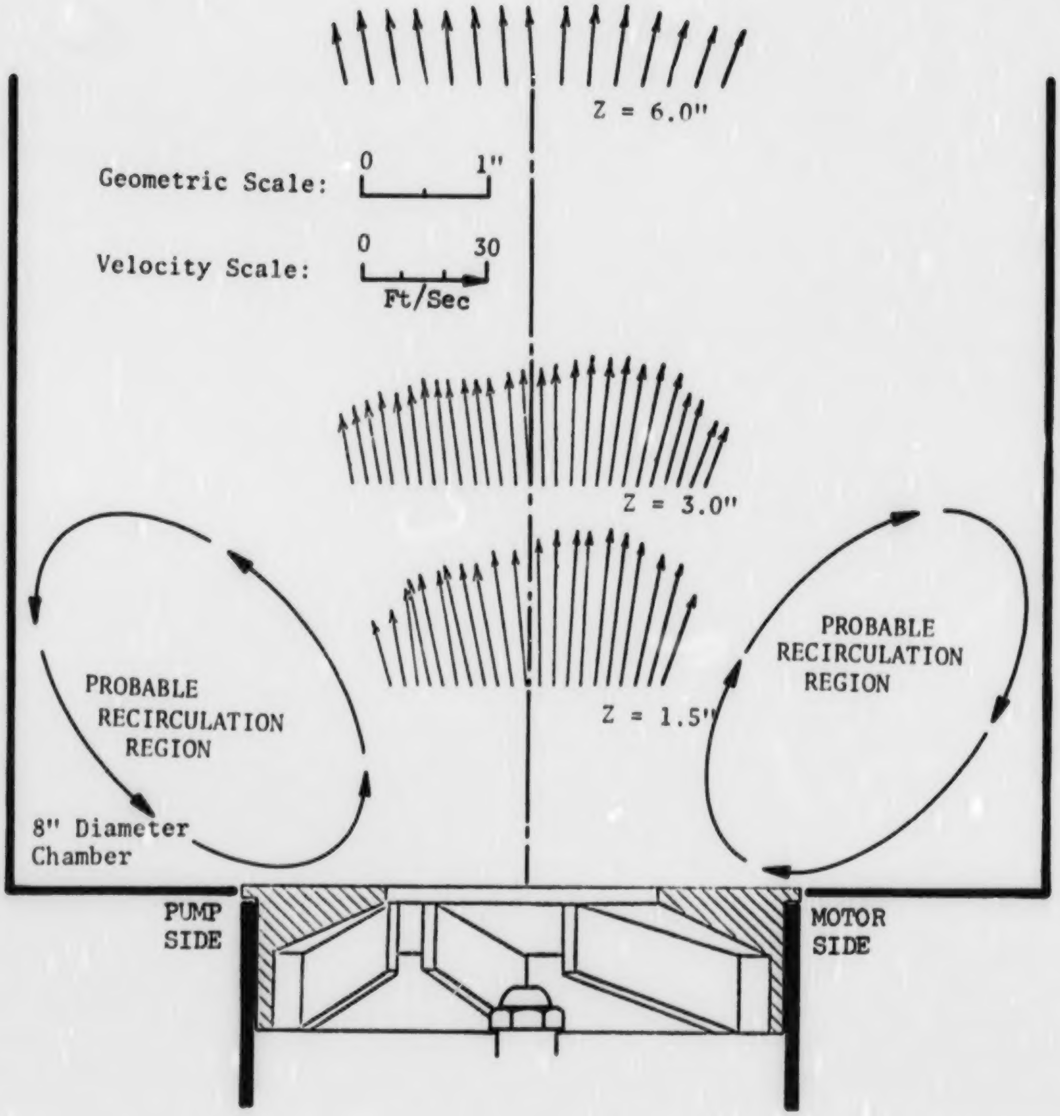
Z = 6.0"
Geometric Scale:
0
1"
Velocity Scale:
0
30
Ft/Sec
Z = 3.0"
Z = 1.5"
PROBABLE RECIRCULATION REGION
PROBABLE RECIRCULATION REGION
8" Diameter Chamber
PUMP SIDE
MOTOR SIDE

Figure 46. Measured cold-flow air velocity vectors in the horizontal plane of a 55-J burner

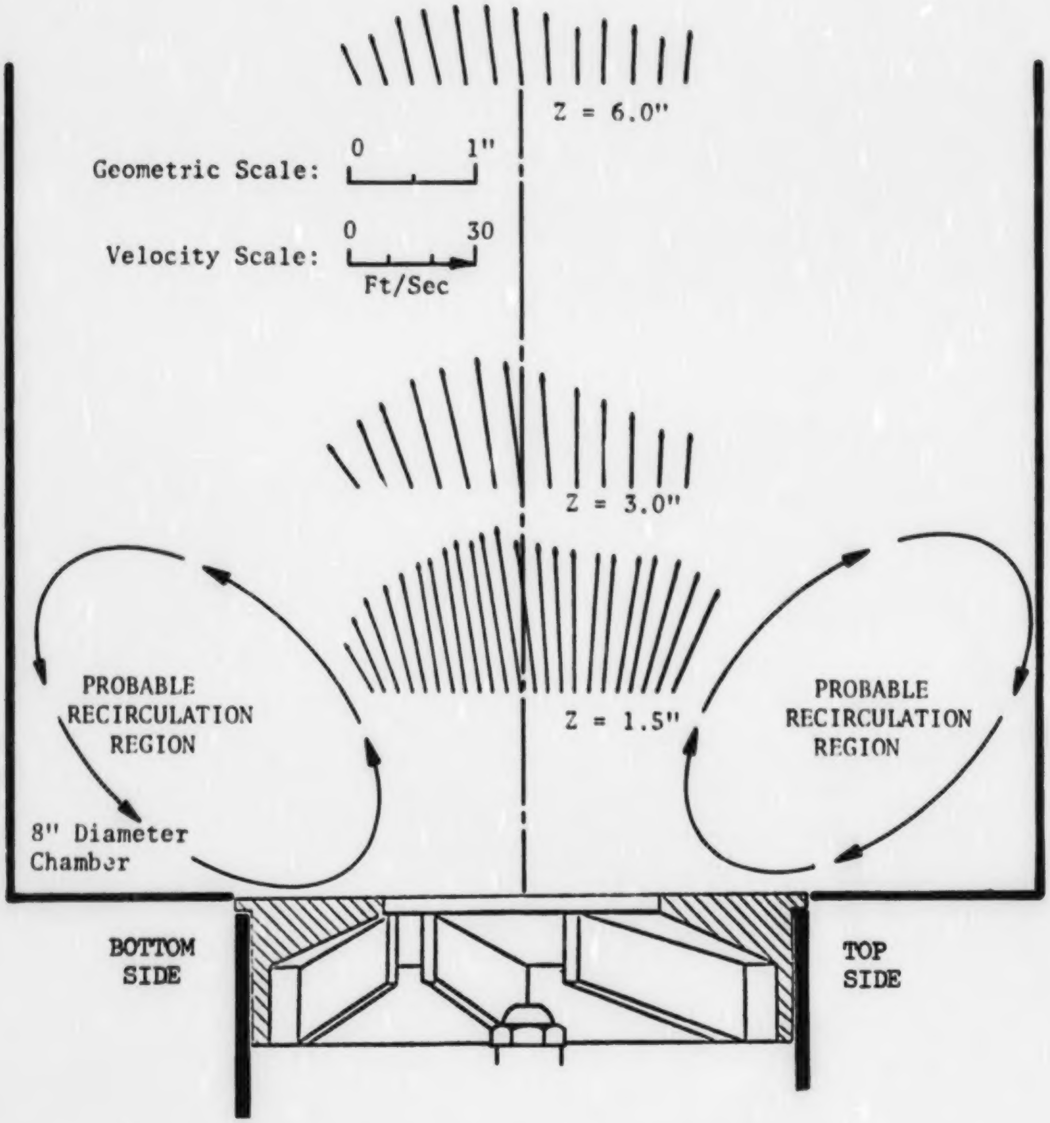
Z = 6.0"
Geometric Scale:
0
1"
Velocity Scale:
0
30
Ft/Sec
Z = 3.0"
PROBABLE RECIRCULATION REGION
Z = 1.5"
PROBABLE RECIRCULATION REGION
8" Diameter Chamber
BOTTOM SIDE
TOP SIDE

Figure 47. Measured cold-flow air velocity vectors in the vertical plane of a 55-J burner

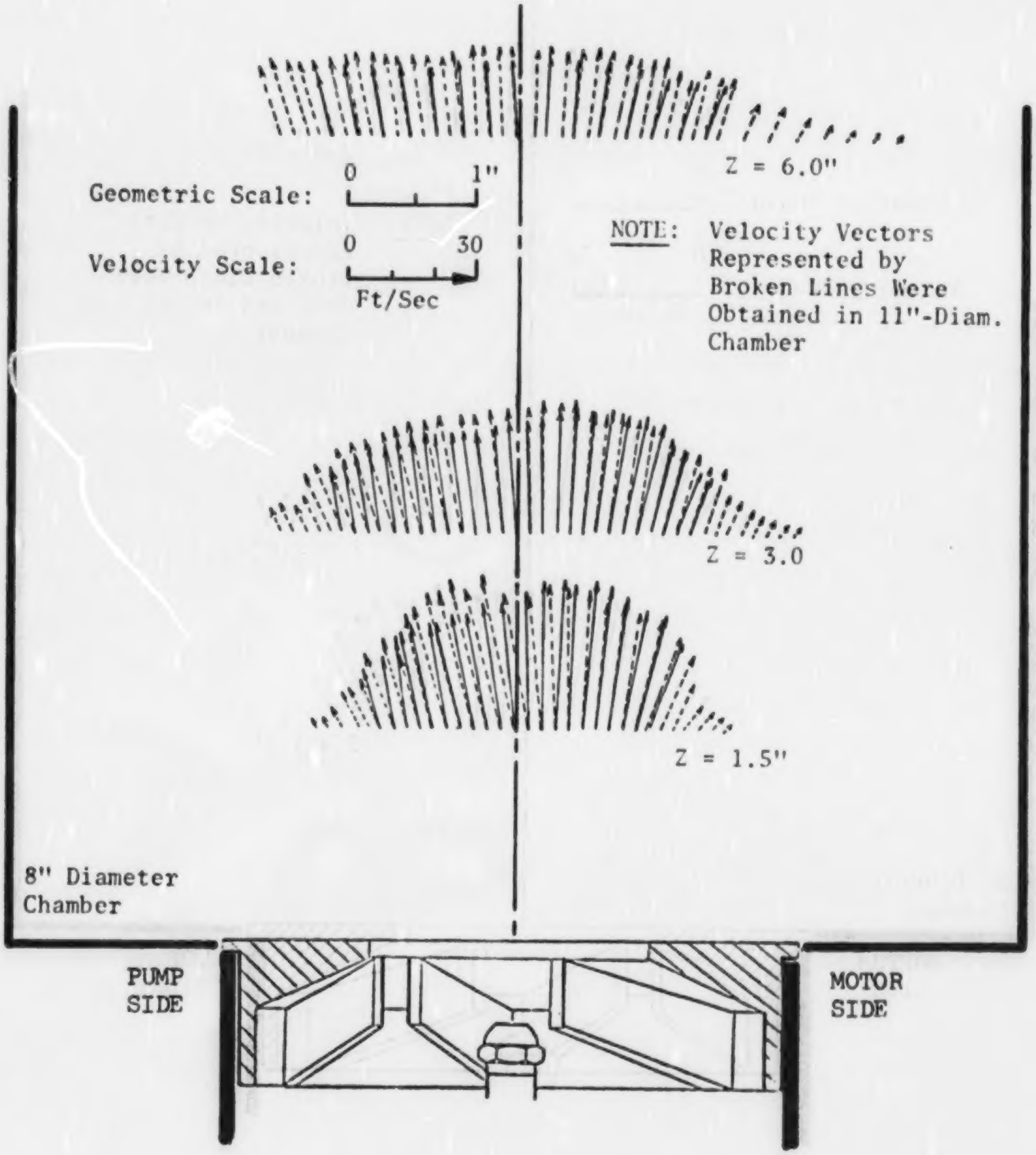

Figure 48. Air velocity vectors for the horizontal plane of a 55-J burner (comparison of data obtained with 8- and 11-inch-diameter chambers)

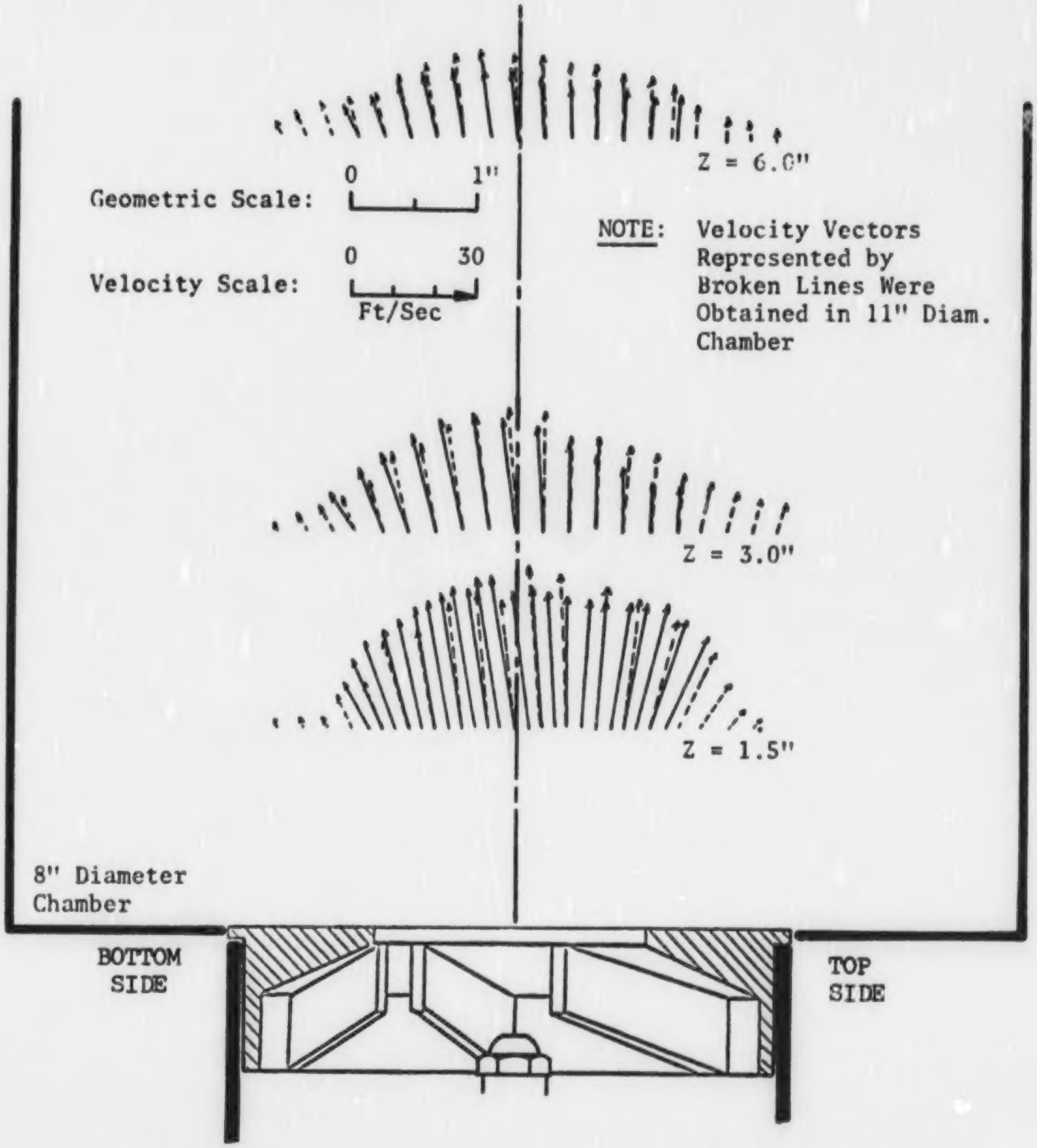
Z = 6.0"
Geometric Scale:
0
1"
Velocity Scale:
0
30
Ft/Sec
NOTE: Velocity Vectors Represented by Broken Lines Were Obtained in 11" Diam. Chamber
Z = 3.0"
Z = 1.5"
8" Diameter Chamber
BOTTOM SIDE
TOP SIDE

Figure 49. Air velocity vectors for the vertical plane of a 55-J burner (comparison of data obtained with 8- and 11-inch-diameter chambers)

Using two different spray nozzles, the local spray mass flux was determined in the flowfield of the 55-J burner, without ignition of the spray. These cold-flow measurements were performed as previously described in the Experimental Apparatus section. The experimental results are shown in Fig. 50 through 52, overlaid on the previously presented air flow velocity vectors. For all of the cold-flow tests, the oil burner air bands were adjusted wide open, which led to the relatively high air-to-fuel ratios shown in the figures. There is a very significant lack of symmetry in the spray mass flux, more than might be expected if the oil spray nozzles were flowed in the absence of the air blast from the burner. It is concluded, therefore, that nonsymmetry in the air flow patterns produced by the burner has also induced nonsymmetry in the oil spray patterns.

Velocity vector measurements were repeated with the burner ignited, so that combustion gas velocities were being measured. These hot-fire results are summarized by data presented in Fig. 53 and 54. The velocities presented in these figures are based on an assumed constant gas density equivalent to 2300 F temperature and a molecular weight of 29. Comparison of the combustion gas velocity profiles with the previously presented cold-flow air velocity profiles show that the essential features of the patterns, other than magnitude, are not significantly altered by the presence or absence of combustion.

The 55-J burner was fired into the 8-inch-ID, coaxial, cylindrical combustion chamber, and experimental techniques previously outlined were used to sample and chemically analyze local combustion products. The results of these experiments are presented in Fig. 55 and 56 for two different overall burner operating stoichiometric ratios. The parameters presented are local burned gas stoichiometric ratio (based on oxygen, carbon monoxide, and carbon monoxide, and carbon dioxide concentrations, and ignoring the presence of liquid or gaseous hydrocarbons), carbon monoxide, and nitric oxide. Carbon monoxide is expressed as grams of carbon monoxide per kilogram of burned fuel

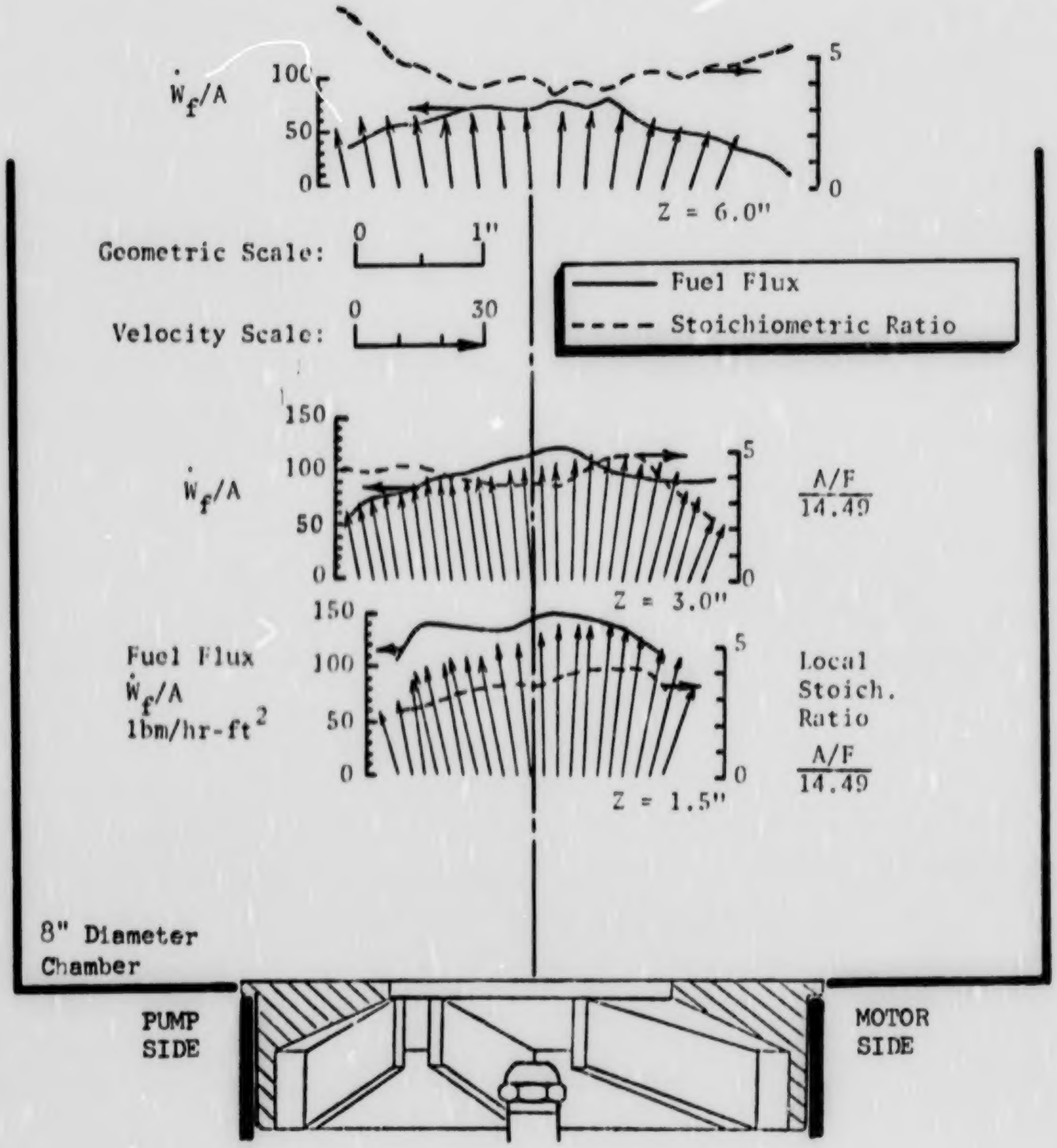

Figure 50. Air velocity vectors and fuel spray mass flux data for a 55-J burner incorporating a 0.75-80°-C nozzle (horizontal plane)

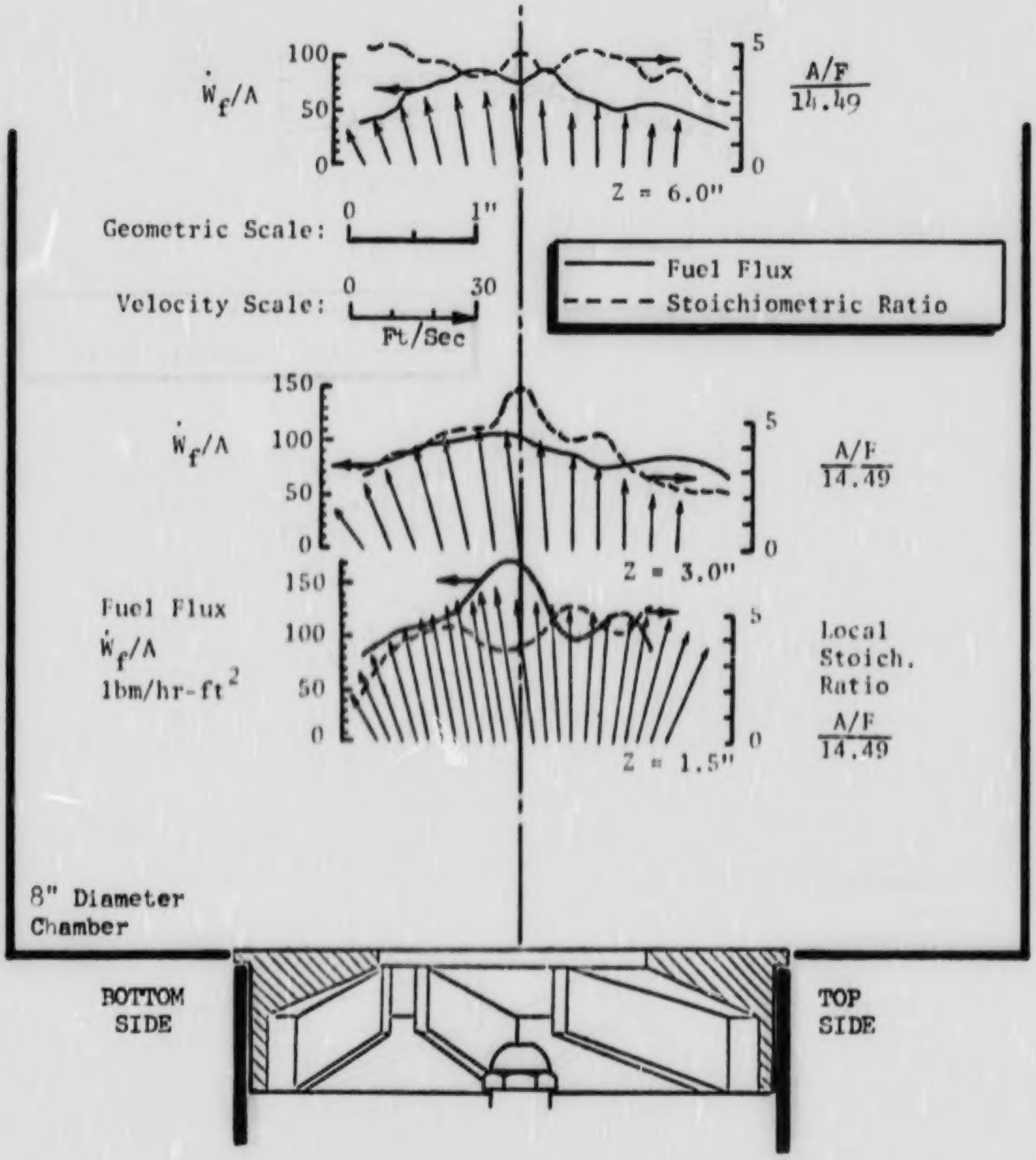

Figure 51. Air velocity vectors and fuel spray mass flux data for a 55-J burner incorporating 0.75-80°-C nozzle (vertical plane)

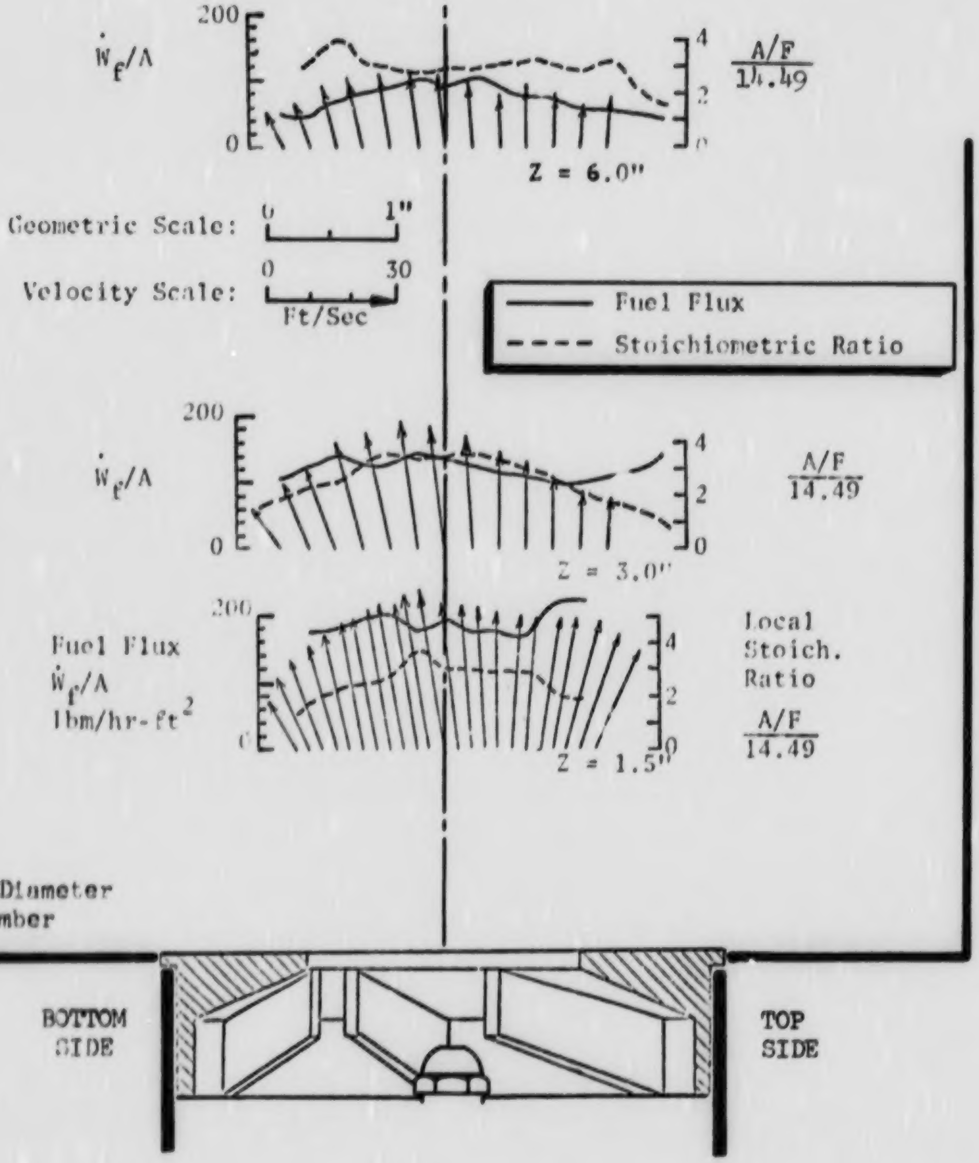

Figure 52. Air velocity vectors and fuel spray mass flux data for a 55-J burner incorporating a 1.50-80°-C nozzle (vertical plane)

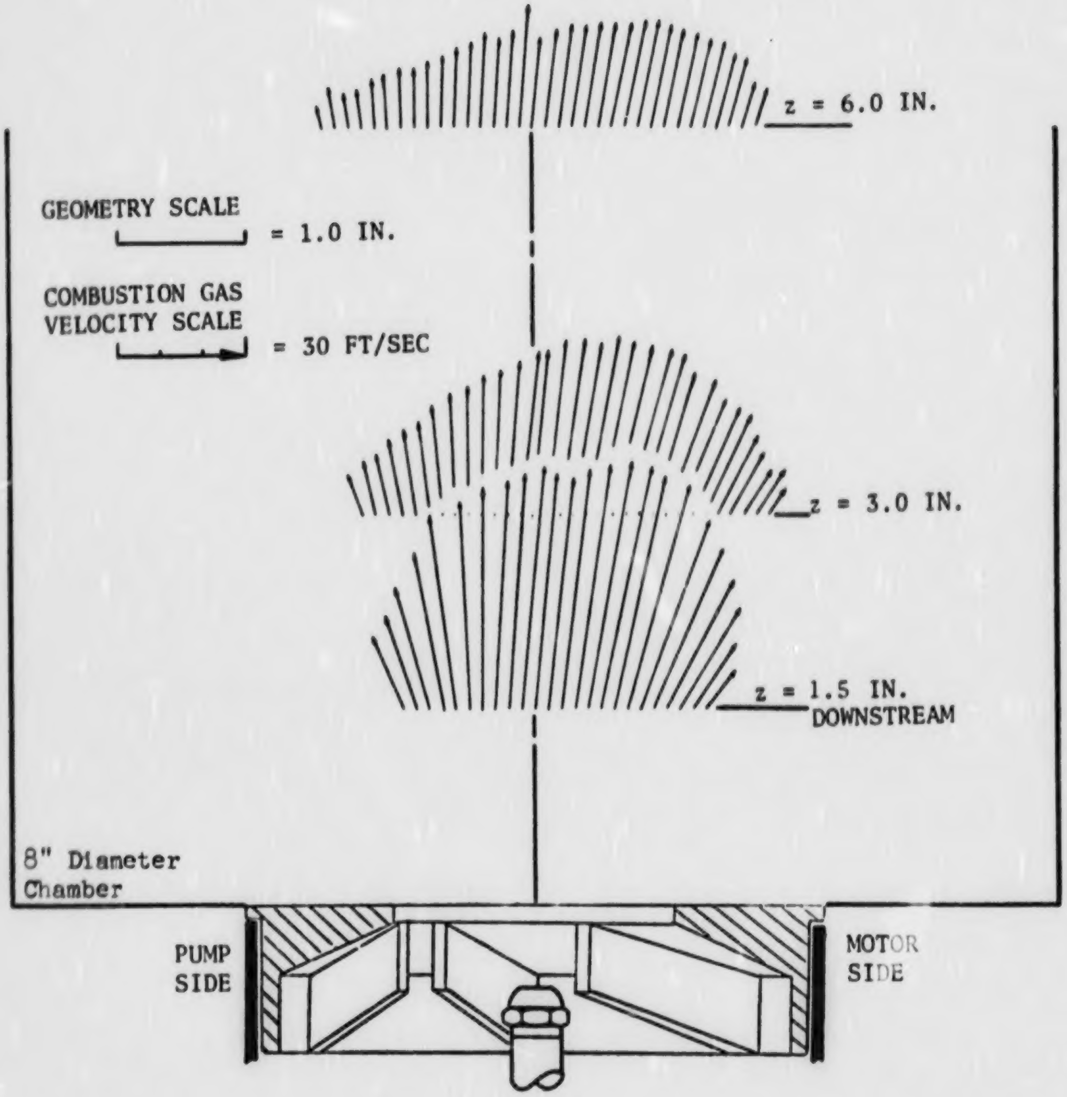
z = 6.0 IN.
GEOMETRY SCALE
= 1.0 IN.
COMBUSTION GAS VELOCITY SCALE
= 30 FT/SEC
z = 3.0 IN.
z = 1.5 IN. DOWNSTREAM
8" Diameter Chamber
PUMP SIDE
MOTOR SIDE

Figure 53. Combustion gas velocity vectors in the horizontal plane for the ABC 55-J burner mounted in an 8-inch-diameter, cylindrical, coaxial chamber

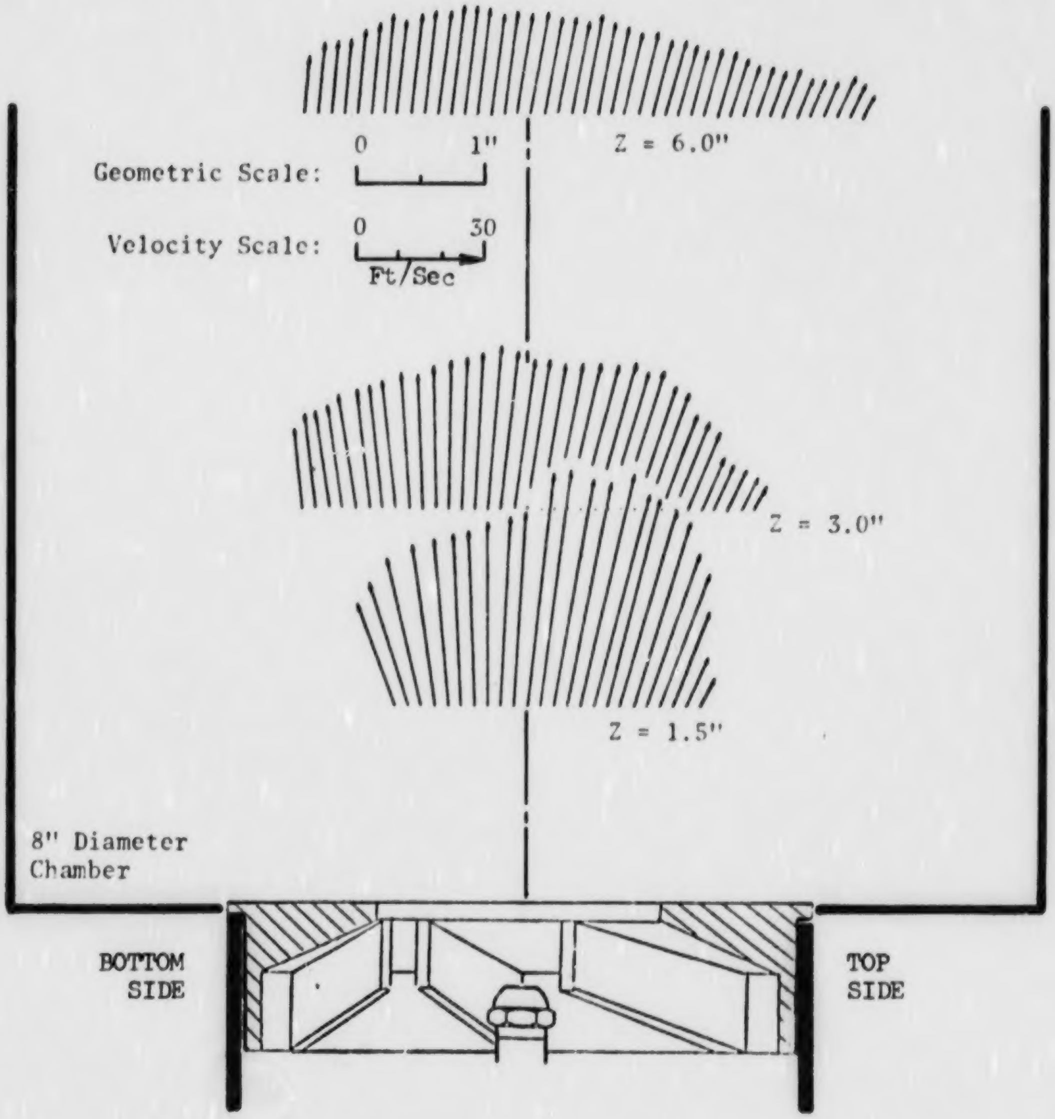
Geometric Scale:
0
1"
Velocity Scale:
0
30
Ft/Sec
Z = 6.0"
Z = 3.0"
Z = 1.5"
8" Diameter Chamber
BOTTOM SIDE
TOP SIDE

Figure 54. Combustion gas velocity vectors in the vertical plane for the ABC 55-J burner mounted in an 8-inch-diameter, cylindrical, coaxial chamber

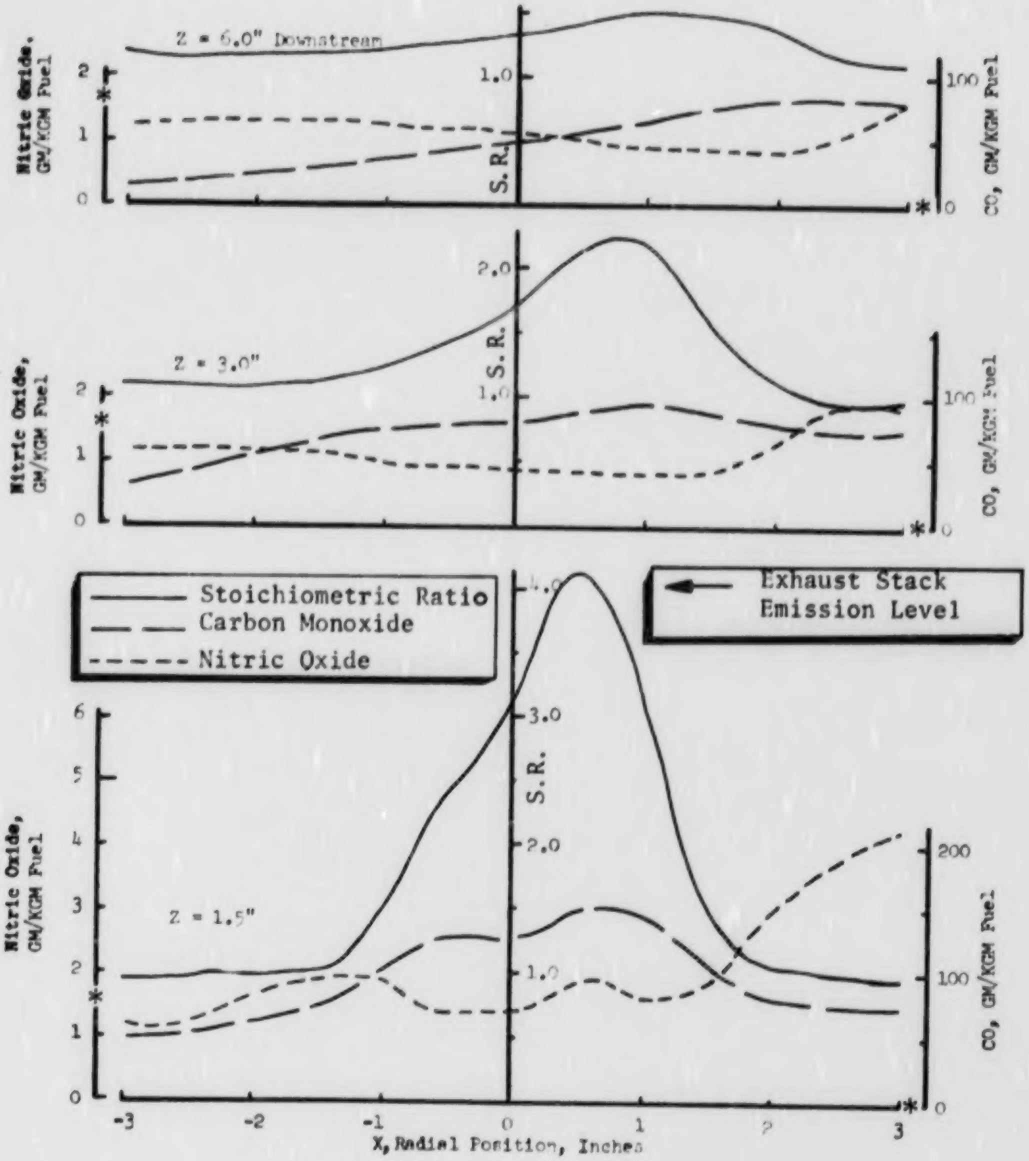

* = Exhaust Stack Emission Levels

Figure 55. Local combustion gas analysis profiles for the ABC 55-J burner at a nominal stoichiometric ratio of 1.25 with a 0.75-70°A nozzle (horizontal plane)

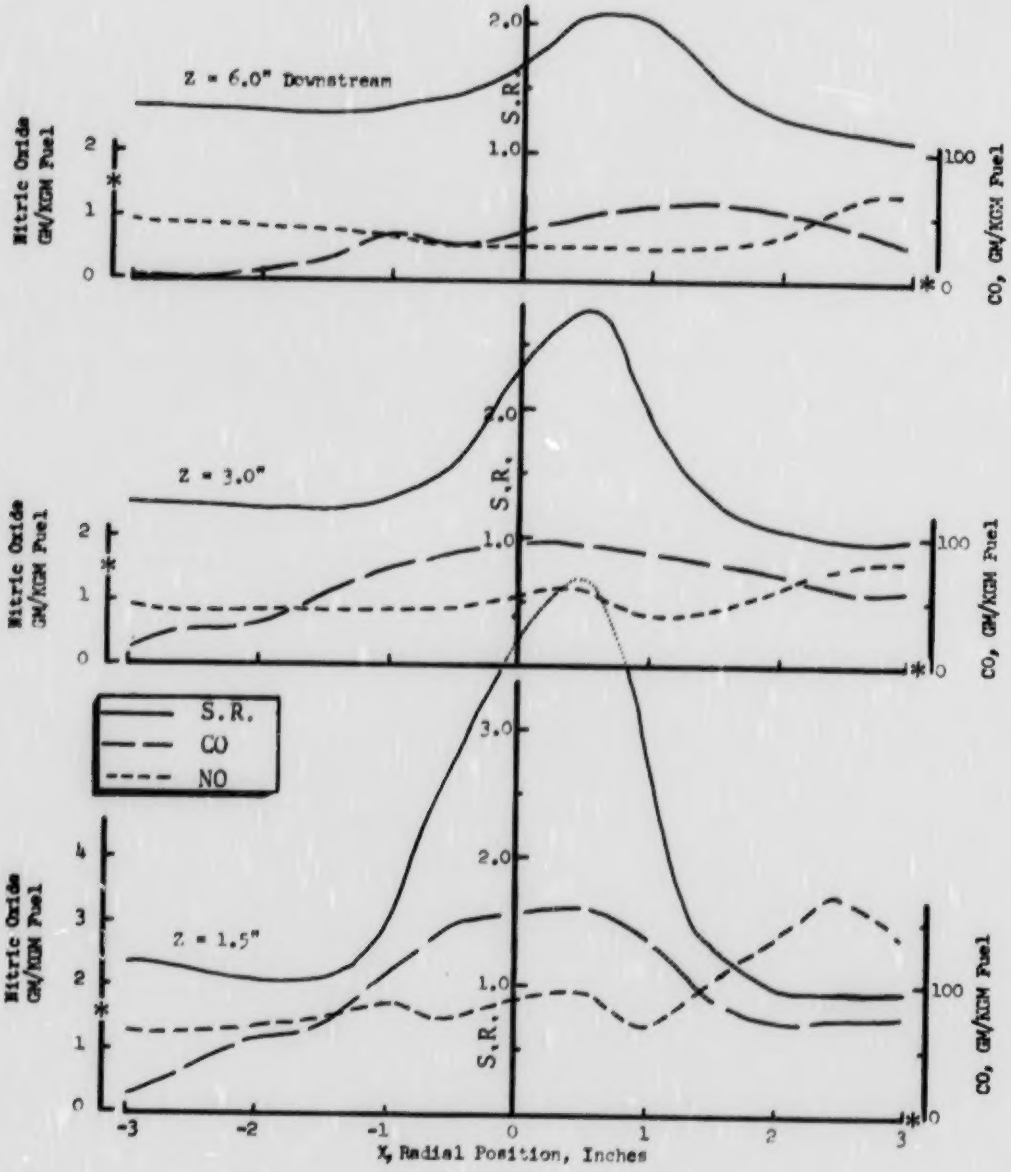

* = Exhaust Stack Emission Levels

Figure 56. Local combustion gas analysis profiles for the ABC 55-J burner at a nominal stoichiometric ratio of 1.50 with a 0.75-70°A nozzle (horizontal plane)

(gm NO/kg fuel) in the local gas sample. Nitric oxide is presented as grams of nitric oxide per kilogram of burned fuel (gm NO/kg fuel) in the local gas sample. Each of these parameters (as described in the Apparatus and Data Reduction section of this report) totally ignores the presence or absence of unburned liquid or gaseous hydrocarbons. Using previously described experimental techniques, the measured concentrations of volatile gaseous hydrocarbons in the gas samples represented by Fig. 55 and 56 were insignificant and, therefore, are not presented here. For reference, the pollutant emission levels in the exhaust stack are shown as asterisks on the ordinates of Fig. 55 and 56.

Data describing the mixed gases, exiting from the baffled, coaxial, cylindrical, 8-inch-diameter combustion chamber are given in Fig. 57 through 59. These figures show that carbon monoxide and smoke emissions are low under all conditions for which the 55-J was tested, with low smoke due most certainly to the absence of fuel-rich stoichiometric ratios throughout the combustion process, as shown in the composition pattern data, and with low carbon monoxide emission due to the same factor as well as the excellent downstream mixing characteristics of the baffled cylindrical combustion chambers. Data are also shown in Fig. 57 through 59 for burners other than the 55-J. Those data are discussed in the sections referring to the specific burners.

Shown in Fig. 60 through 63 are results of flue gas analyses for the 55-J and other burners (discussed later) when fired in the Lennox forced-air furnace having an upright combustion chamber with the burner mounted perpendicular to the combustion chamber axis. Carbon monoxide, unburned hydrocarbons, and nitric oxide emission characteristics do not show significant differences from the data obtained with the coaxial chamber. Smoke emissions, however, are considerably higher, due probably to impingement of liquid fuel on the combustion chamber walls with decomposition thereon to produce smoke, an event which was considerably less likely with the coaxial chamber than with the upright perpendicular chamber. Carbon monoxide and unburned hydrocarbons

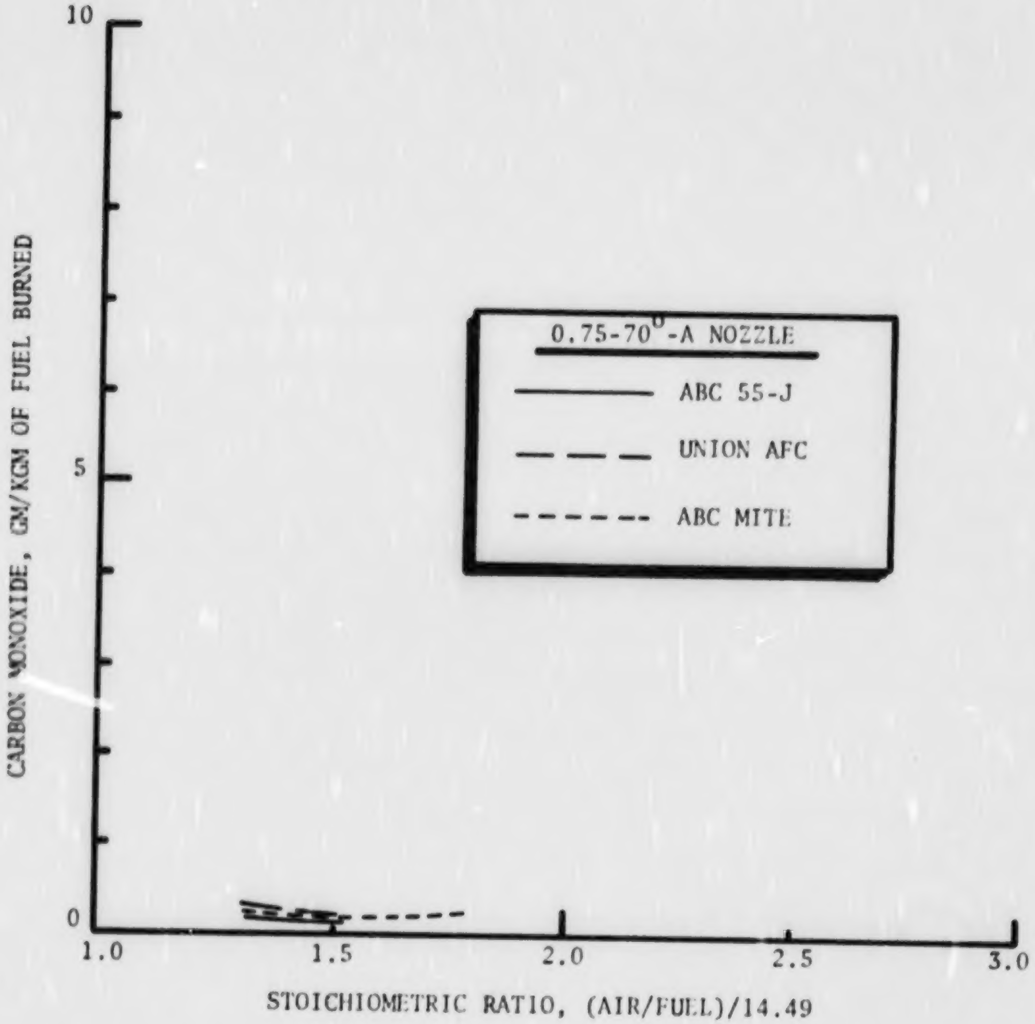

Figure 57. Carbon monoxide emissions measured by mixed combustion gas sampling in the coaxial, 8-inch-diameter cylindrical combustion chamber

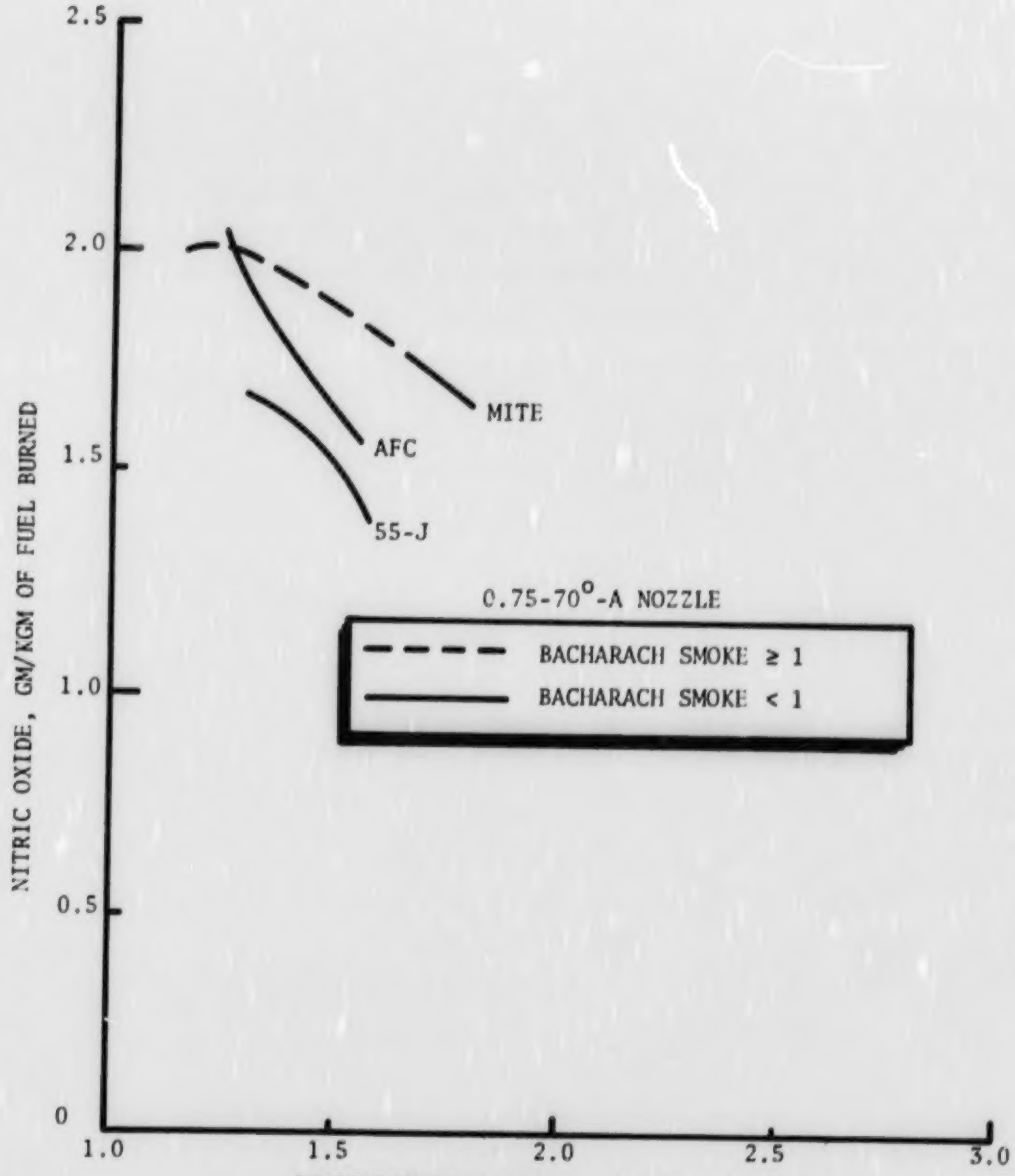

Figure 58. Nitric oxide emissions measured by mixed combustion gas sampling in the coaxial, 8-inch-diameter combustion chamber

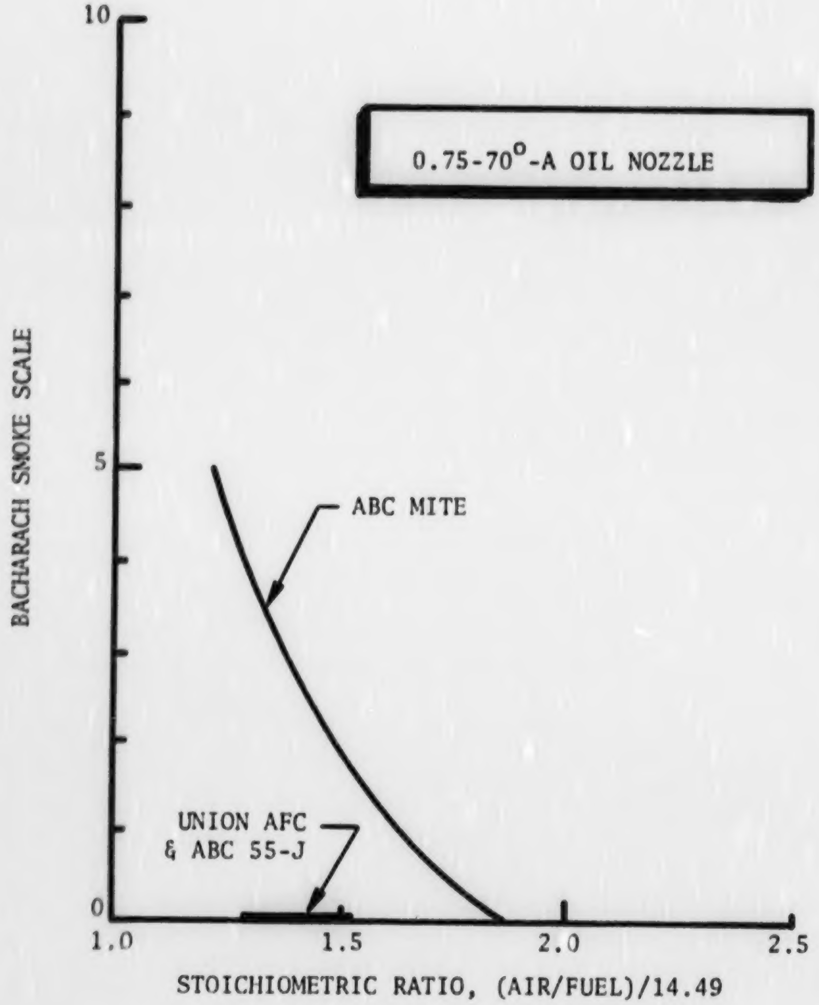

Figure 59. Smoke emissions measured by mixed combustion gas sampling, coaxial 8-inch-diameter combustion chamber

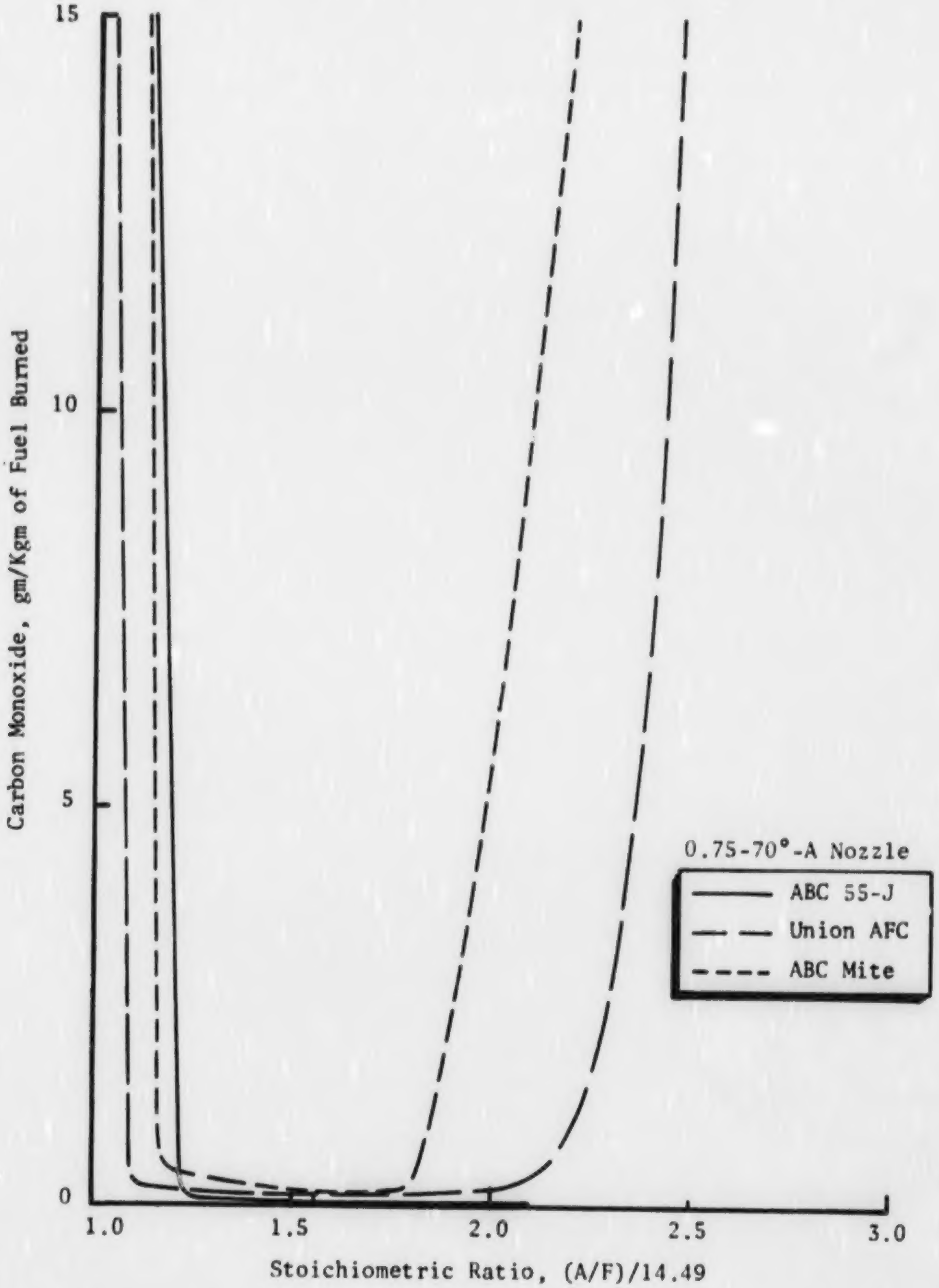

Figure 60. Carbon monoxide emissions measured by Lennox furnace flue gas sampling

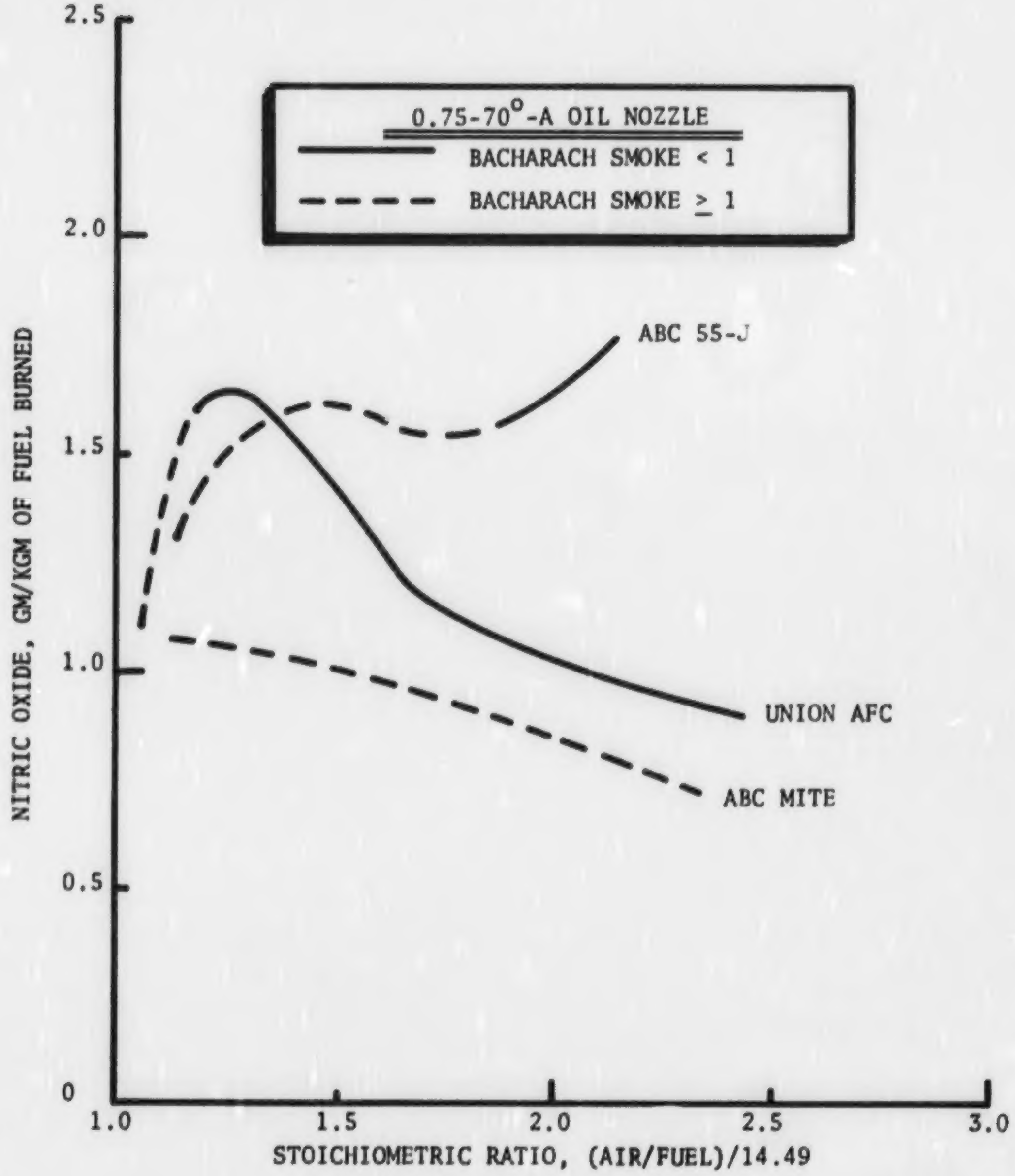

Figure 61. Nitric oxide concentrations measured in the Lennox furnace flue gas samples

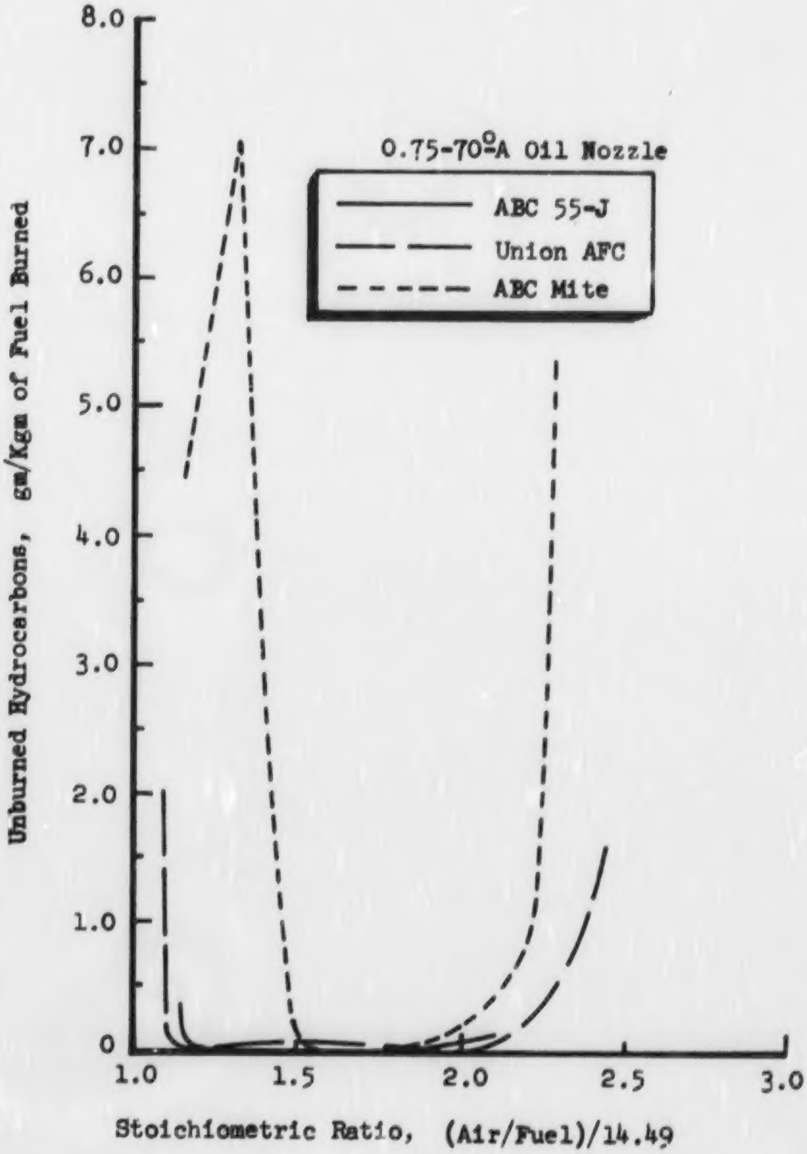

Figure 62. Total hydrocarbon emissions measured by Lennox furnace flue gas sampling

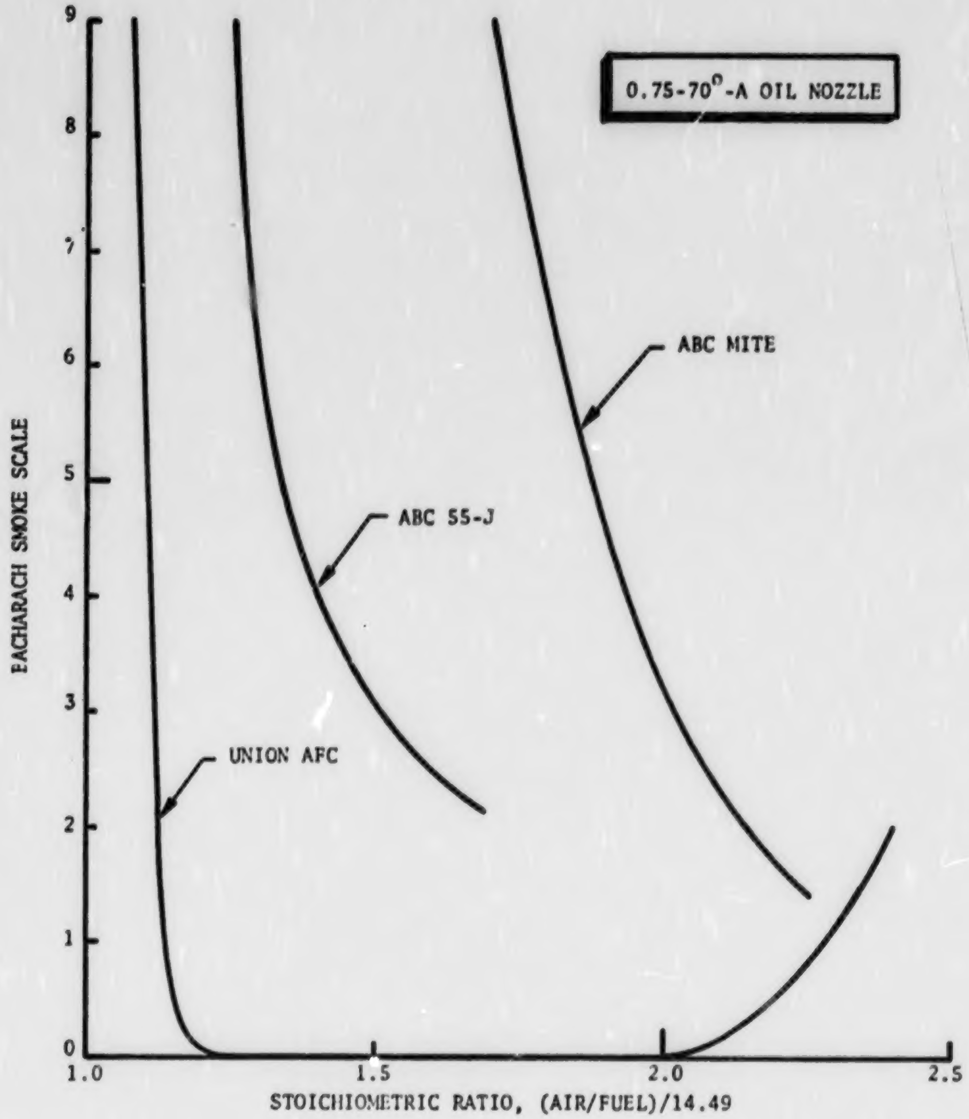

Figure 63. Smoke emissions measured by Lennox furnace flue gas sampling

might also result by the same mechanism; however, their nature is such that they can be eliminated downstream by oxidation, and their absence in the flue gas is therefore not surprising, assuming that only moderate amounts of fuel impinge on the upright combustion chamber walls. Impingement of only a moderate amount of fuel on the upright combustion chamber walls is consistent with the chamber dimensions and the combustion gas flow patterns presented previously as a function of distance from the blast tube end (assuming that similar patterns might result when the 55-J is fired into the upright chamber).

ABC Mite Burner (1.0 gph)

The ABC Mite burner is unique because of the relatively small (3-1/8 inch) OD of its blast tube. It has a 2-1/2-inch-ID choke plate in the end of the blast tube, and a 2-inch-diameter air spinner with windmill-like vanes suspended in the center of the choke plate. The oil spray nozzle is centered within the air spinner.

Cold-flow air flow patterns produced by the Mite burner were relatively complicated, as shown by the data given in Fig. 64 through 66. At the 1.5-inch location, the β angle parameter, which indicates air swirl, is most different from zero at the locations 0.5 to about 1.2 inches radius from the center of the burner. At the 3- and 6-inch downstream locations, the air flow parameters (Fig. 65 and 66) indicate that the flow patterns are less complicated and, in particular, the localized swirl at the 0.5- to 1.2-inch radial locations is considerably less pronounced.

Two-dimensional representations of the air flow velocity vectors are given in Fig. 67 and 68. The swirl (tangential velocity) component cannot be shown in these figures, but the high degree of flow irregularity at the 1.5-inch coaxial location is nonetheless still very evident, with less irregularity at the more downstream locations.

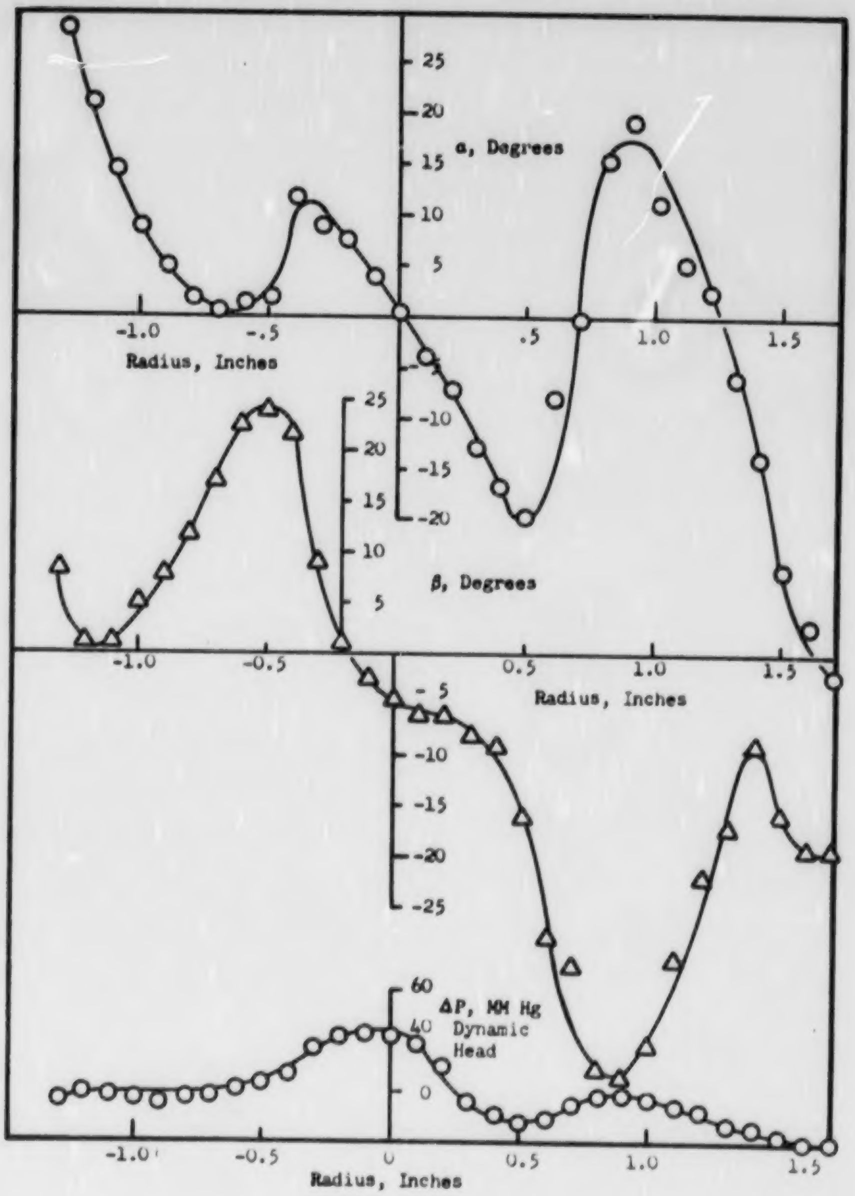

Figure 64. Air flow parameters at 1.5 inches downstream of the Mite burner in an 8-inch-diameter, cylindrical, coaxial chamber (zero oil flow, vertical plane)

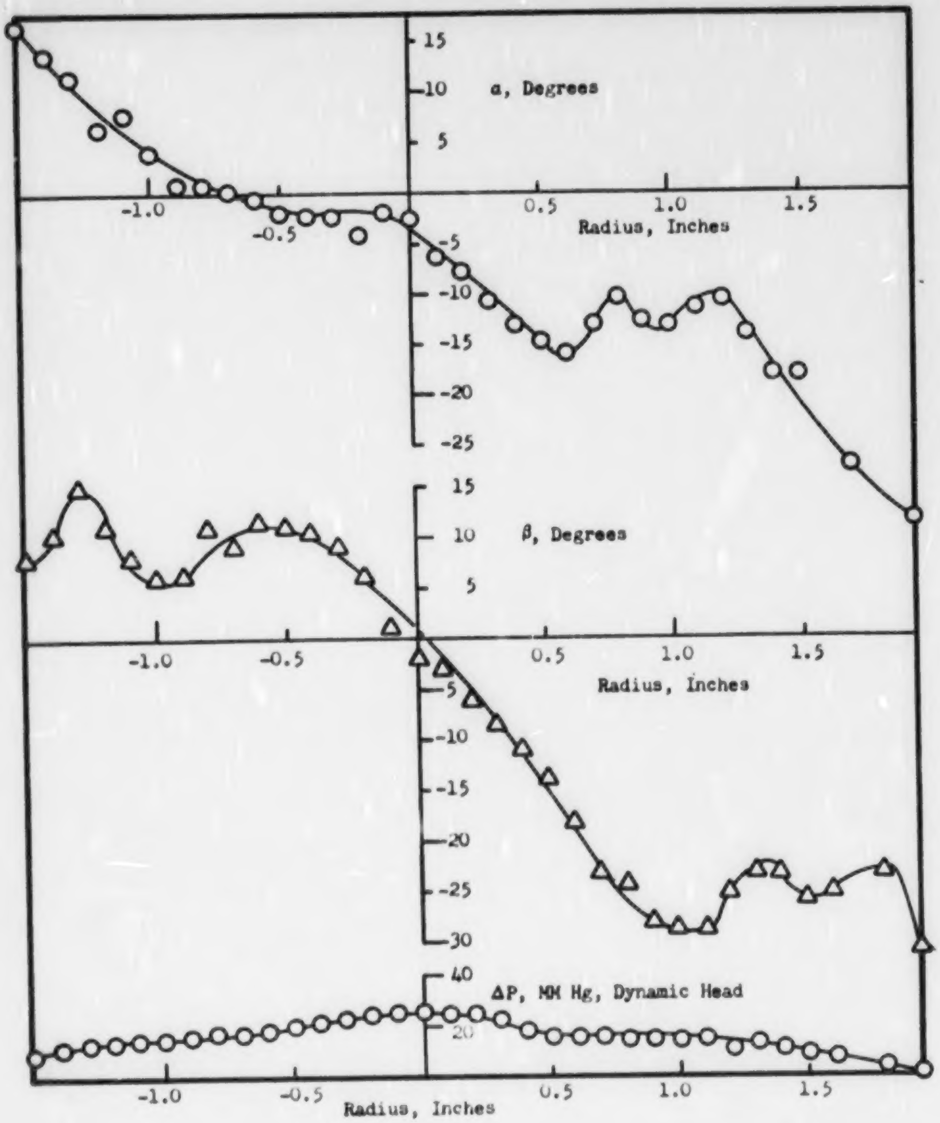

Figure 65. Air flow parameters at 3 inches downstream of the Mite burner installed in an 8-inch-diameter cylindrical, coaxial chamber (zero oil flow, vertical plane)

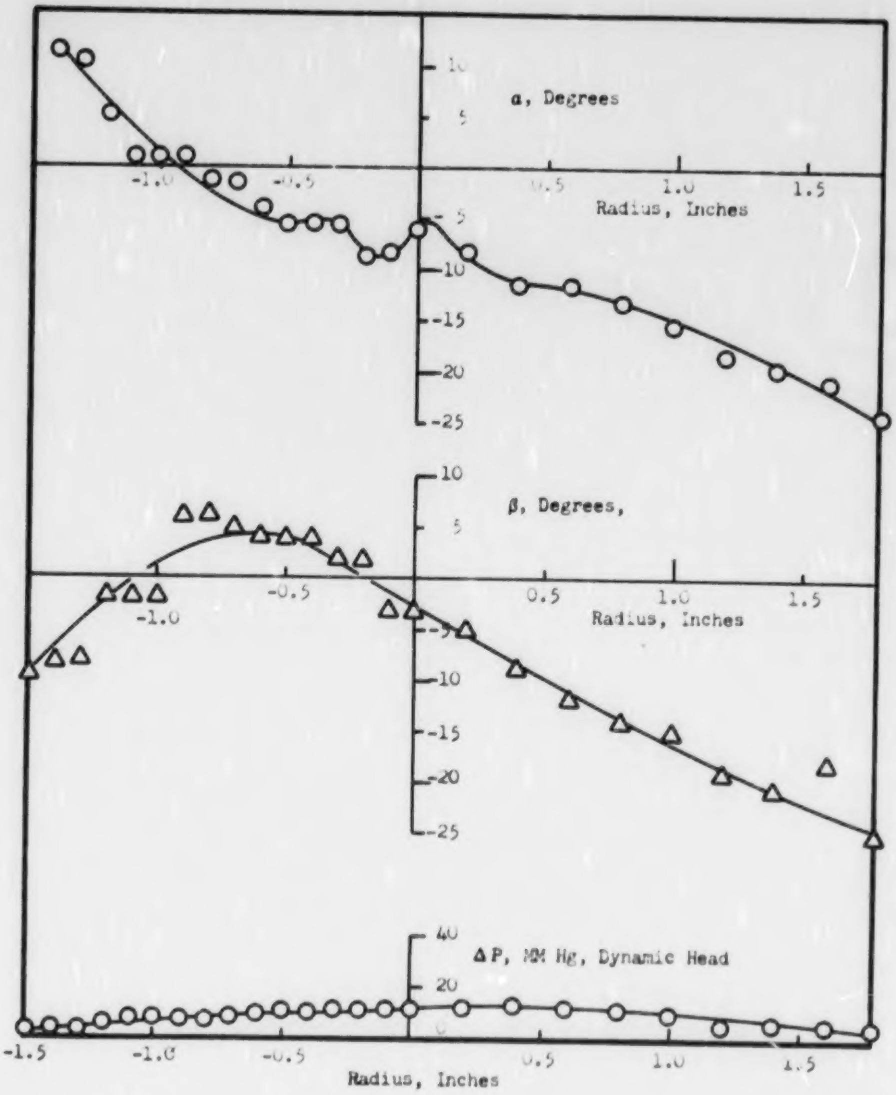

Figure 66. Air flow parameters at 6 inches downstream of the Mite burner in an 8-inch-diameter cylindrical, coaxial chamber (zero oil flow, vertical plane)

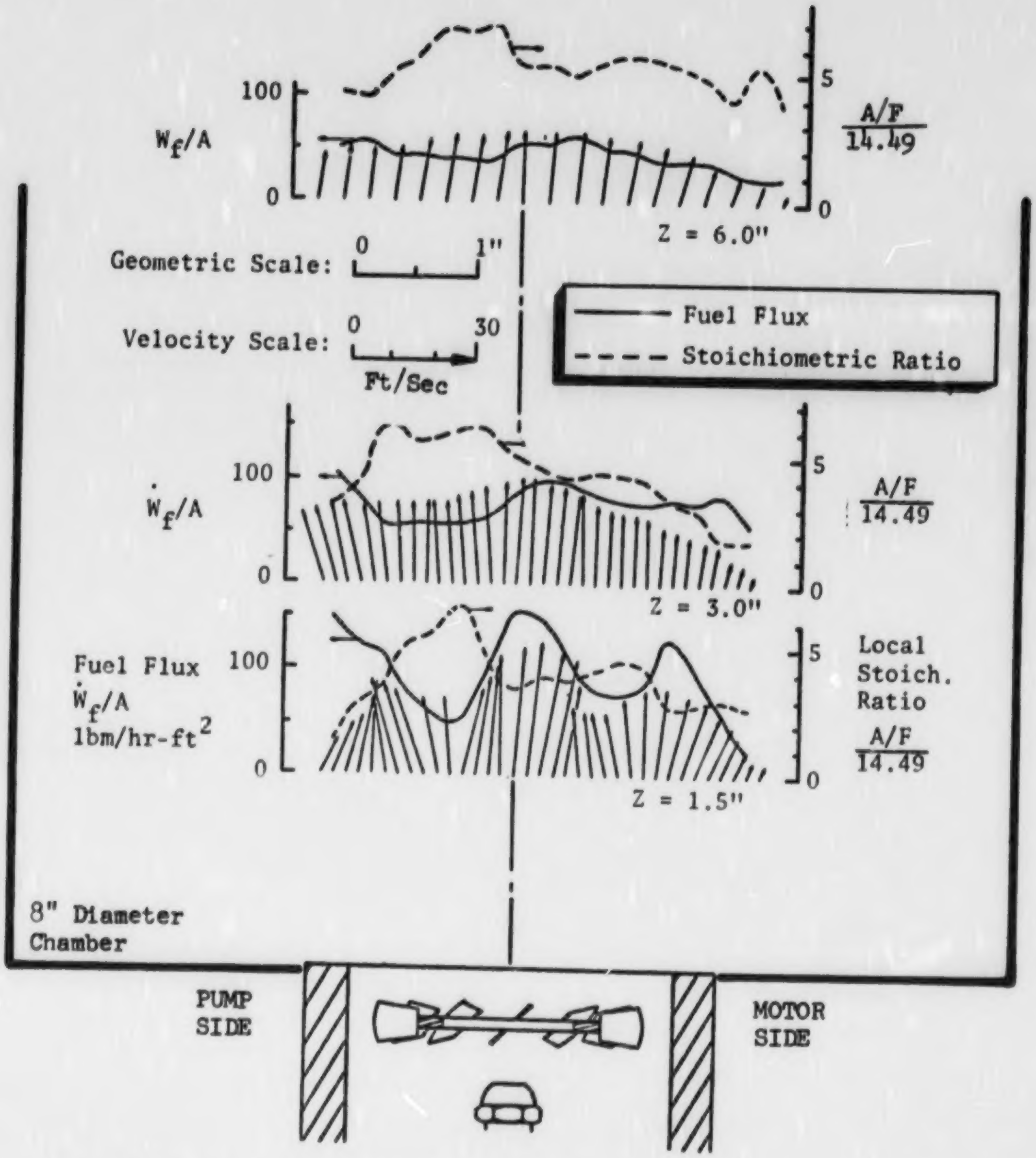

Figure 67. Air flow and oil spray flux patterns in the horizontal plane of the Mite burner mounted in an 8-inch-diameter cylindrical, coaxial chamber (Delavan 1-80°-C nozzle)

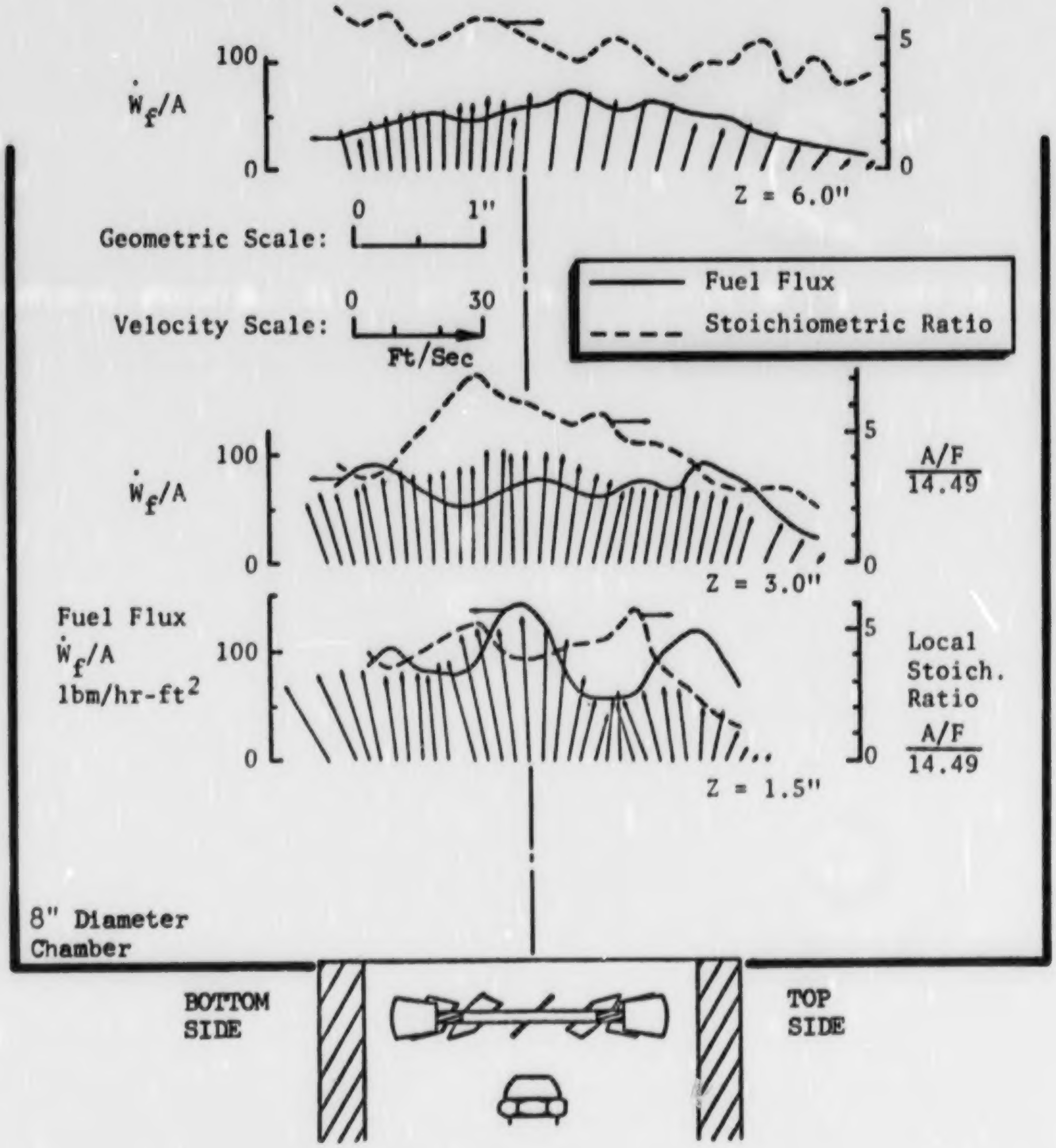

Figure 68. Air flow and oil spray flux patterns in the vertical plane of the Mite burner, mounted in an 8-inch-diameter, cylindrical, coaxial chamber (Delavan 1-80°-C nozzle)

Also shown in Fig. 67 and 68 are cold-flow (nonignition) oil spray flux patterns measured by techniques previously described, with the air band wide open. Note that the oil spray flux appears to be somewhat rarified at the 0.5- to 1-inch radial positions, where it has been noted there exists a high local rate of swirl. These low spray mass fluxes may be a combined result of the spray nozzle design, flow angles, and centrifugal forces, caused by the air swirl, slinging the larger-size oil droplets out of the zone of rotating gases. This same effect is noted in both the horizontal and the vertical planes (Fig. 67 and 68, respectively).

Combustion gas velocity vectors, measured with the burner ignited, are shown in Fig. 69 and 70. Except for magnitude, there is a pronounced similarity between the combustion gas velocity vectors and the cold-flow air velocity vectors. Irregular patterns of the combustion gas velocity vector profiles do propagate further downstream than the analogous irregularities in the air velocity vector profiles.

Local gas sampling for determination of pollutant concentrations was performed for the Mite burner fired into the 8-inch-ID coaxial, cylindrical combustion chamber. The results of the sample gas analyses are shown in Fig. 71 through 73 for overall burner operating stoichiometric ratios of 1.25, 1.50, and 1.80. The most interesting facet of these results is the tendency for very high nitric oxide concentrations, near unity stoichiometric ratios, and minima in carbon monoxide concentrations at the 0.5- to 1.2-inch radial locations where it was previously noted that there exists a high degree of local gas swirl. At these locations, the closeness to unity local stoichiometric ratio and the magnitude of the nitric oxide concentration peaks are most pronounced for the axial locations nearest the blast tube (1.5-inch axial rotation) and for the overall stoichiometric ratios nearest unity. The high temperatures which accompany near unity local stoichiometric ratio and the poor chances for heat loss due to remoteness from the chamber walls undoubtedly are major factors leading to the

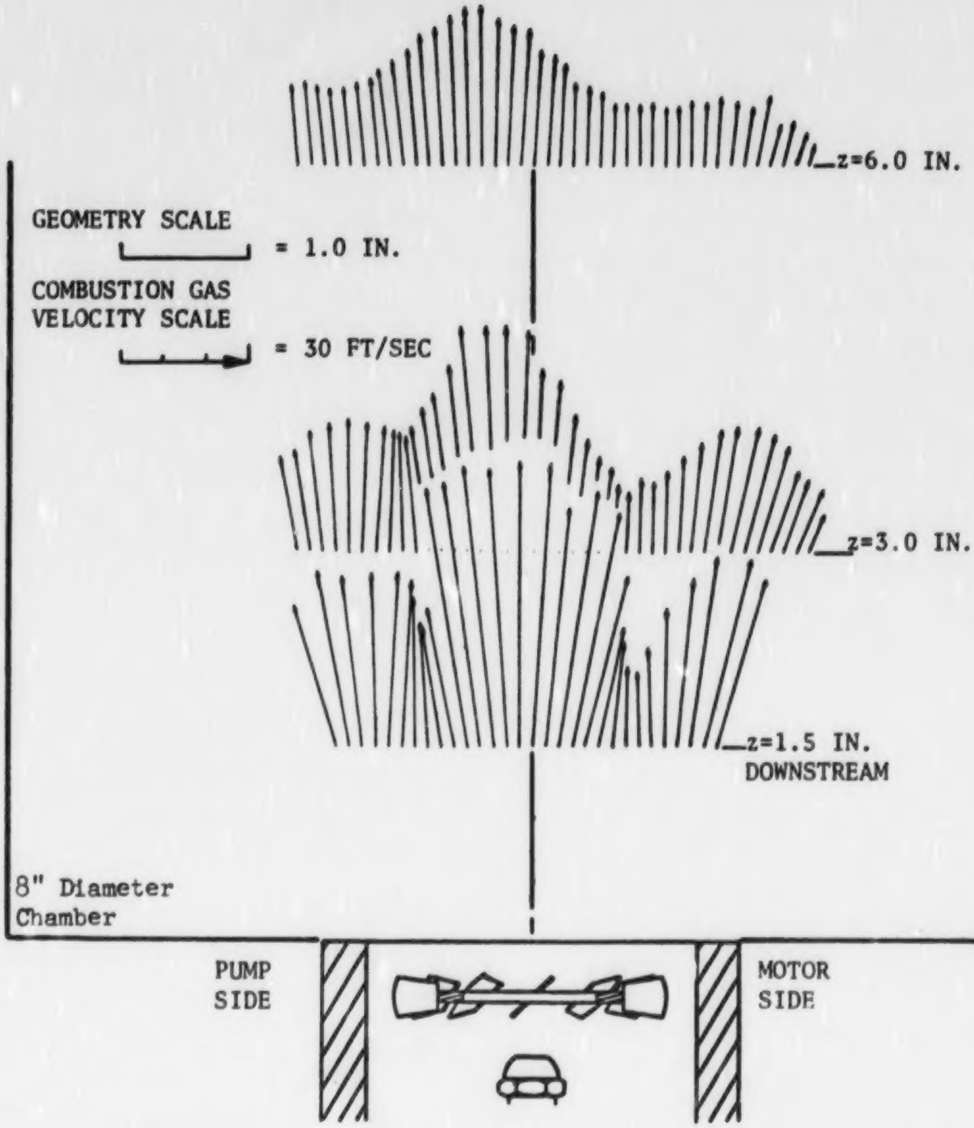
z=6.0 IN.
GEOMETRY SCALE
= 1.0 IN.
COMBUSTION GAS VELOCITY SCALE
= 30 FT/SEC
z=3.0 IN.
z=1.5 IN. DOWNSTREAM
8" Diameter Chamber
PUMP SIDE
MOTOR SIDE

Figure 69. Combustion gas velocity vectors in the horizontal plane for the ABC Mite burner mounted in an 8-inch-diameter, cylindrical, coaxial chamber

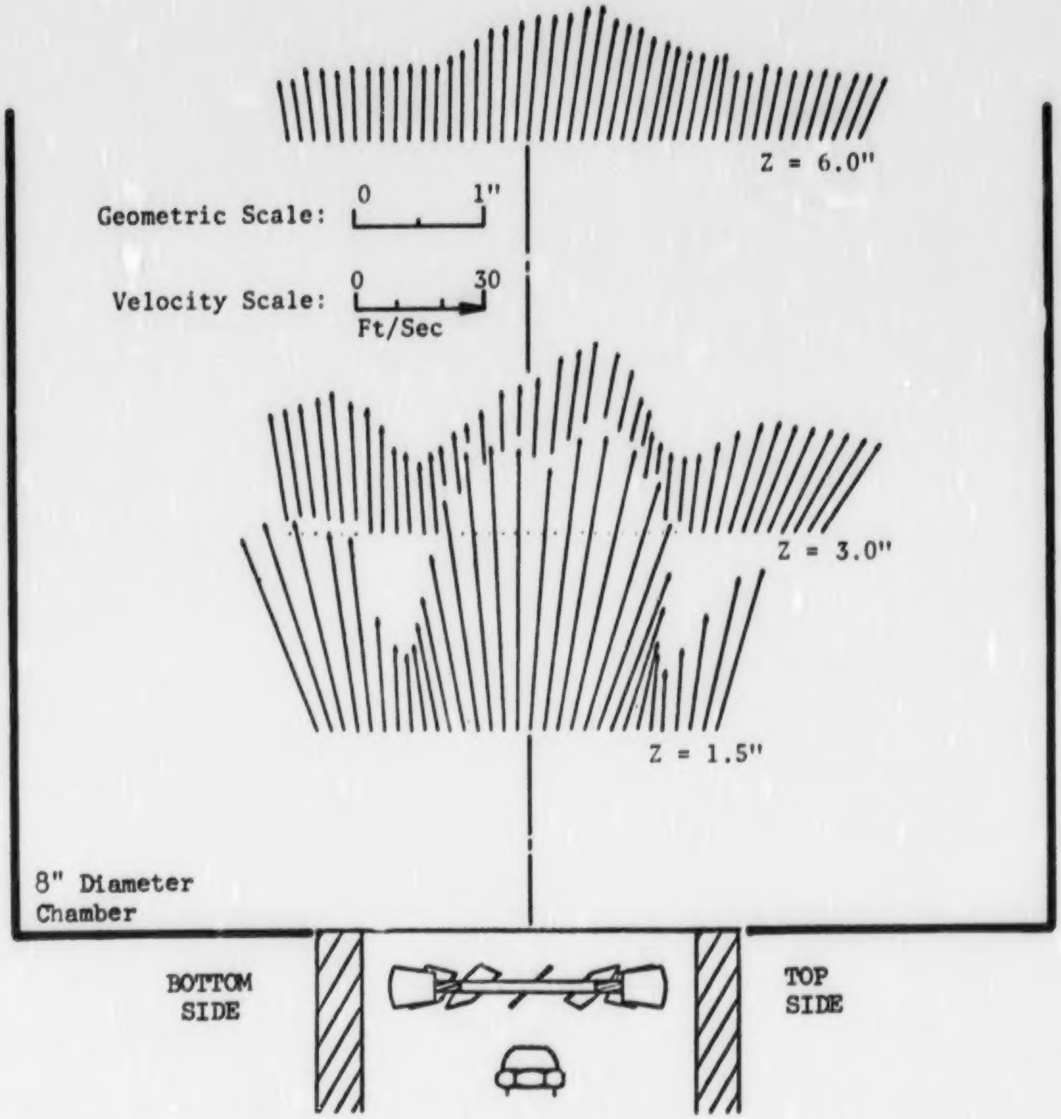
Z = 6.0"
Geometric Scale: 0 1"
Velocity Scale: 0 30
Ft/Sec
Z = 3.0"
Z = 1.5"
8" Diameter Chamber
BOTTOM SIDE
TOP SIDE

Figure 70. Combustion gas velocity vectors in the vertical plane for the ABC Mite burner mounted in an 8-inch-diameter, cylindrical, coaxial chamber

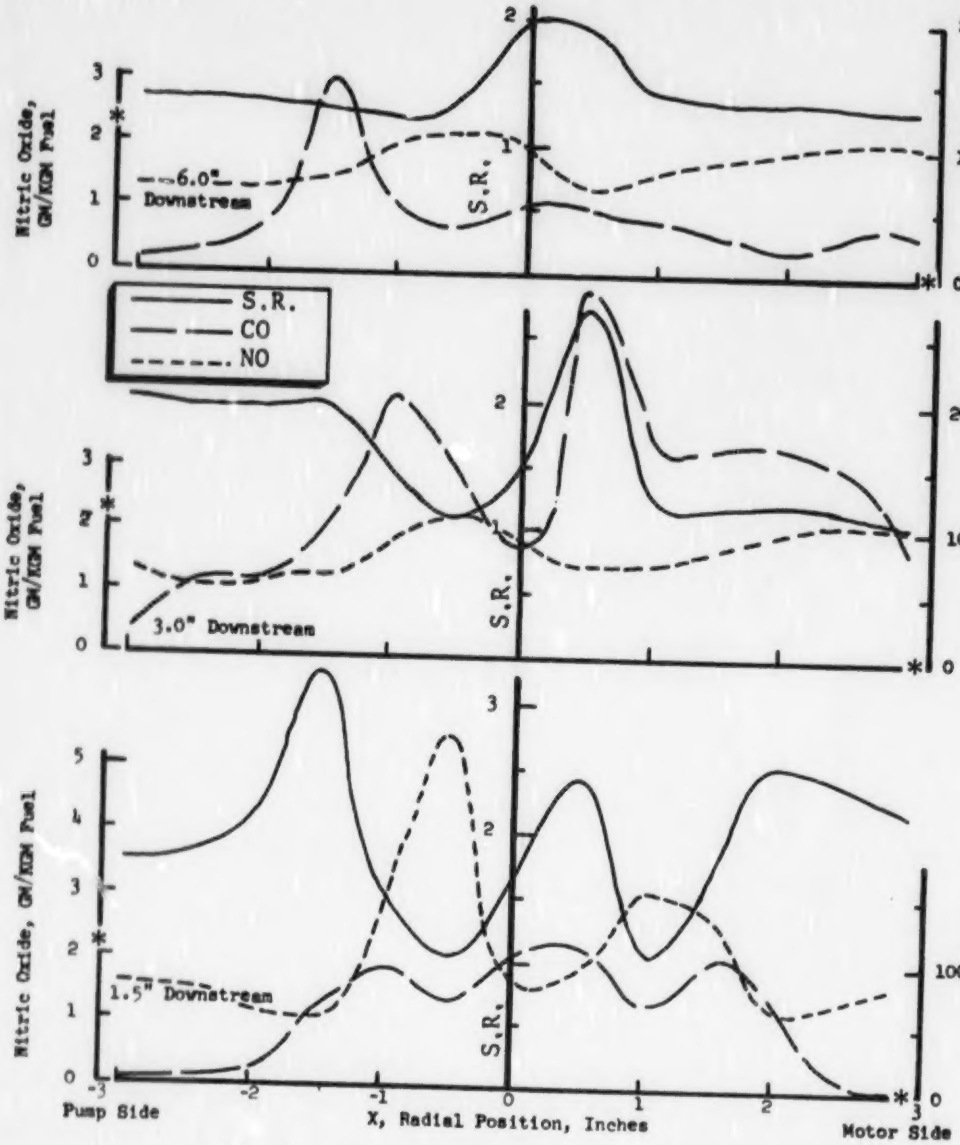

* = Exhaust Stack Emission Levels

Figure 71. Combustion gas analysis profiles for the ABC Mite burner at a nominal stoichiometric ratio of 1.25 with a 0.75-70°-A nozzle

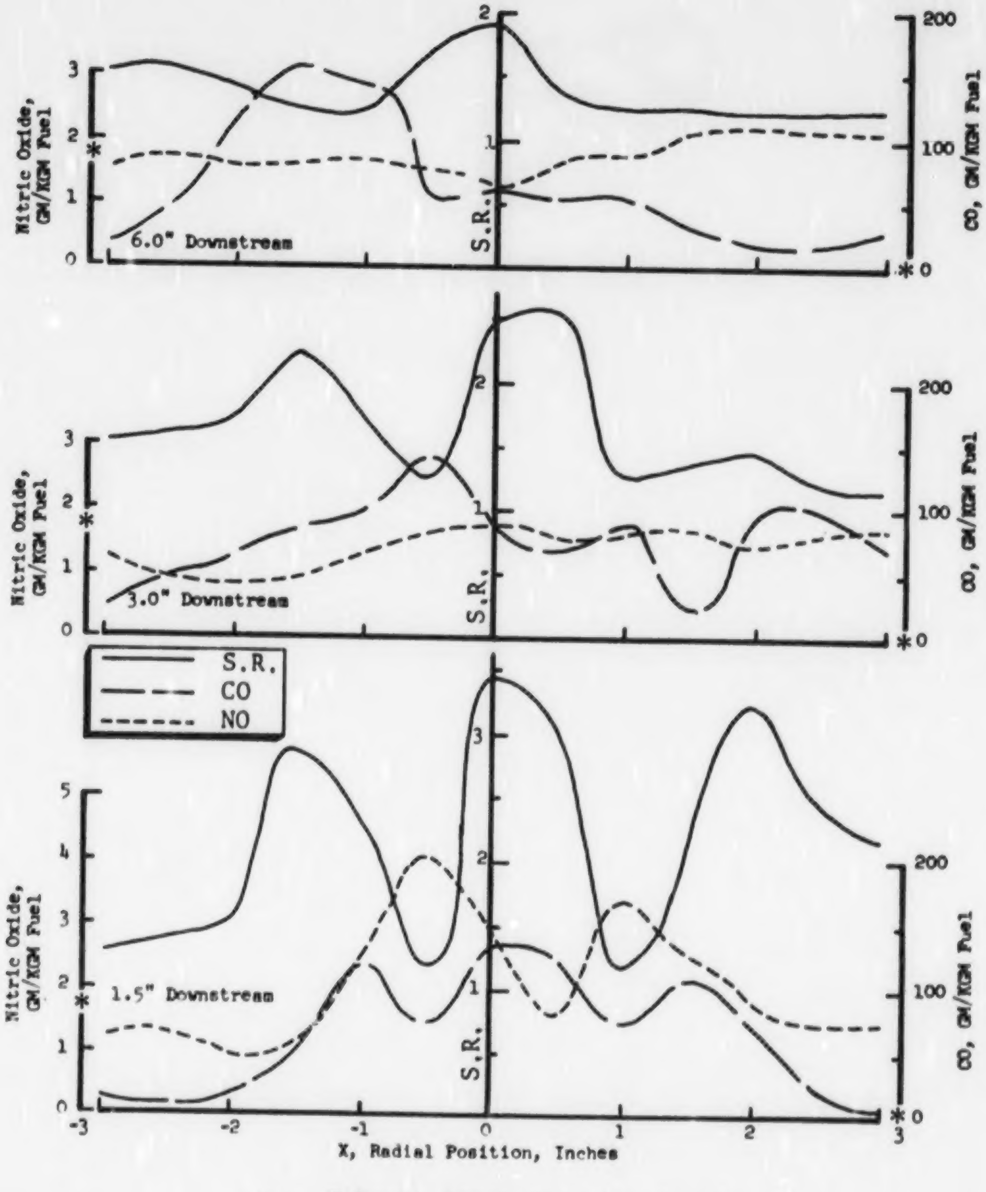

* = Exhaust Stack Emission Levels

Figure 72. Combustion gas analysis profiles for the ABC Mite burner at a nominal stoichiometric ratio of 1.50 with a 0.75-70°-A nozzle

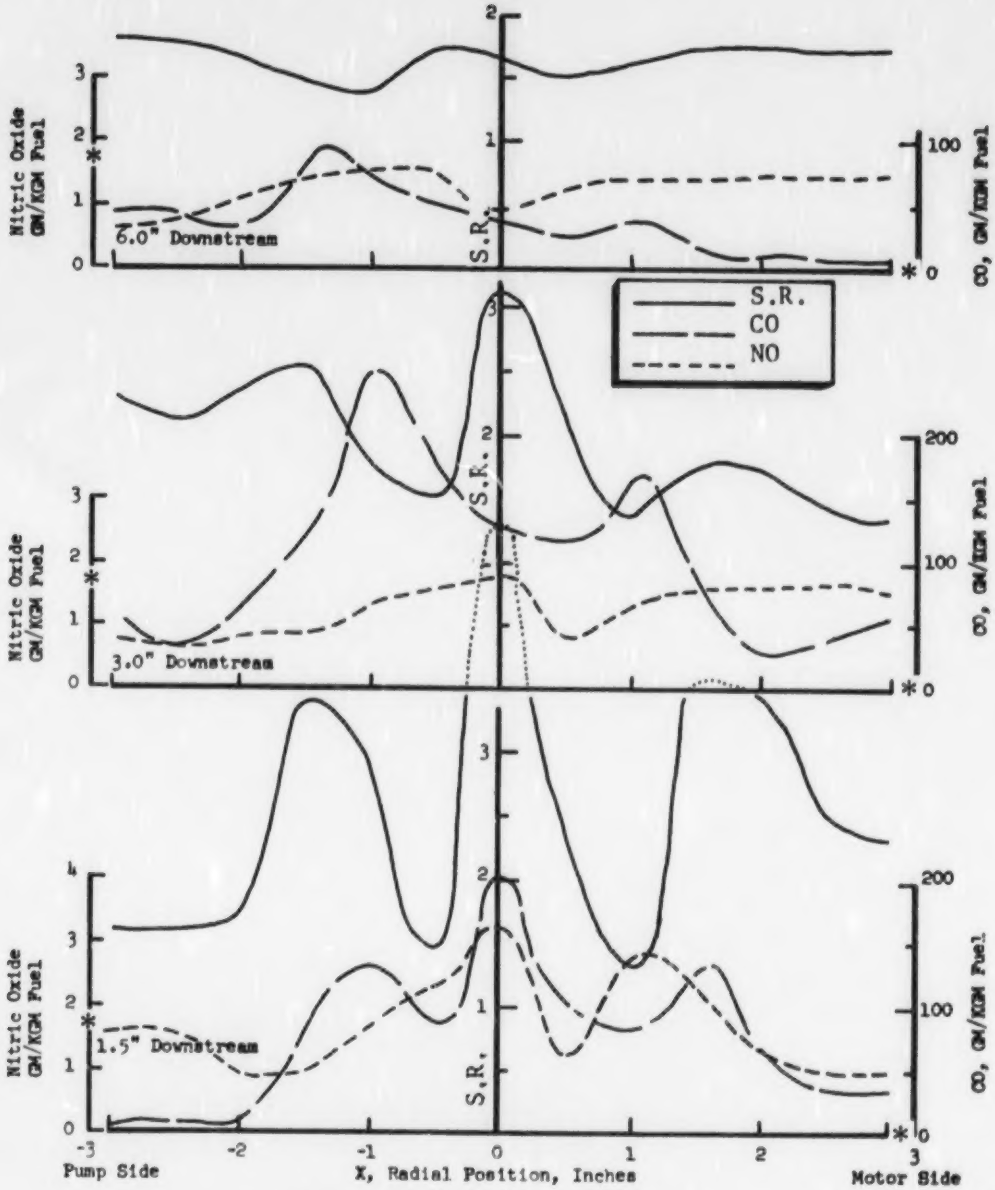

* = Exhaust Stack Emission Levels

Figure 73. Combustion gas analysis profiles for the ABC Mite burner at a nominal stoichiometric ratio of 1.80 with a 0.75-70°-A nozzle

high local nitric oxide concentrations. Comparison of the nitric oxide at the 1.5-, 3-, and 6-inch axial locations indicates a monotonic decrease in the magnitude of the nitric oxide peaks which must be an indication of mixing of the local gases with surrounding gases, rotation due to swirl transporting the nitric oxide-laden gases to a different angular location and/or chemical change of the nitric oxide. Of these three possibilities, the first two seem most likely. Since composition measurements were made only in the horizontal plane of the burner, it is not possible to state whether the new gases replacing the old, due to swirl, were originally high in nitric oxide, but it seems very likely that they were, assuming symmetry. Degradation of the nitric oxide peaks is, therefore, most probably due to mixing of the high nitric oxide concentration gases with surrounding gases having lower nitric oxide concentrations. This seems highly probable in view of the fact that gas velocities (Fig. 69 and 70) in the annular-shaped, high nitric oxide zones are only 1/4 to 1/3 the velocities of the surrounding gases, a fact that tends to enhance mixing and which indicates that the volume flux of the high nitric oxide concentration gases is considerably lower than the volume flux of the surrounding low nitric oxide concentration gases with which it is apt to mix.

As the overall stoichiometric ratio is raised from 1.25 to 1.50, to 1.80, the nitric oxide peaks become less pronounced, apparently because the local stoichiometric ratio becomes further removed from unity.

Carbon monoxide concentrations start low at the 1.5-inch axial locations, become higher at the 3-inch axial location, then become dissipated by the time the gases reach the 6-inch axial location. This behavior is as expected for this combustion intermediate reaction product.

The nitric oxide data presented in Fig. 71 through 73 seem to have a tendency toward minima when the local stoichiometric ratio is in the neighborhood of 1.80, or 80-percent excess air. This general trend also was noted with other burners.

Compositions of the mixed combustion gas from the coaxial cylindrical combustion chamber were previously presented (Fig. 57 through 59) together with the similar data for the 55-J burner. From the coaxial cylindrical combustor, the mixed ABC Mite combustion gases showed low carbon monoxide (probably more due to the large combustor volume than the particular burner), relatively high nitric oxide, and relatively high smoke. The high nitric oxide was undoubtedly provoked, at least partly, by the previously described combustion conditions in the 0.5- to 1.2-inch radius annular locations near the blast tube exit. The relatively high smoke level was a result of the wide variations in local stoichiometric ratio which caused some localized spots having fuel-rich burned gas stoichiometric ratios.

The furnace flue gas composition obtained with the Mite burner (Fig. 60 through 63) are indicative of the occurrence of poor combustion due to combustion stability problems of the Mite burner/Lennox furnace combinations, as operated for these tests. The result was high carbon monoxide and smoke coupled with low nitric oxide emissions, the fundamental symptoms of poor combustion wherein large variations resulting in fuel-rich local stoichiometric ratios occur.

Union Model AFC Burner (0.75 gph)

The third residential-size burner tested was the Union Model AFC burner. The unique construction feature of this burner involves a flame-retention head with a central sheet-metal flame cone which is moveable. Movement of the flame cone causes the air flow to be more or less restricted at the blast tube exit, depending on the direction of the movement. The restriction of the flame cone forces air passing out the blast tube exit to flow along peripheral swirlers located on the choke plate of the blast tube exit.

Air velocity vectors for the Model AFC burner, obtained under cold-flow conditions, are presented in Fig. 74 and 75. The nature of the burner design is such that the air flow is spread out over a relatively

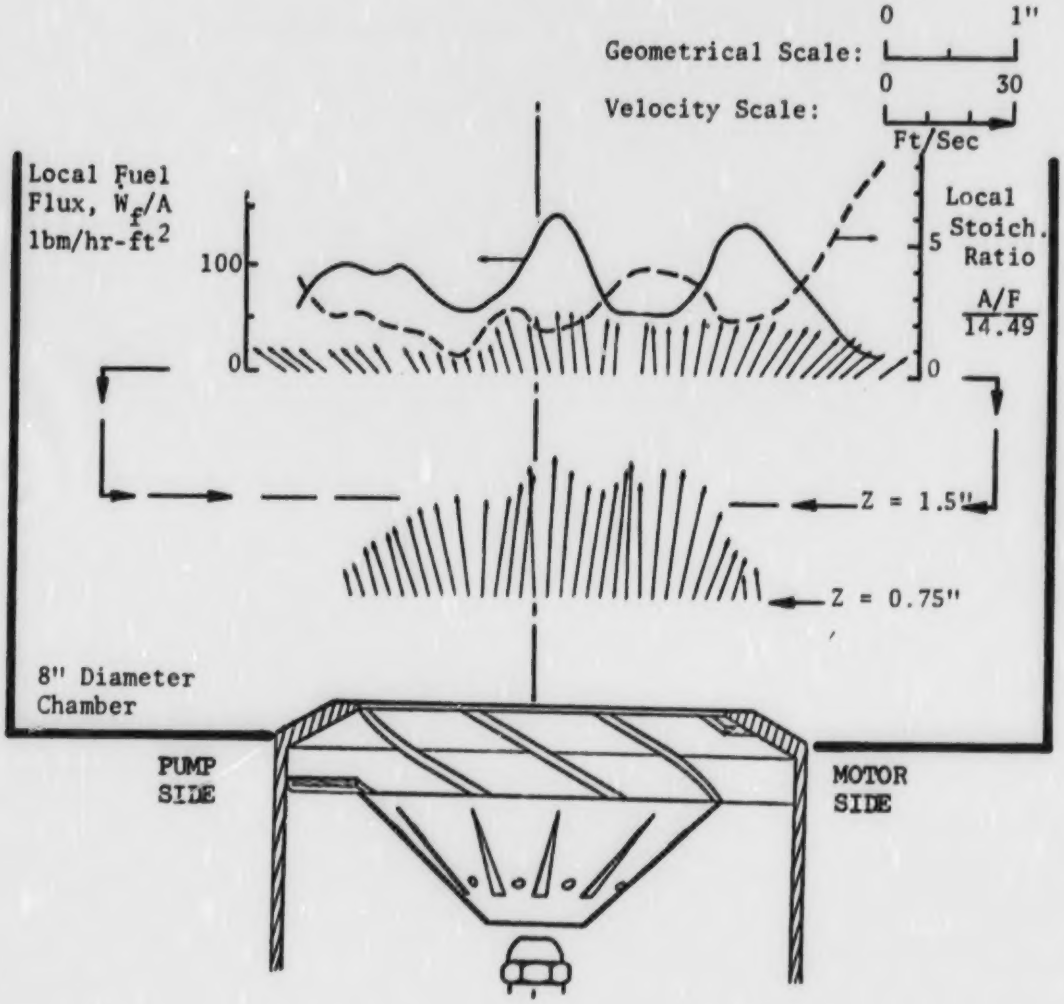
0
1"
Geometrical Scale:
0
30
Velocity Scale:
Ft/Sec
Local Fuel
Flux, W_f/A
lbm/hr-ft^2
100
0
Local
Stoich.
Ratio
$\frac{A/F}{14.49}$
5
0
Z = 1.5"
Z = 0.75"
8" Diameter
Chamber
PUMP
SIDE
MOTOR
SIDE

Figure 74. Air flow and oil spray flux patterns in the horizontal plane of the model AFC burner mounted in an 8-inch-diameter cylindrical, coaxial combustion chamber (Delavan 0.75-70°-C nozzle)

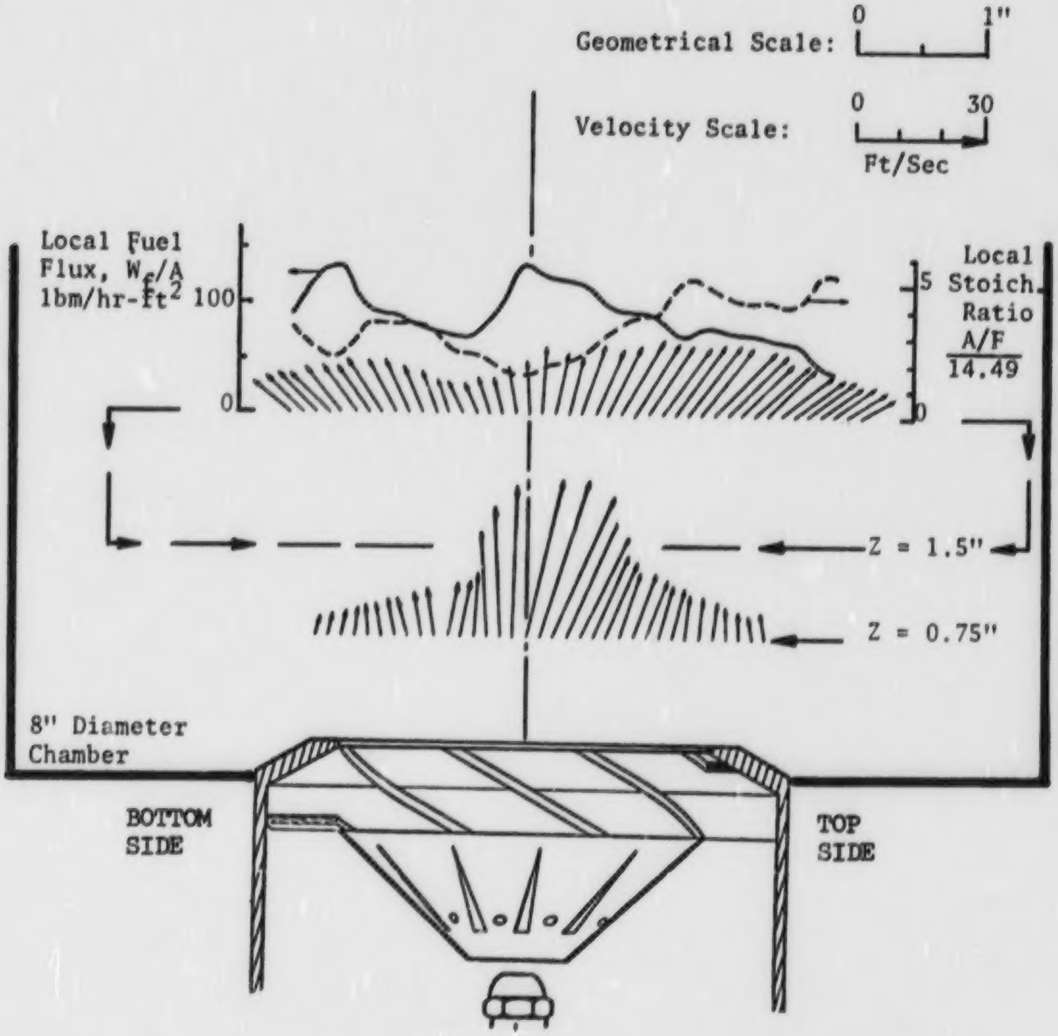
Geometrical Scale:
0
1"
Velocity Scale:
0
30
Ft/Sec
Local Fuel Flux, W_f/A lbm/hr-ft^2
100
0
Local Stoich. Ratio $\frac{A/F}{14.49}$
5
0
Z = 1.5"
Z = 0.75"
8" Diameter Chamber
BOTTOM SIDE
TOP SIDE

Figure 75. Air flow and oil spray flux patterns in the vertical plane of the model AFC burner mounted in an 8-inch-diameter, cylindrical, coaxial chamber (Delavan 0.75-70°-C nozzle)

large area, leading to low local air velocities. Note that for this burner, air velocity measurements were made at 0.75- and 1.50-inch axial positions only, since gas velocities were much lower at the more downstream positions, making the measurements more difficult. The design of the flame-retention head for this burner is such that air from the blast tube is directed radially inward to a center impingement point very near the blast tube exit. After the air impinges upon itself, it reflects in a relatively outward direction, ultimately leading to the well-dispersed flow observed at the 1.5-inch axial location.

Also shown in Fig. 74 and 75 are the local spray mass fluxes determined from cold-flow experiments with the air band wide open. These spray mass fluxes have minima similar to those observed when the same spray nozzle was tested with the ABC Mite burner. The existence of the minima with the Model AFC burner, which has no highly local swirl such as the ABC Mite, indicates that the minima may be the result of the spray nozzle characteristics rather than those of the burner air flow.

Local combustion zone gas samples were obtained with the Model AFC burner mounted in the 8-inch-diameter coaxial cylindrical combustion chamber. The data obtained are presented in Fig. 76 and 77. The relatively uniform mixing characteristics of this burner are evident from these composition profiles. The most significant factor is the effect of overall stoichiometric ratio on the nitric oxide concentrations. The nitric oxide concentrations are lower at the 1.50 stoichiometric ratio than they are with the 1.25 stoichiometric ratio, consistent with previous trends of nitric oxide versus local stoichiometric ratio indicated minimum nitric oxide at stoichiometric ratios near 1.8. Carbon monoxide levels are lowest for the more air-rich operating condition.

Compositions of Model AFC burner mixed exhaust gases from the coaxial cylindrical combustion chamber and from the Lennox furnace were presented earlier, along with data from the 55-J burner in Fig.57 through 63. Those results are consistent with the good mixing behavior of the

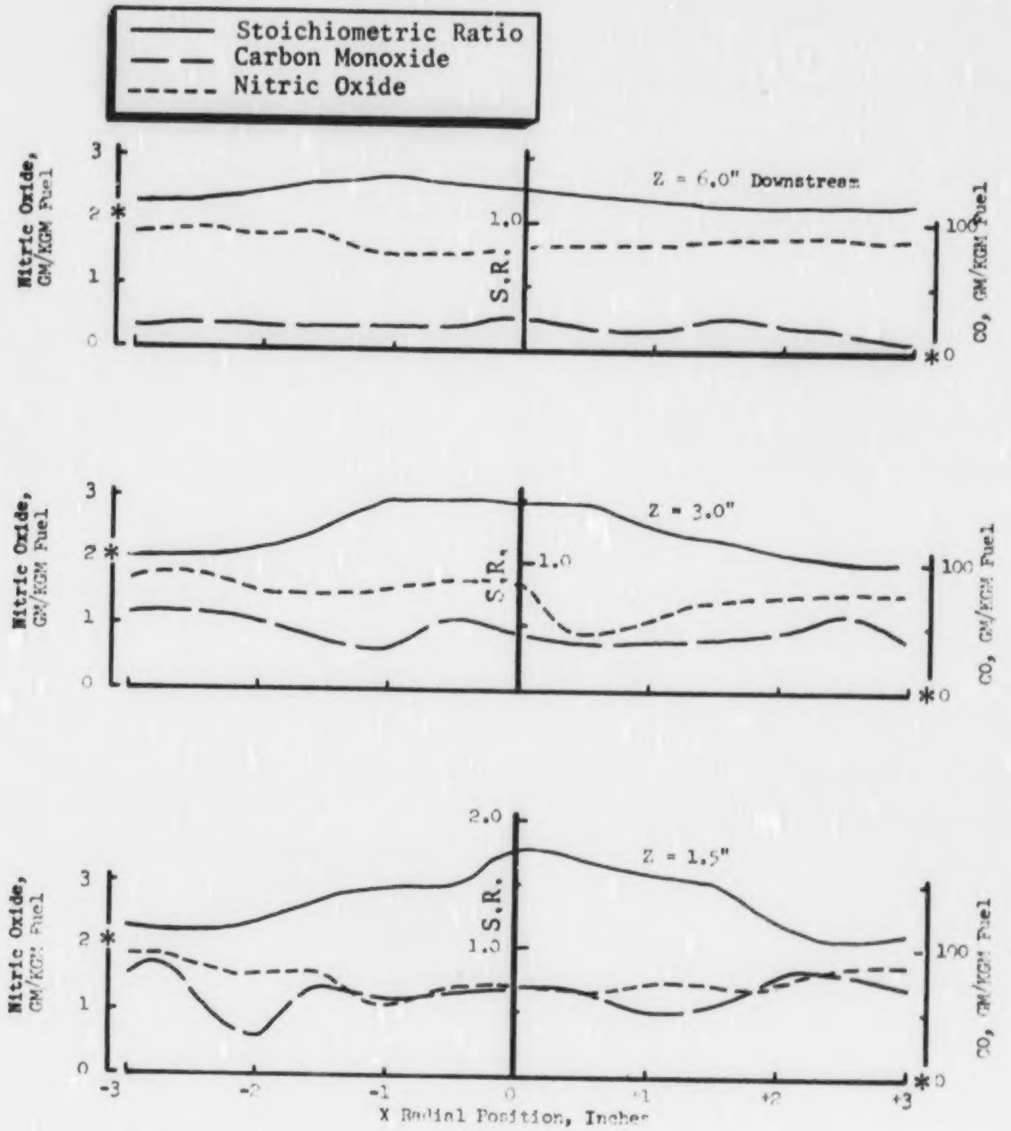

* = Exhaust Stack Emission Levels

Figure 76. Combustion gas analysis profiles for the model AFC burner at a nominal stoichiometric ratio of 1.25 with a 0.75-70°-A nozzle

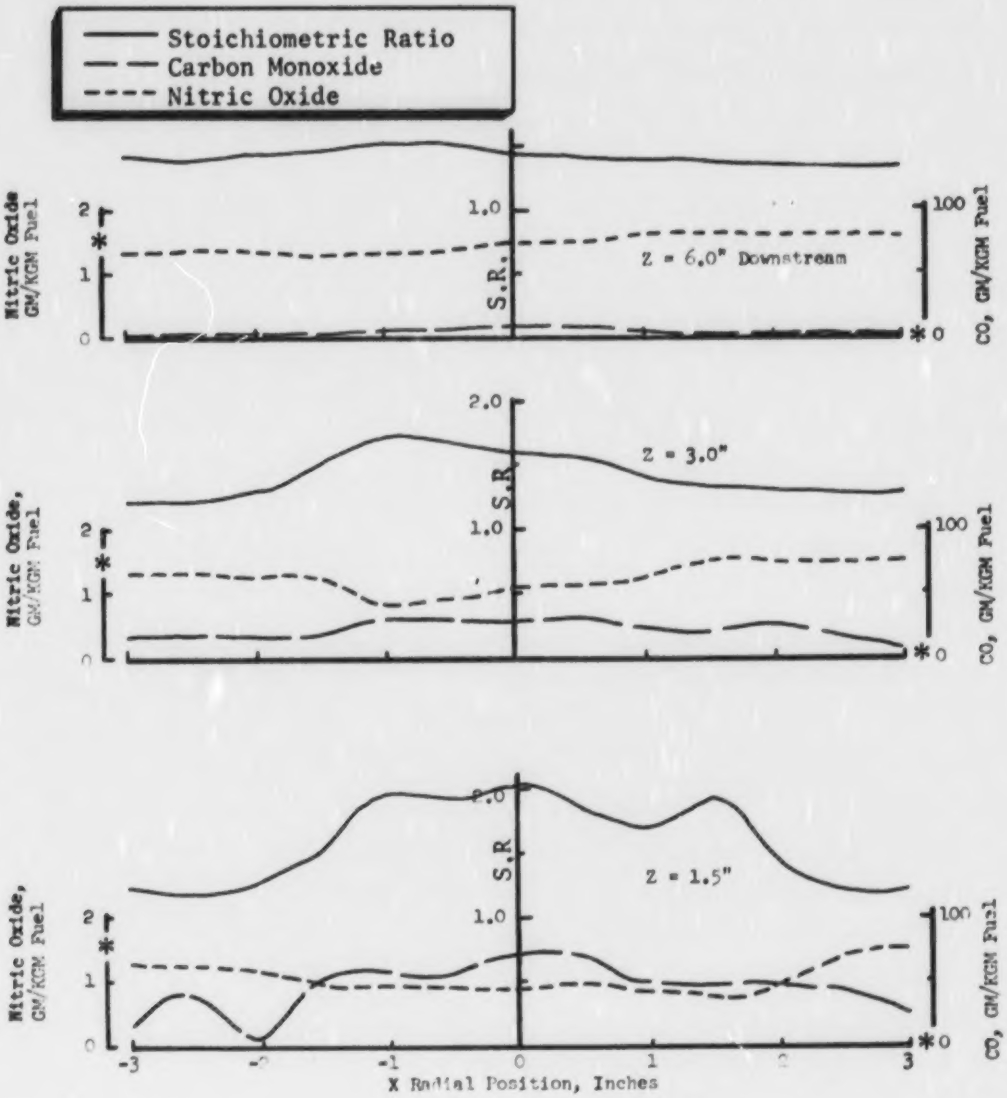

∗ = Exhaust Stack Emission Levels

Figure 77. Combustion gas analysis profiles for the model AFC burner at a nominal stoichiometric ratio of 1.50 with a 0.75-70°-A nozzle

Model AFC burner and the expected influence of uniform local stoichiometric ratio on pollutant emissions. With respect to smoke, hydrocarbon, and carbon monoxide emissions, the Model AFC burner had a relatively wide acceptable overall stoichiometric ratio operating range (from stoichiometric ratio ~1.1 to ~2.2) which was free of significant smoke and CO emissions. The uniform mixing of the Model AFC burner has, therefore, narrowed the spread of local stoichiometric ratios so that, for example, it is possible to operate at an overall stoichiometric ratio relatively close to unity, without having too much local flow at below unity stoichiometric ratios.

Nu-Way Model CO Burner (6.0 gph)

The Nu-Way Model CO burner is a larger than residential-size burner capable of operating in the 6- to 10-gph oil flowrate range. For the experiments conducted, this burner was fired at 6 gph. Construction of the Nu-Way is similar to the 55-J, except it is considerably larger in size, and utilizes dual, side-by-side 3-gph spray nozzles.

Air flow velocity vectors were determined for the Nu-Way burner, as shown in Fig. 78 and 79. In general, the air velocities with this burner were relatively high (~60 ft/sec) compared with velocities observed in the residential-size burners (~30 ft/sec). Note that the velocity vector scale is 60 ft/sec/in. in Fig. 78 and 79 compared to 30 ft/sec/in. for previous presentations. The higher air flow pressure drops coincident with the higher gas velocities lead to a relatively uniform distribution of air velocities near the blast tube exit of the Nu-Way burner.

Fuel spray mass fluxes, experimentally determined under cold-flow conditions, also are shown in Fig. 78 and 79. The spray mass fluxes are not very uniform at the 1.5-inch axial location, but they become relatively uniform at the 3- and 6-inch axial locations, except near the outer edges of the flow patterns.

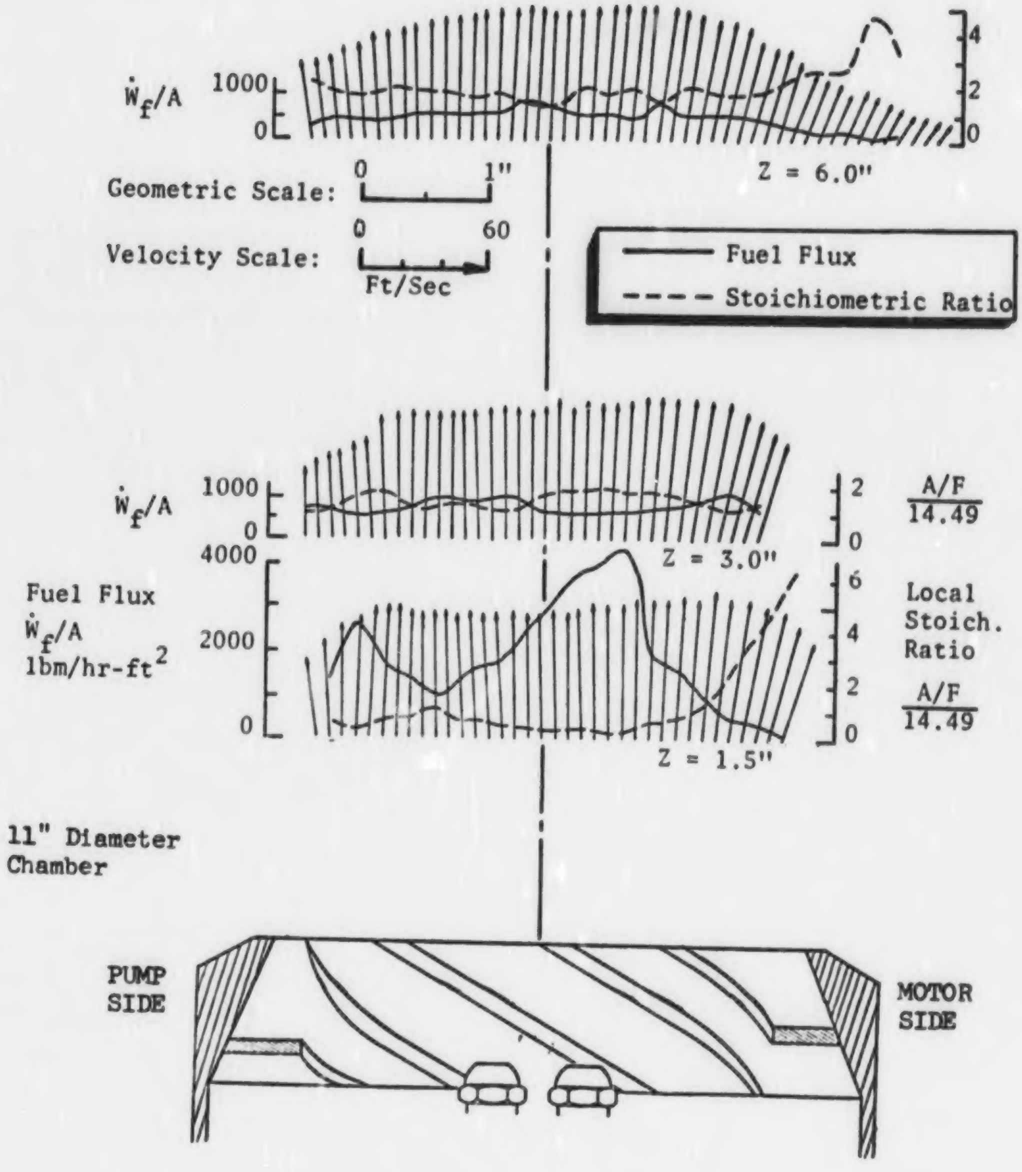

Figure 78. Air flow and oil spray flux patterns in the horizontal plane of the Nu-Way burner mounted in an 11-inch-diameter, cylindrical, coaxial chamber (two 3-gph Delavan nozzles)

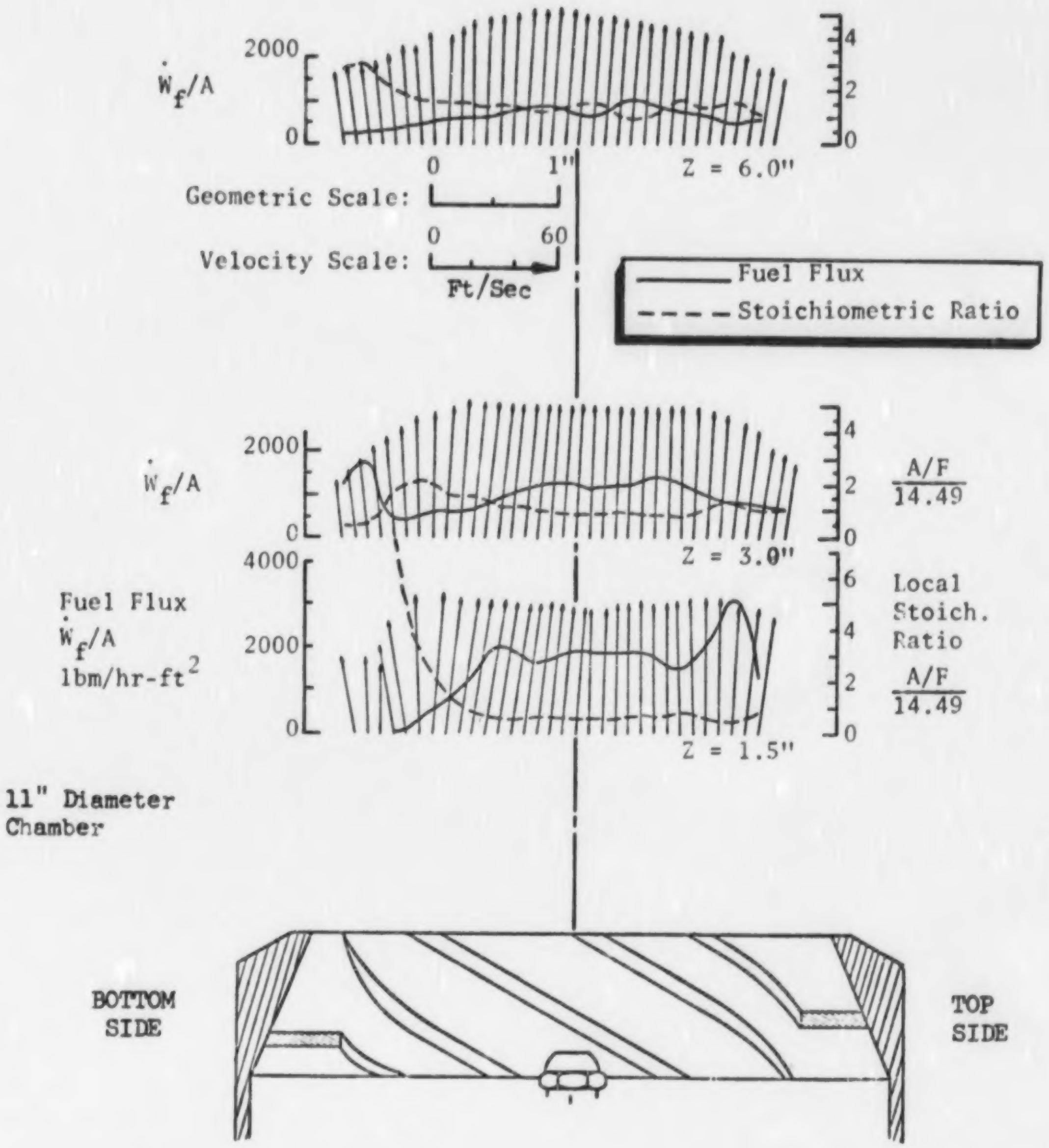

Figure 79. Air flow and oil spray flux patterns in the vertical plane of the Nu-Way burner mounted in an 11-inch-diameter, cylindrical, coaxial chamber (two 3-gph Delavan nozzles)

Combustion gas velocity vectors were also measured with the Nu-Way burner; however, since the flame front was displaced approximately 4 inches away from the blast tube exit (due to high air velocities), combustion gas velocity values are reported only at the 6-inch axial location. The combustion gas velocity profiles (Fig. 80 and 81) appear to be less uniform than the air velocity patterns at the same location, most likely due to the disturbance-amplifying pressure gradient classically present at distinct flame fronts.

The Nu-Way burner was fired in the 30-inch-diameter coaxial combustor, with the combustion chamber configured for cold (water-cooled) wall and hot (refractory-lined) wall. The results for the cold-wall and the hot-wall tests are shown in Fig. 82 and 83. As shown in Fig. 82, the burner was also fired in an 11-inch-diameter coaxial combustion chamber to assess the effects of chamber size on nitric oxide emissions. The nitric oxide emission results shown in Fig. 82 provide insight into the effects of both chamber size and chamber wall temperature.

Lowering the wall temperature by changing from a refractory liner (2500 to 3000 F wall temperature) to a water-cooled wall has a very definite beneficial effect on nitric oxide emissions. This effect is undoubtedly due to the lowering of the flame temperature in the combustion chamber by: (1) convective heat losses from recirculating combustion gases to the cooled wall, and (2) radiative heat loss from the core of the flame zone to the cooled walls.

Decreasing the chamber diameter appears to have detrimental effect on nitric oxide formation. This result may be due to combustion pattern changes in the core of the flow, but it is probably more predominantly a thermal effect resulting from: (1) reduced opportunity for combustion gas recirculation and (2) reduced total heat loss through the smaller area walls of the 18- and 11-inch combustion chambers. The

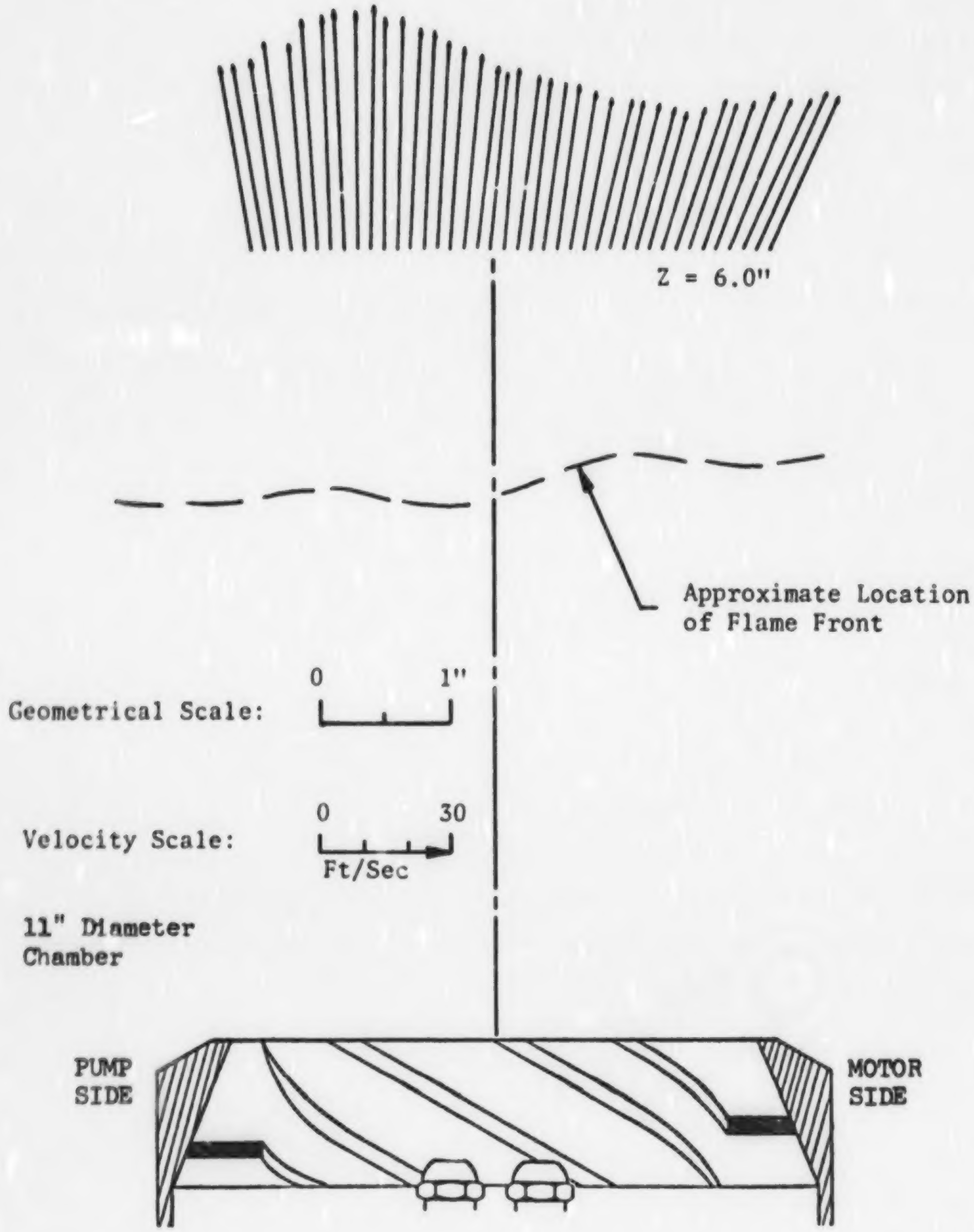
Z = 6.0"
Approximate Location
of Flame Front
0
1"
Geometrical Scale:
0
30
Velocity Scale:
Ft/Sec
11" Diameter
Chamber
PUMP
SIDE
MOTOR
SIDE

Figure 80. Combustion gas velocity vectors in the horizontal plane for the Nu-Way burner mounted in an 11-inch-diameter, cylindrical, coaxial chamber

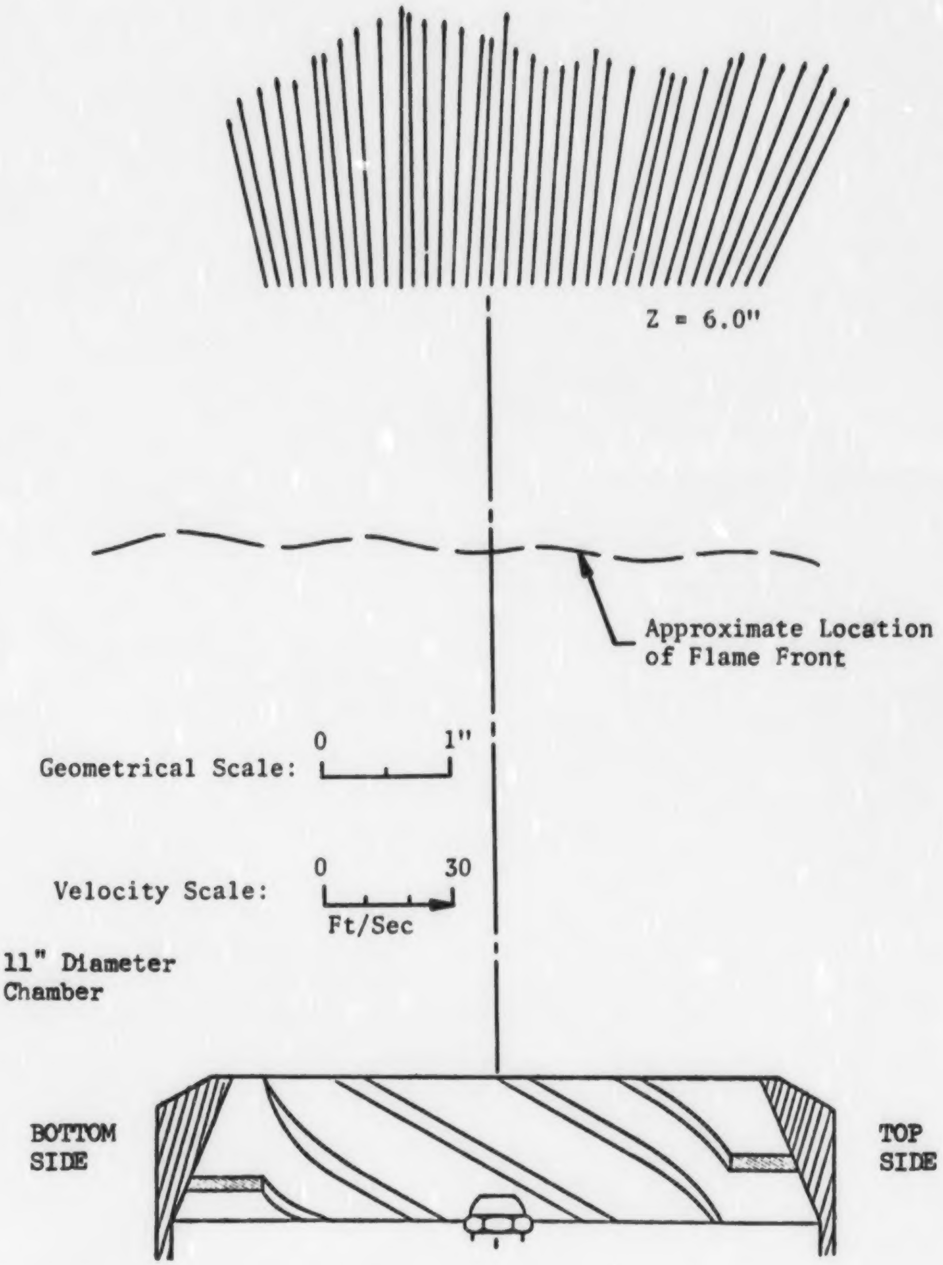
Z = 6.0"
Approximate Location of Flame Front
Geometrical Scale:
0
1"
Velocity Scale:
0
30
Ft/Sec
11" Diameter Chamber
BOTTOM SIDE
TOP SIDE

Figure 81. Combustion gas velocity vectors in the vertical plane for the Nu-Way burner mounted in an 11-inch-diameter, cylindrical, coaxial chamber

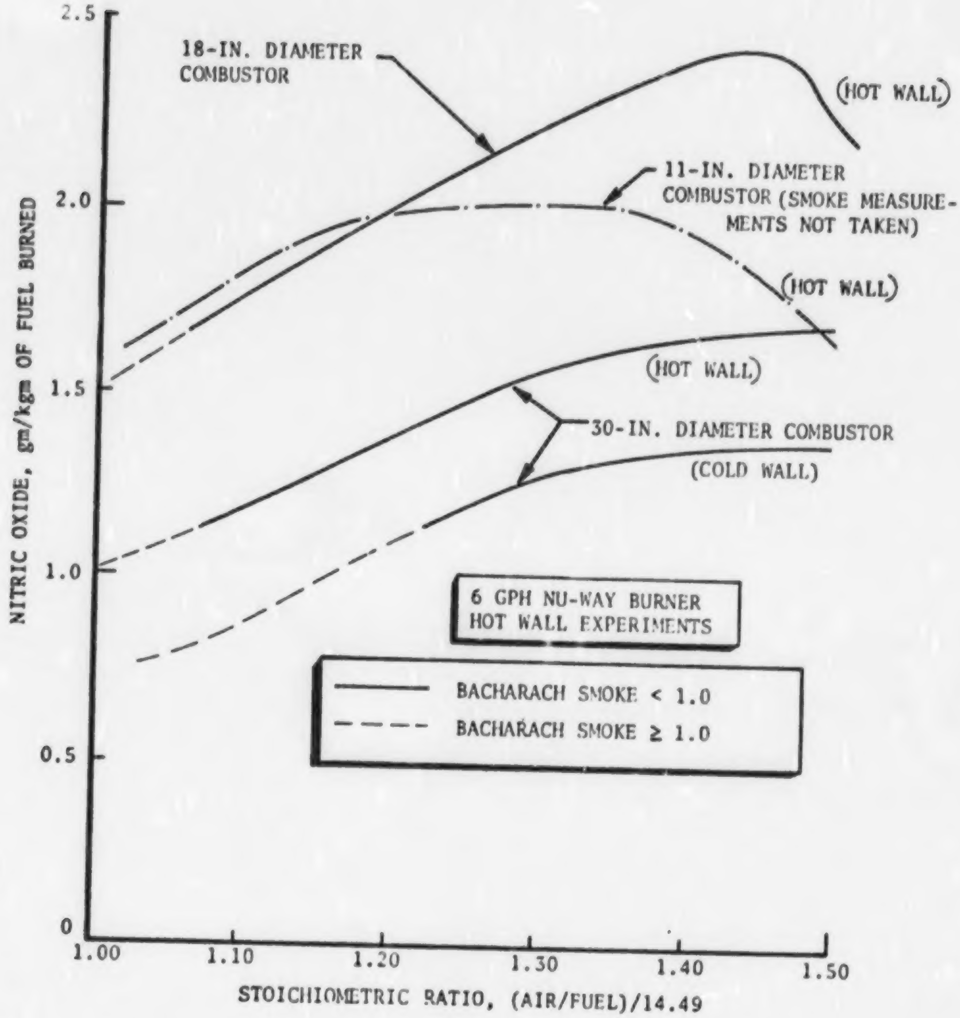

Figure 82. Effect of combustion chamber size on nitric oxide emissions

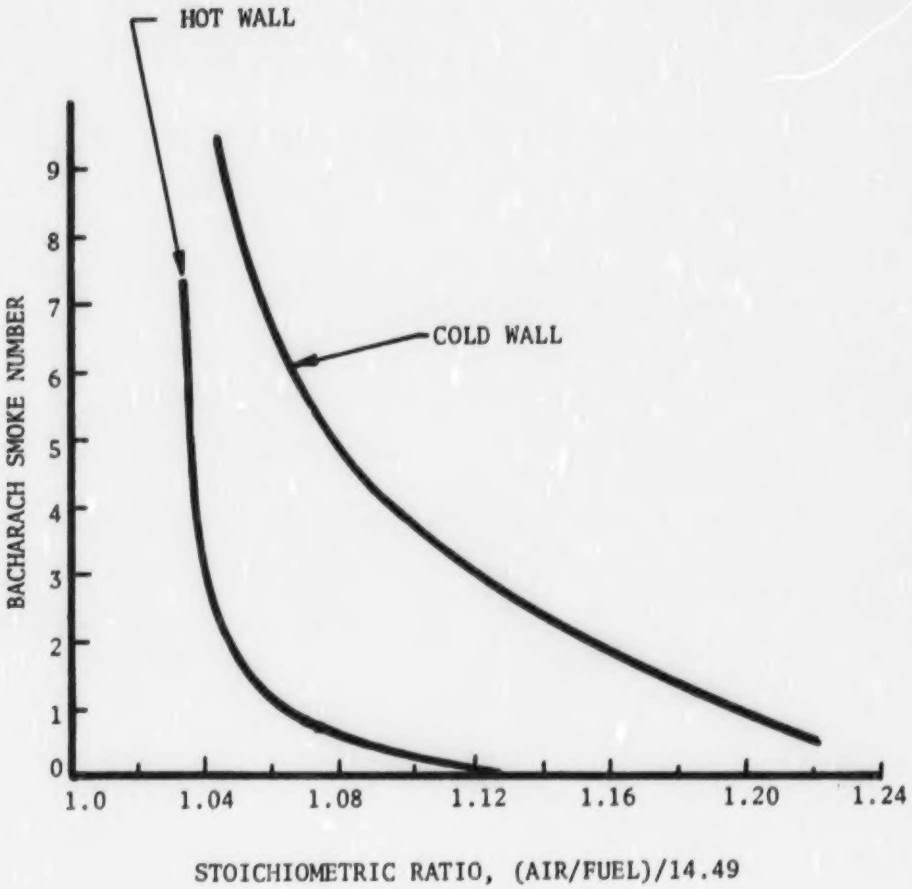

Figure 83. Smoke content of the exhaust gases for the 6-gph Nu-Way burner operating in the 30-inch-diameter, coaxial combustion chamber under cold- and hot-wall conditions

selection of a chamber diameter intermediate between the 30-inch chamber appears to be a reasonable compromise between nitric oxide emissions and combustion chamber capital cost. According to usual industrial practice, the Nu-Way burner, at 6.0 gph, would normally be fired in a combustion chamber intermediate in volume between the 18-inch-diameter chamber (nominally sized for 3 gph) and the 30-inch-diameter chamber (nominally sized for 12 gph). The fact that (according to Fig. 82) a compromise between chamber capital costs and nitric oxide emissions also leads to selection of a chamber diameter intermediate between 18 and 30 inches suggests that typical burner manufacturer design criteria are not unreasonable with respect to nitric oxide emissions. Burner manufacturers claim their chamber size criterion is that the chamber should be sufficiently large to have the entire luminous zone of combustion contained within the chamber.

Shown in Fig. 83 are the Nu-Way smoke emissions as a function of stoichiometric ratio and chamber wall temperature. The cooler wall temperatures lead to higher smoke emissions. This is apparently due to a greater tendency for the cool walls to quench the combustion before its completion. Note that if the usual procedure of setting the burner at number one smoke were followed, the nitric oxide emissions would be nominally the same for both the hot-wall and the cold-wall conditions. For this burner, carbon monoxide emissions were generally negligible when the smoke number was less than one.

Local combustion gas samples also were withdrawn and analyzed during tests with the Nu-Way burner in the 30-inch chamber. The stoichiometric ratio, carbon monoxide, and nitric oxide profiles obtained during the hot-wall tests are shown in Fig. 84 and 85 as functions of radial position (r), and axial position (z) relative to the end of the blast tube centerline. The same data are replotted on a reduced scale in Fig. 86, and compared with similar data from the same burner operating under cold-wall conditions. The cold-wall/hot-wall comparisons shown

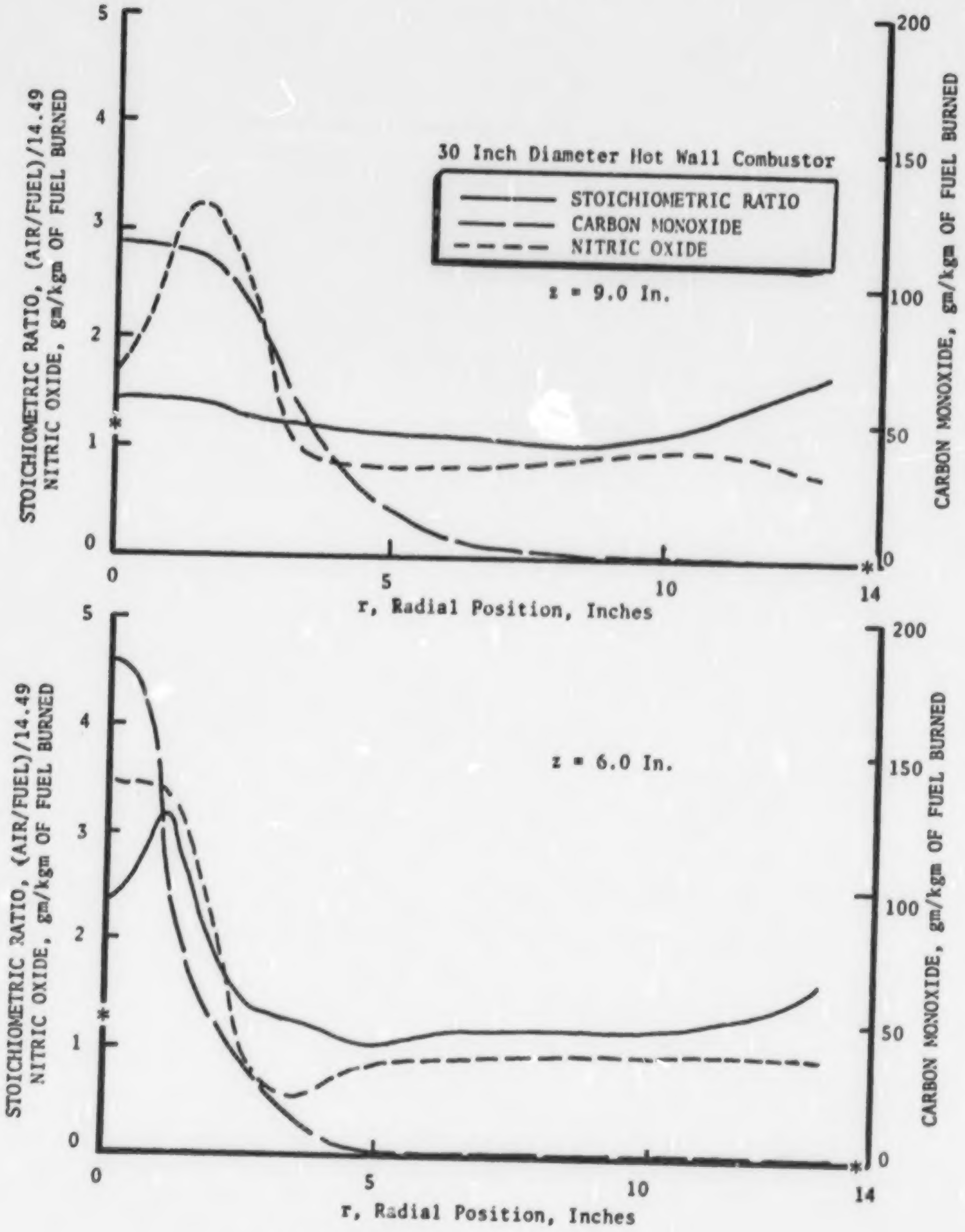

* = Exhaust Stack Emission Levels

Figure 84. Hot-wall, local combustion gas analysis profiles for the 6-gph Nu-Way burner at nominal stoichiometric ratio of 1.16, with twin 3-60°-B oil nozzles

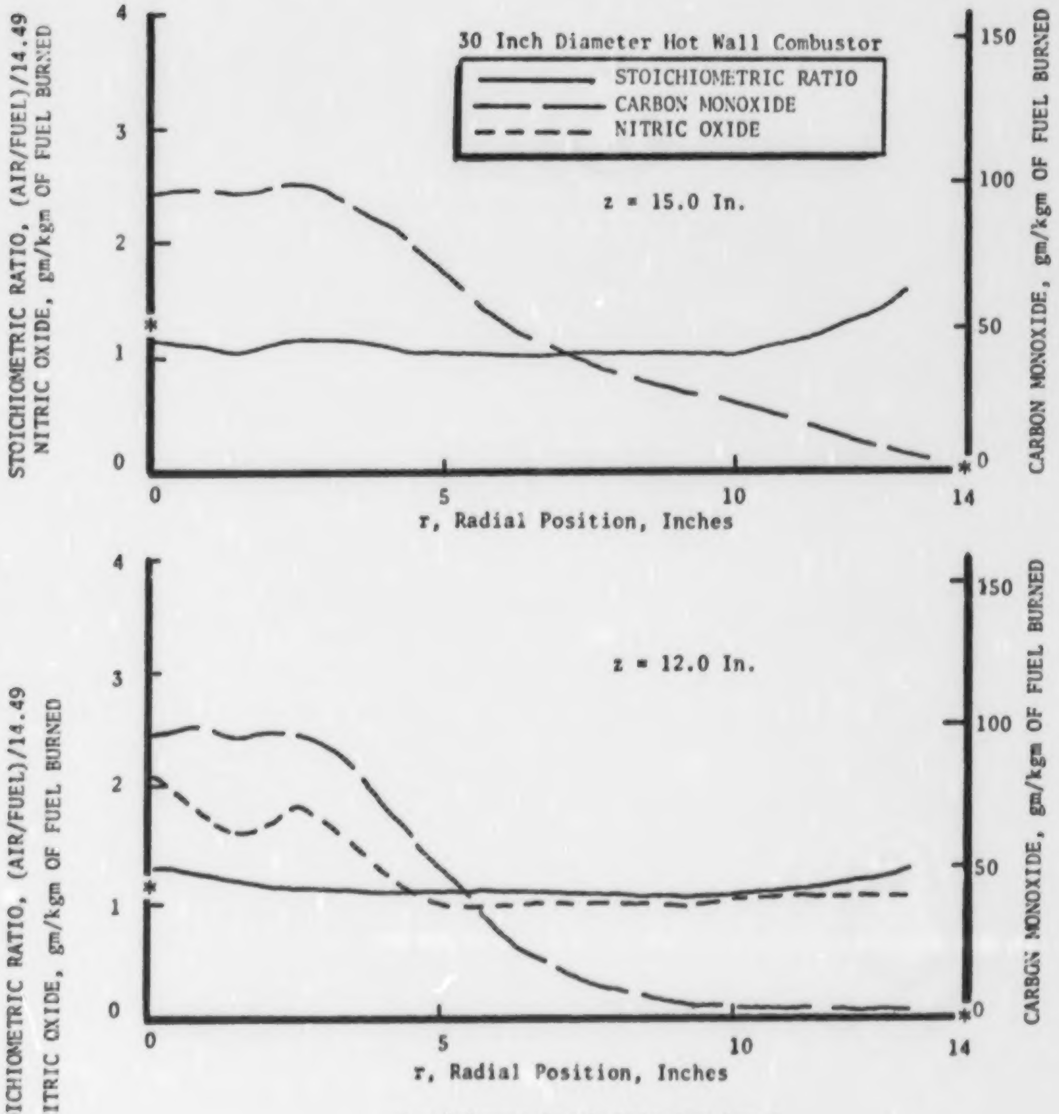

* = Exhaust Stack Emission Level

Figure 85. Hot-wall, local combustion gas analysis profiles for the 6-gph Nu-Way burner at a nominal stoichiometric ratio of 1.16, with twin 3-60°-B nozzles

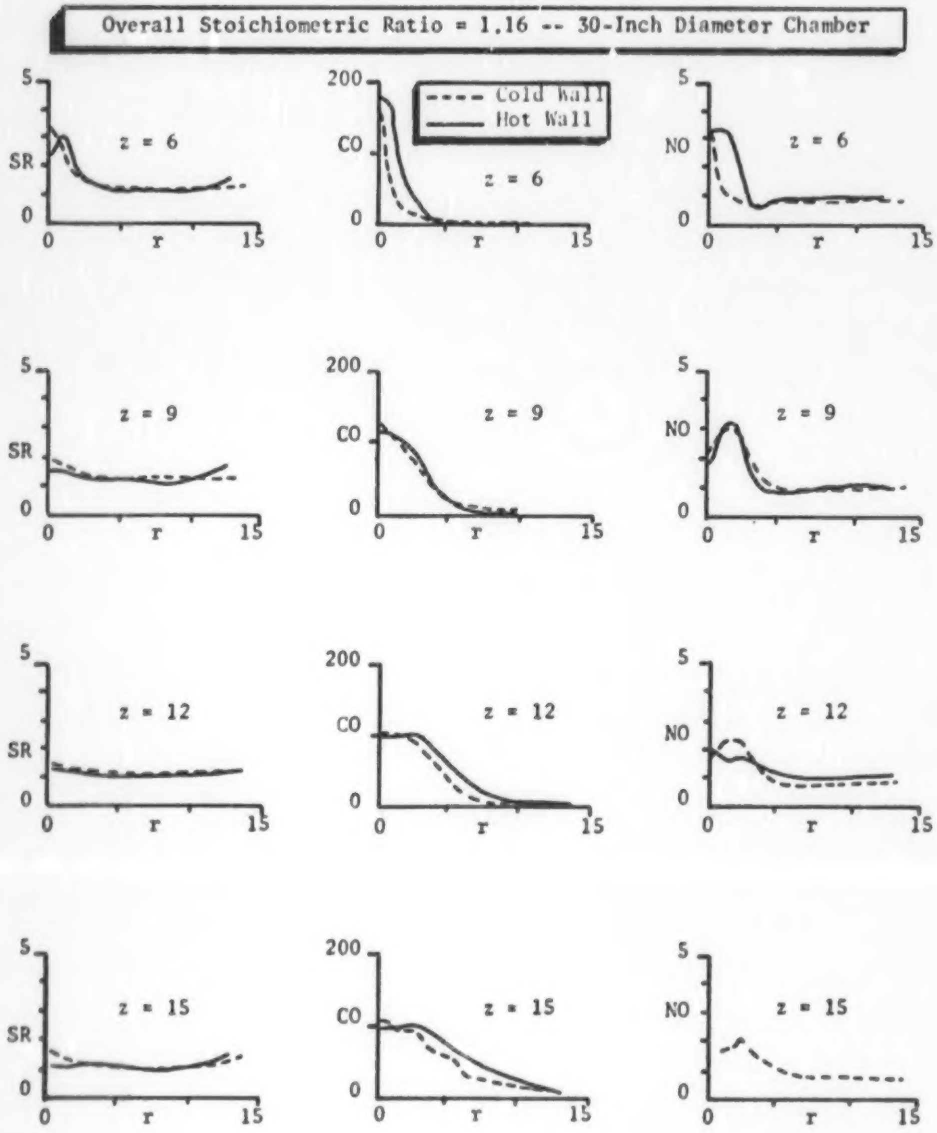

Figure 86. Comparison plots of local combustion zone sampled stoichiometric ratio (SR, AIR/14.49 FUEL), carbon monoxide (gm CO/kg of fuel burned), and nitric oxide (gm NO/kg of fuel burned), as a function of radial location (r = inches) and axial location (z = inches) (Nu-Way burner, 5.5 gph)

in Fig. 86 suggest several interesting observations. Comparison of the stoichiometric ratio profiles suggests that the oil is vaporized and burned slightly earlier in the hot-wall case, as might be expected under conditions of higher temperature. Comparison of the carbon monoxide profiles shows no significant differences except at the 6-inch axial location where the hot-wall profile is more widespread, indicating active combustion processes at larger radii, perhaps due to earlier ignition from hotter recirculating gases. The nitric oxide content has a tendency to peak at radii of 2 to 3 inches, perhaps due to the competing effects of increased nitric oxide due to approaching unity stoichiometric ratio at the larger radii and decreased nitric oxide due to intermixing of the combustion gases with the cooled recirculated gases at the larger radii.

Comparison of the nitric oxide profiles shown in Fig. 86 for hot wall and cold wall indicates the hot-wall nitric oxide is significantly higher than the cold-wall nitric oxide only in the region very near the end of the blast tube (i.e., at $z = 6$ inches). This is reasonable because, when the burner is operating at steady state, the ignition front is maintained by intermixing of hot recirculated gas with the injected air/fuel-spray mixture; and, in the hot-wall case, these intermixed gases are hotter and, therefore, more prone to induce high nitric oxide. The nitric oxide content of the recirculating gases in both hot- and cold-wall cases is about 25 percent lower than the 1.3 and 1.0 gm NO/kg fuel observed in the mixed flue gases, from the two wall conditions, indicating that either: (1) the recirculating gases do not include gas from nitric oxide-rich core of the flame, (2) some additional nitric oxide is formed by thermal processes as the gases pass through the remaining 6 to 8 feet of the baffled exhaust gas mixing section of the combustor, or (3) a combination of these effects. It would seem from inspection of the data that the most likely of these three alternate reasons is (1).

As shown in Fig. 87, composition profiles also were measured when the Nu-Way burner was fired in the 11-inch-diameter hot-wall chamber. Also shown in Fig. 87 are comparative 30-inch-diameter cold-wall data. Both sets of data were taken at 9 inches downstream of the blast tube exit. Surprisingly, at this axial location, the combustion appears to be more nearly complete in the 11-inch chamber, so that the composition profile at the 9-inch axial location in the 11-inch diameter chamber more nearly resembles the composition profiles (Fig. 86) at the 12-inch axial location in the 30-inch-diameter chamber. This may be due to the flame being held closer to the blast tube in the 11-inch-diameter chamber as a result of increased radiant heat exchange from the walls of the smaller diameter chamber.

Nu-Way Burner Radiation Measurements. The 6-gph Nu-Way burner was fired in the 11-inch-diameter cylindrical combustion chamber for radiant energy measurements. A Land Instruments Inc., 2π steradians radiometer was used to measure the radiant energy flux profile across radial traverses at five axial locations of $Z = 1.5$, 3, 6, 9, and 12 inches downstream of the burner head. The radiant energy flux profiles are presented in Fig. 88 and 89, showing data for nominal stoichiometric ratios of 1.25 and 1.50, respectively. The Land radiometer measures radiant energy flux by means of the temperature rise of a blackbody contained in a highly reflective cavity with a small hole for admission of the radiant energy. The radiometer is calibrated and operated with a positive gaseous nitrogen purge to prevent combustion contaminants from entering the blackbody cavity. However, oil spray from the Nu-Way oil burner proved to be capable of penetrating the protection provided by the gaseous purge. Accumulation of small amounts of fuel oil within the sensor head cavity caused deterioration of the black, heat-absorbent coating. Therefore, the data presented in Fig. 88 and 89 should be used for qualitative evaluation only, as the calibration curve probably shifted with the deterioration of the coating. Radiometric probing was initiated at the 12-inch location which, with the least amount of coating deterioration, should be the

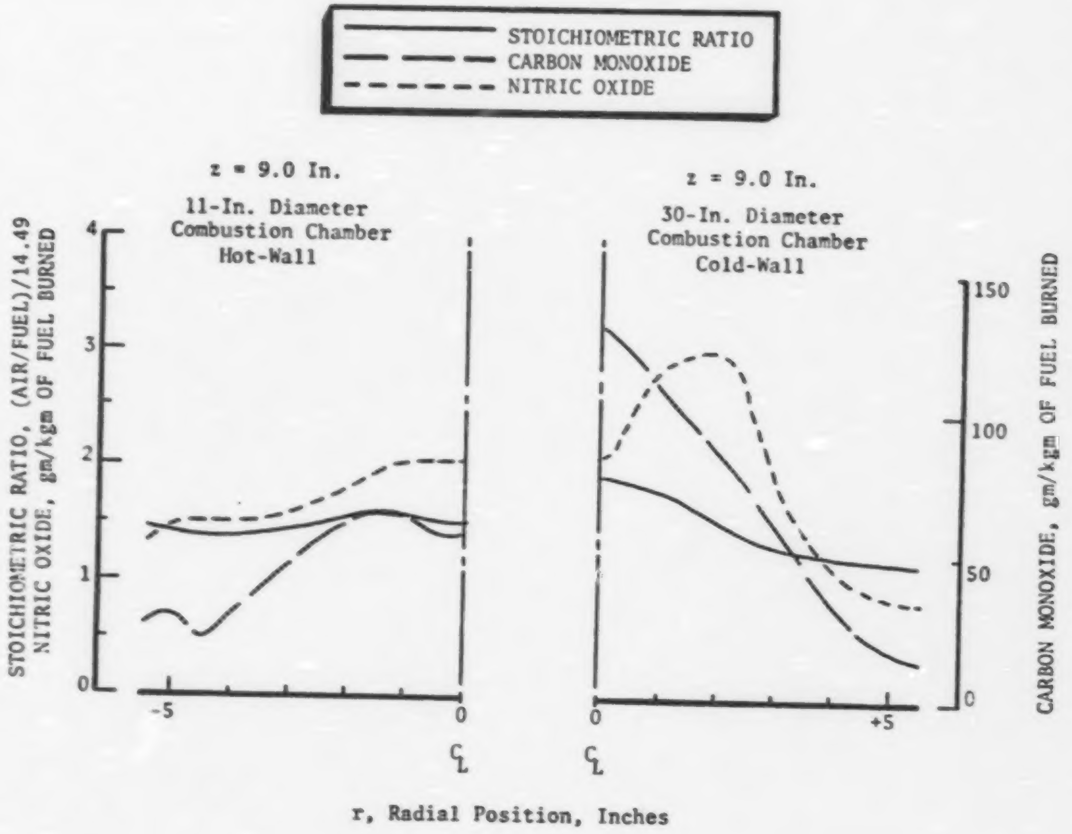

Figure 87. Comparison of combustion gas composition profiles of the 6-gph Nu-Way Model CO burner in hot- and cold-wall enclosures of different diameters

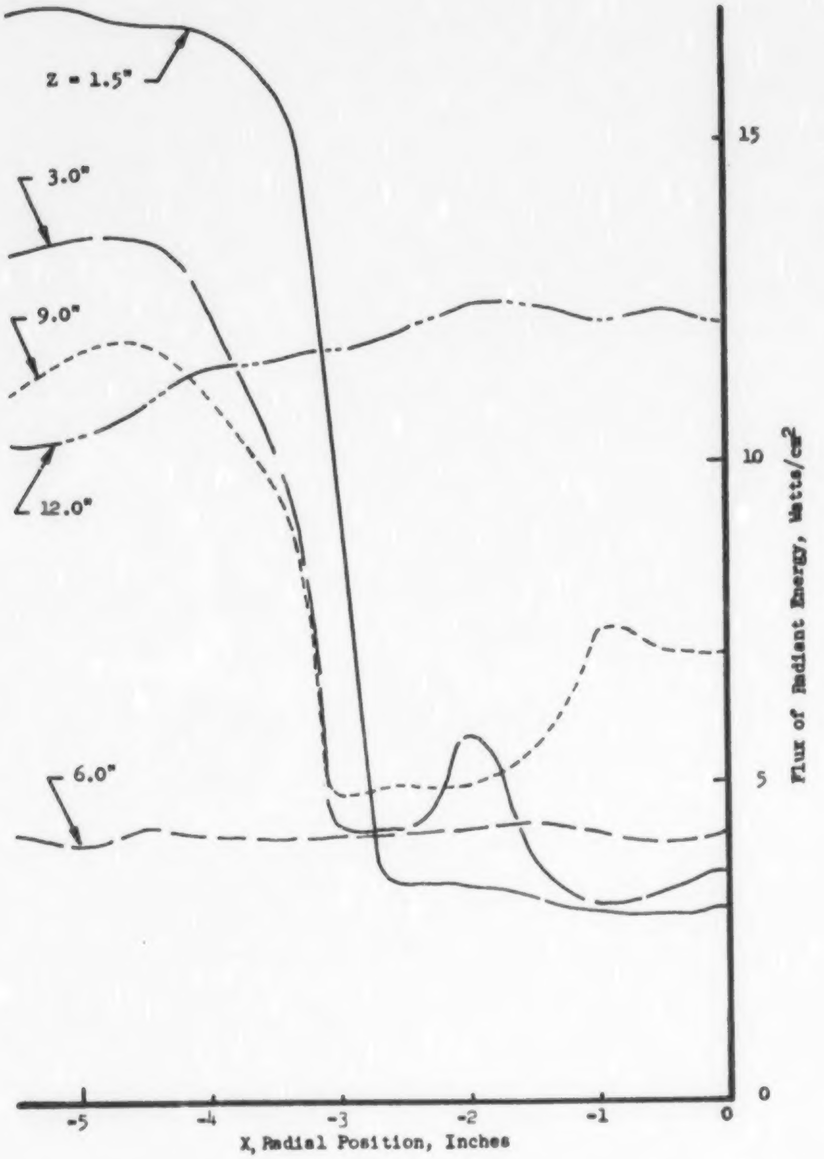

Figure 88. Radiant energy profiles for the 6-gph Nu-Way burner at a nominal stoichiometric ratio of 1.25 (at various distances downstream)

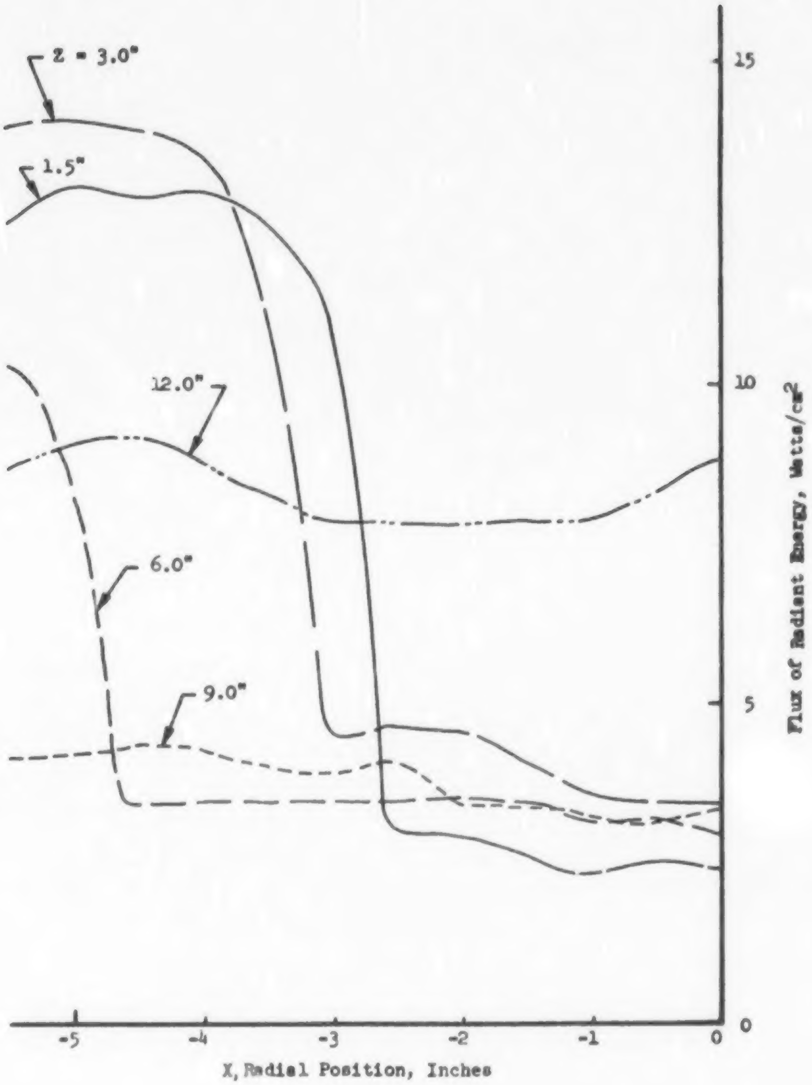

Figure 89. Radiant energy profiles for the 6-gph Nu-Way burner at a nominal stoichiometric ratio of 1.50 (at various distances downstream)

most accurate for any quantitative evaluation. At the 1.5-, 3-, and 9-inch axial locations, a rapid decrease in indicated radiant energy flux was observed between the radial positions of 3 to 4 inches from the burner axis. This drop in indicated flux may be due either to a change in the flame-holding characteristics of the probe itself (if any) or, more likely, to the presence and evaporation of oil within the blackbody cavity. The low, flat curves at 6 and 9 inches also may have been influenced strongly by oil accumulation in the probe.

The data presented in Fig. 89 indicate that an average radiant flux of 10 to 15 watts/cm^2 might be expected at any typical location. It is of interest to determine how important this energy flux might be relative to the droplet vaporization and combustion processes. The flux, as measured, is received from 2π steradians (a hemisphere) just as the radiant flux would be received by a differential segment of droplet surface area. The radiant energy flux can therefore be compared with the energy flux required per unit droplet surface area to vaporize a typical droplet at a rate characteristic of burning. The total flux for droplet vaporization is received by a combination of forced convection and radiation. For a droplet burning in stagnant air, the burning rate can be described by the burning rate parameter k' as follows:

$$k' = \frac{d(D^2)}{dt} = \frac{4(dm/dt)}{\rho_L \ \pi D} = \text{constant}$$

where

k' = burning rate constant, cm^2/sec
D = droplet diameter, centimeter
t = time, seconds
m = droplet mass, gram
ρ_L = droplet density, gm/cm^3

The above expression is easily used to determine the necessary energy flux to sustain droplet vaporization at a rate consistent with the burning rate constant k':

$$\frac{Q}{A} = \frac{(dm/dt)\ \Delta H_v}{\pi D^2} = \frac{k'\ \rho_L\ \Delta H_v}{4\ D}$$

where

Q/A = thermal energy flux per unit droplet surface area, cal/cm^2-sec

ΔH_v = latent heat of vaporization, cal/gm

For a typical hydrocarbon droplet burning in stagnant air, k' $\simeq$ 0.01 cm^2/sec (see, e.g., Goldsmith, M. and S. S. Penner, "On the Burning of Single Drops of Fuel in an Oxidizing Atmosphere," Jet Propulsion, V. 24, pp 245-251, 1954), $\rho_L \simeq 0.8$ and $\Delta H_v \simeq 100$ cal/gm. Typical droplet size in the burner tested is about 0.01 centimeter and, for these parameters, the above equation yields a required energy flux for vaporization of 20 cal/cm^2-sec or about 83 watt/cm^2. The observed radiant energy flux of 15 watt/cm^2 is about 18 percent of the 83 watt/cm^2 required for vaporization if the droplets were burning in a stagnant atmosphere. In the convective environment of the oil burner, the burning rate constant k' can be larger by a factor of about 2 or 3 than the k' for stagnant conditions and, thus, the radiant energy flux is probably only about 6 to 9 percent of the total flux required for vaporization. This is a relatively insignificant percentage; however, during droplet ignition, just after droplets leave the spray atomization nozzle, the surrounding gas is cold and the radiant energy flux must be the major source of thermal energy for ignition of the droplets. Therefore, the radiant energy fluxes observed are concluded to have little influence on the combustion processes after ignition, but to have major influence on the spray droplet ignition processes.

Since the radiant energy flux has a strong influence on the spray droplet ignition process, and since the chamber geometry will, in turn, influence the radiant energy flux (as well as hot-gas recirculation), oil burner operation in different chambers should be more consistent if the spark ignition is left on. When the spark ignition is left on, droplet ignition is less dependent on radiation and hot-gas recirculation from the rest of the chamber. It should be noted, however, that consistent operation does not necessarily imply best operation, and thus there may be more compelling reasons for not leaving the spark ignition turned on, such as reduction of total power consumption or reduction of nitric oxide emissions.

Carlin Model 250 FFD Burner (6.0 gph)

This burner (shown in Fig. 90) is a somewhat unique design that encloses the most upstream portion of the flame in a funnel-shaped addition on the end of the blast tube. Inside the flame funnel, at the point of transition from the cylindrical blast tube to the conical flame funnel, a radially louvered flame retention cone is located. The air that passes through the swirl-inducing louvers participates in the combustion that takes place inside the flame funnel, while the air that passes around the flame-retention device serves to insulate the large cone from the thermal effects of the combustion which it contains. The position of the flame-retention cone in the flame funnel is adjustable by means of an escutcheon on the outside of the burner; this adjustment allows the burner to operate over a fairly wide oil flowrate range.

The Carlin Model 250 FFD burner was test fired in the 30-inch-diameter, hot-wall chamber. The maximum recommended firing rate for this burner is 12 gph; however, with the existing motor/fan combination, it was not possible to flow sufficient air through this burner to achieve air-rich combustion, presumably because of the small draft available from the 30-inch-diameter combustor which has no significant exhaust

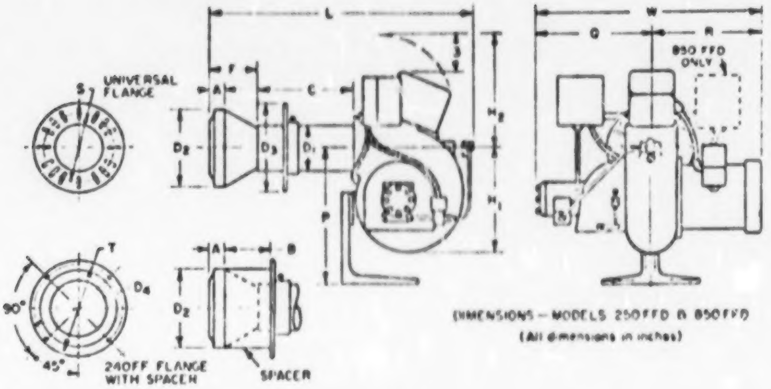
L
W
Q
R
850 FFD ONLY
S
UNIVERSAL FLANGE
F
A
C
D2
D3
D1
H2
H1
P
J
T
D4
90°
45°
240FF FLANGE WITH SPACER
A
B
D2
SPACER
DIMENSIONS – MODELS 250FFD & 850FFD
(All dimensions in inches)

MODEL NO	A	B	C	D_1	D_2	D_3	D_4	D_5	D_6	F	H_1	H_2	L	P	Q	R	S	T	W
250 FFD	1½	4-8	10 or 15	4⅛	7	8½	10	5⅛	7⅛	4⅛	9⅝	10½	26½-31½	9⅝-12⅝	9½	11	5⅝-7⅝	9	20½

(a) Overall geometry

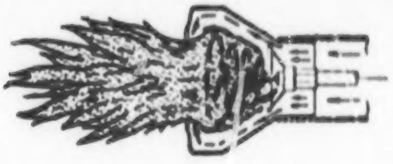

(b) Flame funnel detail

Figure 90. Diagram of the Carlin Company FFD flame funnel series burner showing the semi-staged combustion

stack height. For the 250 FFD, the minimum recommended firing rate is 5 gph. In this burner, twin oil nozzles are used; however, the only near-matched nozzles available were a 3-gph, 45 degree hollow-cone nozzle and a 3-gph, 45 degree solid-cone nozzle. The 250 FFD burner was fired with these nozzles, which have a total flowrate of 6 gph. The nitric oxide emissions obtained with these nozzles is shown in Fig. 91. Results are shown for two positions of the flame-retention cone, the recommended position for 6 gph (1/7-inch forward) and full forward. The manufacturer recommends positioning the flame-retention cone at proportionate locations between its full-back position (i.e., in the throat of the burner flame funnel) for the lowest, 5-gph flowrate, and full forward (1 inch ahead of full back) for 12 gph. The results shown in Fig. 91 indicate the burner produces less nitric oxide at the full-forward position than at the recommended position. At high excess air with the the recommended position, the flame tended to detach itself and move downstream of the flame cone. Also shown in Fig. 91 are emission results from the 6-gph Nu-Way, and the 7- and 12-gph Sun-Ray burners. The 250 FFD burner does not have as high emissions as the 12-gph Sun Ray, but neither does it have as low emissions as the Nu-Way burner. Both the Sun-Ray (discussed next) and the Carlin are flame-retention burners, while the Nu-Way has only modest peripheral swirler vanes. Since emissions of both the flame-retention burners are close together at low excess air, while the Nu-Way is lower, these results support the conclusion that nonflame-retention burners tend to have lower emissions at low excess air conditions.

Sun-Ray Model PHC-34 Burner (12 gph)

The Sun-Ray PHC-34 burner is a 5- to 14-gph burner incorporating a single oil nozzle when used at the nominal oil flowrate of 12-gph for the reported experiments. This burner has a 4-inch-diameter conical flame-retention device located inside the 5-inch-ID blast tube. The spray nozzle is located at the center of the conical deflector, and there is no choke ring on the blast tube end.

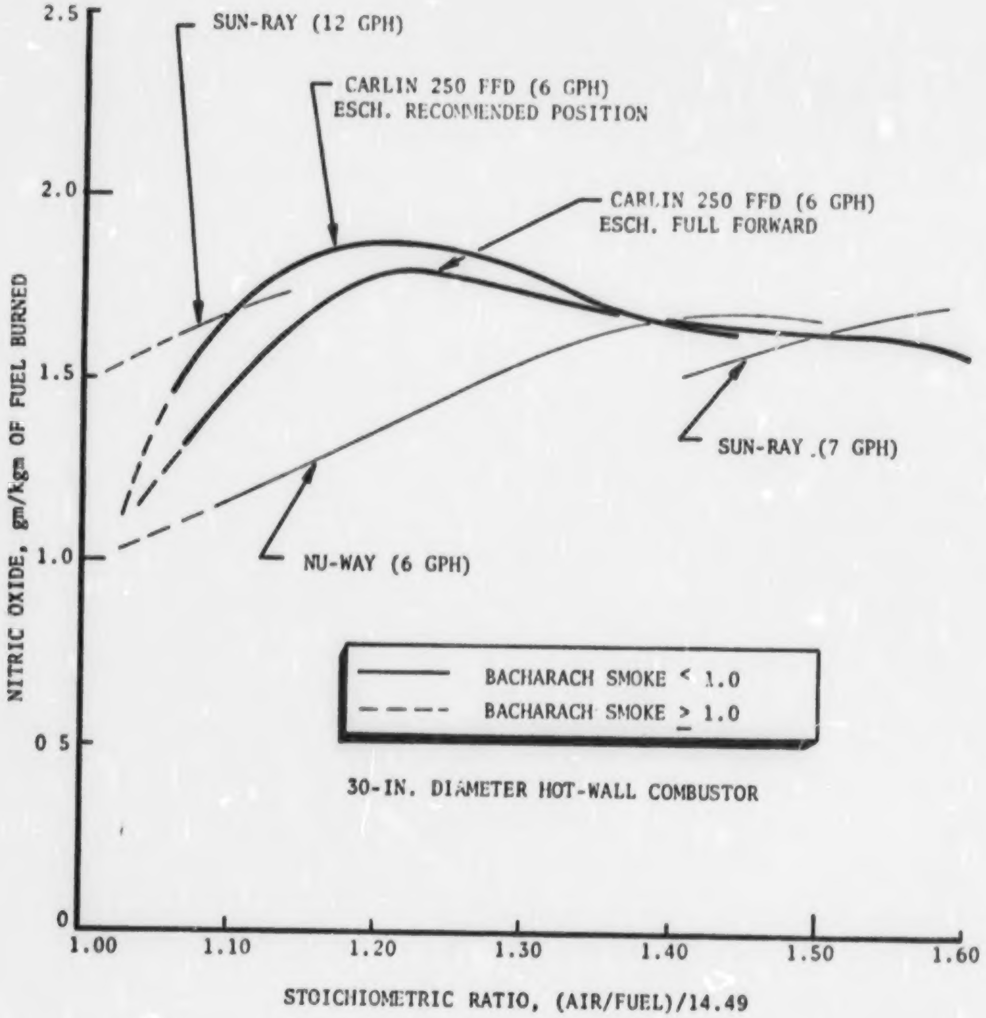

Figure 91. Nitric oxide emissions obtained from the Carlin 250 FFD flame funnel, the Nu-Way Model CO, and the Sun-Ray Model PHC burners

Air velocity vectors were determined using the Sun-Ray burner. These tests were conducted in an open-air environment. The data are presented, for the horizontal plane, in Fig. 92 through 94, and the vectors are two-dimensionally displayed in Fig. 95 and 96. At the 1.5- and 3-inch axial locations, there exist regions in which it was not possible to measure finite air velocities with the equipment used for these experiments, and it is concluded that these areas must be slow moving zones of recirculation caused by the presence of the flame-retention device in the blast tube exit.

Nitric oxide and smoke emission data for the Sun-Ray burner fired into the 30-inch-diameter coaxial combustion chamber are shown in Fig. 97 and 98. The burner was tested at two different oil flowrates, using the same spray nozzle, by adjusting the oil supply pressure. At 7 gph, the results are very similar to those previously presented for the 6-gph Nu-Way burner while, at 12 gph, the nitric oxide emissions are approximately 30 percent higher, probably due to the lesser percentage of heat lost through the chamber walls at the higher flowrate. The effects of cold- and hot-wall operation are also similar to those same effects discussed previously in the Nu-Way burner.

Local combustion gas samples were also withdrawn and analyzed for the Sun-Ray burner operating in the 30-inch-diameter hot-wall chamber. The stoichiometric ratio, carbon monoxide, and nitric oxide profiles obtained from these tests are shown in Fig. 99 through 101, as functions of radial position (r), and axial position (z), relative to the end of the blast tube centerline. The same data are replotted on a reduced scale in Fig. 102 for comparison with similar data for the same burner operating under cold-wall conditions. This burner has a flame-holding cone in the end of the blast tube which serves as a large zone of ignition for the air/oil spray mixture injected by the burner. The recirculation pattern caused by this flame cone is surrounded by an annulus of high velocity-injected air and, thus, should be relatively insensitive (at short z distances) to the temperature of the

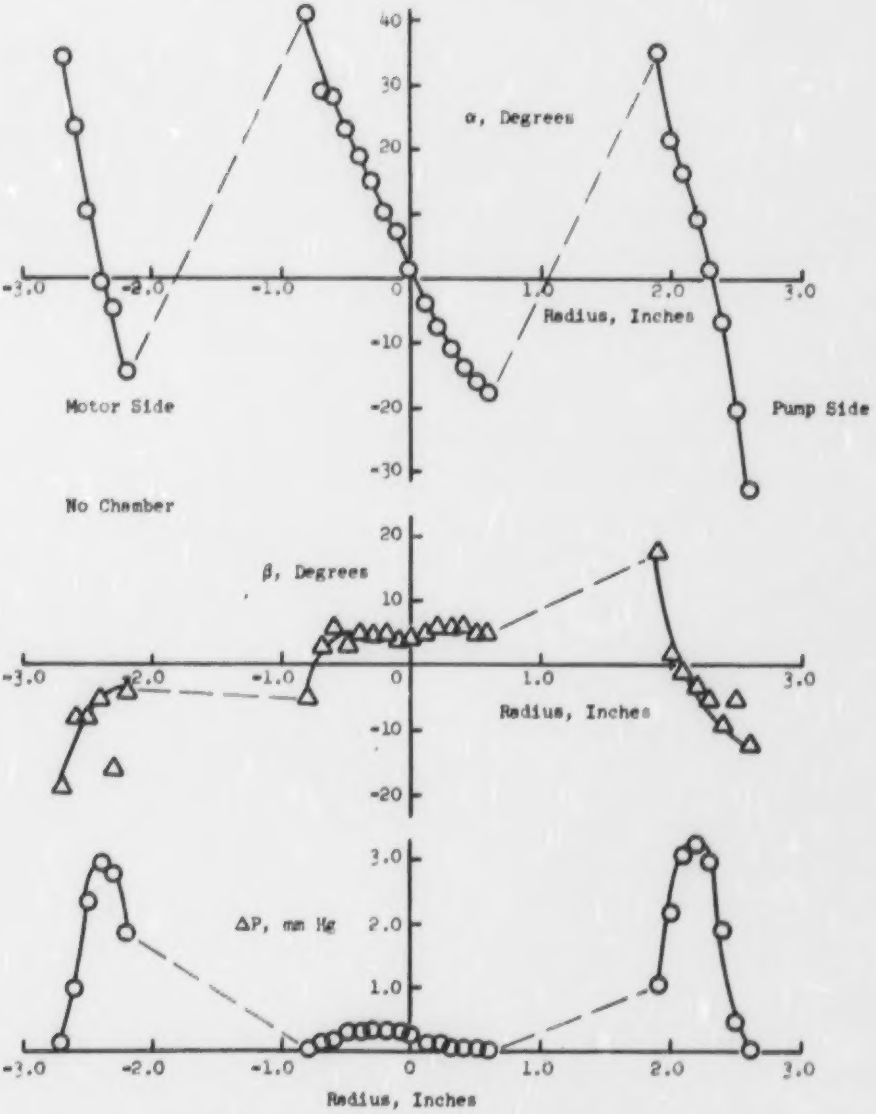

Figure 92. Air flow parameters in the horizontal plane at 1.5 inches downstream of the Sun-Ray burner with no chamber and no oil flow

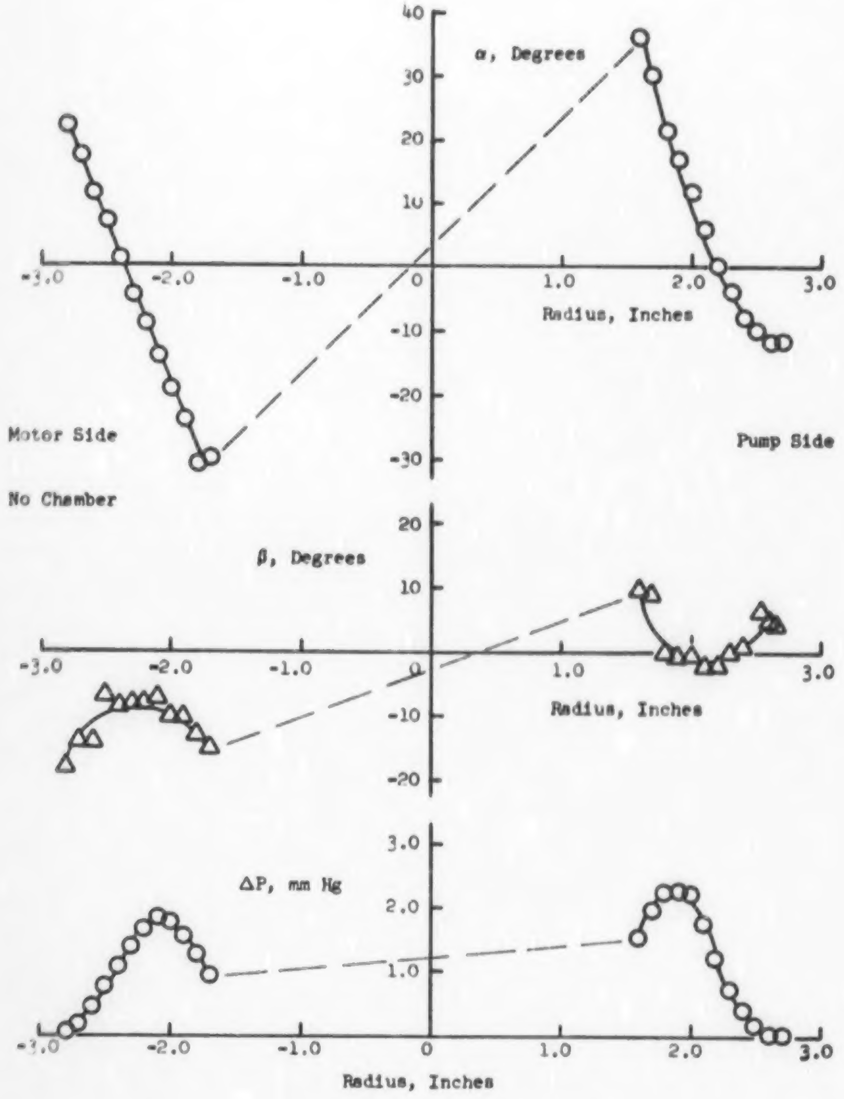

Figure 93. Air flow parameters in the horizontal plane 3 inches downstream of the Sun-Ray burner with no chamber and no oil flow

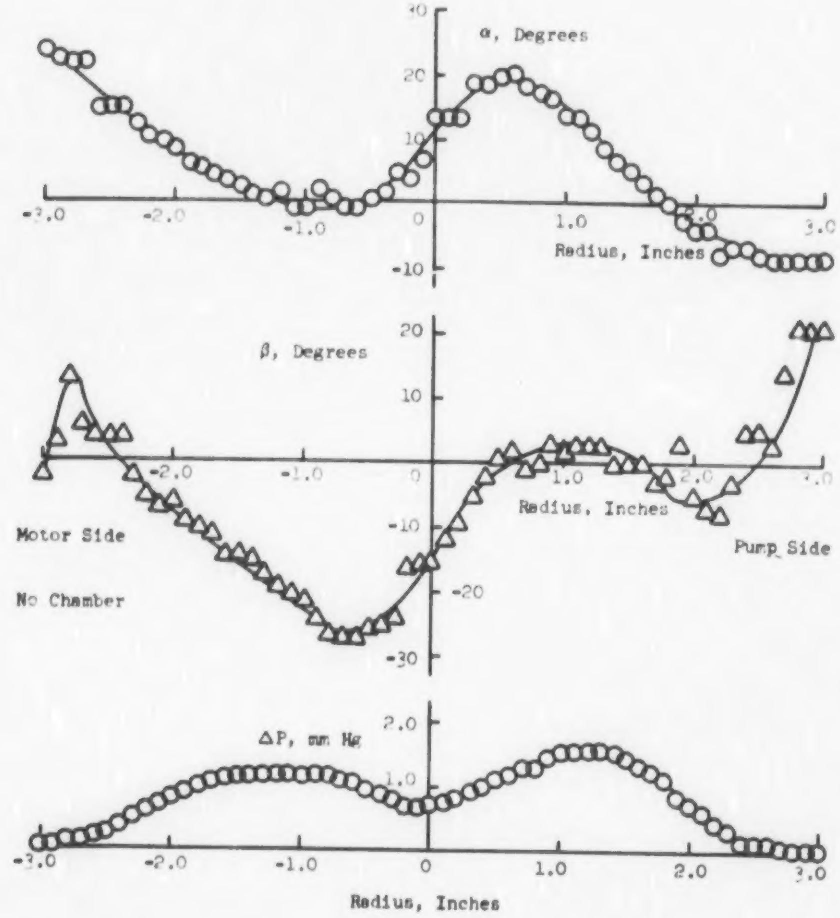

Figure 94. Air flow parameters in the horizontal plane at 6 inches downstream of the Sun-Ray burner with no chamber and no oil flow

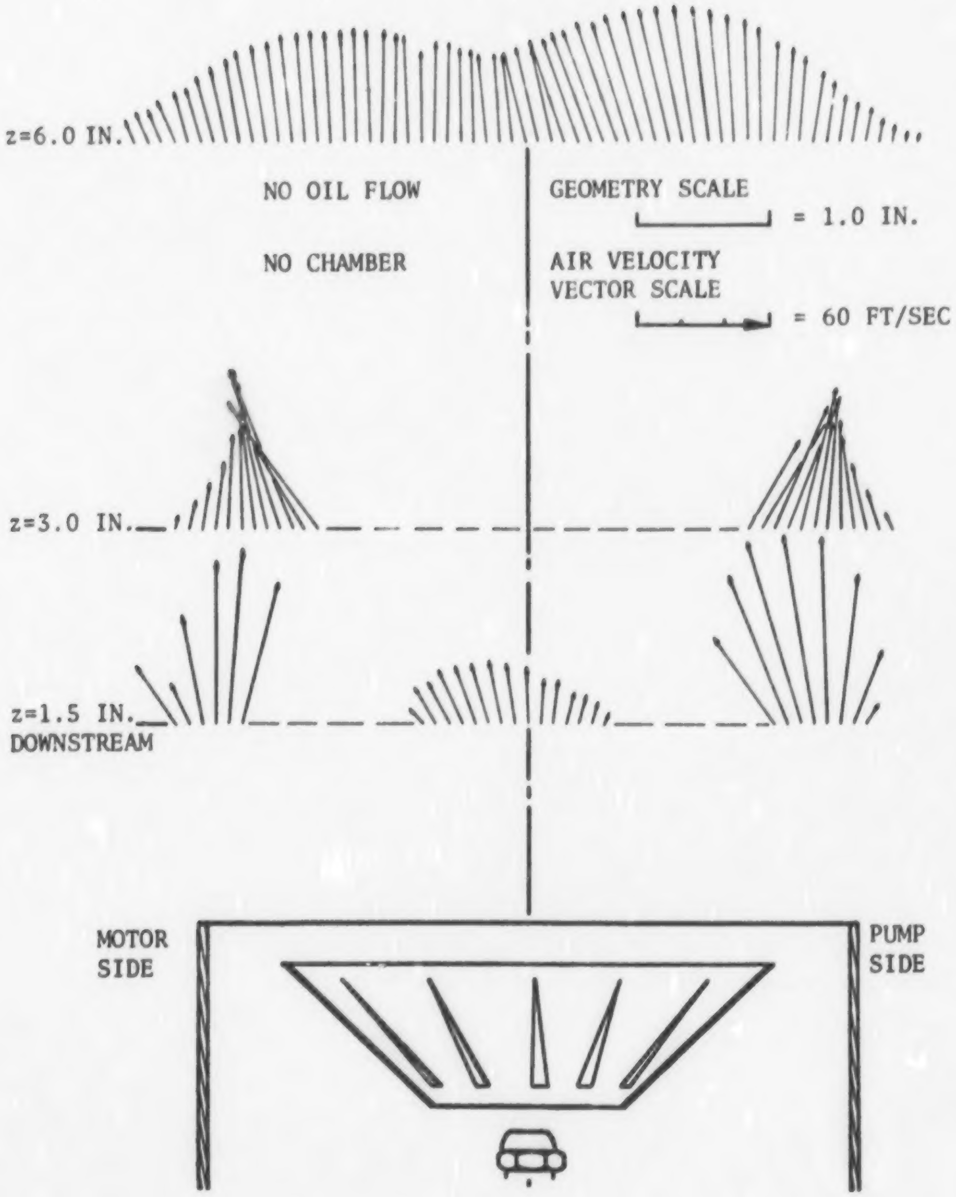
z=6.0 IN.
NO OIL FLOW
NO CHAMBER
GEOMETRY SCALE
= 1.0 IN.
AIR VELOCITY
VECTOR SCALE
= 60 FT/SEC
z=3.0 IN.
z=1.5 IN.
DOWNSTREAM
MOTOR
SIDE
PUMP
SIDE

Figure 95. Air velocity vectors in the horizontal plane for the Sun-Ray PHC-34 burner with no chamber and no oil flow

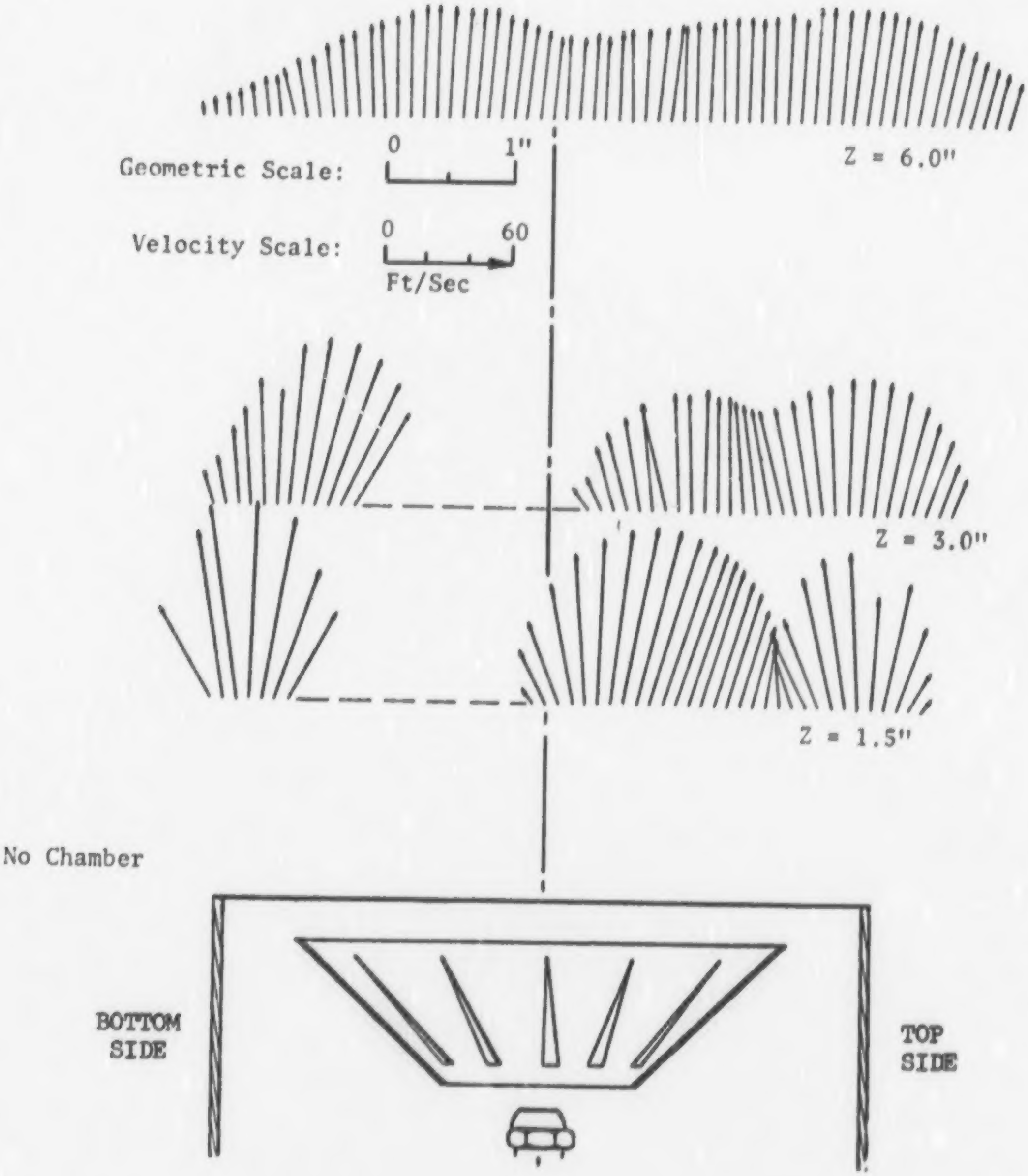
Geometric Scale:
0
1"
Velocity Scale:
0
60
Ft/Sec
Z = 6.0"
Z = 3.0"
Z = 1.5"
No Chamber
BOTTOM SIDE
TOP SIDE

Figure 96. Air velocity vectors in the vertical plane for the Sun-Ray PHC-34 burner with no chamber and no oil flow

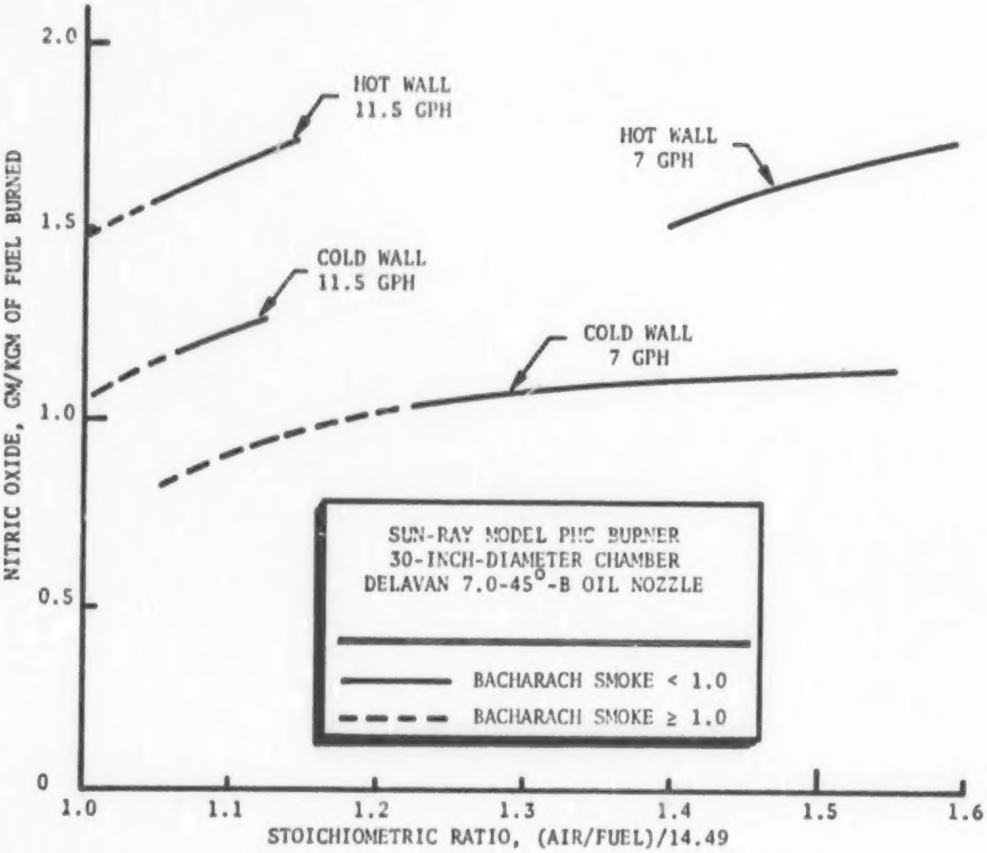

Figure 97. Comparison of nitric oxide emissions in the flue gas for the Sun-Ray Model PHC burner operating at 11.5 gph (300 psig oil pressure) and 7 gph (100 psig oil pressure) in the 30-inch-diameter chamber under cold- and hot-wall conditions

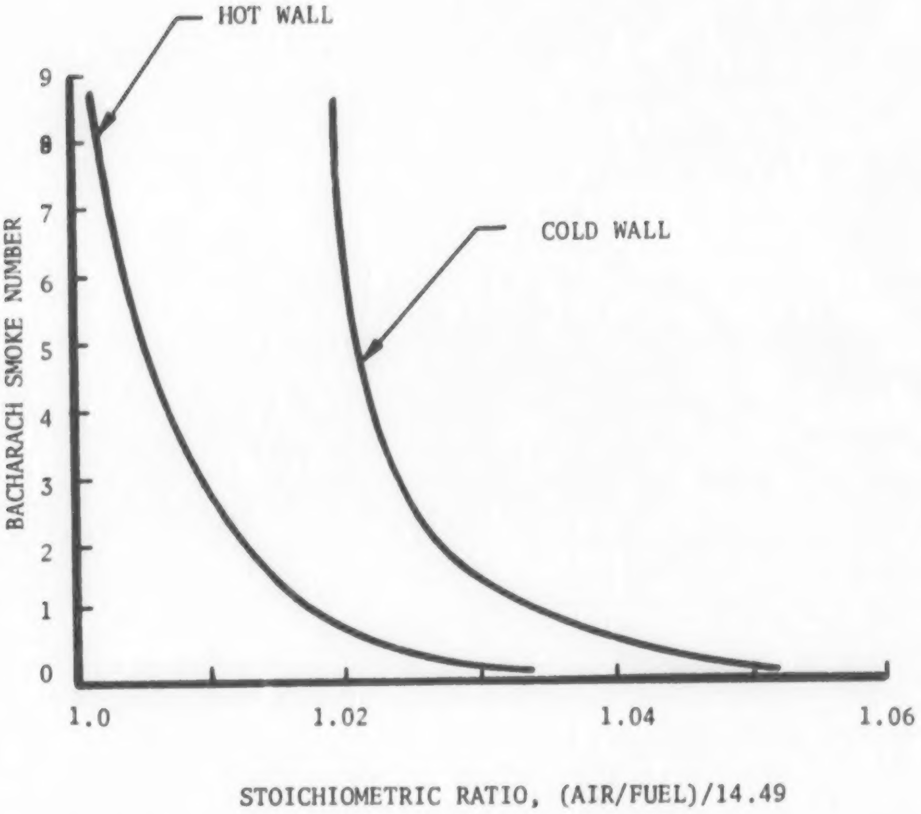

Figure 98. Smoke content of the flue gases for the Sun-Ray Model PHC burner fired at 11.5 gph in the 30-inch-diameter coaxial combustion chamber under cold- and hot-wall conditions

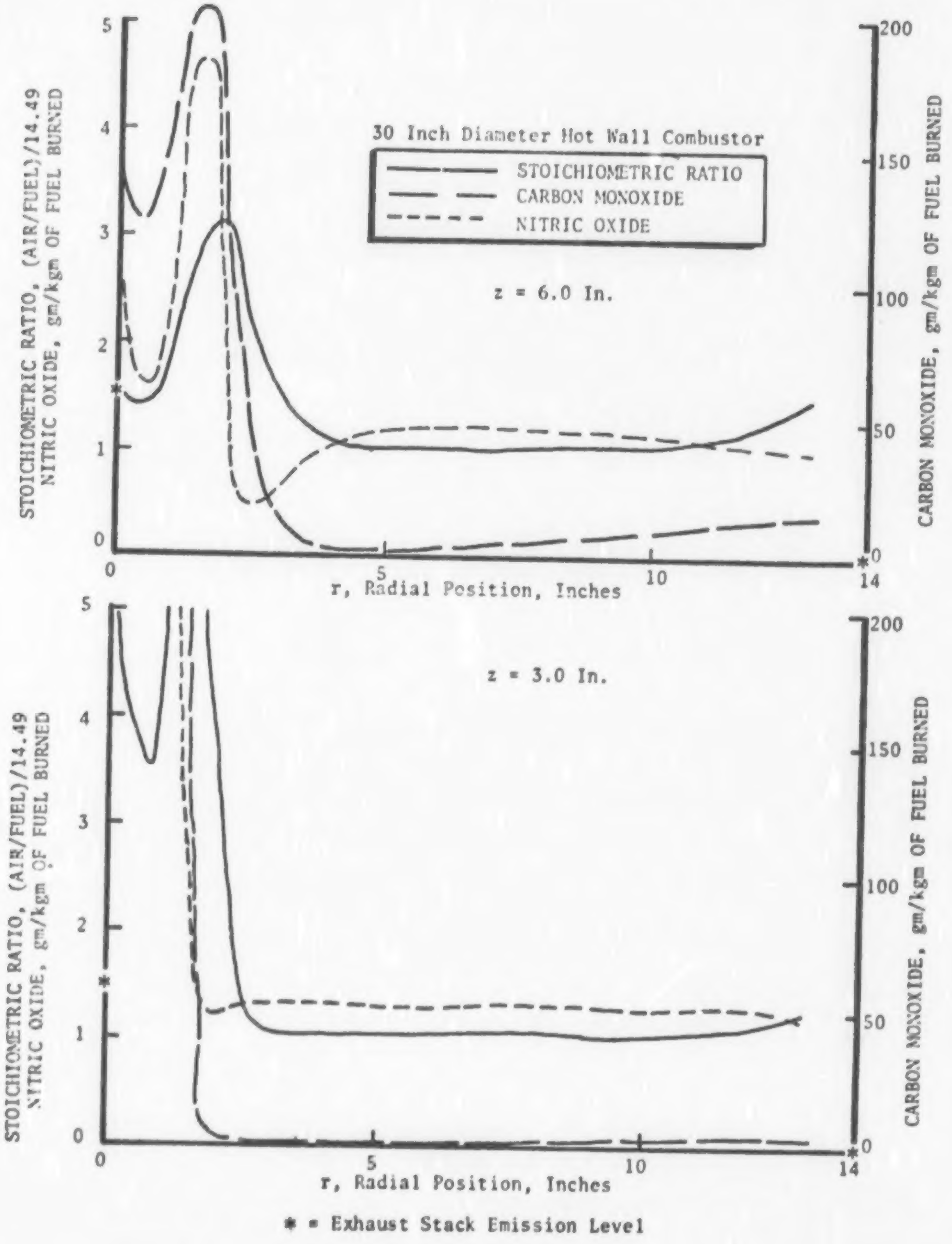

* = Exhaust Stack Emission Level

Figure 99. Hot-wall, local combustion gas analysis profile for the Sun-Ray burner at 11.5 gph and a nominal stoichiometric ratio of 1.03 (single 7-45°-B oil nozzle)

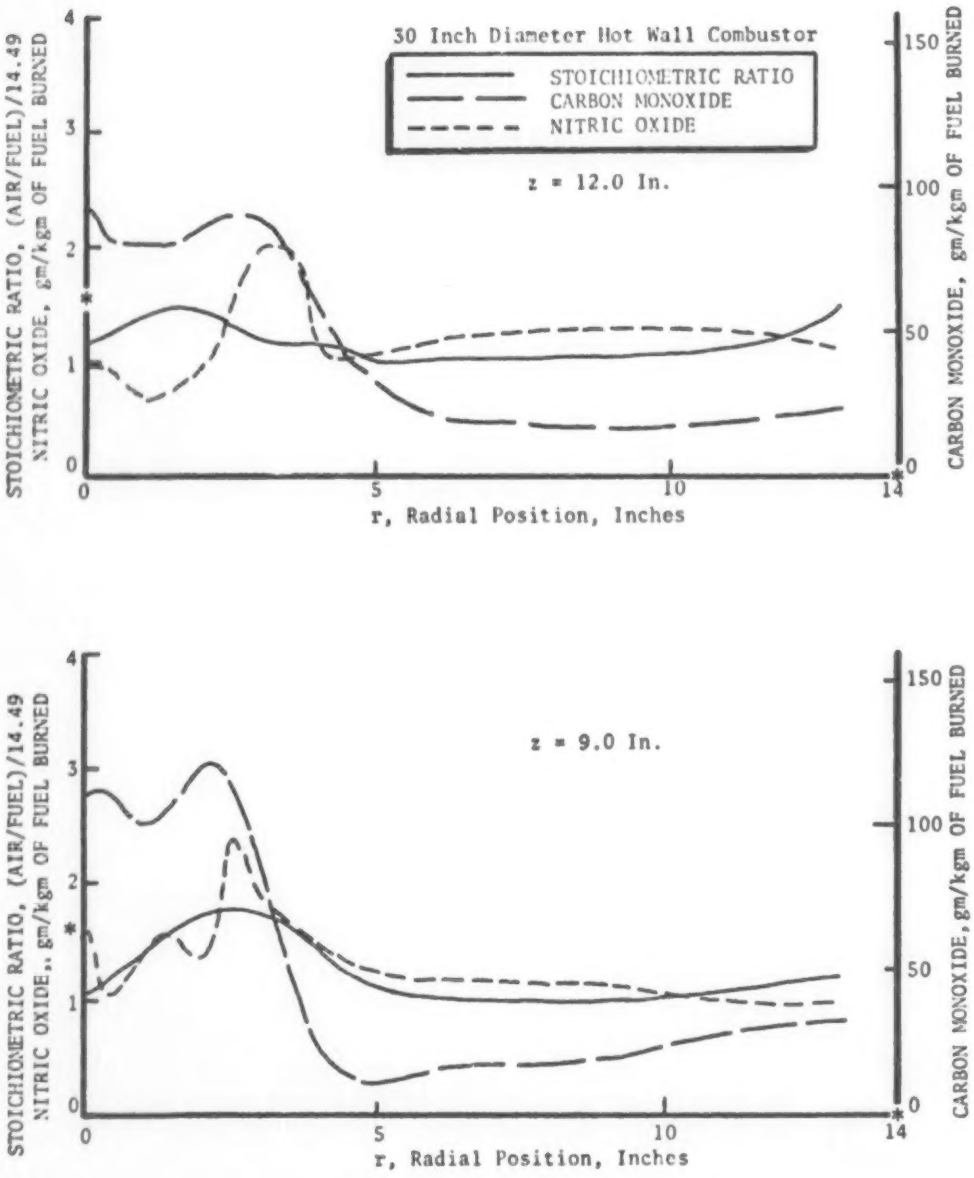

* = Exhaust Stack Emission Level

Figure 100. Hot-wall, local combustion gas analysis profiles for the Sun-Ray burner at 11.5 gph and a nominal stoichiometric ratio of 1.03 (single 7-45°-B oil nozzle)

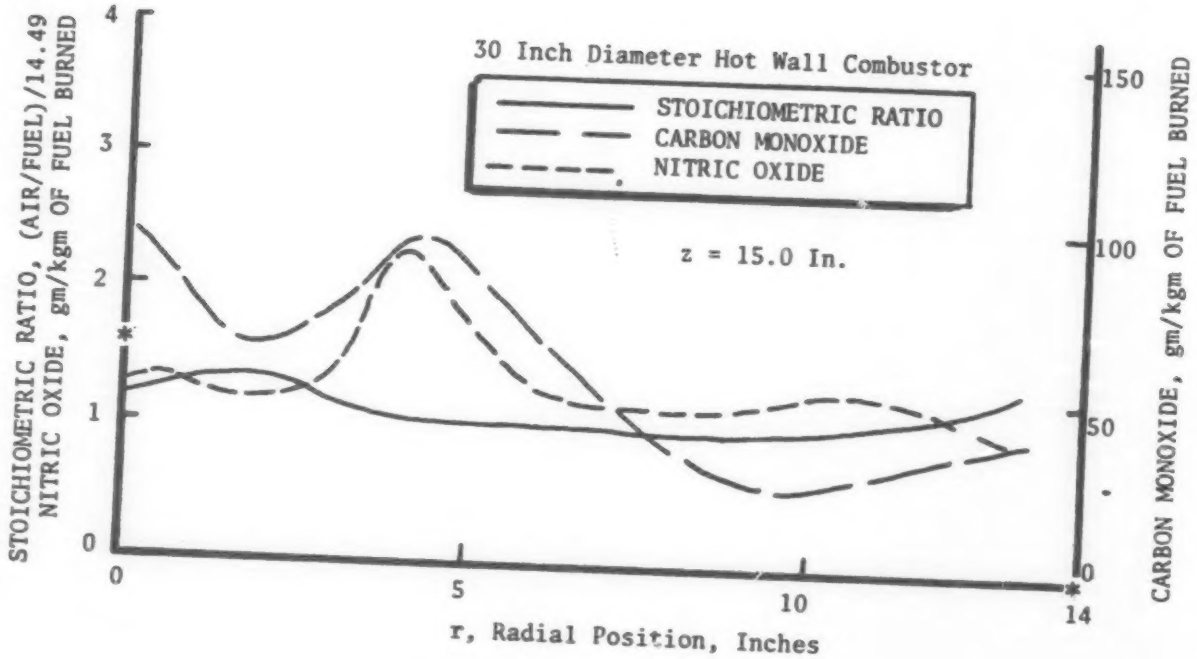

* = Exhaust Stack Emission Level

Figure 101. Hot-wall, local combustion gas analysis profiles for the Sun-Ray burner at 11.5 gph and a nominal stoichiometric ratio of 1.03 (single 7.0-45°-B oil nozzle)

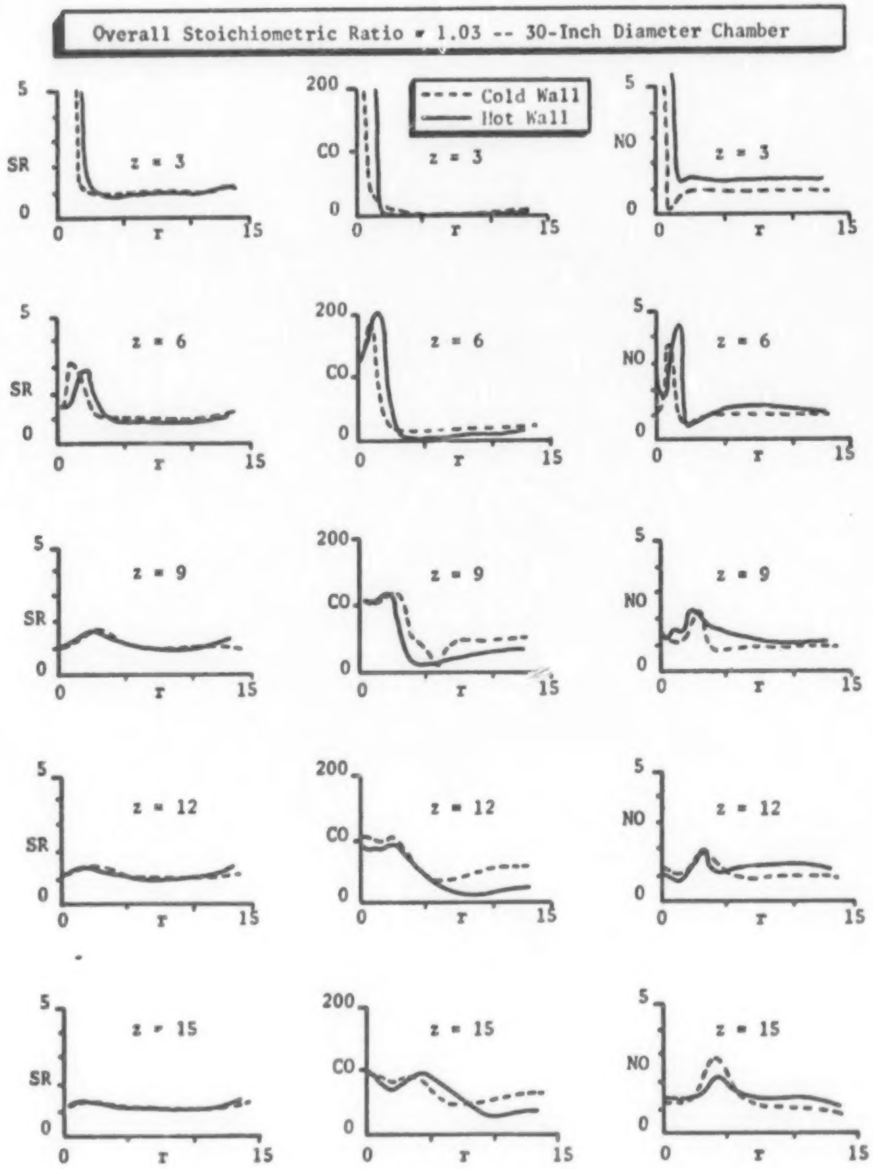

Figure 102. Comparison plots of local combustion zone sampled stoichiometric ratio (SR, air/14.49 fuel), carbon monoxide (gm CO/kg of fuel burned), nitric oxide (gm NO/kg of fuel burned), as a function of radial location (r = inches) and axial location (z = inches) (Sun-Ray burner, 115 gph)

recirculated gases and, hence, insensitive to whether hot- or cold-wall conditions are being tested. The gases recirculating behind the flame cone are a main source of ignition for the injected air/fuel spray mixture and, in agreement with the fact that these flame cone recirculating gases should be insensitive to wall temperature, the stoichiometric ratio profiles for hot- and cold-wall conditions show a high degree of correspondence to one another, particularly near the centerline, $r = 0$. The carbon monoxide profiles show few differences, except at $z = 3$ inches, where the outer radial limit of the active combustion zone (i.e., high CO) is higher in the hot-wall case. The nitric oxide profiles are generally higher for the hot-wall case, as compared to the cold wall, except for a portion of the profile at $z = 15$ inches. With this burner, as with the Nu-Way burner, the nitric oxide content of the recirculating gases, out along the chamber wall, is about 20 percent lower than the content of the flue gases. Here again, the difference is probably due to the lack of recirculation of the nitric oxide-rich gases in the core of the flow.

INTERPRETATION OF COMMERCIAL BURNER RESULTS

In this section, limited portions of the experimental results presented previously are discussed. The objective of this discussion is to make the point that burners tend to operate in one or the other or a combination of two fundamental modes, which are referred to herein as the plug-flow reactor and the well-stirred reactor modes. The experimental measurements of local flame-zone pollutant concentrations are interpreted to show that burners that tend to behave as plug-flow reactors produce lower nitric oxide emission levels when less than 80-percent excess air is utilized, while those that tend toward the well-stirred reactor behavior produce lower nitric oxide emission levels only with the impractically high excess air levels greater than 80 percent.

Finally, because of these interpretations, it is concluded that burner designs should be of the plug-flow type to achieve low nitric oxide emissions. This requires that burners be of the nonflame-retention type and well designed so that they can achieve: (1) uniform dispersion of the fuel spray in the air flow, and (2) eliminate or minimize turbulent mixing in the combustion zones. These conclusions are reached by reference to previous results, as described in the following paragraphs.

Velocity vector and composition profile maps are shown in Fig. 67 through 73 for a Mite burner. The combustion gas velocity vectors measured at three axial locations downstream of the burner's blast tube discharge are shown in Fig. 69 and 70. Also shown in Fig. 69 and 70 is a diagram of the blast tube end and the combustion chamber. The large disturbances in the flow pattern that result from the presence of the multiple-blade swirler device in the end of the blast tube are shown later to have an effect on nitric oxide formation. Figures 71 through 73 show combustion gas composition profiles measured at the same three axial locations at which the Mite velocity profiles were obtained. The most interesting features in Fig. 71 through 73 is the presence of the prominent peaks of nitric oxide content that happen to be located at the flow disruptions caused by the vaned-swirler device. The local stoichiometric ratio near the nitric oxide peaks is near unity. The results in Fig. 71 through 73 suggest that thorough mixing (due to the vaned swirlers) in regions of near stoichiometric combustion leads to excessive nitric oxide formation.

Velocity vector and composition profile maps were shown in Fig. 46 through 56 for the 55-J burner. The construction of the 55-J burner blast tube, as shown in Fig. 53, is considerably different from the flame-retention-type burner. There are swirler vanes, but these are located inside the blast tube choke ring at diameters larger than the inside diameter of the choke ring, so that they do not lead to major disruptions of the flow pattern. Note that the flow pattern is slightly nonsymmetrical, with a larger velocity gradient on the motor side of the velocity profile than on the pump side. This nonsymmetry is caused by the blower arrangement and various components inside the blast tube upstream of the components illustrated in Fig. 53. Note also, in Fig. 54 and 55, that there is a definite tendency for the local nitric oxide content of the combustion gases to be higher on the side near the largest velocity gradients. This, once again, infers that strong mixing (a result of the large velocity gradients) leads to excessive nitric oxide formation. In this case also, the nitric oxide formation is highest in the strong mixing, nearly stoichiometric regions.

Similar results were also obtained with the larger burners. Figures 95 through 101 illustrate results obtained with the 12-gph Sun-Ray burner, for example. Because of the high flowrates involved, it was more convenient to measure velocity vectors only under a no-combustion condition. The velocity vector profiles shown in Fig. 95 and 96 include large regions near the blast tube with no vectors shown. In those regions, the velocities were either too small for accurate measurements, or directed backwards (recirculation) so that they were not measurable with the apparatus used. Therefore, there appears from Fig. 95 and 96 to be a large region of low velocities and recirculation caused by the flame-holding cone located in the end of the blast tube. The combustion gas composition profiles shown in Fig. 99 through 101 indicate very high nitric oxide content in that recirculation zone. Once again, these results suggest that regions of strong mixing are not desirable for minimization of nitric oxide formation.

The velocity vector and gas composition results presented in this section all suggest that vigorous mixing at near stoichiometric conditions should be avoided if nitric oxide formation is to be reduced. Carried to an extreme, it might logically be concluded that a burner that simulates a plug-flow reactor might be expected to have lower nitric oxide emissions than one that simulates a well-stirred reactor.

A plug-flow reactor is characterized by the manner in which the reactants are allowed to react. In a plug-flow reactor, any particular differential volume of reactants is allowed to carry out the reaction in a timewise progressive manner without the addition of any other components (i.e., no fresh reactants and no products from outside the differential volume) throughout the course of the reaction. In a two-phase, liquid/gas reaction, such as the vaporization and combustion of oil spray in air, strictly speaking, the oil droplets originally associated with a given differential volume of air should remain with that differential volume of air until the droplets are completely vaporized and the combustion process is completed. However, as far as the reaction chemistry is concerned, it is of no significant consequence if those specific droplets are removed from the differential gas volume and replaced by other droplets. In other words, an oil spray combustion process can be considered to be essentially a plug-flow-type process, in spite of gross changes in the spray location, as long as no intermixing of the gas phase occurs during the combustion process. That is, the differential reaction volume starts out as a pocket of pure air, to which modest amounts of fuel vapor and heat are added by droplet vaporization and heat conduction. This leads to ignition, and then the process proceeds with fuel vapor addition to the air pocket, by vaporization, and reaction of that fuel vapor with the available oxygen in the air pocket. The process continues until no more fuel is available to be added. If the overall process is near stoichiometric (S.R. = 1.0), the end point for each differential volume of gas should be such that little or no unreacted oxygen will remain.

A well-stirred reactor is also characterized by the manner in which the reactants are allowed to react. In a well-stirred reactor, reactants are added quickly and uniformly to a relatively large volume of material in which the reactions are already nearly complete. In an oil burner operating in the well-stirred mode, air and oil spray are added to a strongly stirred volume of material consisting primarily of reaction products. If the overall process happens to be operating air rich, this volume of products will contain excess oxygen and very little fuel vapor whereas, if the overall process happens to be operating fuel rich, the volume of products will contain significant amounts of fuel vapor or fuel pyrolysis products and very little oxygen.

The primary chemical difference between a well-stirred reactor and a plug-flow reactor is, therefore, the bulk gas composition under which the reaction takes place. In a well-stirred reactor, the chemical reactions take place entirely in bulk gas having a composition equivalent to the combustor exhaust whereas, in the plug-flow reactor, the chemical reactions take place throughout the entire continuous spectrum of bulk gas composition, ranging from essentially pure air to the combustor exhaust composition. For chemical species that reach equilibrium quickly, such as H_2O, and even CO/CO_2, the concentrations in the exhaust will be very near the equilibrium amounts no matter whether the reaction is carried out as a plug-flow or a well-stirred process. However, the mode of reaction, be it plug flow or well stirred, would be expected to have a strong influence on the amount of particular reaction products in the exhaust that have slow kinetics and are characteristically found in concentrations far from equilibrium (e.g., NO). This expectation constitutes a primary thesis of this section, i.e., the NO produced by an adiabatic combustion chamber oil burner is largely dependent on whether the burner tends to operate as a plug-flow burner, or as a well-stirred burner, or as some intermediate combination of the two modes.

Nitric oxide is generally thought to be formed by either of two similar processes which are labeled "prompt" and "thermal." Thermal NO is produced by allowing combustion products to exist for a period of time without significant heat loss, so that reactions such as the following can occur:

$$N_2 + O \rightleftharpoons NO + N$$

$$O_2 + N \rightleftharpoons NO + O$$

$$N + OH \rightleftharpoons NO + H$$

where, for the thermal NO process, the species such as O and OH exist in chemical equilibrium with the other combustion products.

Prompt NO, on the other hand, is formed by chemical reactions similar to those above, but under conditions in which the active species such as atomic oxygen (O) exist in super-equilibrium concentrations. These super-equilibrium concentrations exist because the species are reaction intermediates. That is, the very active intermediate species such as O exist for short durations in super-equilibrium amounts because many chemical bonds are being broken and formed in the process of oxidizing the available fuel. The rate at which these super-equilibrium amounts of active species are destroyed by non-objectionable reactions (i.e., those which do not produce NO) must vary significantly depending on the composition and temperature of the bulk gas in which they are found. The amount of prompt NO formed per unit of fuel oxidized should not depend on the total bulk gas product residence time in the combustion chamber (as it does for thermal NO) because the super-equilibrium amounts of active intermediate species do not exist for time periods anywhere near comparable to chamber residence times.

A separate mechanism for the formation of NO, with chemical kinetics which are far different from the kinetics in the equilibrium bulk gas, can occur in the boundary layer flame fronts surrounding individual droplets, or in the flaming wakes of individual droplets. In these regions, localized temperatures are near the stoichiometric, adiabatic flame temperature, depending somewhat on the surrounding bulk gas temperatures. At these high, localized temperatures, NO kinetics are more rapid and large amounts of NO might be formed. This mechanism might be referred to as a "quick" mechanism, since the chemical species exposed to the high temperature are exposed only briefly, as they pass through the localized flame fronts. The amount of NO formed by this mechanism is dependent on the fraction of the combustion volume which is at the high temperature which, in turn, is proportional to the amount of fuel being burned. Thus, NO being formed by this quick mechanism is dependent on the amount of fuel which has been burned, and not at all on the bulk gas residence time after completion of burning.

Formation of thermal NO, in contrast to the quick and prompt NO's discussed above, is primarily dependent on temperature and residence time (i.e., time for reaction) after the bulk gases have reached their maximum temperatures. Thus, the amount of prompt NO and quick NO will both be functions of the amount of fuel burned and somewhat dependent on bulk gas composition and temperature (as it affects the super equilibrium oxygen atom lifetimes, and the local flamefront temperature), but not dependent on bulk gas residence times. The amount of thermal NO, on the other hand, is dependent on bulk gas residence times and not particularly on the amount of fuel being burned.

Assuming for the moment that the NO with which we are dealing is only quick and/or prompt NO, then it must be possible to relate NO formation in plug-flow combustion processes to NO formation in well-stirred combustion processes. As stated above, the amount of NO formed per unit mass of fuel oxidized should depend only on the bulk gas temperature and composition at which the oxidation takes place. But, for an adiabatic process at near-equilibrium conditions for the major components, these are continuous functions of the bulk gas stoichiometric ratio. Therefore,

$$\frac{dW_{NO}}{dW_{FUEL}} = f(SR) \tag{11}$$

where

W_{NO} = amount of prompt NO formed

W_{FUEL} = amount of fuel oxidized

SR = stoichiometric ratio of the bulk gases

f(SR) = a continuous function of stoichiometric ratio, to be defined experimentally

Now, in a well-stirred reactor, the stoichiometric ratio of the bulk gases is constant throughout the reactor at the value of the exhaust composition (SR_{WS}) where the subscript WS refers to well stirred. The function f(SR) can thus be moved outside the integral sign and integration of Eq. 11 under these conditions yields:

$$\int_0^{(W_{NO})_{WS}} dW_{NO} = \int_0^{(W_{FUEL})_{WS}} f(SR_{WS})dW_{FUEL} = f(SR_{WS}) \int_0^{(W_{FUEL})_{WS}} dW_{FUEL} \qquad (12)$$

$$(W_{NO})_{WS} = (W_{FUEL})_{WS} \; f(SR_{WS}) \qquad (13)$$

In a plug-flow reactor, the stoichiometric ratio of the bulk gases varies as the fuel is oxidized, so that $SR = W_{AIR}/(14.49 \; W_{FUEL})$, so that:

$$\int_0^{(W_{NO})_{PLUG}} dW_{NO} = \int_0^{(W_{FUEL})_{PLUG}} f(W_{AIR}/14.49 \; W_{FUEL})dW_{FUEL} \qquad (14)$$

or

$$(W_{NO})_{PLUG} = \int_0^{(W_{FUEL})_{PLUG}} f(W_{AIR}/14.49 \; W_{FUEL})dW_{FUEL} \qquad (15)$$

and, in this case, the function cannot be moved outside the integral sign.

Now, according to the discussion presented just prior to Eq. 11, the function f(SR) used in Eq. 12 through 15 remains the same regardless of whether the reactor is a plug-flow or a well-stirred type. In this case, the function can be evaluated from well-stirred reactor NO emission data by algebraic manipulation of Eq. 13 to yield:

$$f(SR) = \left.\frac{(W_{NO})_{WS}}{(W_{FUEL})_{WS}}\right]_{SR_{WS} = SR} \qquad (16)$$

Or, it can be evaluated from plug-flow reactor data by differentiation of Eq. 15 to yield:

$$f(SR) = \left.\frac{\partial (W_{NO})_{PLUG}}{\partial (W_{FUEL})_{PLUG}}\right]_{SR_{PLUG} = SR} \qquad (17)$$

Having used Eq. 16 to obtain the required function from well-stirred combustor NO emission data, it should be possible to apply that function to Eq. 15 to predict the NO emission data for a plug-flow combustor. Conversely, having obtained the function from differentiation of plug-flow reactor data according to Eq. 17, it should be possible to predict well-stirred combustor NO emissions. As shown below, this has been successfully done during this program with emission data from burners operating predominantly in the plug-flow mode and the others operating in the well-stirred combustor mode. The important factor here is that the function f(SR) has been experimentally determined, so that it is possible to define: (1) the conditions for which plug-flow combustors are superior to well-stirred combustors, and vice-versa; and (2) the lowest level of NO emission that it is possible to obtain in adiabatic combustors. This information allows one to decide which type of combustor development to pursue, and it defines the NO level at which further refinements in burner design for adiabatic combustors will not result in further significant decrease in NO emission.

It should be emphasized that the above arguments are based on the use of an adiabatic combustion system, either plug flow or well stirred, where there is no significant heat removal during the course of combustion, heat loss by radiation or convection to combustion chamber walls, or effective heat loss by techniques such as flue gas recirculation. As such, the above arguments are applicable to luminous-flame burners fired into refractory combustion chambers which are a principal subject of this research program. On the other hand, the above arguments are not applicable to water- or air-cooled combustion chambers for which significant flame-zone heat losses must be considered.

One condition for the applicability of the arguments related to Eq. 11 through 17 was that "prompt" or "quick" rather than "thermal" NO formation mechanisms are predominant. The reactions for production of thermal NO depend largely on the presence of atomic oxygen, which exists in adiabatic equilibrium combustion products in significant amounts only when less than 35 to 40 percent excess air is utilized. With 40 percent or more excess air, the thermal NO mechanism would be expected not to produce significant amounts of NO from equilibrium combustion products due to the absence of O, leaving only the prompt mechanism for NO formation. Therefore, the arguments with respect to NO formation, as related to Eq. 11 through 17, should be valid for greater than 35 to 40 percent excess air, or under conditions of minimum chamber volume (i.e., low residence time at peak temperature), or with slight radiant heat loss (slightly reduced flame temperature and hence lower O concentrations). On this basis, the relations of Eq. 11 through 17 might be expected to be valid to as low as, say, 10- to 15-percent excess air under conditions of low chamber residence time. The experiment interrelationship of well-stirred and plug-flow combustor NO emission data, as described below, has been attempted only in the 35- to 100-percent excess air range.

If an oil burner were to act as a true plug-flow reactor, the process could be visualized as a plug of air to which fuel vapor is continuously added (by vaporization from droplet) and reacted. As the process continues, the buildup of combustion product concentrations would be expected to increase monotonically until a near-stoichiometric condition is reached, at which time the process would be considered complete. For a practical oil burner, the entire combustion might not be a single plug-flow combustion process; however, if the air flow were separated into several different stream tubes, each of the stream tubes might be considered to be individually undergoing a plug-flow combustion process if turbulent mixing were not excessive. Then, if local combustion gas composition profiles were measured, each combustion gas sample could be considered to be a sample from a typical plug-flow combustor at a particular degree of completion.

Among the commercial burners tested, the 55-J has the least vigorous mixing, and the resulting combustion would be expected to provide the best simulation of a plug-flow reactor. Even though the flow is in the turbulent regime, the results obtained from combustion profile sampling of the 55-J might reasonably be expected to exhibit streatube flow characteristics.

Combustion zone sampling data for the 55-J, including the data from Fig. 54 are shown plotted in Fig. 103 in such a manner that consistent trends should be observed if the streamtubes from which the samples were obtained actually simulate plug-flow reactor behavior. Figure 103 shows the weight of nitric oxide per unit weight of air as a function of the mass of fuel per unit mass of air. The data in Fig. 103 include combustion sample analyses from throughtout the combustion zone of the 55-J. Since the sample analysis train does not permit liquid fuel or fuel vapor to enter the sample analyzers (both are removed by passage of the gas sample through a cold trap), the weight of fuel per unit weight of air for Fig. 103 has been calculated from the carbon dioxide and carbon monoxide concentrations and, hence, the fuel referred to on the abscissa of Fig. 103 is burned fuel. The plug-flow combustion process starts with pure air, followed by monotonic increase in fuel/air ratio, which can be visualized as moving rightward from the origin on the abscissa of Fig. 103.

The data of Fig. 103 show a relatively consistent trend. If the data truly describe the characteristics of a plug-flow combustion process, then it is apparent that little or no nitric oxide is generated when the plug composition passes from an abscissa value of 0.01 to 0.04 gm fuel/gm air. Most of the nitric oxide is formed at 0.05 to 0.07 gm fuel/gm air, with some apparently formed from 0.0 to 0.01. The curve drawn in Fig. 103 is related to the function f(SR) from Eq. 11 through 17, as shown by the equation in the figure. The curve drawn in Fig. 103 is purposely placed near the lower limit of the experimental

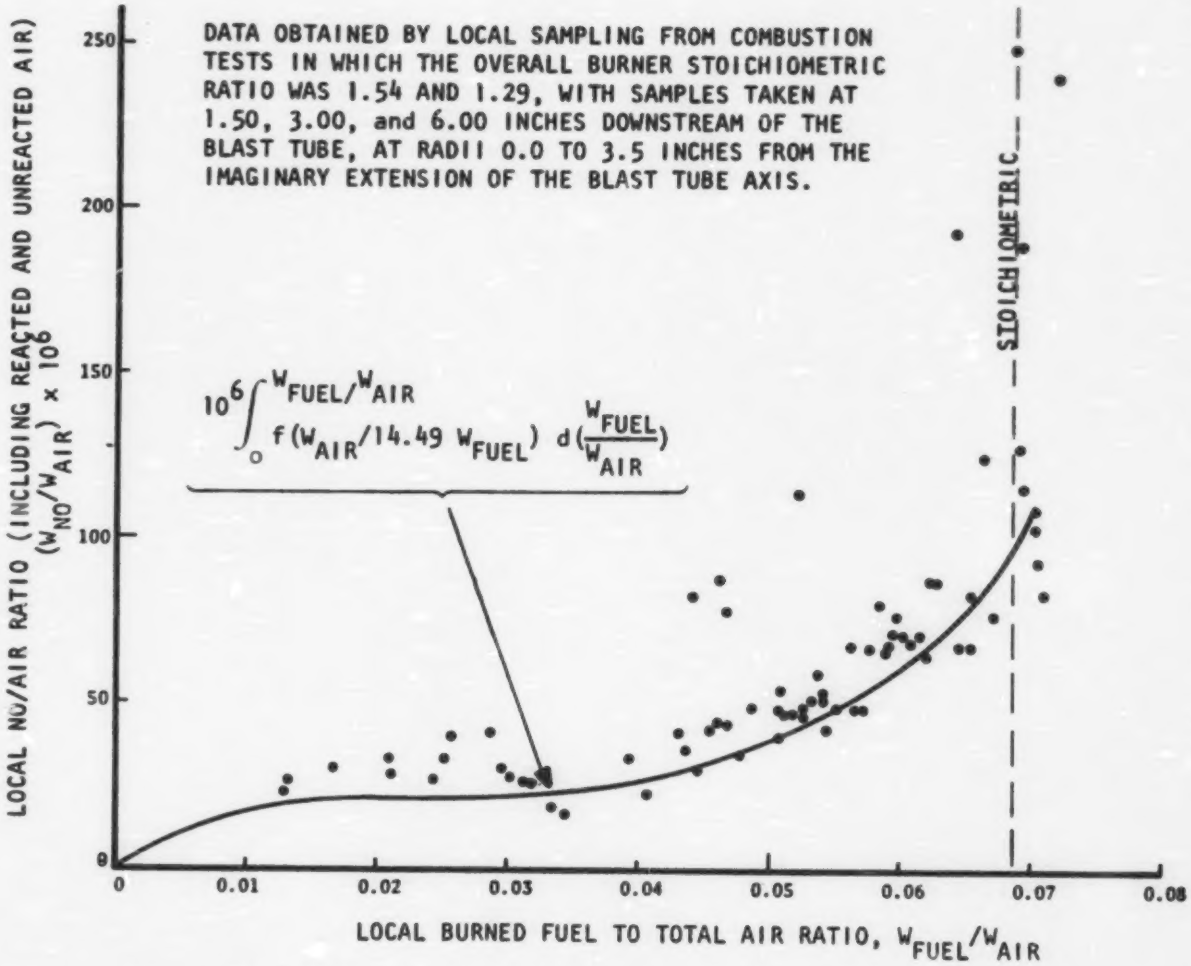

Figure 103. Nitric oxide content of locally sampled combustion gases, as a function of combusted fuel content, for the ABC 55-J burner (which has relatively streamlined flow)

data because of the predominantly positive value of the second derivative of the curve. (That is, if two equal weight streamtubes having fuel/air ratios of 0.03 and 0.07 were to become mixed by turbulent actions, the mixed gas fuel/air ratio would be 0.05; but, the weight of nitric oxide per unit weight of air in the sample would be about 65×10^{-6} rather than the value of 40×10^{-6} which would result if a single plug-flow streamtube reached the fuel air ratio of 0.05 by the plug flow combustion process. Since the turbulent mixing which does occur tends, by this effect, to elevate the data points, the true curve for plug-flow combustion must lie near the lower limit of the data, as it is drawn in Fig. 103.)

The large scatter in Fig. 103 is not surprising, since the flow produced by the burner is not truly plug flow, but somewhat turbulent. The other burners tested, which have devices tending to promote turbulence, produced data trends similar to those of Fig. 103, but with relatively larger scatter. If it were important to obtain good data representative of plug flow, a burner operating in the laminar flow regime could be designed, and the gases sampled from its combustion zone would probably have much reduced scatter when plotted according to the format of Fig. 103.

In a well-stirred process, the gas composition in the combustion chamber is stationary as fuel is added, and the amount of nitric oxide formed per unit of fuel added should (according to Eq. 16 and 17) be proportional to the slope of the curve representing the data in Fig. 103. The large slope in Fig. 103 at the stoichiometric condition, therefore, indicates that a well-stirred reactor operating at near stoichiometric would produce large amounts of nitric oxide. This is consistent with the trends discussed in relation to the combustion zone flow pattern and gas sample concentration data presented earlier in which high nitric oxide content was found at near-stoichiometric, "well-stirred" zones. It is noticeable that the slope of Fig. 103 is near zero at the intermediate range of the abscissa. Obviously, a well-stirred reactor operating in this more air-rich zone would produce relatively low nitric oxide emissions.

A special oil burner, discussed in the nonconventional burner section, was fabricated to test the characteristics of the well-stirred burner concept. This burner achieves the well-stirred characteristics by vigorously swirling the air before it is injected into the combustion chamber. The air swirl is induced by rotating a six-vane paddle wheel in the end of the burner at 3450 rpm. The flue gas emissions data obtained with this intense swirl, "well-stirred" burner are shown in Fig. 104. The curve was obtained by differentiating the corresponding portion of the plug-flow curve shown in Fig. 103, and multiplying the local burned gas fuel/air ratio, indicating that the plug-flow and well-stirred reactor data are related to each other by the function f(SR) as they should be if the above-described assumptions are true. The function f(SR) has been evaluated numerically and, in terms of fuel to air weight ratio, it is:

$$\frac{dW_{NO}}{dW_{FUEL}} = f(SR) = 26.126 - 34.951\ (SR) + 16.152\ (SR^2) - 2.5369\ (SR^3)\ \text{(gm NO/kg fuel)};\ 1.0 < SR < 4.6 \qquad (18)$$

If the curve from Fig. 104 were superimposed on Fig. 103, the crossover between the plug-flow and well-stirred reactor curves would occur at about 0.04 gm fuel/gm air (i.e., about 80 percent excess air). To the left of the crossover point, the well-stirred reactor design produces lower nitric oxide emissions while, to the right of the crossover point, the plug-flow reactor has lower nitric oxide emissions.

The crossover point between the two reactor types occurs at a relatively high excess air level. At high excess air levels, the flame temperature is reduced, making it more difficult to transfer heat from the combustion gases to the heated media and, therefore, generally

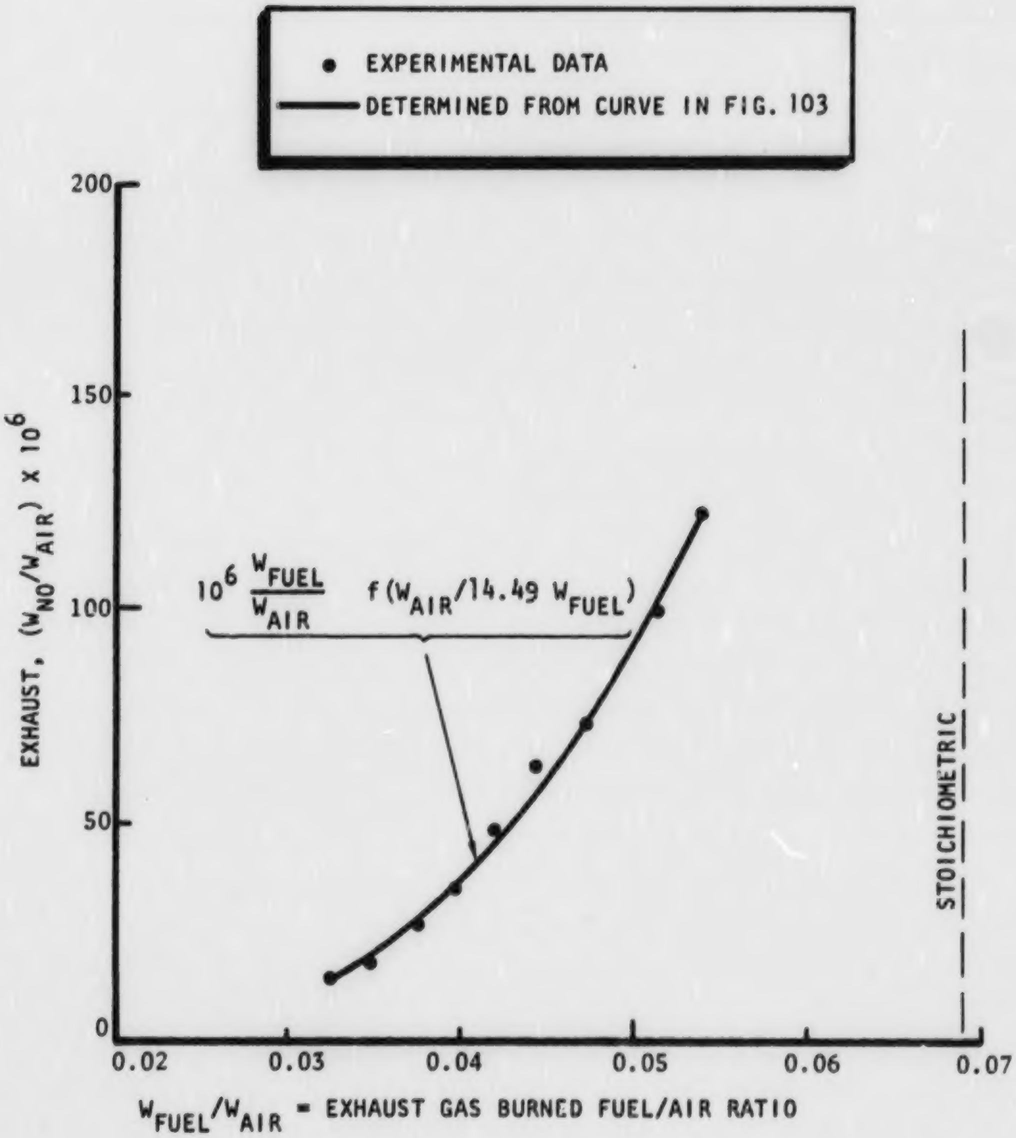

Figure 104. Nitric oxide content of flue gases produced by the well-stirred burner

lowering the overall furnace thermal efficiency (typically by 10 to 15 percent at 80-percent excess air versus 10-percent excess air). This loss in efficiency is not tolerable in existing furnaces and, hence, low excess air levels must be used; therefore, burner designs which promote plug-flow mode behavior must be selected. With this selection, at 10-percent excess air ($W_{FUEL}/W_{AIR} = 0.063$), Fig. 103 indicates that about 70×10^{-6} grams of nitric oxide per gram of air, or about 1 gm NO/kg fuel will be produced. For adiabatic combustors (i.e., uncooled combustion chamber systems with little radiant or convective heat loss, and no cooled flue gas recirculation), this 1 gm NO/kg fuel level is about the lowest that should be expected since, to achieve it, the oil burner must operate as a plug-flow burner, uniformly for all of the flow it passes. In practice, non-uniformities and some turbulent mixing will be difficult to avoid, and the ideal goal of 1 gm NO/kg fuel for an adiabatic combustor might be expected to be somewhat exclusive.

Considerations of furnace efficiency, as discussed above, dictate that all burners operate at low excess air. As also discussed above, at low excess air, burners operating in the plug-flow mode have lower nitric oxide emissions than burners operating in the well-stirred mode. Therefore, the burner optimization experiments described in the following section were conducted with burners that tend to operate in the plug-flow mode. This eliminated the possibility of using flame-retention devices or other devices that tend to promote vigorous turbulence in the air injected through the blast tube.

BURNER GEOMETRY OPTIMIZATION STUDIES

The results discussed in the previous section strongly suggest that plug flow-type burners have the greatest likelihood of operating with low nitric oxide emissions in refractory-lined combustion chambers. Furthermore, it is apparent that burners that do not utilize flame-retention devices are most likely to produce plug-like flow. The burner geometry optimization studies described in this section have, therefore, made use of versatile geometry burners that do not incorporate flame-retention devices. Instead, they have only peripheral swirlers which resemble those found on the 55-J-1 and model CO burners discussed previously. The variable angle swirlers allow a controlled amount of turbulent mixing to be induced into the flow, varying from zero to a moderate amount.

Two versatile geometry burners were constructed for this study, one for application from 0.75 to 3 gph, and one for application from 3 to 12 gph. The 3- to 12-gph version is shown in Fig. 105. Geometry variation effects on pollutant emissions were studied at 0.75 and 3 gph with the smaller version, and at 7 and 12 gph with the larger version of the versatile burner. The most detailed studies were conducted at the 12-gph flowrate.

A photograph of the large, 3- to 12-gph versatile burner is shown in Fig. 105. It has a six-leaf, iris-type variable choke plate which results in a hexagonal-shaped outlet that can be varied in area from about 3 to 15 sq in. while the burner is running. The choke plate settings, as reported herein, are given in terms of the equivalent area circle diameter. The versatile burner also has six variable angle swirler blades, which can be seen just inside the blast tube exit in Fig. 105. These swirler vanes are mounted so that their angle relative to the blast tube axis can be varied from 0 to 60 degrees while the burner is running. In the earliest studies with the 1- to 3-gph versatile burner, the variable angle swirler vanes were relatively short in the radial direction, with the innermost edges located at a radius of 1.5 inches relative to the blast tube centerline. Experimental results showed these short swirler vanes to have no significant effect on emissions. For all subsequent experiments, the swirler vanes were made taller so that their innermost edges were located at a radius of 0.6

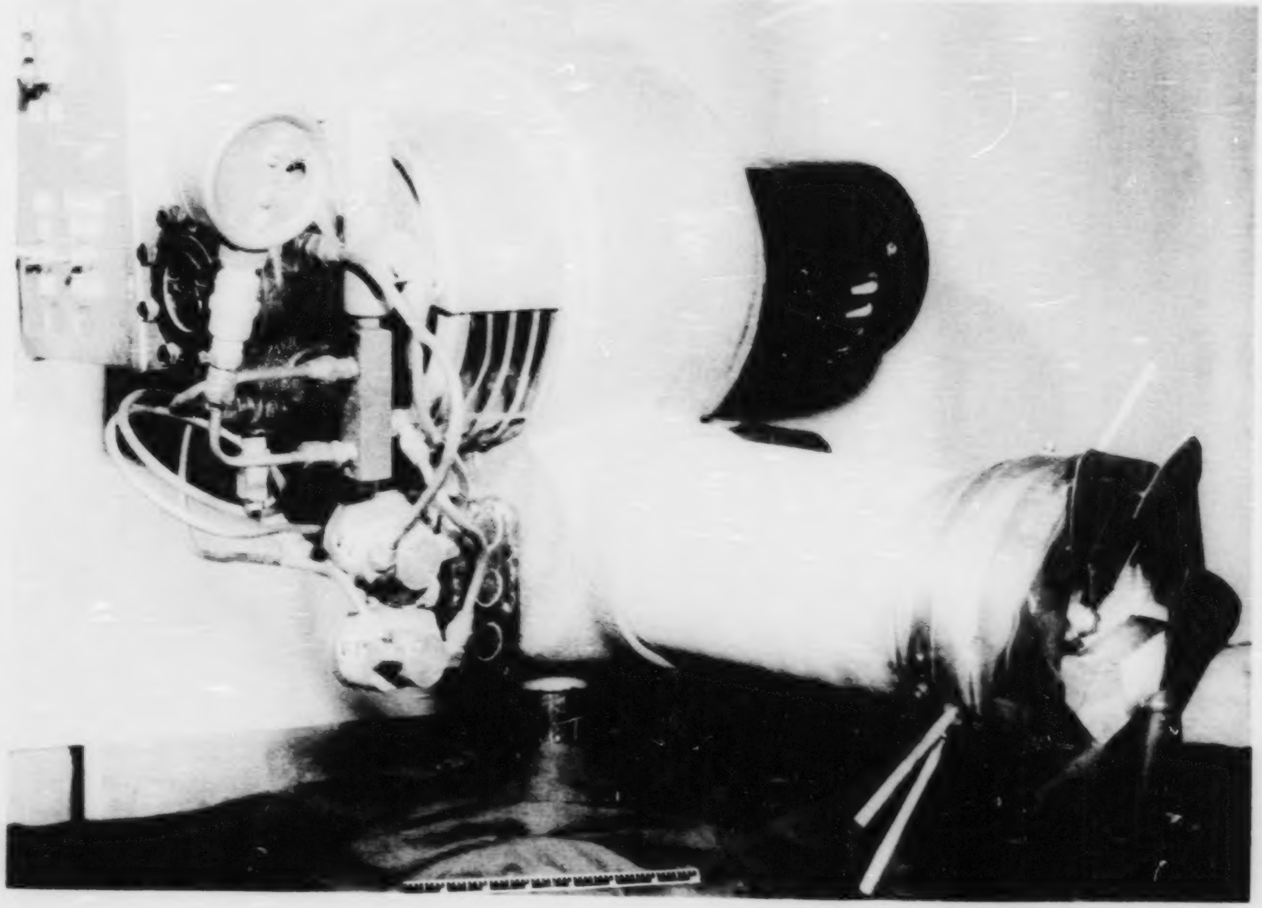

5AD26-7/17/73-S1B

Figure 105. Overall photograph of the 3- to 12-gph versatile research burner

inch from the blast tube axis (this radius is just slightly larger than the radius of the oil spray nozzle). The experimental results with these tall swirler vanes showed significant effects of swirl angle on emissions.

Photographs of the head ends of the 3- to 12-gph and 1- to 3-gph versatile burners are shown in Fig. 106.

The 12-gph studies were conducted using the 30-inch-diameter coaxial combustion chamber 35 inches in length. The chamber was internally lined with a 1/2-inch-thick layer of Pyroflex insulation. The exhaust from the coaxial combustor was passed through the mixing and exhaust section to thoroughly mix the gases to provide a sample having average composition for the analyses. The oil spray nozzles used for these studies were all Delavan brand, either A = hollow cone spray, or B = solid cone spray, with spray angles of 45, 60, or 90 degrees. The oil nozzles are nominally rated for flow at 12 gph; however, a nominal 7-gph nozzle, when operated at an elevated pressure of 300 psig, also flows at about 12 gph.

Experiments conducted with the versatile burners in coaxial chambers generally had very low emissions of unburned hydrocarbons and carbon monoxide when operated at those conditions that yielded low smoke; however, low nitric oxide emissions did not necessarily coincide with the low smoke emissions. It should be noted that, in some instances, significant smoke was observed in the absence of significant hydrocarbon or carbon monoxide emissions. This may have been due, for example, to impingement of fuel on the chamber walls followed by formation of smoke, vaporized hydrocarbon, and carbon monoxide; subsequently, the hydrocarbons and carbon monoxide may have become oxidized, but the smoke (which is more difficult to oxidize) persisted into the exhaust. However, the reverse was not generally observed, i.e., significant hydrocarbons or carbon monoxide in the absence of smoke. Therefore, the

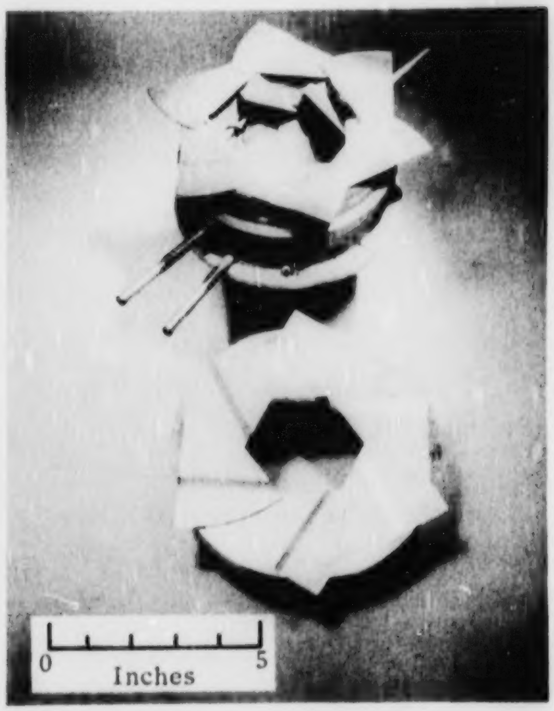

1- TO 3-GPH HEAD (COMPLETE)

6- TO 12-GPH HEAD (LESS VARIABLE SWIRLERS)

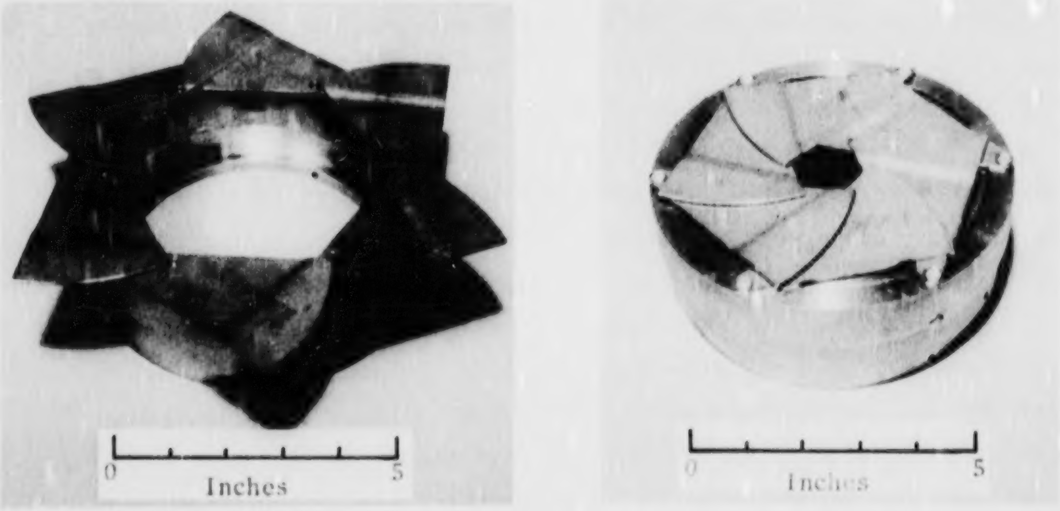
0
Inches
5
0
Inches
5

6- TO 12-GPH VARIABLE CHOKE, FULL OPEN

6- TO 12-GPH VARIABLE CHOKE, FULL CLOSED

Figure 106. Photographs of the variable geometry burner heads of both the 1- to 3-gph and the 6- to 12-gph versatile burners

problem of selecting the optimum burner geometry reduces to selecting those conditions where low smoke emissions coincide with low nitric oxide emissions.

The results of the 12-gph studies are presented in Fig. 107 through 110. Figure 107 shows the results of an attempt to determine the effects of dropsize by using two nozzles of the same spray pattern, but requiring different operating pressures to obtain the same flowrate. Figure 107 also shows the effects of choke diameter and air swirl angle. Figure 108 is similar to Fig. 107, except it is for wider angle spray nozzles. Figure 109 is also similar to Fig. 107, except for spray angle, and it also includes the effects of the hollow cone versus the solid cone spray nozzle. Figure 110 shows the effects of oil spray nozzle recess with respect to the blast tube exit. Figures 107 through 109 indicate that dropsize has little or no significant effect on the minimum achievable NO levels, but that the smaller dropsizes (i.e., those obtained from the highest operating pressure nozzles) have a lesser tendency to produce smoke.

According to Fig. 107 through 109, increasing the air swirl vane angle results in an almost monotonic increase in the NO emissions under the no-smoke condition. This result is not surprising, since the commercial burner studies described in the previous section indicated that well-stirred combustion at low excess air levels tends to produce higher levels of NO than plug-flow combustion. Increasing the air swirl angle obviously makes the combustion more like the well-stirred process and, therefore, leads to the monotonic increase in NO. At very low swirl angles, there is a definite tendency toward the formation of smoke. Apparently, some degree of stirring (by means of the air swirl vanes) is necessary to achieve sufficiently uniform flow to avoid fuel-rich zones of combustion where smoke is produced. Therefore, the optimum air swirl vane angle obviously becomes a compromise between an angle sufficiently large to eliminate smoke, but as low as possible to minimize

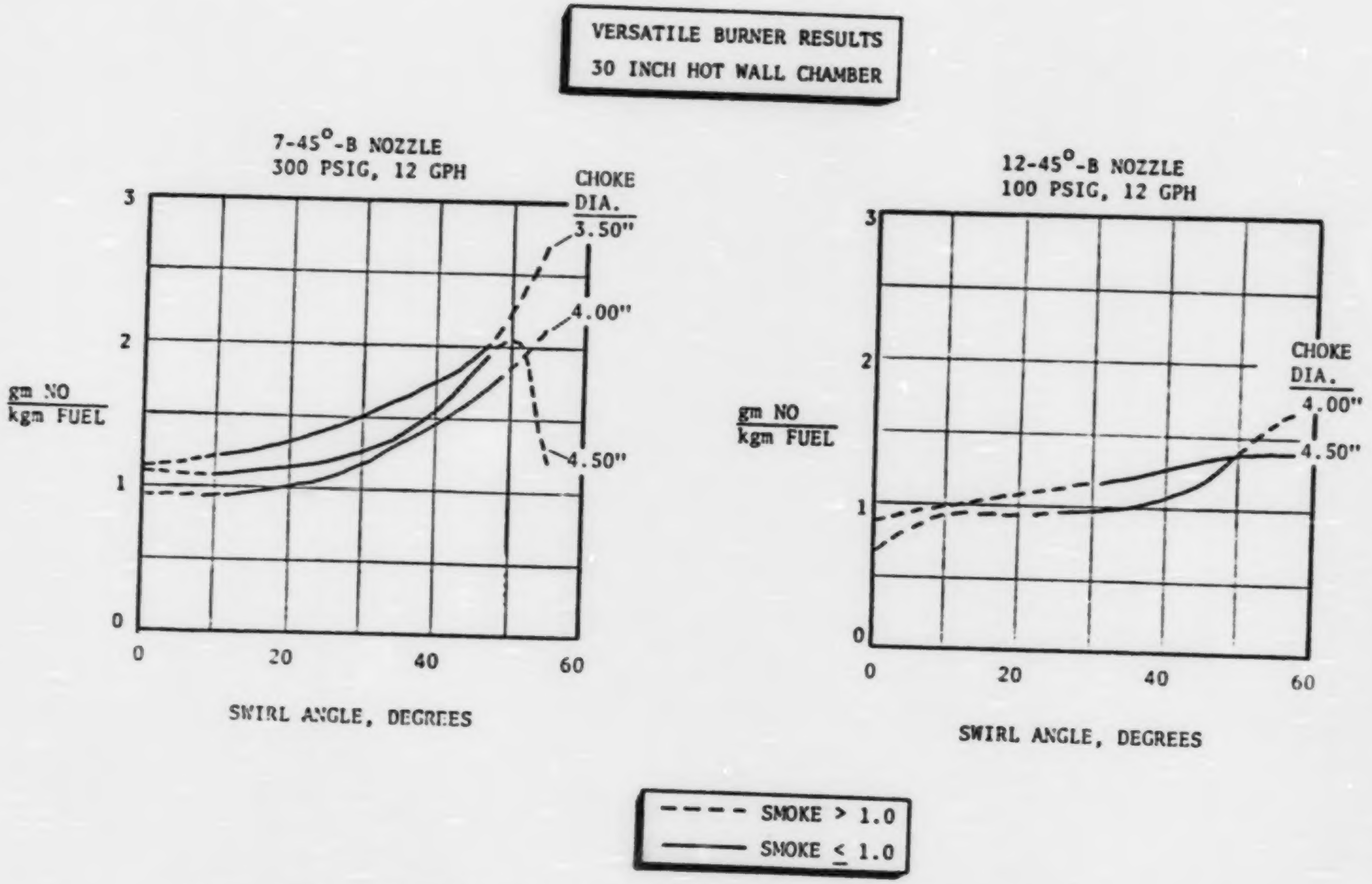

Figure 107. Versatile burner flue gas emissions obtained with 10-percent excess air in the 30-inch-diameter hot-wall chamber (45° nozzles)

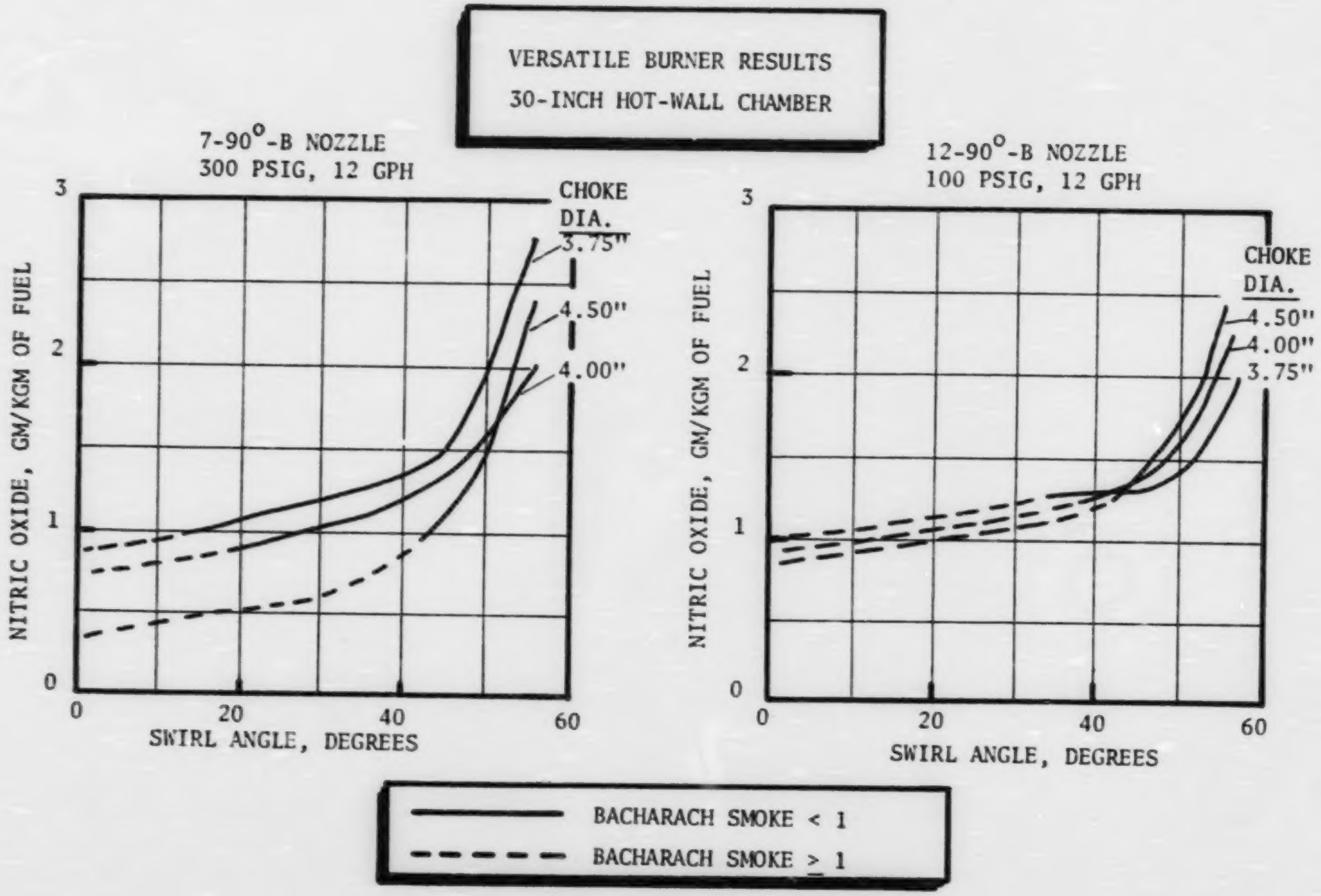

Figure 108. Versatile burner flue gas emission obtained with 10-percent excess air in the 30-inch-diameter hot-wall chamber (90° nozzles)

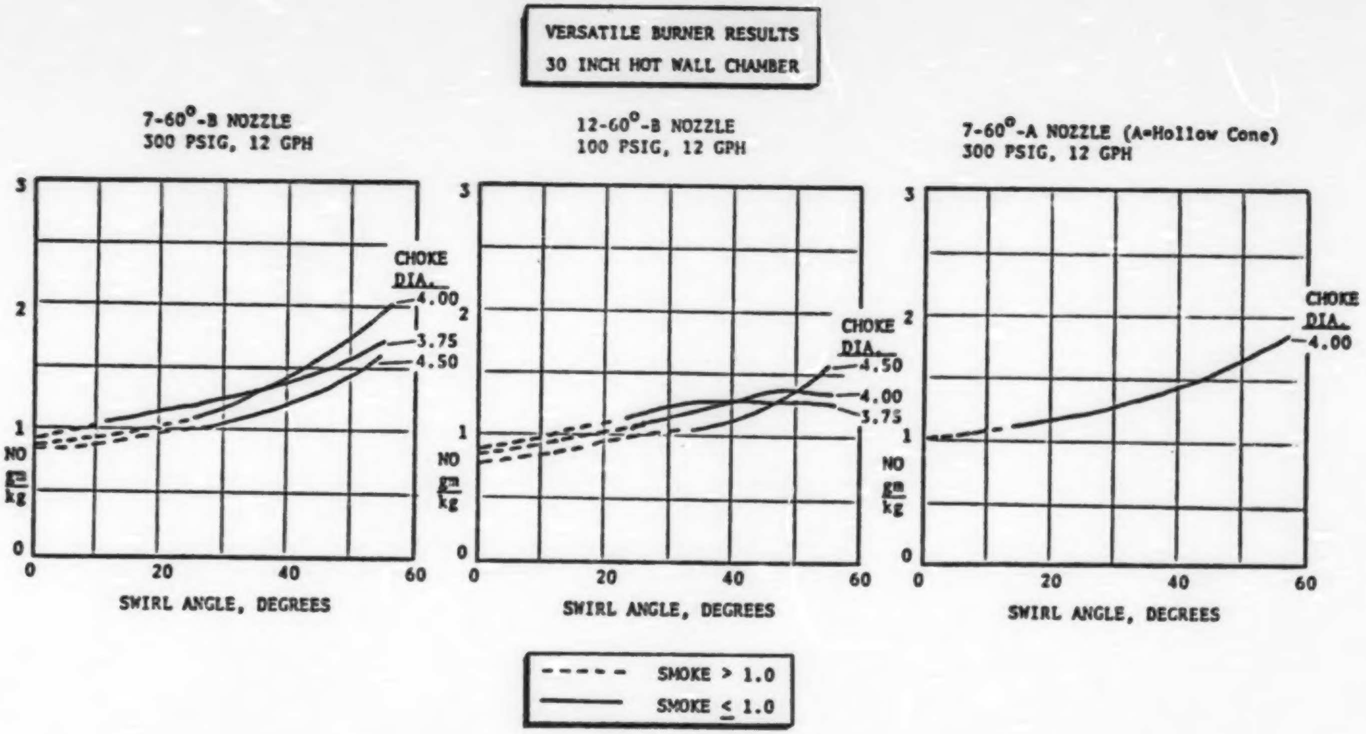

Figure 109. Versatile burner flue gas emissions obtained with 10-percent excess air in the 30-inch-diameter hot-wall chamber (60° nozzles)

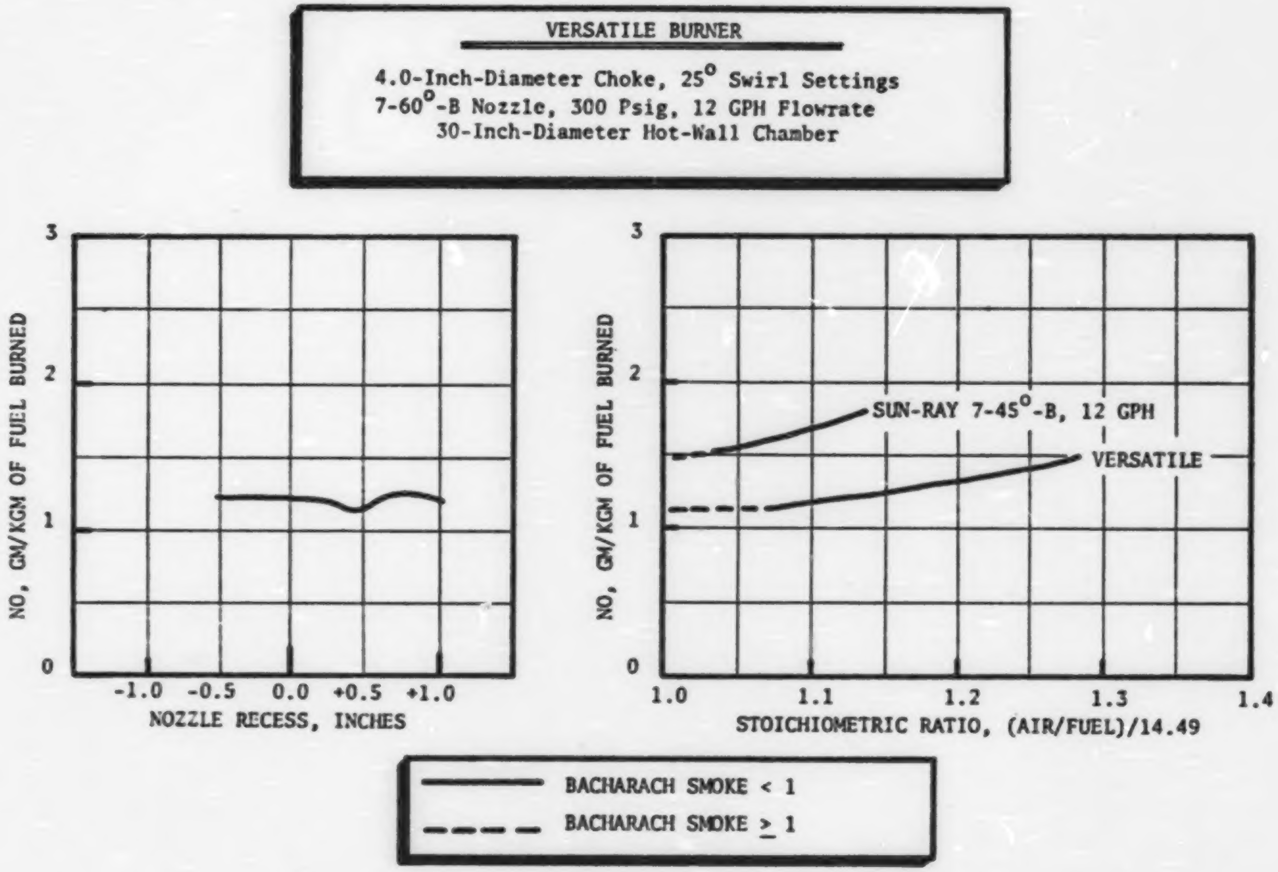

Figure 110. Versatile burner flue gas emissions obtained with 10-percent excess air in the 30-inch-diameter hot-wall chamber

NO formation. Examination of Fig. 107 through 109 suggests that an air swirl vane angle of about 25 degrees is a reasonable compromise between smoke and nitric oxide.

The effects of choke diameter at 12 gph, as shown in Fig. 107 through 110, are not totally unambiguous. However, the 3.50-inch choke diameter (Fig. 107) produced relatively high NO emissions, and the 4.5-inch choke diameter also produced somewhat high NO emissions, and/or required a large air swirl angle to eliminate smoke. The 3.75- and 4-inch choke diameters appear, therefore, to be the best compromise.

The effects of spray nozzle recess, as shown in Fig. 107, were not significant, and the effects of stoichiometric ratio, also shown in Fig. 110, were minimal with respect to nitric oxide. Also shown in Fig. 110 are NO emissions from a commercial 12-gph burner tested under similar conditions, indicating the optimum adjustment of the versatile burner leads to the lower NO emissions.

In Fig. 107 through 110, it is interesting to note that the nominal level of 1 gm NO/kg fuel appears to be a lower barrier, as suggested by the analyses described in the previous section. This lends credence to the conclusion that 1 gm NO/kg fuel is the nominal minimum that can be achieved by adiabatic, near-stoichiometric oil spray/air combustion without smoke. A lower value should, of course, be possible when air-cooled or hydronic combustion chambers are utilized, since combustion gases cooled by contact with the chamber wall can be aspirated into the air flow and, also, the flame temperature is lowered due to radiation losses from the flame to the cool wall. These cooling methods, however, are not possible with refractory wall combustors.

Using the same 30-inch-diameter coaxial combustor, versatile burner experiments were conducted at 7 gph. The results of these experiments are shown in Fig. 111. Choke diameters of 3 to 3.5 inches and an air

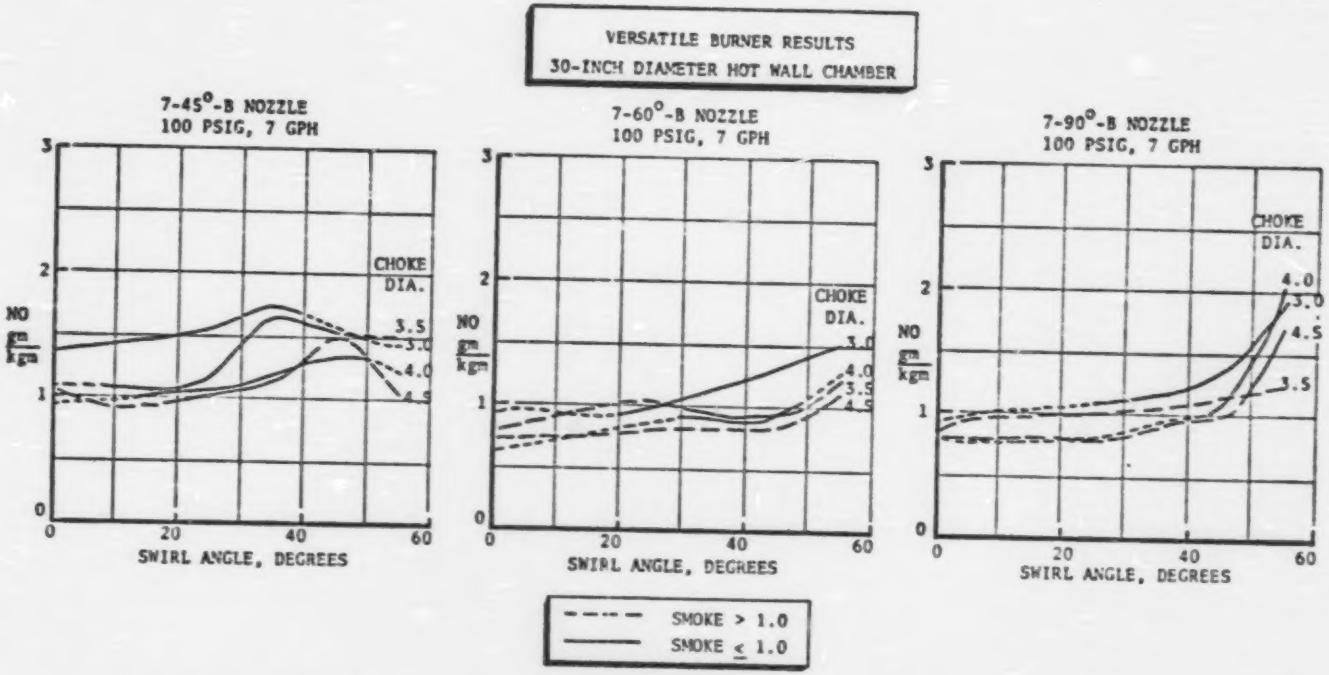

Figure 111. Versatile burner flue gas emissions obtained with 10-percent excess air in the 30-inch-diameter hot-wall chamber, 7 gph

swirl angle of 25 degrees appear to be generally near optimum at this flowrate. Note that, at this 7-gph flowrate, the 1 gm NO/kg fuel minimum appears still to be applicable for refractory wall (i.e., near adiabatic) combustors.

An 18-inch-diameter coaxial chamber, internally insulated with 1/2 inch of Pyroflex, was used for 3-gph versatile burner tests. The small version of the versatile burner was used for these experiments. The results are shown in Fig. 112. Here again, a 25-degree swirl angle appears to be a good compromise, while the 2.5-inch choke diameter is the better of the two shown.

At the 0.75-gph level, versatile burner experiments were conducted in an 8-inch-diameter, Pyroflex-lined coaxial combustion chamber. For those experiments, the air swirler vanes were relatively small (1/2-inch radial dimension by 2 inch length) and ineffective (placed at the periphery of the blast tube) so the only major geometry variable was the choke diameter. Shown in Fig. 113 is a spread of NO emission data obtained as a function of choke diameter. The data spread is for various nozzle recesses. The optimum choke diameter appears to be at about 1.5 inches. These were the first versatile geometry burner tests conducted and, since the experimental results indicated no swirler angle effects, all later versatile burner tests were conducted with swirler blades extending radially inward to within about 0.3 inch from the oil nozzle. Although no effective air swirl was tested at 0.75 gph, the data trends at higher flowrates suggest that an air swirler angle of 25 degrees might be most acceptable at this 0.75-gph level also.

Throughout the 0.75- to 12-gph range, the use of about a 25-degree air swirler angle appears to be a good compromise to eliminate smoke without inducing high NO emission. However, the optimum, or best compromise choke diameter is apparently dependent on the oil flowrate. The nominal best compromise choke diameters are shown in Fig. 114 as a

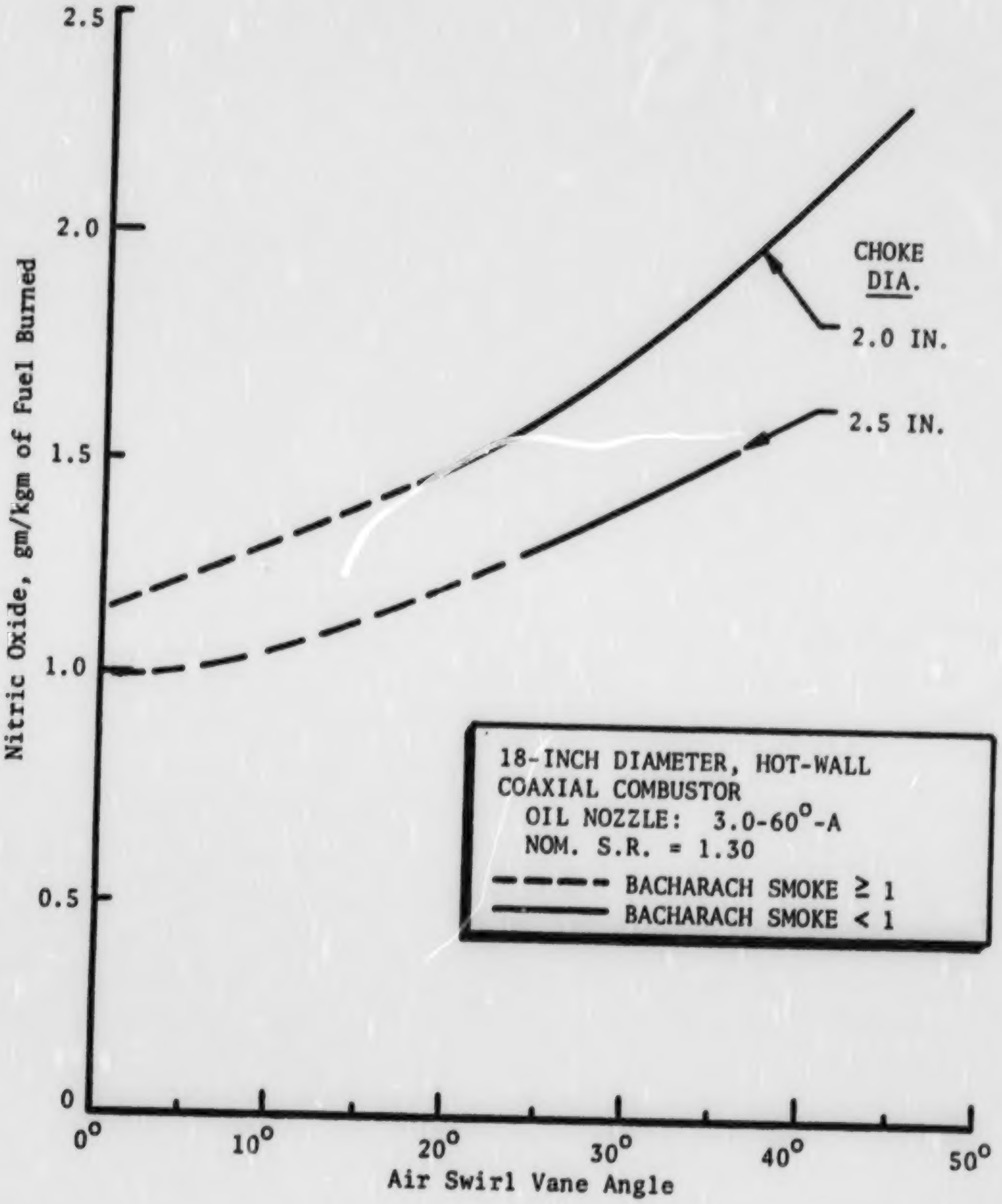

Figure 112. Comparison of nitric oxide emission results from the 1- to 3-gph versatile burner experiments as a function of air swirl vane angle

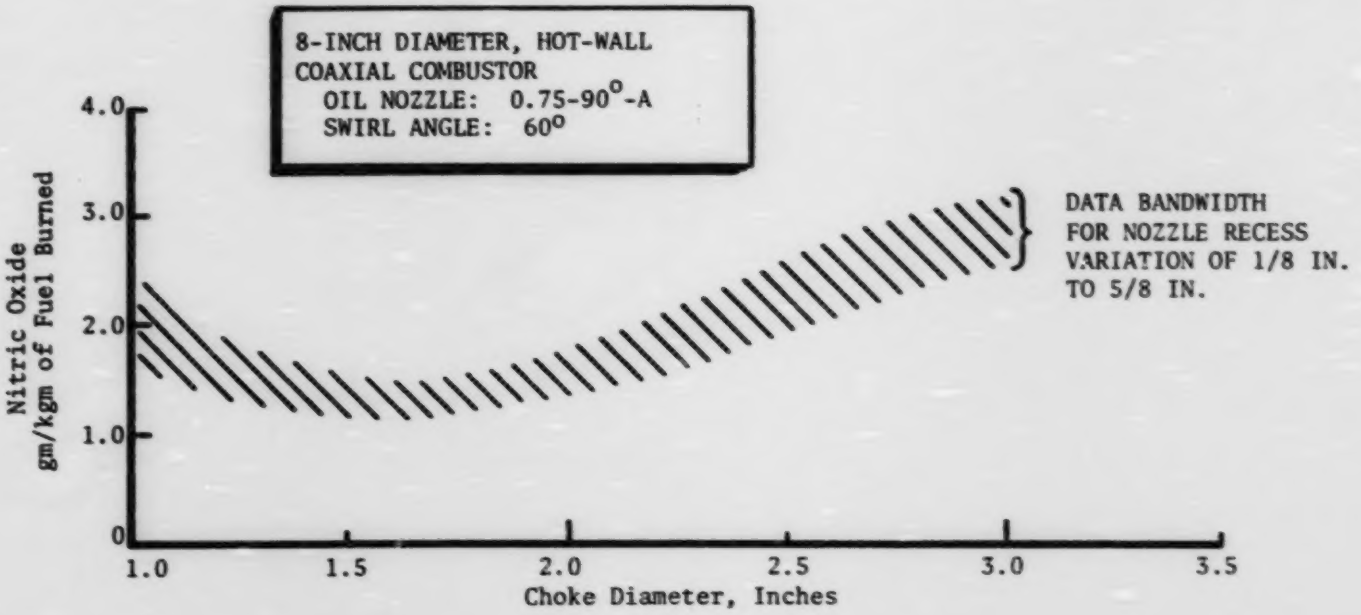

Figure 113. Nitric oxide emissions as a function of choke diameter for the versatile research oil burner at a nominal oil flowrate of 0.75 gph with 25-percent excess air

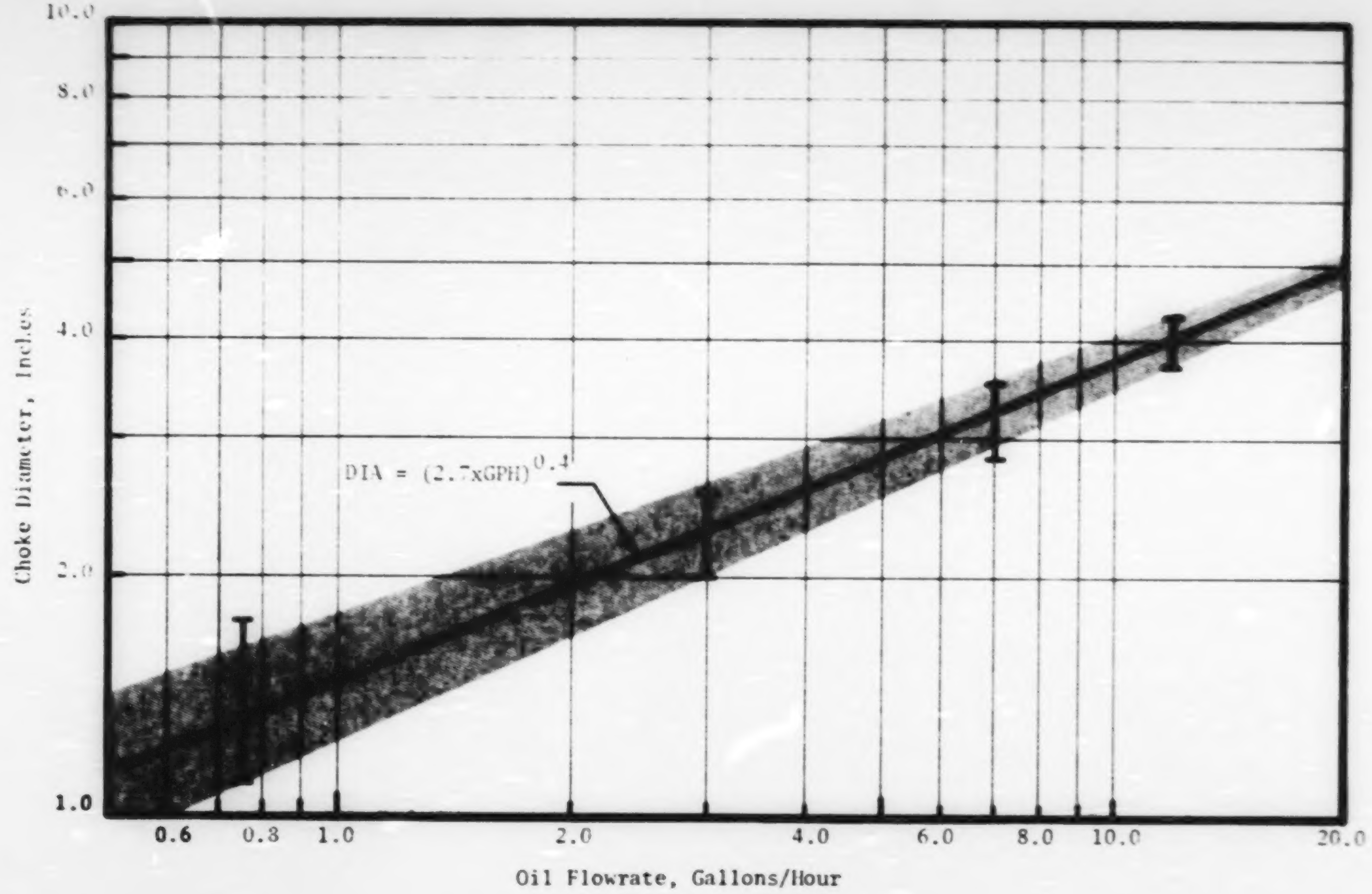

Figure 114. Choke diameter versus oil flowrate for minimum nitric oxide emissions, low smoke, and carbon monoxide emissions (applicable to burners incorporating a six-vane, 25-degree air swirler)

function of oil flowrate. The assessment of the compromise is at best only semiquantitative and, therefore, the optimum diameter ranges are shown as shaded areas. A single, straight line appears to adequately represent the center of the ranges. The equation of that line is:

$$\mathrm{DIA} = (2.7 \times \mathrm{gph})^{0.4}$$

where

DIA = optimum choke diameter, inches
gph = oil flowrate, gal/hr

If an oil burner is designed with the choke diameter obtained from the above equation, and if a six-vane set of 25-degree air swirler blades is used in the end of the blast tube, a near-optimum compromise between smoke and nitric oxide emissions should be expected when the burner is fired into an appropriately sized coaxial combustion chamber.

All of the versatile geometry burner experiments described above were conducted in refractory-lined combustion chambers which had their axes oriented coaxially with the burner blast tube axes. Perhaps a more common configuration in the 1-gph, residential burner size is the perpendicular orientation. For the perpendicular orientation, the burner blast tube axis is directed radially into the combustion chamber, near its closed end. The perpendicular orientation requires that flow from the blast tube make a right-angle turn after entering the combustion chamber. The right-angle turn tends to disrupt smooth flow patterns, and probably makes the flow resemble a well-stirred reactor which was previously shown to promote the formation of nitric oxide. The use of a perpendicular port combustion chamber is, therefore, expected to be detrimental to the objective of minimizing nitric oxide emissions; however, since such a large portion of the burners in the 1-gph, residential size range utilize the perpendicular port combustion chamber, a series of experiments was conducted with the 1-gph versatile burner mounted in the perpendicular port combustion chamber. The results of those experiments are shown in Fig. 115. It is observed that there is a considerably greater tendency for smoke formation in the perpendicular port combustion chamber and, also, a higher level of nitric oxide emissions. The smoke probably results from oil impingement on the chamber walls, and the high nitric oxide emissions from the flow disruptions which "stir" the combustion process. For the data in Fig. 115, the 1.0-90°-A nozzle, a 1.5-inch-diameter choke and about a 25- to 30-degree swirler angle appear to be near optimum. The choke diameter and swirler angle values are very close to the optimum values previously shown for coaxial combustion chambers. In conclusion, it was very apparent that the perpendicular port combustion chamber resulted in much worse pollutant formation than coaxial chambers.

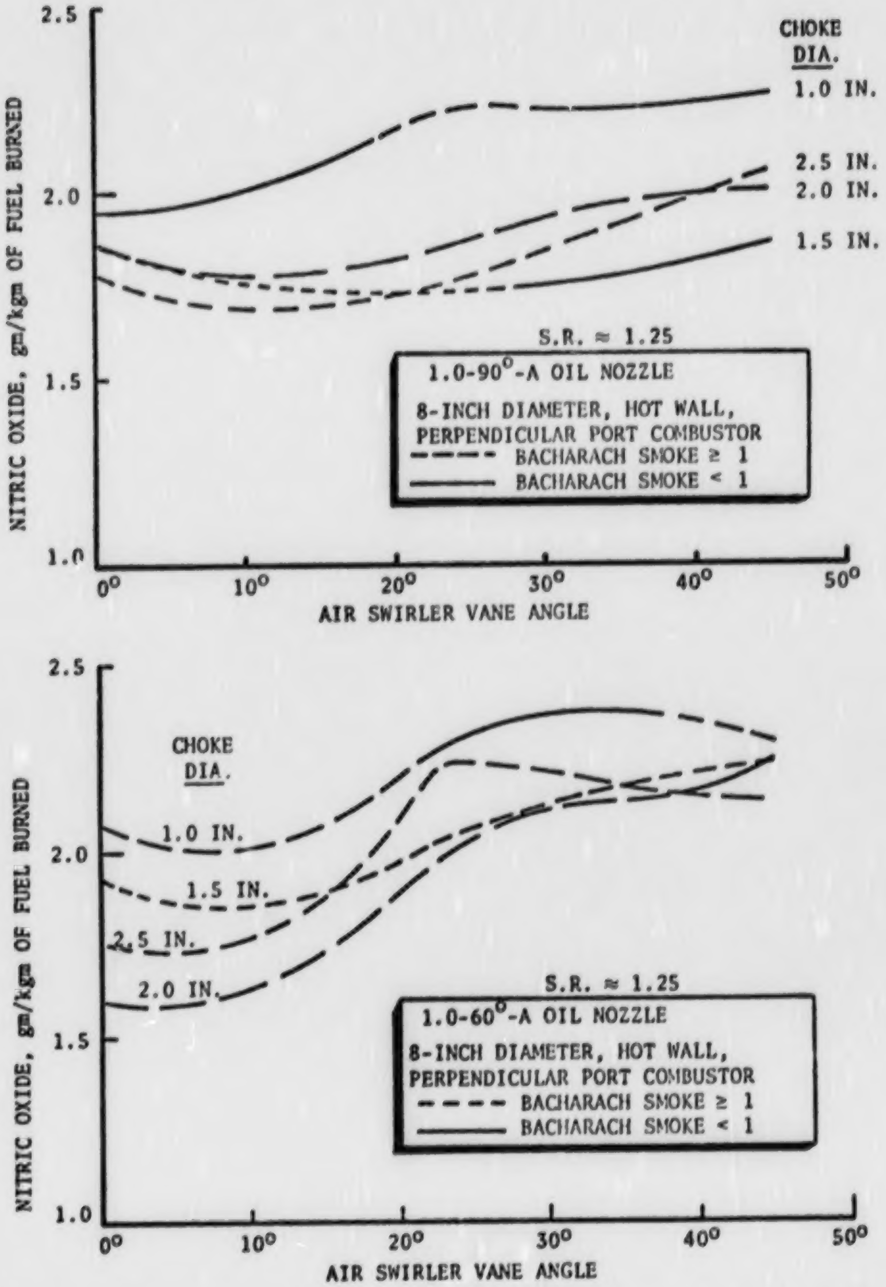

Figure 115. Nitric oxide emission results from 1-gph versatile burner experiments in a perpendicular port combustor

SIMULATED FIELD TESTING OF OPTIMUM GEOMETRY BURNERS

To verify the optimum burner geometry design criteria described in the previous section, two fixed geometry burners were fabricated according to those criteria, and subjected to an extensive series of tests. The two burners were designed for 1 and 9 gph, respectively. The 1-gph design represented an "extrapolation" since the 1-gph versatile geometry results did not include the use of effective air swirler blades, and it was assumed that the 25-degree air swirler angle found to be optimum for the larger 3-, 7-, and 12-gph size burners would also be optimum for the 1-gph size. The 9-gph design represented an "interpolation"of the versatile geometry results, which were conducted at 1, 3, 7, and 12 gph.

1-gph Fixed Geometry Optimum Burner

The 1-gph fixed geometry burner based on the optimum design criteria, included a 1.5-inch choke ring diameter and 25-degree air swirler vanes installed in a 4-inch-diameter blast tube. The air swirler blades extended inward to the 0.6-inch radius and were 2.06 inches long in the axial direction. A photograph of this burner is shown in Fig. 116. Test results obtained with this burner are shown in Fig. 117, indicating that it did achieve the desired result of 1 gm NO/kg fuel without smoke. Also shown in Fig. 117 is the range of NO of emissions experienced using several commercially available burners under similar conditions. These results indicate that the use of the optimum geometry criteria described above do provide a definite reduction of NO compared to the typical commercially available burners for smoke-free conditions. Shown in Fig. 118 are optimum burner and commercial burner data obtained using a cylindrical combustor with the burner blast tube port perpendicular to the axis of the chamber. The NO levels with the perpendicular port chamber are significantly higher than with the coaxial chamber, apparently because of the flow disruptions (i.e., combustion zone stirring) induced by the geometry change. However, note that under low smoke conditions, the optimum geometry burner is still lower in NO than the typical

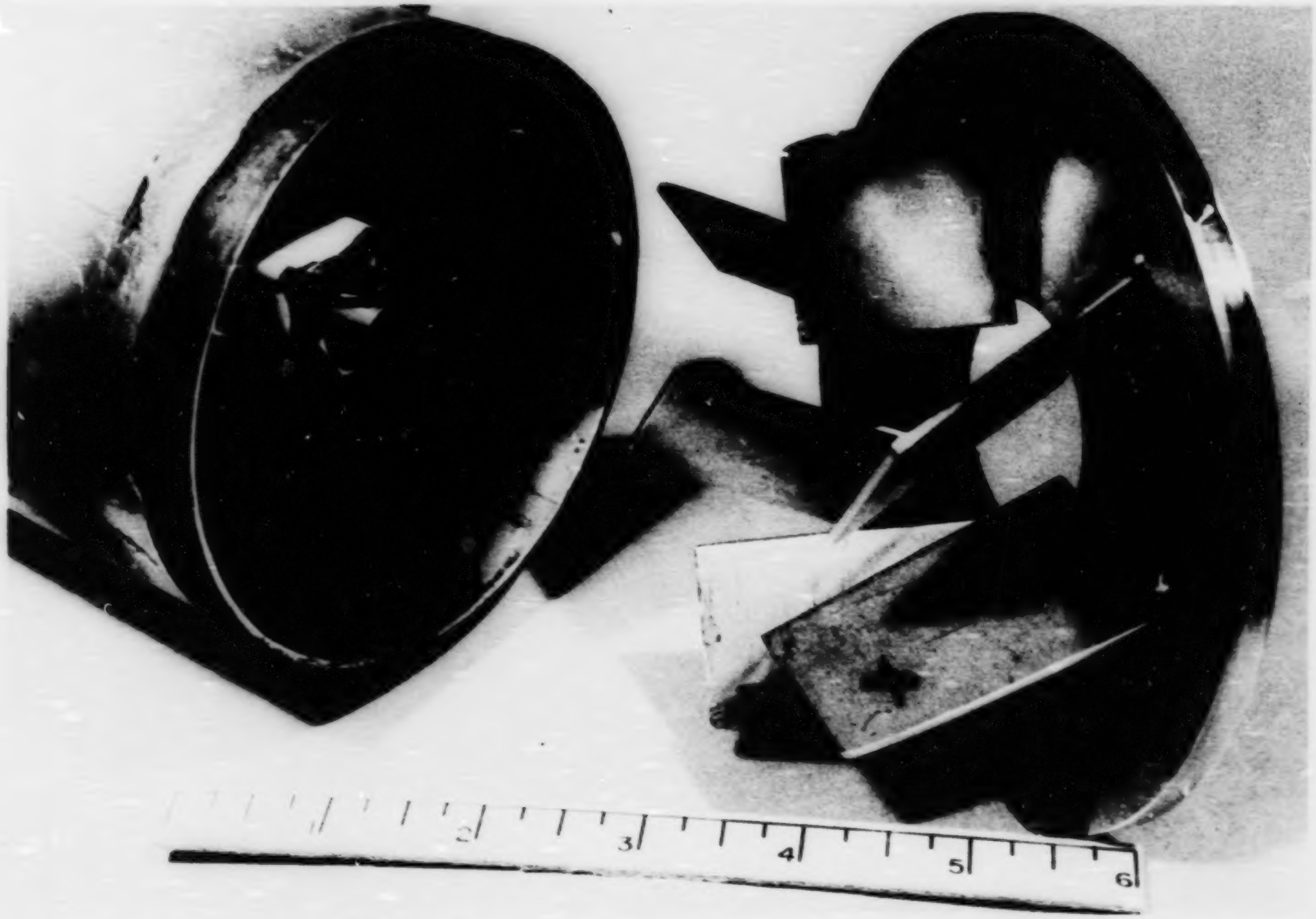

5DZ21-8/6/73-S1A

Figure 116. Closeup photograph of the 1-gph optimum oil burner head

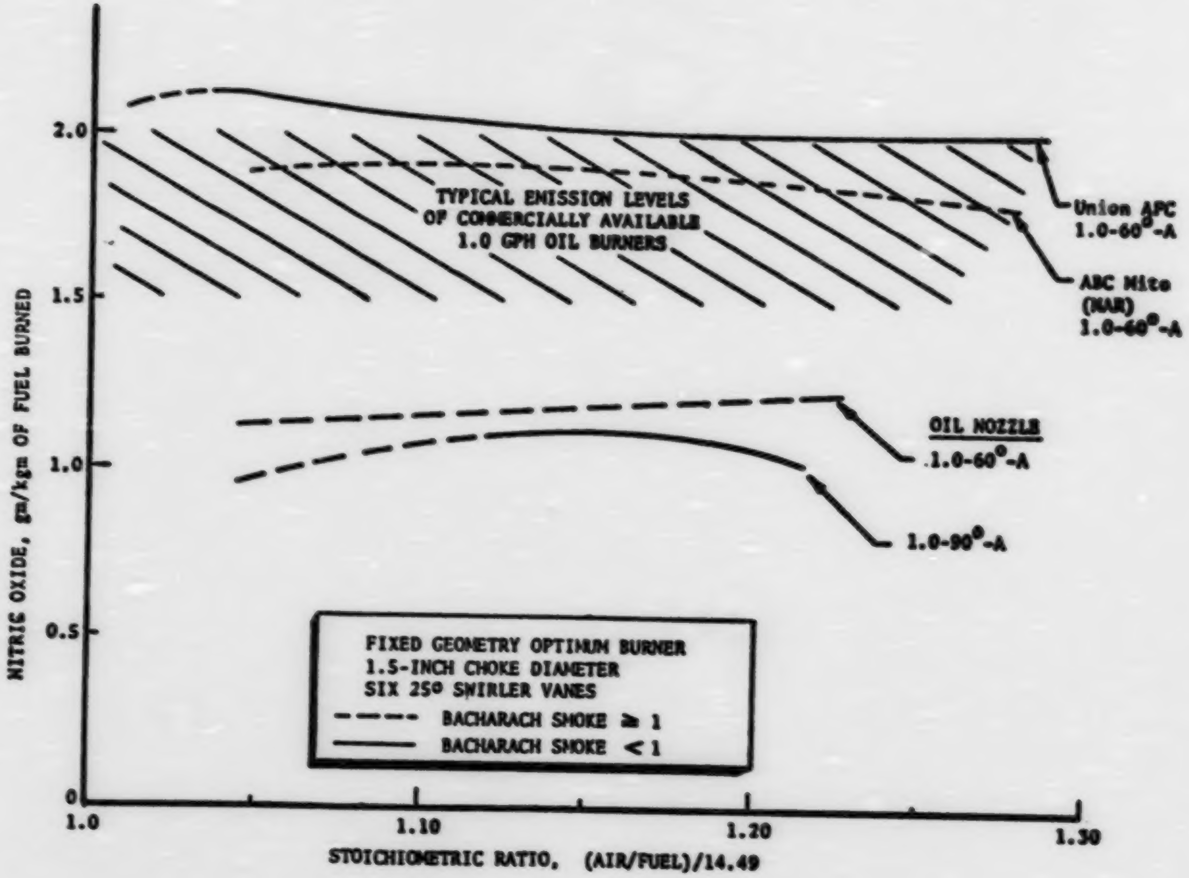

Figure 117. Nitric oxide emissions from the fixed geometry, 1-gph optimum burner fired in the 8-inch-diameter, hot-wall, coaxial combustor

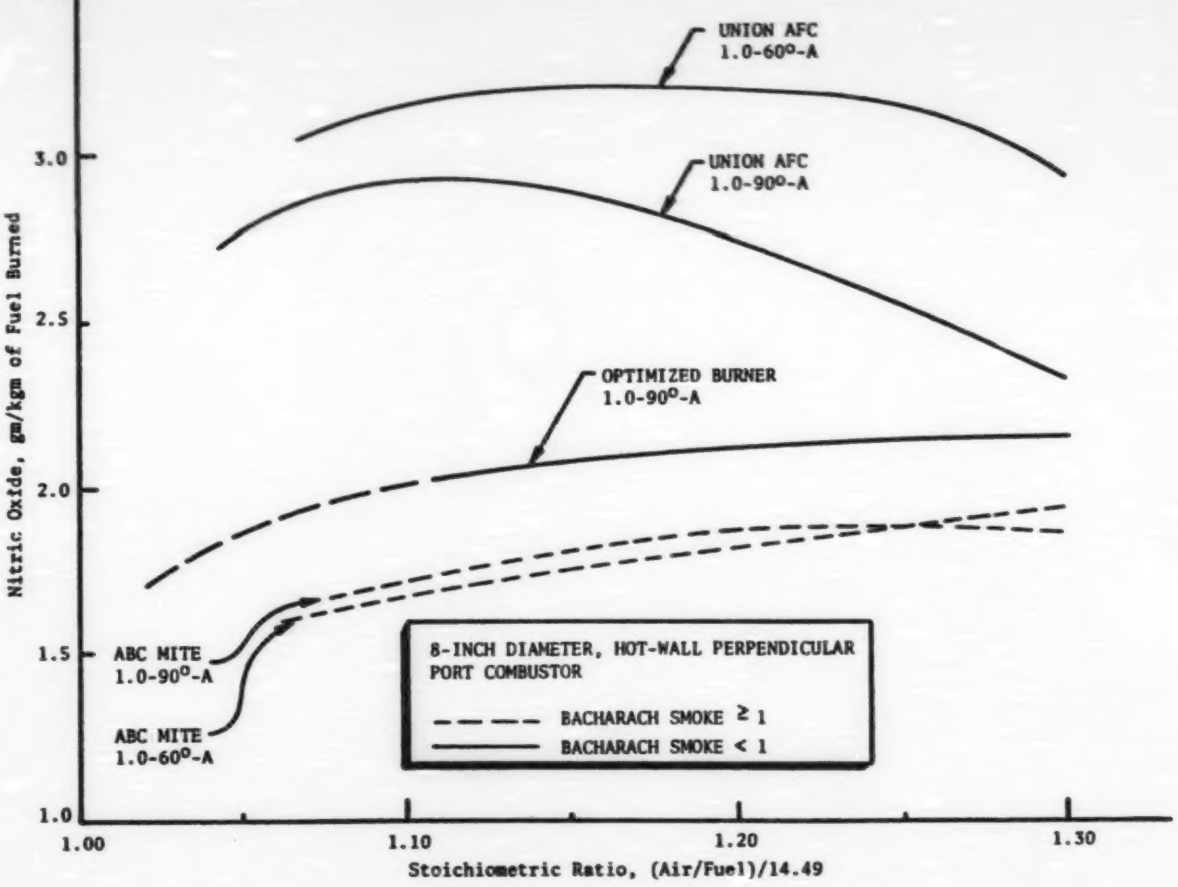

Figure 118. Comparison of nitric oxide emission profiles for several 1-gph oil burners fired in the 8-inch-diameter, hot-wall, perpendicular combustor

commercial burners, even though the optimum was determined from coaxial combustion chamber studies. Comparison of Fig. 117 and 118 supports the desirability of plug-flow-type combustion (which apparently cannot be achieved in a perpendicular part combustor due to flow disruption in the required right-angle turn) and the superiority of combustion chambers which are oriented coaxially to the burner blast tube.

Perpendicular port combustion chambers are very common in the 0.5- to 1.5-gph home heating applications where minimum floor space is available for the furnace. It is unfortunate that the very common perpendicular port geometry generally leads to higher NO emissions (by disrupting the flow, making the combustor resemble a near-stiochiometric well-stirred combustor rather than a near-stoichiometric, plug-flow combustor). The lower NO levels characteristic of coaxial chambers should be an incentive to alter furnace designs to allow universal use of coaxial combustion chambers.

A total of 128 hours of cyclic testing time (42 hours burning time) was accumulated as a part of simulated field testing with this burner in the Unitron A100 hydronic/warm-air furnace. The cycles were 5 minutes on, 10 minutes off, 5 minutes on, 10 minutes off. Nitric oxide, unburned hydrocarbon, and carbon monoxide emissions as a function of time are shown in Fig. 119. The high carbon monoxide and unburned hydrocarbons at the termination of the firing cycle are not extremely significant since the analysis system was sampling stagnant gas from the stack. The performance of the 1-gph optimum burner over the entire test period showed little variation and no noticeable degradation. The nominal stoichiometric ratio, with no mechanical readjustment, drifted upward slightly, ~2 percent (from about 1.08 to 1.10 to 1.10 to 1.12). This was probably due to changes in ambient conditions associated with the outdoor test facility being used. None of the exhaust pollutant emission concentrations increased during the testing, with nitric oxide at about 0.95 gm NO/kg fuel burned, no measurable unburned hydrocarbons, no smoke (Bacharach smoke scale = 0), while carbon monoxide improved

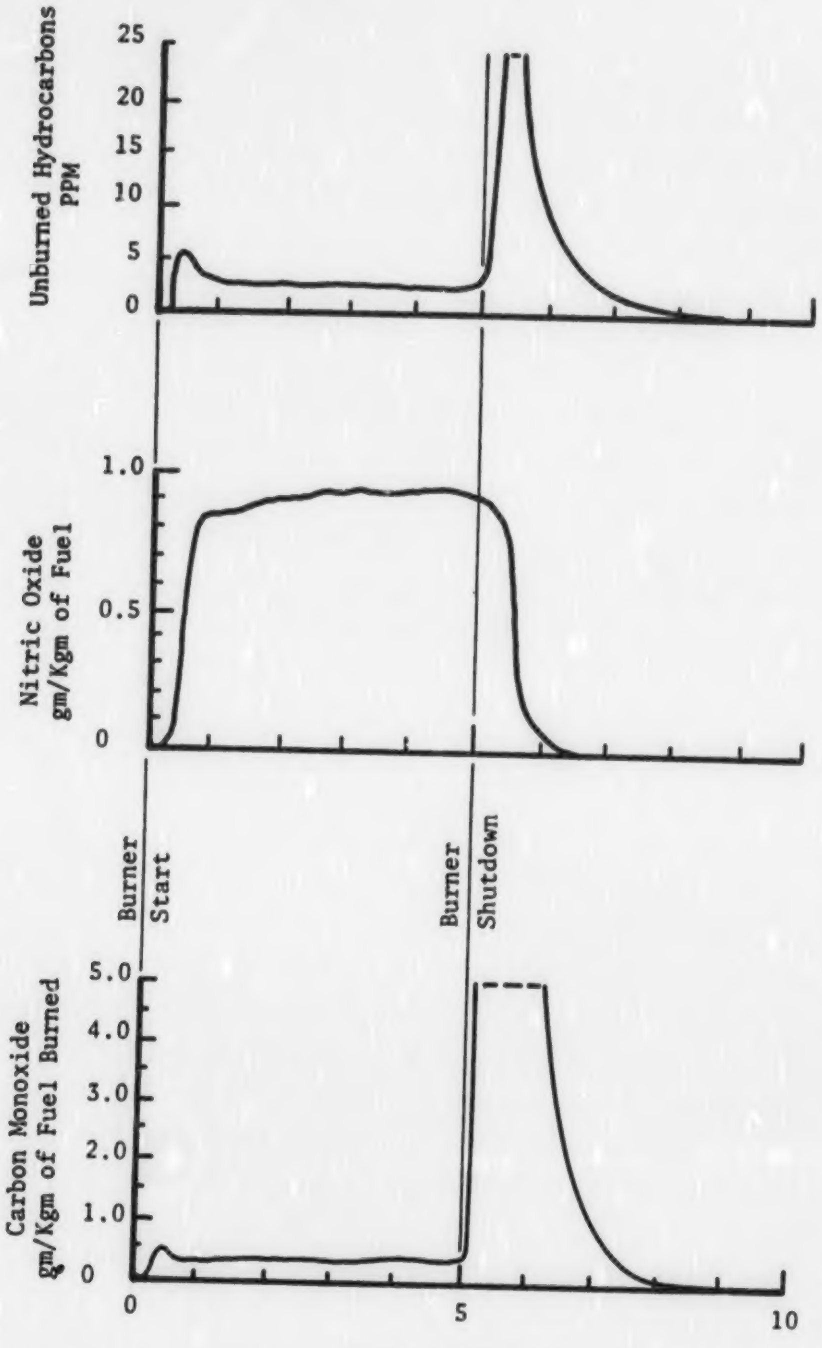

Figure 119. Exhaust gas composition profiles as a function of time for the 1-gph optimum oil burner in a refractory-lined chamber, hydronic furnace

(0.60 → 0.35 gm CO/kg fuel) probably due to the stiochiometric ratio shift. Removal and inspection of the 1-gph optimum burner after completion of testing revealed no soot or sludge accumulation nor any evidence of deterioration of either the burner or the furnace.

In summary, the 1-gph fixed geometry burner behaved as well, or better, than expected in all respects.

9-gph Fixed Geometry Optimum Burner

The 9-gph fixed geometry optimum burner blast tube was mounted on the Sun-Ray burner body. It had a 3.75-inch-diameter choke ring installed in a 6-inch-diameter blast tube, with six 25-degree air swirler vanes extending into the 0.6-inch radius, and 2.8 inches long in the axial direction. This optimum burner, with a 9.0-45°-B oil nozzle, was fired in the 30-inch-diameter, water-cooled, coaxial combustor. The resultant nitric oxide emission as a function of stoichiometric ratio is shown in Fig. 120 along with corresponding profiles from the 12-gph Sun-Ray and the 6-gph Nu-Way burners. The differences are quite substantial, the 9-gph optimum burner producing clearly 50-percent lower nitric oxide emissions in the smoke-free operating range than either of the other burners. The 9-gph optimum burner operated smoke-free to near-stoichiometric conditions ($SR \simeq 1.02$), and at a nominal nitric oxide emission level of about 0.65 gm NO/ kg fuel burned. This level of NO emissions for the 9-gph optimum burner is very low, relative to the 1-gph optimum burner data shown in Fig. 117 ($NO \approx 1.10$ gm NO/kg fuel) primarily because of the effect of the cold-wall ($T_{wall} \approx 400$ F) combustor and probably due in part to the large combustor volume.

The 9-gph fixed geometry optimum burner consistently ran somewhat noisier than the conventional burners in the 10-foot-long, 30-inch-diameter combustor, whereas the 1-gph fixed geometry burner was noisy only under rare circumstances. Whether the noise was being generated as a result of combustor resonance and/or as a result of flame instability was not

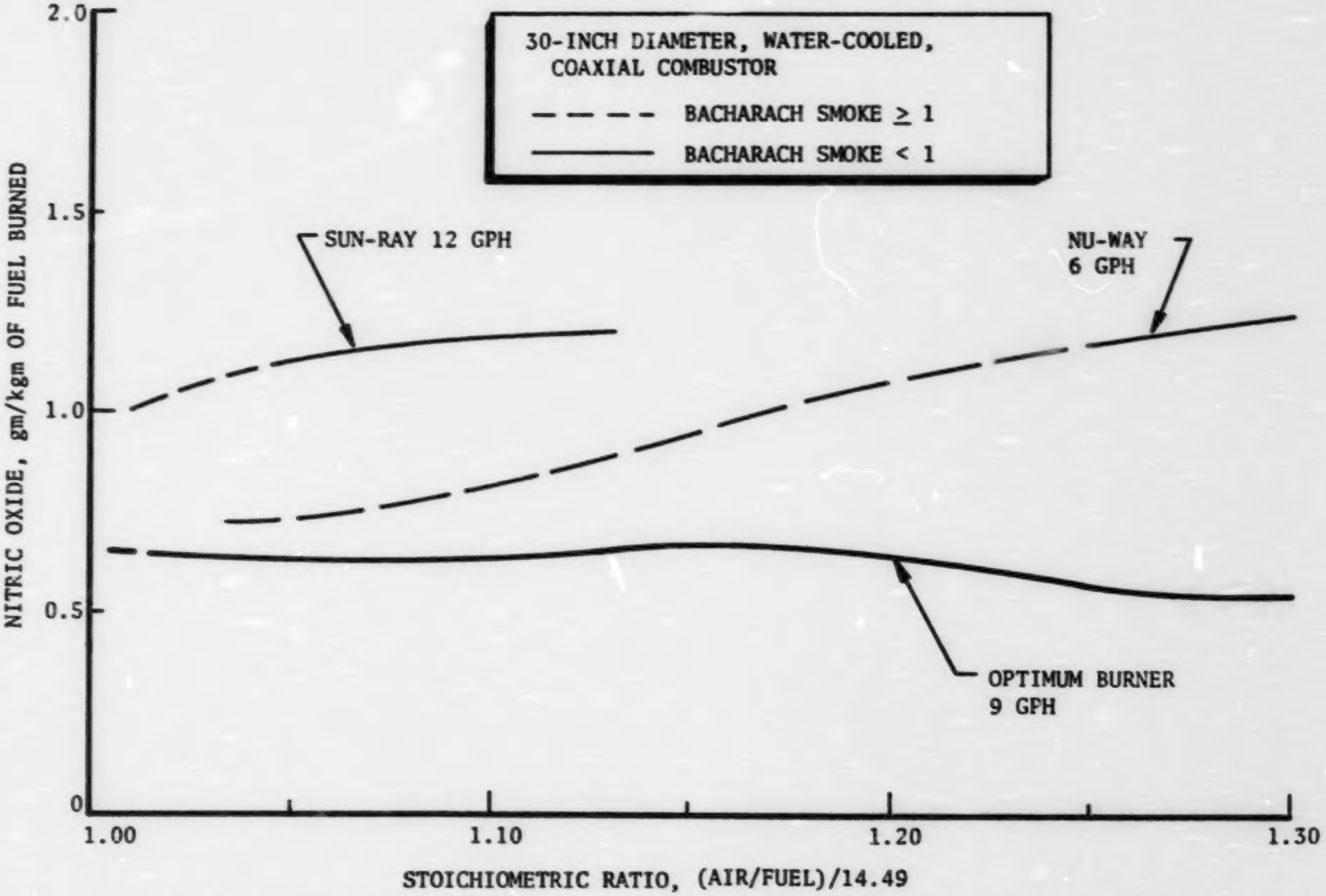

Figure 120. Comparison of nitric oxide emission profiles for various oil burners in the 6- to 12-gph firing rate range

apparent. A high sensitivity microphone was used to measure the noise being generated by the 9-gph fixed geometry optimum burner in the 30-inch-diameter, cold-wall combustor. Figure 121 shows a photograph of an oscilloscope display of the noise (microphone output) obtained during the burner firing. These data indicate that the frequency of the noise is about 39 to 40 Hz. Assuming an average temperature in the chamber of 2000 R, the acoustic velocity was calculated to be about 2100 ft/sec. The estimated effective length of this combustor has a quarterwave resonance which corresponds to a resonant frequency of 43 Hz, which is reasonably compatible with the measured frequency. Therefore, it appears likely that the noise is due to a quarterwave resonance in the combustor. This being the case, it is likely that if the burner were installed in a combustor of smaller volume, the resonance would disappear and the burner would run quietly. In practical commercial applications, the use of combustors of smaller volume than the one used here is standard practice.

Simulated field testing of the 9-gph optimum burner also was conducted with a total cycle time of 112 hours (27 hours of burning time) being accumulated with this burner in the 30-inch-diameter, water-cooled, coaxial combustor. The most usual cycle was 5 minutes on, 10 minutes off. The performance of this larger, optimum burner also showed little variation and no noticeable degradation. The stoichiometric ratio increased slightly from 1.02 to 1.03 to 1.03 to 1.04 during the test series. A slight improvement was noted in the NO emission level which decreased from about 0.5 to 0.6 gm NO/kg fuel to 0.45 to 0.50 gm NO/kg fuel burned. The CO emission level varied slightly, probably with changes in ambient conditions, but CO emissions as low as 0.6 to 0.7 gm CO/kg fuel burned were still being obtained at the end of the test series. The unburned hydrocarbon emission level was zero, and the Bacharach smoke level was zero. Time-dependent hydrocarbon and nitric oxide emissions for a typical cycle are shown in Fig. 122. Inspection of the 9-gph optimum burner at the end of the test series revealed only a slight oily accumulation around the perimeter of the 5-inch-diameter burner head,

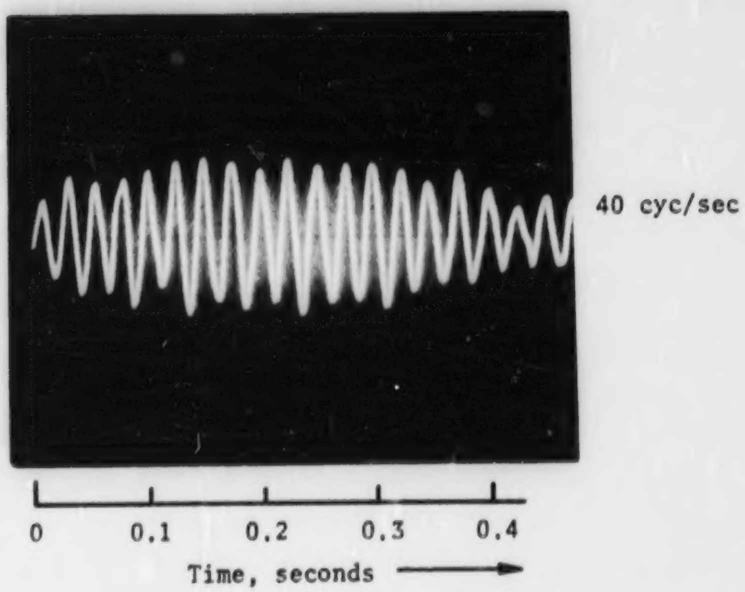

Figure 121. Oscilloscope frequency trace of noise generated by the 9-gph fixed geometry optimum burner, measured at the exhaust of the 30-inch-diameter, 10-foot-long coaxial combustor

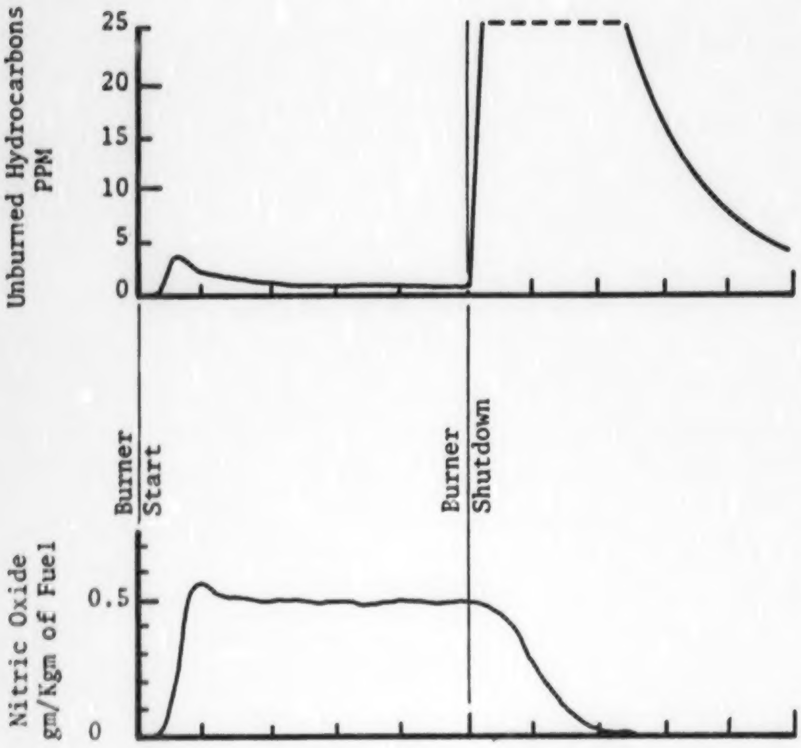

Figure 122. Exhaust gas composition profiles as a function of time for the 9-gph optimum oil burner in a cold-wall, 30-inch-diameter, coaxial combustor

and no evidence of deterioration of the burner head assembly. An interesting characteristic of this burner is the almost invisible flame it produced, implying an extremely low particulate concentration in the flame, and a high degree of recirculation.

This optimum geometry burner also behaved as well as, or better than, expected in all respects.

NONCONVENTIONAL BURNERS

The primary emphasis in this program was on relatively conventional, high-pressure atomizing, luminous flame, No. 2 distillate oil burners fired into refractory combustion chambers. The objective was to make minor changes in the burner blast tube end which would result in a reduction in emissions and improvement in efficiency. The changes were desired to be such that they could be retrofitted onto existing burners and they should not introduce any new or special servicing requirements.

In addition to the conventional burner development, a portion of the program effort was set aside for application to nonconventional burners. These nonconventional burner concepts were generally felt to be potentially applicable to future burners, but cost and serviceability were not a significant consideration in selection of the concepts to be tested. Several different nonconventional burners were tested, including the intense swirl burner, the forced combustion gas recirculation burner, the displaced injection burner, the two-stage burner, the three-stage burner, and the nonswirl optimum geometry burner. These burners and the results obtained with each are described in the following sections.

Intense Swirl Burner

Results obtained with the commercial burners suggested that a well-stirred combustion process would produce relatively small amounts of nitric oxide when operated at high excess air levels. To verify this, an existing 0.5- to 3-gph commercial burner was modified to accept a variable rate, mechanically rotated, multiple-vane swirler assembly to be used to investigate low to very high air swirl rates. This intense swirl burner has been described earlier, in the Apparatus section of this report. Figures 23 and 25 in that section show a schematic and a photograph of the modified burner with the motorized swirler assembly.

The high-swirl burner was tested with maximum (3450 rpm, swirl No.=8.8) swirl, with low (812 rpm swirl No.=2.2) swirl, and with no swirl. The burner was fired in the 8-inch-diameter, perpendicular port, refractory-lined combustion chamber. The nitric oxide emissions determined from analysis of the mixed exhaust gases are shown in Fig. 123. When there was no swirl, the nitric oxide emissions were similar to those observed with typical commercial burners, except there was a very noticeable lack of repeatability. The lack of repeatability was later determined to be due to a nonstationary flame front location. Apparently, the smooth convergence of the choke device, combined with the lack of any swirl at all, and the absence of a continuous spark igniter, allowed the flame front to shift from test to test.

At low swirl, the nitric oxide emissions were moderately high, and varied irregularly with stoichiometric ratio.

At very high swirl rates, the nitric oxide emissions decreased monotonically with increasing stoiochiometric ratio. This is the well-stirred reactor trend which was expected from interpretation of results from the commercial burner studies, as discussed in pages 173 through 188. The well-stirred burner obviosuly has the potential for extremely low nitric oxide emissions at high excess air, especially considering the fact that these results were obtained in a refractory-lined chamber; however, the furnace efficiency penalties (due to lower temperatures for heat transfer) which result from operations at high excess air are not tolerable.

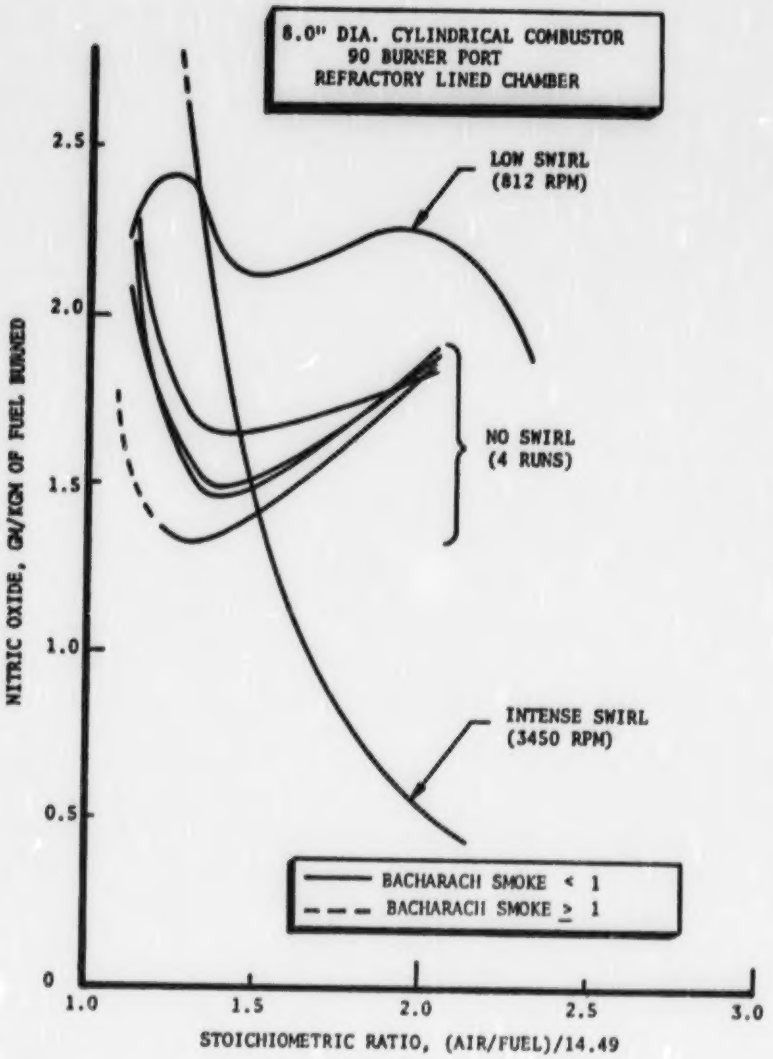

Figure 123. Nitric oxide emissions, comparison of the effect of swirl on the 30-degree convergence, 1.65-inch-diameter, mechanically rotated, six-vane swirler, with no spark igniter

If this same burner were fired at high swirl in a water-cooled combustor, the nitric oxide levels would undoubtedly be much lower, and the enhancement of heat transfer to the combustion chamber walls by virtue of the high swirl velocities might wholly compensate for the penalties of high excess air operation.

Forced Combustion Gas Recirculation Burner

The benefits of flue gas recirculation for the control of nitric oxide emissions are well known. However, it is not convenient to arrange for flue gas recirculation in typical domestic applications. A special burner was fabricated to achieve the benefits of flue gas recirculation without any modifications to the heating plant, other than the burner itself. This burner is constructed to suck combustion gases out of the combustion chamber and mix them with the incoming air. The burner was designed to operate in a cooled combustion chamber, so that the combustion gases withdrawn by the burner would be at least partially cooled to yield the same benefits as flue gas recirculation. The flow directions are shown schematically in Fig. 27, in the Apparatus section, and a photograph of the assembled burner is shown in Fig. 28.

Tests were conducted with this burner, using an 0.5-gph spray nozzle, varying the overall stoichiometric ratio and varying the ratio of recirculated combustion gas to primary air in the burner. The overall stoichiometric ratio was determined by chemical analysis of the flue gas composition. The recirculation ratio in the burner was determined by measuring the composition of the mixed gases in the burner blast tube. Since, in the analysis of the mixed gases, it was not possible to differentiate between oxygen coming in with the fresh air and unburned oxygen coming in with the recirculated gas, the recirculation ratio is reported as the weight ratio of burned gases to unburned gases. For this definition, the burned gases include CO, CO_2, H_2O, and NO, as well as the inert atmospheric gas (N_2) associated with the oxygen in the combustion products; the unburned gases are the free oxygen and the inert atmospheric gas associated with it. This recirculation ratio can be calculated from O_2, CO, and CO_2 concentrations in the mixed gases according to the following formula:

Recirculation Ratio =

$$\frac{CO_2\ [44 + \frac{x}{2}\,18 + (1 + \frac{x}{4})\,\frac{79}{21}\,28] + CO\ [28 + \frac{x}{4}\,18 + (\frac{1}{2} + \frac{x}{4})\,\frac{79}{21}\,28]}{O_2\ (32 + \frac{79}{21}\,28)}$$

where

recirculation ratio = grams of burned gas per gram of unburned air
CO_2 = volume percent CO_2 in the mixed gases, dry basis
CO = volume percent CO in the mixed gases, dry basis
O_2 = volume percent O_2 in the mixed gases, dry basis
x = hydrogen to carbon atomic ratio for the fuel, $x = 1.814$

The forced combustion gas recirculation burner was tested in the 8-inch-diameter coaxial combustion chamber. For these tests, the coaxial combustion chamber did not have a refractory lining, and the exterior of the steel combustion chamber was cooled by natural air convection. The flame produced by this burner was mostly nonluminous, with a few streaks of blue. The nitric oxide emissions measured for these tests are shown in Fig. 124. This burner produces very low nitric oxide emissions, even at near-unity stoichiometric ratios. A recirculation ratio of 0.16 grams burned gas per gram of unburned air appears to be about optimum for this burner. The highest recirculation ratio of 0.4 produced slightly more nitric oxide than the ratio of 0.16, presumably because the gases recirculated at the higher ratio were apparently drawn from the uncooled core of the combustion process whereas those at a ratio of 0.16 were mainly from the cooler regions near the wall. This presumption is supported by the observation of a higher carbon monoxide-to-burned fuel ratio for the high recirculation ratio cases.

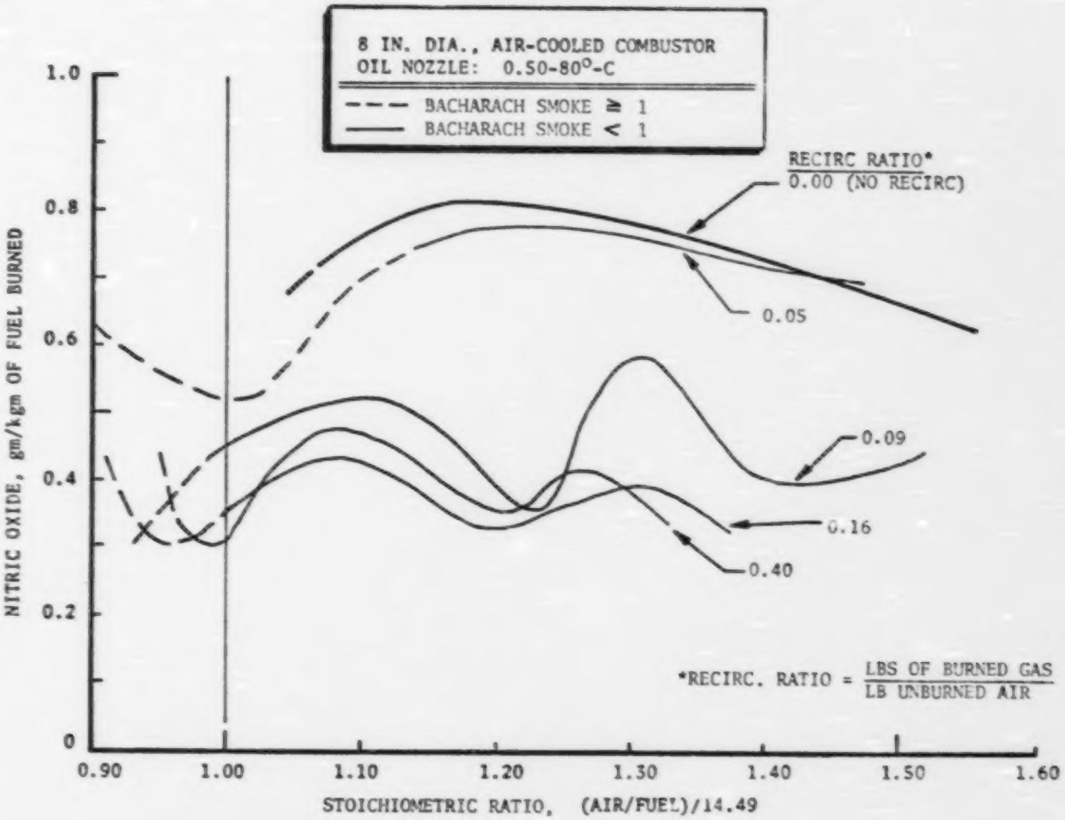

Figure 124. Effects of varying recirculated combustion gas with the forced combustion-gas recirculation burner

It is notable that the nitric oxide emissions for this 0.5-gph burner are a factor of 2 or 3 lower than for the 1-gph optimum geometry burner. This is due to: (1) operation in a cool wall chamber (as opposed to a refractory wall chamber for the optimum burner, and (2) the recirculation of cooled combustion gas products through the burner, where the cooled gases lose even more heat through the walls of the burner to the surrounding environment.

An additional factor of interest in Fig. 124 is the tendency for this burner to operate smoke-free. At the high recirculation ratio of 0.4, the burner operated smoke free even in the fuel-rich region to the left of unity stoichiometric ratio in Fig. 124. Under this condition, there was, of course, a considerable amount of carbon monoxide, but very low nitric oxide and smoke emissions. The tendency for smoke-free operation appears to be enhanced by the higher recirculation ratios, suggesting that the temperature of the mixed primary gas is a strong factor. Apparently the hotter primary gas tends to prevaporize the fuel, prior to the start of combustion, reducing the tendency for smoke formation. This factor may also explain the general flame appearance, which was largely nonluminous with a few streaks of blue.

Using the same combustion chamber, but installing a 1/2-inch-thick Pyroflex liner, the burner was fired in the hot-wall configuration. The results of these tests are shown in Fig. 125, compared to some of the previously presented cool-wall results. The results with the hot-wall configuration are essentially as might be expected from consideration of the fact that the recirculated combustion gases are hotter with the hot-wall chamber. The nitric oxide emissions are considerably higher, undoubtedly an effect of the higher temperatures. The smoke-free region also appears to be wider, apparently due to the greater tendency for prevaporization of the fuel.

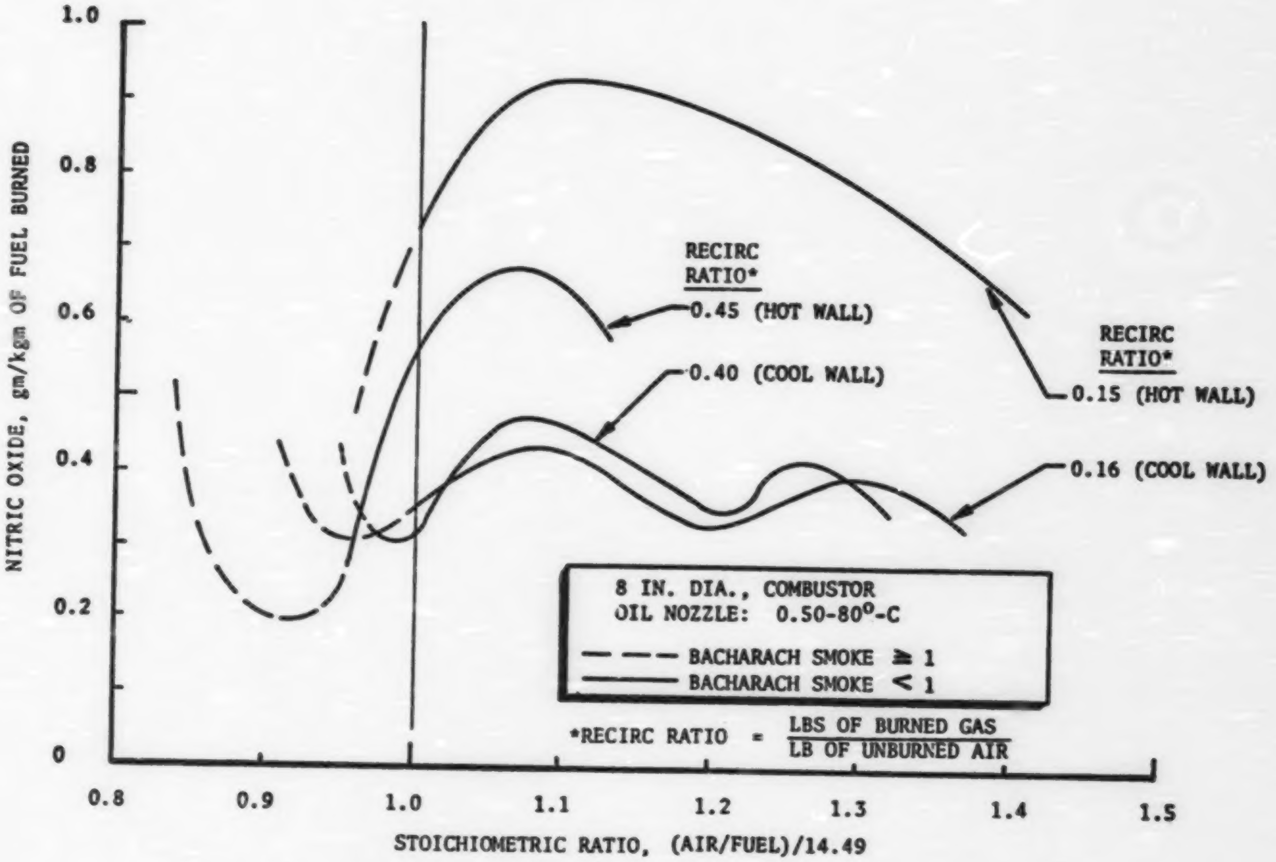

Figure 125. Effects of combustion chamber wall temperature with forced combustion-gas recirculation burner

Tests were also conducted with a larger flowrate spray nozzle in the forced combustion gas recirculation burner. The results of these tests are shown in Fig. 126. To achieve recirculation ratios above 0.08 gram of burned gas per gram of burned air required.the use of a lesser number of lower-angle swirler vanes (because the blower power was limited and the swirler vanes were the main pressure drop). Note that, in general, the 0.75-gph flowrate resulted in higher nitric oxide emissions, presumably because of the higher heat loads at 0.75 gph and the higher rates of recirculated gas flowrate combining to cause higher mixed gas temperatures (but perhaps affected by the different swirler vane configuration). The higher mixed gas temperatures are less effective in reducing nitric oxide formation. The forced combustion gas recirculation burner nitric oxide emissions at 0.75 gph would very likely be improved by use of combustion gas entry ports (Fig. 27) located at a larger radius where they would have a greater tendency to pull in combustion gases from the vicinity of the cooled walls.

In conclusion, burners incorporating forced combustion gas recirculation appear to offer the combined benefits of smoke-free operation at very near to stoichiometric air/fuel ratios and low nitric oxide emissions. They must, however, be operated in conjunction with air-cooled or water-cooled combustion chambers. Some additional advantage might also be obtained if the combustion chamber geometry were specially tailored to enhance recirculation of gases to the burner end of the chamber.

Displaced Injection Burner

The displaced injection burner concept is shown schematically in Fig. 26 for two configurations that were tested. The burner design is intended to take advantage of combustion gas circulation induced by tangential injection of the combustion air. As shown in Fig. 26 (Apparatus section), the tangential injection of combustion air imparts a strong circulation to the gases, causing combustion gases to be intermixed with the fresh air. The oil injection nozzle is located so that the oil is sprayed into

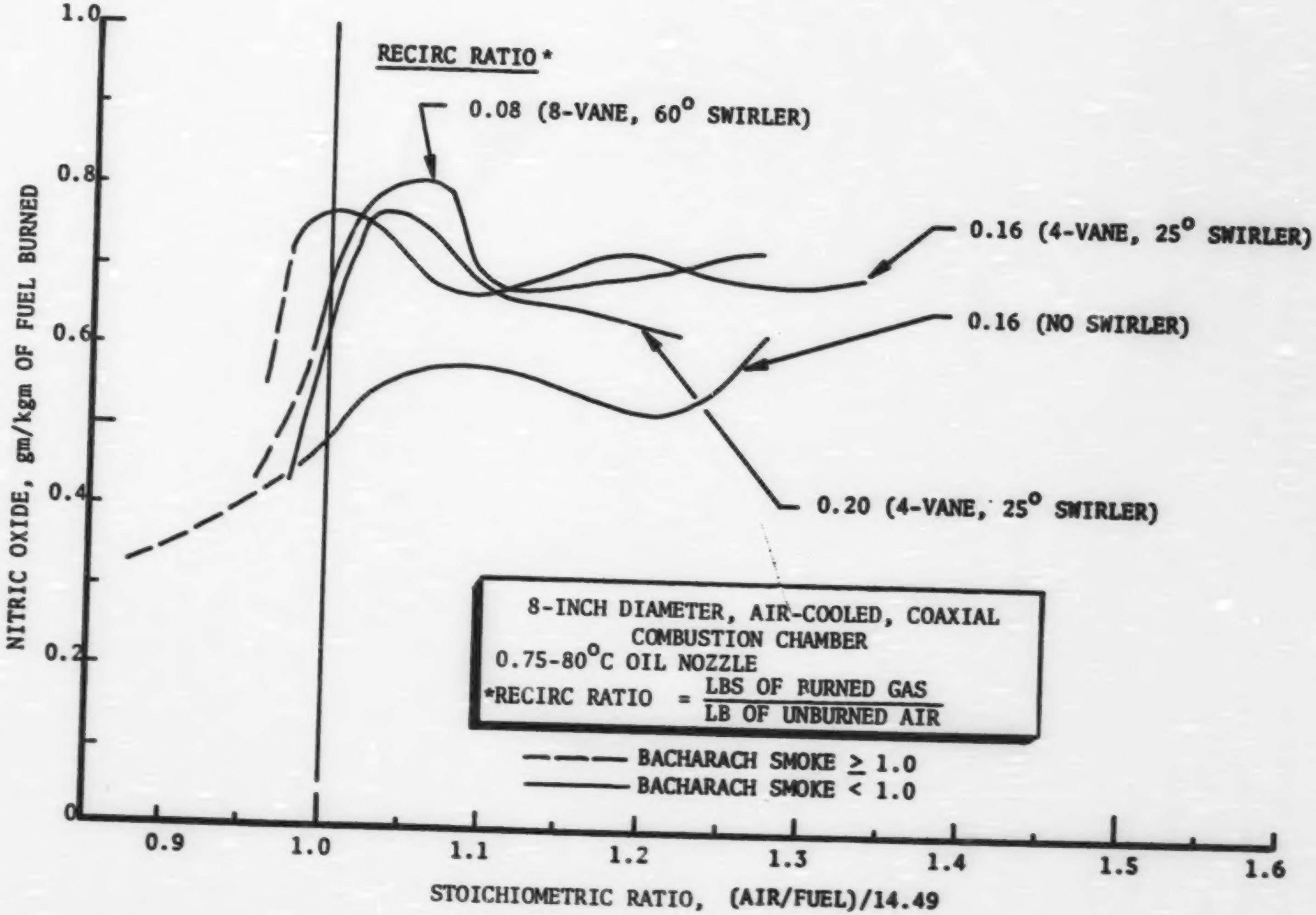

Figure 126. Forced combustion gas recirculation burner emissions at an oil flowrate of 0.75 gph

a mixture of burned gases and fresh air. The recirculation pattern induced by the burner was intended to take advantage of the combustion gas cooling which results as the gases pass along the wall. Thus, the design shown in Fig. 26 was intended to achieve the same results as the forced combustion gas recirculation burner described in the previous section, but without requiring the passage of combustion gas through the air fan.

The displaced injection burner was tried only in the two configurations shown in Fig. 26 and, for each of these, it resulted in relatively heavy smoke emissions, even though it was tested in a refractory-lined chamber. The smoke apparently was caused by impingement of oil spray on the combustor walls, and/or poor mixing of the air/oil spray mixture. Further studies of this burner concept, employing a larger combustion chamber, and/or variations in the oil spray injection site, would be worthwhile.

Two-Stage Burner

If combustion takes place under fuel-rich conditions and chemical equilibrium is achieved, there is a tendency for relatively low nitric oxide emissions. This may or may not be offset because of superequilibrium amounts of nitric oxide formed by the prompt reaction mechanisms. Most oil burners operate with all of the combustion taking place under air-rich conditions where nitric oxide chemical equilibrium is unfavorable to the objective of low nitric oxide emissions. A burner (Fig. 127) was designed that carried out all but the last stage of combustion under fuel-rich conditions.

It was hoped that the fuel-rich portion of the combustion could be carried out smoke free with the use of intensely swirled air (3450 rpm). The grounds for this optimism was the smoke-free nature of fuel-rich combustion in the forced combustion gas recirculation burner, and with the intense swirl burner. However, preliminary tests with the burner shown in Fig. 127 did not result in smoke-free operation, so further testing was not conducted.

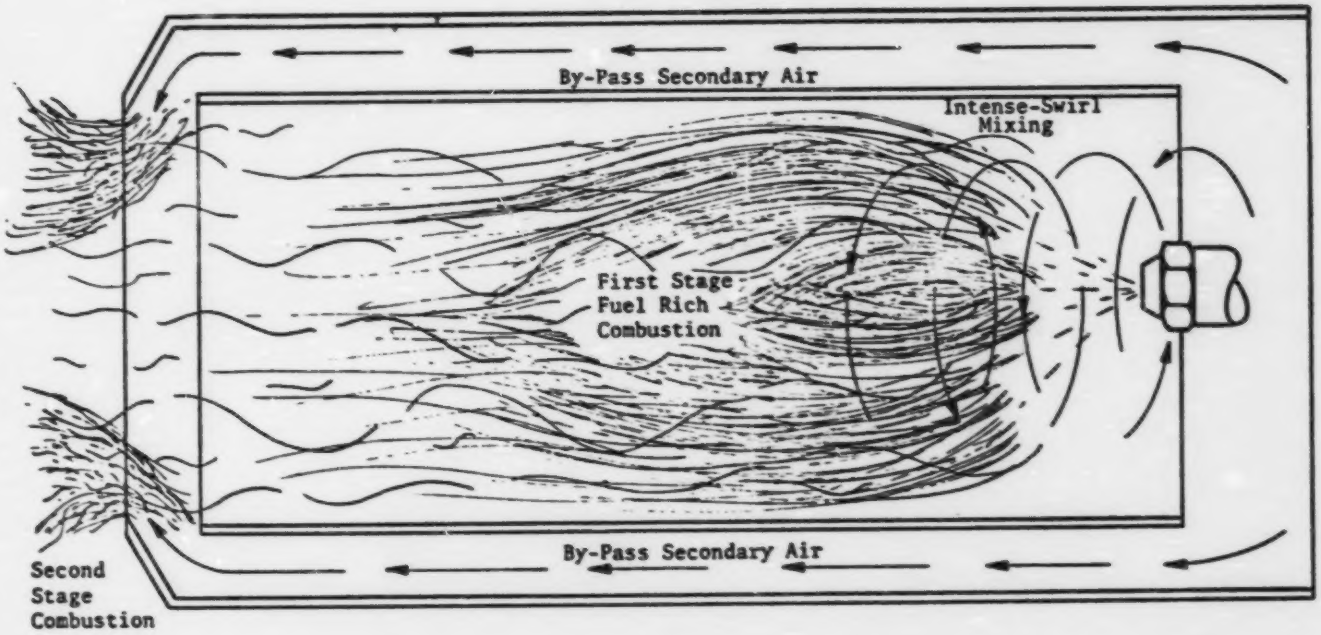
By-Pass Secondary Air
Intense-Swirl Mixing
First Stage Fuel Rich Combustion
By-Pass Secondary Air
Second Stage Combustion

Figure 127. Schematic of the two-stage, intense-swirl, concentric-tube oil burner head extension

Three-Stage Burner

As a further effort to achieve smoke-free, fuel-rich combustion, a three-stage burner was conceived. The three stages of combustion are: (1) preheat the inlet air to 400 to 600 F, (2) use the air for fuel-rich, low nitric oxide, hopefully smoke-free combustion, and (3) add the last bit of air to make the overall combustion air rich, thus eliminating carbon monoxide and unburned hydrocarbons with a minimal increase in nitric oxide. The test configuration for this burner is shown in Fig. 29 (Apparatus section). The test configuration included only the first two stages of the three-stage device. The device shown in Fig. 29 was tested to determine whether or not it could burn fuel rich with no smoke emissions. The results from these tests are shown in Fig. 128, where it is noted that the nitric oxide emissions are very low but, in all cases, the Bacharach smoke level exceeded a reading of 1. The smoke readings ranged from 2 to greater than 9 in the fuel-rich region. Since smoke-free operation was not achieved in the first stage, testing of the remaining two stages of combustion was not conducted.

No-swirl Optimum Geometry Burner

The earliest burner geometry optimization experiments utilized a versatile burner that had relatively ineffective swirler vanes and, hence, a fixed geometry burner was constructed that had a choke diameter corresponding nominally to the optimum geometry criterion (dia. = $[2.7\ \text{gph}]^4$) but which had no swirler vanes. In a further attempt to streamline the flow, the burner was built, as shown in Fig. 129, with the choke in the form of a smoothly converging and diverging contour. The diverging part of the contour was made removable so that the burner could be tested with only the converging section.

Several tests were conducted with this burner, a few of the results of which are shown in Fig. 130. The tests were conducted with two oil spray nozzles, and with/without the 45-degree expansion section on the nozzle.

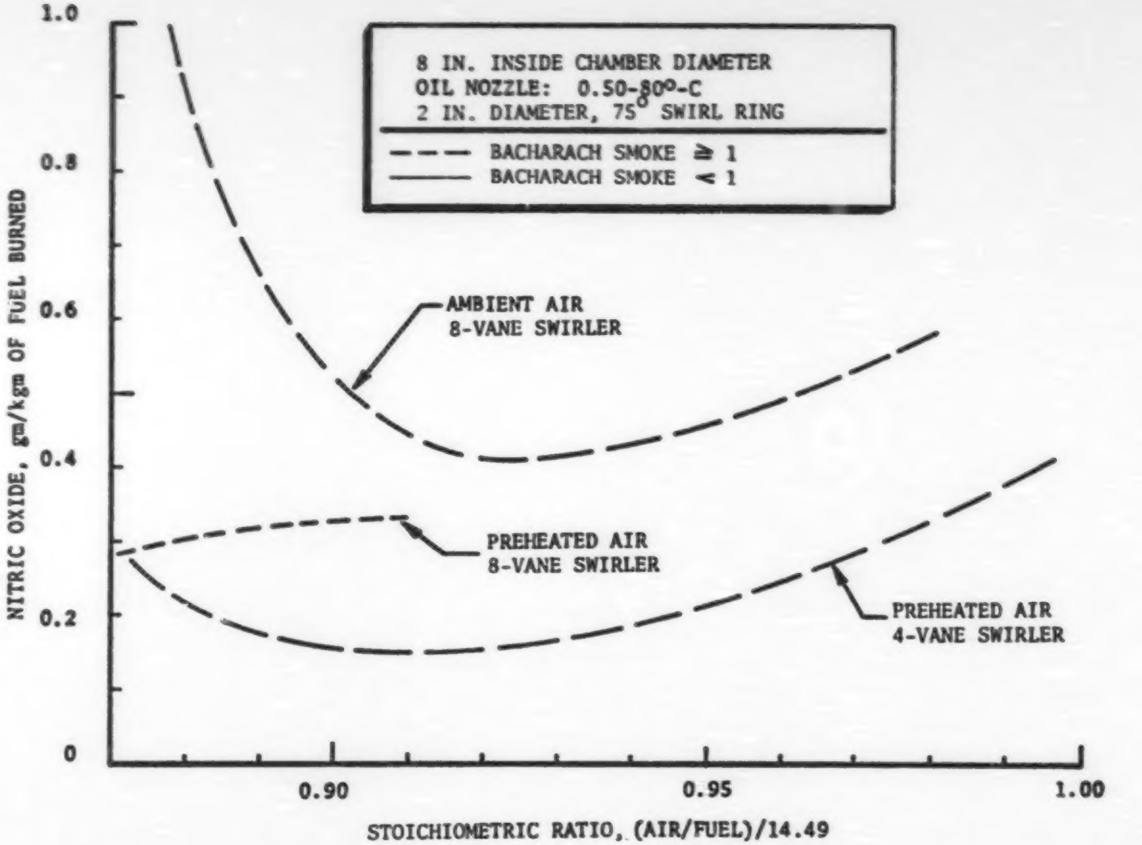

Figure 128. Nitric oxide emission results of fuel-rich combustion experiments with a fixed-vane intense-swirl burner head

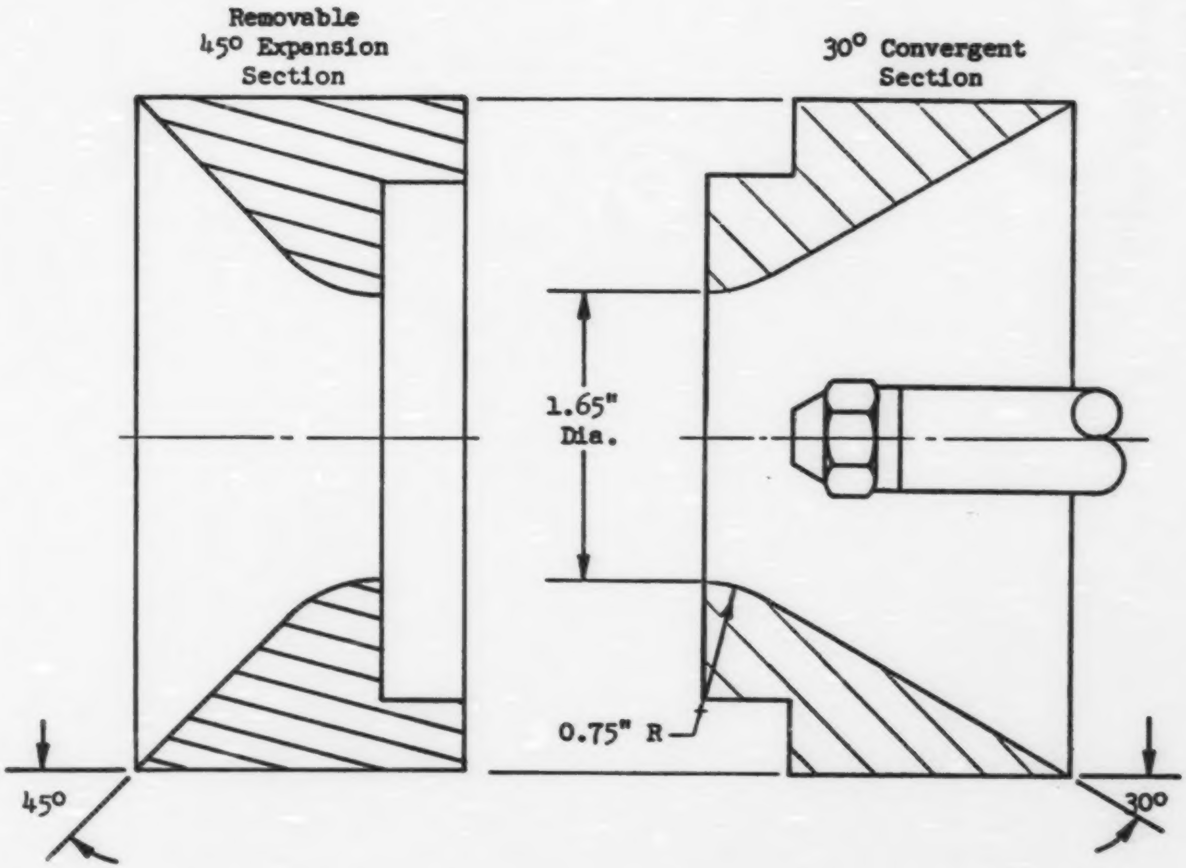
Removable
45° Expansion
Section
30° Convergent
Section
1.65"
Dia.
0.75" R
45°
30°

Figure 129. Cross-section view of the fixed geometry, 1.65-inch-diameter no-swirl optimum burner head

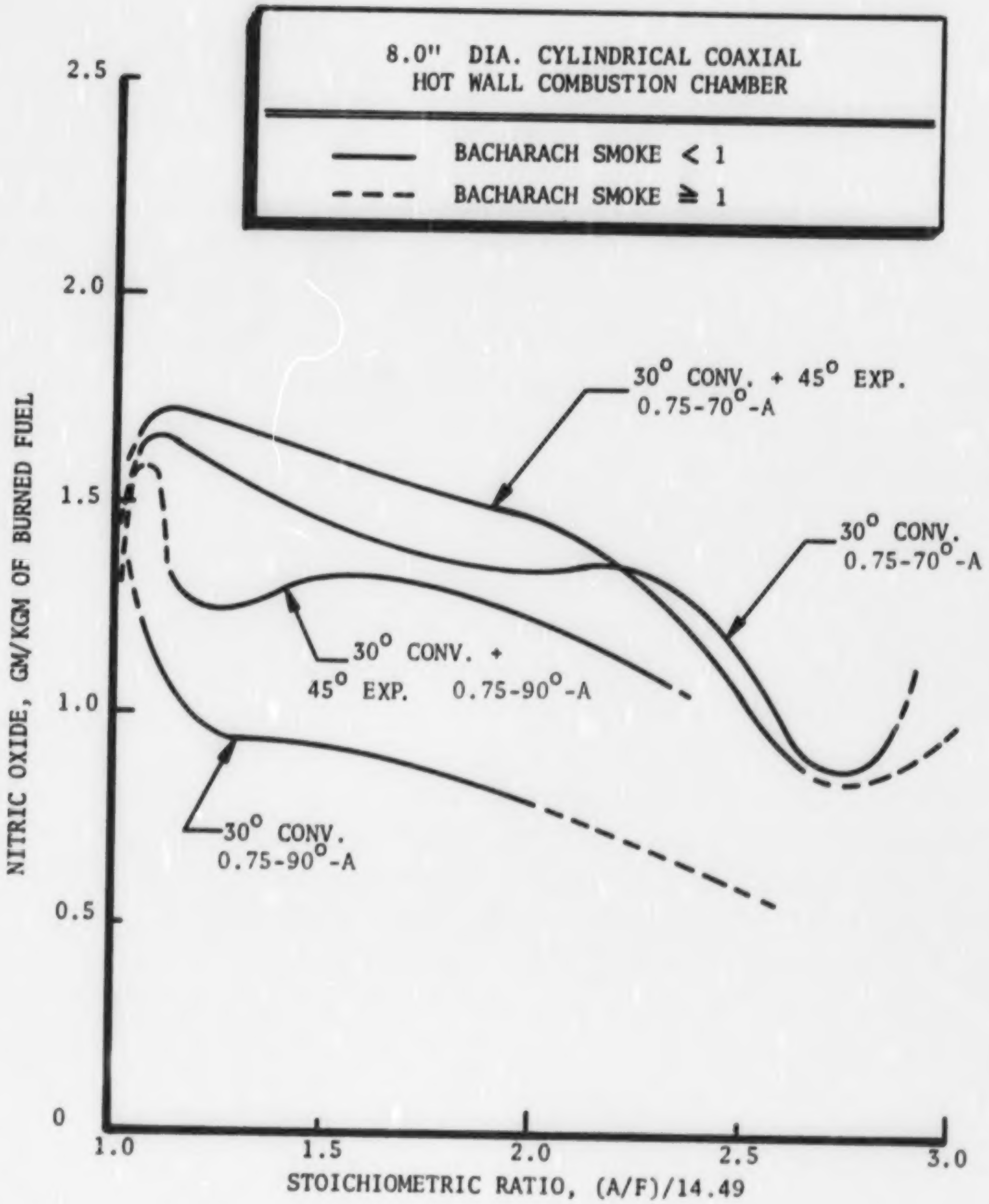

Figure 130. Nitric oxide emissions of the fixed geometry, convergent and expansion sections head, optimum geometry, no-swirl burner

Operation with the 90-degree nozzle and without the 45-degree expansion section was found to be best, as shown in Fig. 130. However, later attempts to repeat the low nitric oxide emission data resulted in a wide data spread, as shown in Fig. 131.

Because of the smooth flow profiles that should be expected from the smoothly contoured choke, it was suspected that the poor data repeatability was due to poor stability of the flame front location. A series of tests was conducted with an annular-shaped, flame-holding ring, and this seemed to stabilize the data. It was further suspected that the spark ignition device was influencing the flame front location, and so a series of experiments, shown in Fig. 132, was conducted (no flame ring), varying the location and condition of the igniter. As shown in Fig. 133, the nitric oxide emission level was lowest and most repeatable when the igniter was either turned off or extended downstream of the spray nozzle. This suggests that the flame front location is optimum when it is relatively far downstream of the spray nozzle.

The difficulty with data reproducibility resulting in the occasional relatively high nitric oxide emissions was apparently the combined effect of the smooth, no-swirl flow, and test-to-test variation in the effectiveness of the igniter. The fixed geometry optimum burner test results, reported in a previous section of this report, did not have similar data reproducibility problems, apparently because those burners incorporated six 25-degree air swirler vanes which tended to stabilize the flame front location.

To determine if the spark igniter had a similar effect on the action of other burners, tests were conducted with the ABC 55-J burner, and a EPA-furnished version of the ABC Mite burner (similar, but not identical to the Mite burner described in other parts of this report). The results of those tests are shown in Fig. 132, where it is apparent that, in some cases, turning the igniter off improves nitric oxide emissions while, in others, it increases them.

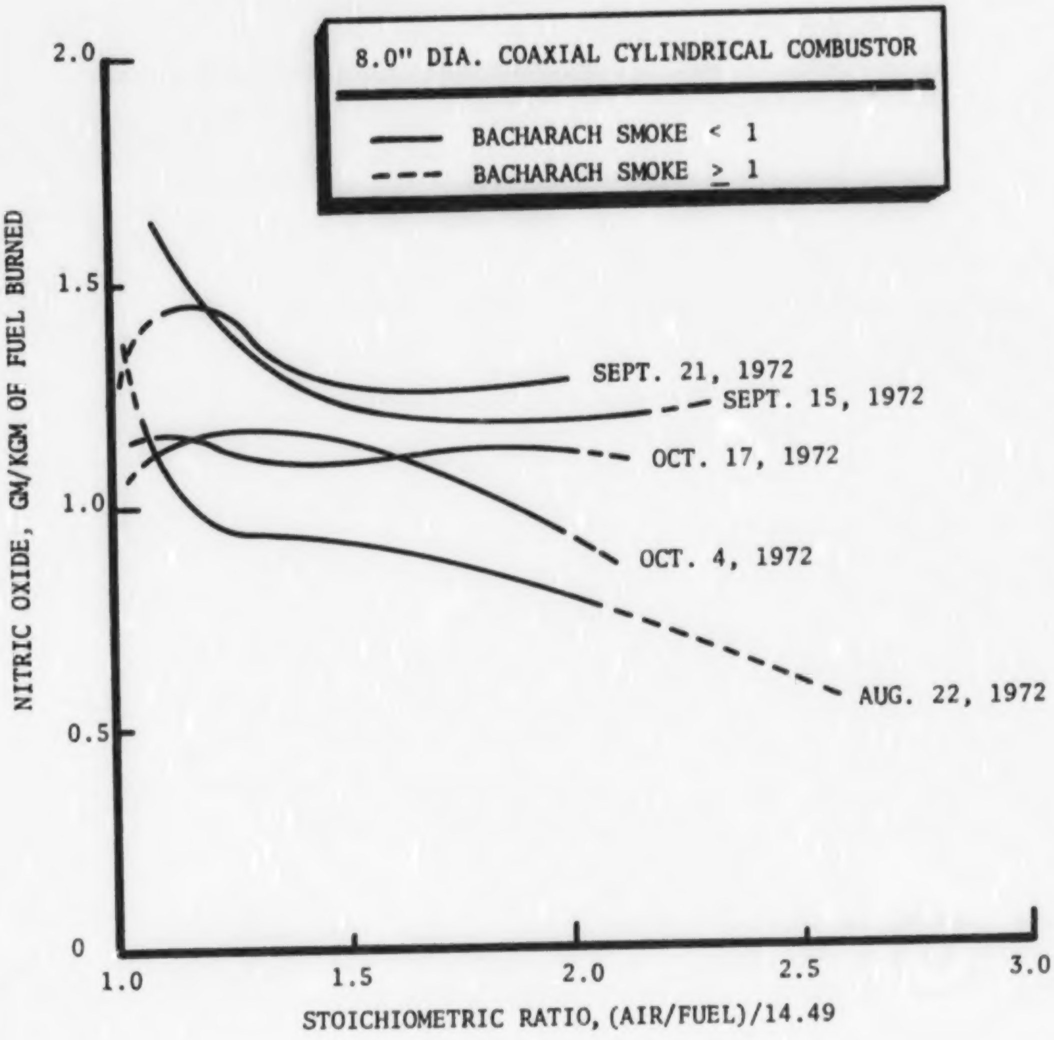

Figure 131. Variation of the nitric oxide profiles for the 1.65-inch-diameter, fixed geometry versatile burner with a 0.75-90°-A nozzle tested on different days

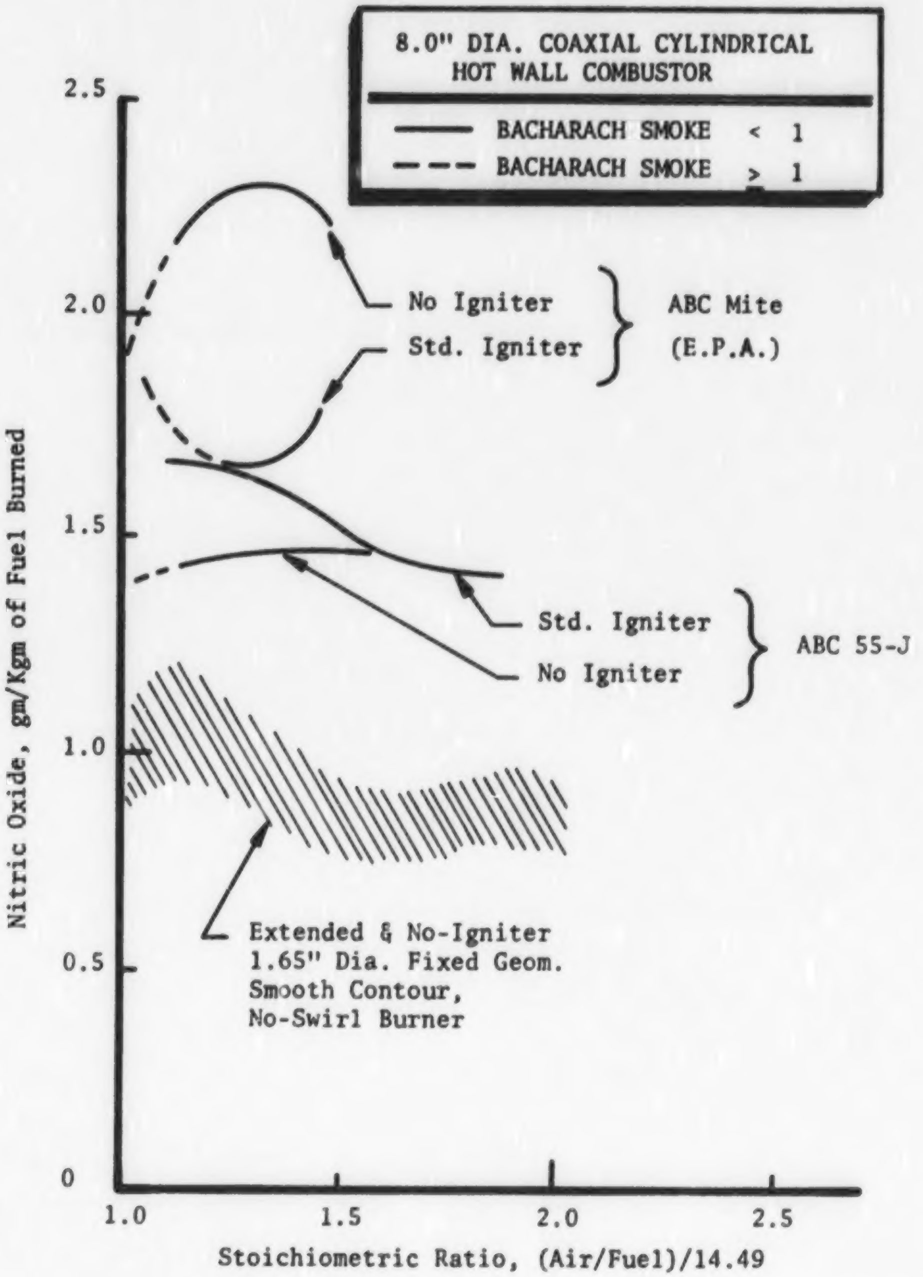

Figure 132. Comparison of nitric oxide emissions of commercially available burners with spark igniter modifications

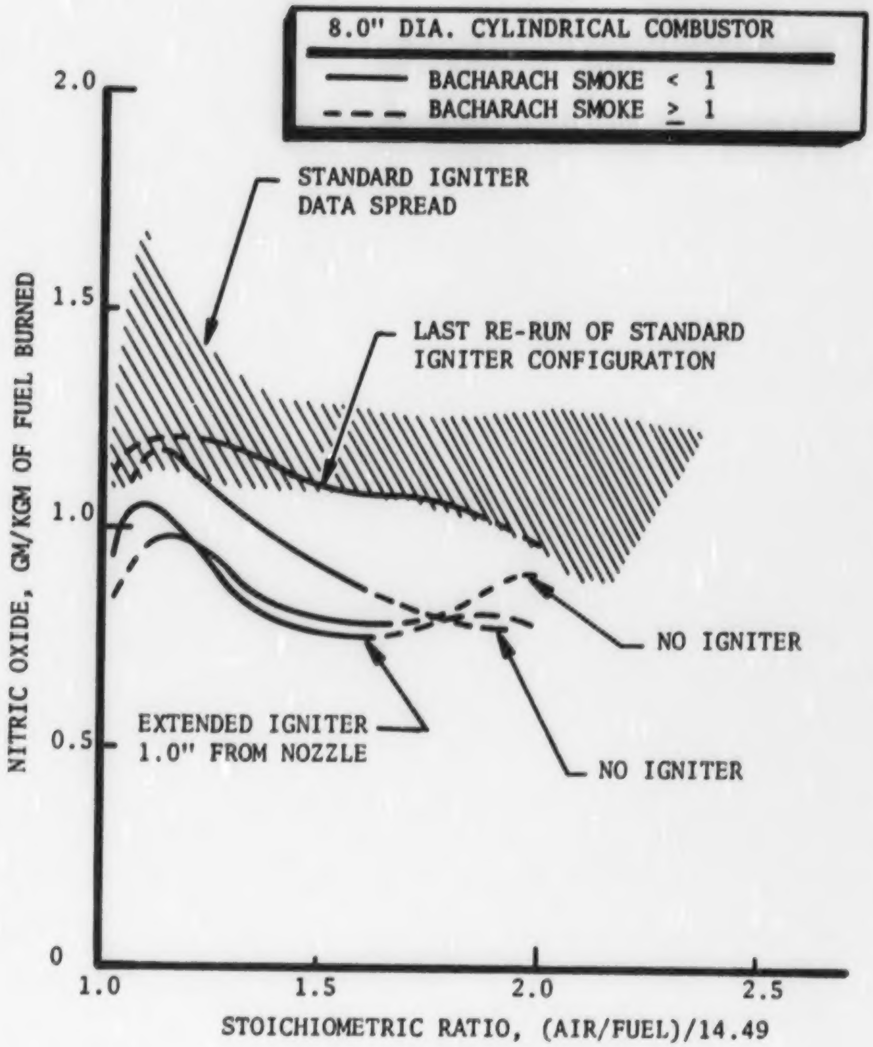

Figure 133. Comparison of nitric oxide emissions from the 1.65-inch-diameter, no swirl, fixed geometry, versatile burner with spark igniter modifications

CONCLUSIONS

Several major conclusions can be drawn from the results of this study, as described in the following paragraphs.

OPTIMUM BURNER GEOMETRY

For high-pressure atomizing, luminous flame burners fired into refractory-lined combustion chambers, minimum pollutant emissions are obtained with burners having: (1) no flame-retention device, (2) choke diameters equal to $(2.7 \text{xgph})^{0.4}$ (inches), and (3) peripheral swirler vanes oriented at 25 degrees relative to the blast tube axis. This swirler vane angle gives the best compromise between smoke emissions and nitric oxide emissions, while the recommended choke diameter produces minimum nitric oxide emisions.

BURNER DESIGN PHILOSOPHY

With oil burners fired into adiabatic combustion chambers (i.e., refractory lined chambers) at low excess air levels, formation of nitric oxide is minimized by the absence of strong mixing and recirculation and the absence of steep gradients in the combustion zone. That is, with low excess air and a refractory chamber, a uniform dispersion of fuel spray in air flowing and reacting smoothly down the combustion chamber, in the manner of a plug flow reactor, produces the least nitric oxide emissions. On the other hand, a vigorous intermixing of incoming fresh air with combustion products (as a result of adiabatic internal recirculation or steep gradients in the combustion field) tends to promote the formation of nitric oxide.

For adiabatic combustion chambers, the minimization of vigorous mixing and steep gradients prevents the use of flame-retention devices because these flame-retention devices promote undesirable mixing and recirculation in the flame zone. Flame-retention devices are used primarily because they promote stability of the flame front location so that a particular burner can be fired into a wide variety of combustion chambers without special changes or "tuning" of the design for each of the chambers. The detrimental effects of the flame-retention devices, with respect to pollutant emissions, suggests that they should not be used with adiabatic combustion chambers and, instead, burners designed according to the optimum burner geometry criteria presented herein should be used, with trial and error selection of the most suitable oil spray nozzle where necessary.

When oil burners are fired into nonadiabatic combustors (i.e., water-cooled or air-cooled chambers), the recommended design philosophy is somewhat different. In this case, external recirculation (i.e., recirculation between the flame core and the cool wall) is beneficial, whether it is produced by the forced recirculation technique described in the Nonconventional Burners section or by other techniques. In this case, the recirculated gases are cooled by the cool chamber wall, and when these cooled gases are mixed with the incoming fresh air, benefits similar to those obtained with flue gas recirculation, are realized because of a reduction in peak flame temperature reduction. It appears likely that internal recirculation (i.e., recirculation within the core of the flame where there is no opportunity for significant heat loss from the recirculated gases) is probably most detrimental to nitric oxide emissions, even in the case of nonadiabatic combustion, for essentially the same reasons it is detrimental in the case of adiabatic combustion chambers. Consequently, flame-retention devices are probably not desirable in cool-wall chambers either.

COMBUSTION CHAMBER WALL TEMPERATURE

Water-cooled or air-cooled combustion chambers characteristically lead to lower nitric oxide emissions than chambers of similar geometry that have refractory linings. This is undoubtedly the result of higher flame temperatures in the refractory-lined chambers. In the cool-wall chambers, peak flame temperatures are reduced because of heat lost to the chamber walls by radiation and because of recirculation of cooled combustion gases, which tends to dilute air injected through the burner blast tube. The advantages of cool-wall combustion chambers can be exploited through the use of burner designs that promote the recirculation of cooled combustion gases and the intermixing of these gases with the injected air.

COMBUSTION CHAMBER GEOMETRY

In the case of refractory-lined combustion chambers, it has been shown that cylindrical, coaxial combustion chambers (i.e., with the chamber and blast tube aligned along a common axis) result in lower nitric oxide emissions than cylindrical combustion chambers with the axis of the burner blast tube perpendicular to that of the chamber. Whether or not a similar effect occurs with cooled combustion chambers has not been determined experimentally.

APPENDIX A

COMMERCIAL DESIGN PRACTICES

The objective of this portion of the effort was to define present-day commerical burner design practices. Initially, a listing of oil burner manufacturers was made from: (1) the Thomas Register, and (2) the Oil Burner Rating Handbook by Edwin M. Field (printed by Oildum Publications, Bayonne, N. J.). For each company line, this handbook contains the capacity, nozzle type, nozzle angle, motor, fuel pump, transformer, controls and electrode specifications. From this list, companies located throughout the mid-west and eastern states were contacted by telephone. Brochures of the product line, installation manuals, and service manuals were requested from each company that manufactured oil burner units in the 0.5- to 12-gph size range. A list of all companies contacted by telephone is contained in Table A-1. A high attrition rate of small companies in the oil burner business is evidenced by the large number of companies that no longer produce oil burners. (Other companies whose telephone listings were no longer connected were not included in Table A-1; an additional 17 companies.) Brochures were requested from 26 companies, and 19 were received. Without exception, company representatives were interested and eager to discuss all aspects of their designs and willing to share their experience and whatever test results they had with us. At each company, both engineering and sales personnel were contacted so that some indication of the business aspects of the company, as well as the type of development efforts being conducted, could be determined. Based on the information obtained from the company brochures and the telephone conversations, and recommendations made by Dave Locklin of Battelle (a member of NOFI), five companies were then chosen for plant visits. All of the

Table A-1. OIL BURNER MANUFACTURERS CONTACTED BY TELEPHONE

Company Name	State Location	Remarks	Brochure Received
Preferred Utilities Mfg.	Connecticut	Burners 20 gph only	No
Victor Mfg. & Distr.	↓	No longer manufactures oil burners	No
Dunham-Busch Inc.		Commercial sizes only	Yes
Carlin Co.		Also made plant visit	Yes
Ace Engineering Co.	Illinois	Commercial sizes only	No
Auto Burner Co.	↓	Also made plant visit	Yes
Croak Engineering		-	No
Nu-Way (White-Rogers)		Also made plant visit	Yes
Aldrich Div.		-	No
Wayne Home Equip. Co.	Indiana	Major Company	Yes
Power Flame Div.	Kansas	-	Yes
General Automatic Prod.	Maryland	No longer manufactures oil burners	No
Lynn Products Co.	Massachussetts	No longer manufactures oil burners	No
American Steel Works	Missouri	Make heaters for tar only	No
American Furnace Co.	Missouri	-	No
Majic Servant Prod.	Michigan	Gas burners only	No
Calmac	New Jersey	-	No
W. N. Best Comb. Engr. Co.	↓	Commercial sizes only	No
Quiet Auto. Burner Co.		-	Yes
Hydrotherm Inc.		-	Yes
Aeroil Prod. Co.		Commercial sizes only	Yes
Acme Heat & Power Inc.	New York	-	No
Sun Ray	↓	Also made plant visit	Yes
Way-Wolff Assoc.		0.5 to 8 gph only	Yes
Reif-Rexoil Inc.		Going out of business	No
Superior Combustion		0.5 to 225 gph units	Yes
Cowan Frederick & Co.		International Co.	No
Gold Start Oil Burner		-	Yes

Table A-1. (concluded). OIL BURNER MANUFACTURERS CONTACTED BY TELEPHONE

Company Name	State Location	Remarks	Brochure Received
Babcock & Wilcox	Ohio	Primarily boilers	No
Smokeless Oil Burner		Commercial sizes only	No
North American Mfg.		-	Yes
Pyronics		Primarily gas burners	Yes
R. W. Beckett		Also made plant visit	Yes
Bethlehem Corp.	Pennsylvania	No longer manufactuctures	No
Thermal Research & Engr.		Commercial sizes only	No
Burnham Corp.		Boilers only	No
Hauck Mfg. Co.		Commercial application	Yes
Orr & Sembower		-	Yes
Forin Foundary & Mfg.		No longer makes oil burners	No
National Airoil Burner		Commercial sizes only	No
Amsler Morton Div.		Gas burners only	No
Bloom Engineering		Commercial applications	Yes
York-Shipley Inc.		Distribution for Wayne	Yes

companies visited were members of NOFI and individuals within each company were chairmen of various NOFI committees. The companies selected were representative of major oil burner manufacturers in terms of sales and research. However, these companies can all be classified as small businesses ($\leq$ 500 employees). This is understandable because the total market for domestic oil burners is only about 800,000 units per year, of which 45 percent are new installations and 55 percent are replacement units. The market should, however, increase in the future. In the past, applications have been limited primarily to heating units for homes, apartments, and industrial and office buildings. New markets, which are growing each year, are Marine applications and mobile home heating units. In addition, because of the natural gas shortage, more and more existing units are being converted to oil operation, and new installations are oil burners alone. It appears that future heating units may be primarily oil burners, rather than natural gas burners.

The companies selected for plant visits are tabulated in Table A-2. A complete day was spent at each company in discussions with both management and staff covering sales, production, engineering, and field service. The areas of discussion were broad because the burner design is affected by burner operation, cost, appearance, ease of service, as well as sales promotions. The companies are largely controlled by sales considerations and the function of engineering is to provide a product that is compatible with the overall marketing strategy. For the most part, all of the oil burners look alike and have identical locations for the pump, blower, transformer, and controls. In fact, these component parts are frequently identical on different burners, which facilitates obtaining replacement parts anywhere in the country. The various burners are competitive costwise and produce nearly identical efficiencies, with only a trace of smoke. The major sales arguments are: (1) our product is more versatile and requires less inventory (attractive to distributors or original equipment manufacturers), (2) the product is tailored or engineered to your specific application, (3) fixed geometry so that no adjustments are necessary, and

Table A-2. LIST OF COMPANIES VISITED

Company Name	Location	Date of Visit	Telephone No.	Initial Contact	Co. Members at Meeting
The Carlin Co.	Wethersfield, Conn.	2-12-73	(203) 529-2501	Mr. Burt S. Watling Vice President	B. Watling-V.P. Len Fisher-Chief Engineer
Sun Ray Burner Mfg. Co	Plainview, N. Y.	2-13-73	(516) 293-6800	Mr. Bob Skarda Sales Manager	Bob Skarda (Chief Engr. recently deceased)
Nu-Way Division, White-Rogers Corp.	Milan, Illinois	2-14-73	(309) 787-4461	Mr. Bud Rettke General Manager	Bob Krump-Supv. Project Engr. Les Olsen Manager Field Services
R. W. Beckett Corp.	Elyria, Ohio	2-15-73	(216) 365-4141	Mr. Myron Cooperrider Chief Engineer	M. Cooperrider-Chief Engr. R. Dumboys-Ass't. Chief Engr. F. Deuble } Sales O. Faulnaber } Mgr. J. Beckett-Pres. B. Cook-V.P.
Automatic Burner Co.	Chicago, Illinois	2-16-73	(312) 733-1707	Mr. William Lord Vice President	W. Lord, V.P.

(4) factory-trained installation service to "fine tune" the burner. The information and considerations relating to design practice, service problems, and independent research were almost the same for all companies, so no attempt will be made to categroize by company.

The evolution of oil burner designs has been based on cut-and-try techniques aimed at obtaining CO_2 levels of about 12.5 percent (with $\approx$20-percent excess air) and no more than a trace of smoke. The oil burner designs are now virtually fixed and little, if any, industrial manufacturer research is being conducted to improve existing designs or develop new approaches. Only two basic types of No. 2 oil burners are marketed today: (1) flame-retention type and (2) conventional. The major difference between these types is that in the flame-retention type, a cone-shaped bluff body or other obstruction is added that locally reduces the air and oil velocities sufficiently below the turbulent flame speed so that ignition is maintained at the retention device location. With the conventional burner type, the flame location is dependent on burner and boiler design, as well as operating conditions. Both types employ swirl vanes. In a flame-retention-type burner, the swirl vanes are sometimes located on the flame cone while, in the conventional burner, they are positioned along the blast tube wall. An advantage of a centrally located flame cone with an annulus between the cone and the wall is that it is possible to vary the input air between the central portion of the flow area and the peripheral zone and thereby adjust the mass distribution uniformity.

STATIC PLATE

Static plates are placed upstream of the oil nozzle and are designed to reduce the air flow bias introduced by the centrifugal blower. The static plates are primarily used to control air flow distribution when short blast tube lengths are required, but with a pressure loss.

BLAST TUBE

The length of the blast tube should be sufficiently long, usually in excess of 3 inches, to ensure that the air flow is uniform at the burner head. The maximum length of blast tube currently used is about 20 inches. The actual length is usually determined by the furnace wall thickness.

SWIRL VANES

The swirl vanes are used to promote mixing of the oil and air.

BLAST TUBE END PLATE

End plates (choke plates or choke rings) are used to induce a high combustion gas velocity and thereby promote oil droplet breakup and additional mixing.

OIL NOZZLES

Primarily hollow cone nozzles are used in the smaller 0.6- to 3-gph burners. These nozzles are designed to provide a very thin annular sheet of oil with tangential swirl. The thinner the sheets, the smaller the final droplets. Swirl promotes breakup and mixing with the air. The larger burners use either hollow or solid cone, depending on specific characteristics of each burner. At the low flowrate capacities, only a single nozzle is used; however, for sizes larger than 12 gph, multiple nozzles are sometimes used to control oil distribution and reduce dropsizes. The multiple nozzle also is conducive to a low-fire, high-fire programmed start sequence commonly found in the larger burners through use of one nozzle for low-fire startup.

FLAME DETECTORS

Three types of flame detectors are currently being used as safety cutoff devices; all are photoelectric devices. Cadmium sulfide cells are often used and ultraviolet-sensitive cells have been used. The devices operate satisfactorily although ultraviolet-sensitive cell creates a mounting location problem, because it responds to ultraviolet-sensitive radiation from the spark igniter and must be shielded from it.

SAFETY CONTROLS

If flame is not detected after the burner is turned on, the safety controls must shut down the burner within an acceptable time. Underwriter's Laboratories has specified the following times:

Capacity, gph	Required Shutoff Time, seconds
0.75 to 3.0	30
3.0 to 7.0	15
7.0 to 20.0	4

OTHER STANDARD PARTS

- Ignition rods--all standard; however, U.L. requires that the electrodes be at least 1-1/2 inches away from any other metal part
- Oil pump--100- or 300-psig discharge pressure
- Motor--1725- or 3450-rpm units
- Ignition Spark Transformer--10,000 to 12,000 volts

DESIGN PROBLEMS

The major problems that face the design engineer in burner/boiler matching are:

1. Instability
    a. Instability of the flame due to burner/boiler "mismatching" or combustion coupling

   b. Instability induced from feed system vibrations

2. Noise
   a. Pump or fan mountings and bearing vibrations which couple easily with the boiler and associated ducts
   b. Flame front and burner/boiler instabilities
3. Determination of insertion length (thickness of boiler wall and the burner flange)
   - Defines the blast tube length
4. Operation
   - The burner must provide CO_2 levels of 12.5 percent (with 20-percent excess air) with no more than a trace of smoke at all design flowrates and, at its maximum rated oil flowrate, it must demonstrate a 50-percent excess air capability to allow for degradation.

Unfortunately, there is little, if any, interchange of design requirements between the boiler and the oil burner manufacturers, so that the burner designer is often faced with a combustion chamber configuration that will not support efficient combustion.

The current practice in original equipment manufacturers' burner sales is for the boiler manufacturer to ship a prototype boiler to the selected oil burner manufacturer for use in testing at his plant. The oil burner designer first inspects the boiler for furnace dimensions, refractory-lined and uninsulated surfaces of the furnace, and required blast tube length. With this information, a burner configuration is selected and it is tested in the boiler furnace. Adjustments are made until the burner operates satisfactorily. With some boilers, it has not been possible to produce stable, efficient, noise-free operation, and the boiler design has been rejected by both the burner and boiler manufacturer. In cases where instability is encountered, current design practice is to do one of the following:

1. Change stack pressure to provide less flow resistance
2. Leave the boiler furnace door slightly ajar (boilers operate at subatmospheric pressure)
3. Build in leaks around the furnace and burner installation flange, which has the same effect as (2) above.

Although these fixes are crude, they work. Unfortunately, if the burner is adjusted for efficient operation with no leaks, then introducing air leaks will result in the boiler operating at a higher than desirable stoichiometric ratio. This condition usually does not result in increased smoke, but the efficiency may be decreased.

A major problem facing the burner manufacturer is good field service. Generally, the manufacturer provides no additional service after the burner leaves the plant. Usually, the boiler manufacturer or distributor provides service installers whose job is to ensure that the burner is properly set up. The burner people universally agreed that service and installation are generally poor. Service personnel often have only a minimal knowledge of good operating practice, and no standards are maintained. The burner manufacturers indicated that the units should be removed and serviced at least once a year to prevent fouling of the nozzle, carbon deposits on the burner, and ensure that the igniters are working properly. Owners, however, generally service their burners only when they fail. The oil burner manufacturers are not inclined to change their burner designs because they believe that field service personnel are reluctant to learn new procedures and stock additional replacement parts. This is the reason why new innovations should be relatively straightforward modifications of existing designs.

APPENDIX B

FACTORS FOR THE CONVERSION OF UNITS TO THE METRIC SYSTEM

Physical Quantity	To Convert From	To	Multiply by
Length	inch	meter	0.0254
	foot	meter	0.3048
	micron	meter	0.000001
Mass	pound	kilogram	0.45359
Pressure	psi	pascal	6894.8
	newton/meter^2	pascal	1.0000
Speed	foot/second	meter/second	0.3048
Temperature	Celsius (C)	Kelvin (K)	K = C + 273
	Fahrenheit (F)	Kelvin (K)	K = (F + 460)/1.8
	Fahrenheit (F)	Celsius (C)	C = (F - 32)/1.8
	Rankine (R)	Kelvin (K)	K = R/1.8
Time	hour	second	3600
Volume	gallon (U.S. liquid)	meter^3	0.0037854